Exploring the Reactivity of 4-Hydroxydithiocoumarin to Access Novel Organosulfur Compounds and Some of Their Anticancer Activity Study

A Dissertation Submitted to the
Indian Institute of Technology Guwahati
As partial fulfilment of the degree of
DOCTOR OF PHILOSOPHY

Submitted by

Ahmad Ali

Roll No.: 216122051

Under the Supervision of

Prof. Abu Taleb Khan

Department of Chemistry
Indian Institute of Technology Guwahati
Guwahati-781039, Assam
India

November 2025

DEDICATION

Dedicated to my beloved Grandparents
in heaven, and my loving Parents

DECLARATION

I do hereby declare that the matter embodied in this thesis entitled "***Exploring the Reactivity of 4-Hydroxydithiocoumarin to Access Novel Organosulfur Compounds and Some of Their Anticancer Activity Study*** " is the result of investigations carried out by me under the supervision of Professor Abu Taleb Khan in the Department of Chemistry, Indian Institute of Technology Guwahati, Guwahati, Assam, India.

In keeping with the general practice of reporting scientific observations, due acknowledgements have been made wherever the work described is based on the findings of other investigators.

IIT Guwahati
14th November 2025

Ahmad Ali
(Roll No.: 216122051)

Indian Institute of Technology Guwahati
Guwahati – 781039, India
Tel. No.: +91-361-2582305
Fax No.: +91-361-2582349
e-mail: atk@iitg.ac.in

Dr. Abu T. Khan
Professor of Chemistry

CERTIFICATE

This is to certify that Mr Ahmad Ali, Roll Number-216122051, has been working under my guidance since 21st October 2021 as a regular registered PhD student. Due to the COVID-19 pandemic, he was not permitted to join the institute, despite being admitted in July 2021.

I am forwarding his thesis entitled "**Exploring the Reactivity of 4-Hydroxydithiocoumarin to Access Novel Organosulfur Compounds *and Some of Their Anticancer Activity Study***", which is being submitted for the PhD Degree in Science from this institute.

I also certify that he has fulfilled all the requirements set forth in the rules & regulations of this institute for the investigations embodied in his thesis, and that this work has not been submitted elsewhere for any other degree.

IIT Guwahati
14th November 2025

Prof. Abu T. Khan
(Thesis Supervisor)

ACKNOWLEDGEMENT

I would like to express my sincere gratitude to my thesis supervisor, Professor Abu Taleb Khan, for his unwavering support, guidance, encouragement, constructive advice, and tireless efforts in assisting me throughout my PhD journey. His patience and valuable suggestions are always encouraging and greatly help me with my research.

I am also very much thankful to him for giving me the opportunity and the freedom to explore my own ideas during my research. I feel fortunate to have worked under his kind guidance.

I also express sincere gratitude to the Chairperson, Professor. Bhisma Kumar Patel, as well as other Doctoral Committee Members, namely Professor Subhas Chandra Pan and Professor Siddhartha Sankar Ghosh, for their valuable advice and suggestions throughout my PhD journey, starting from my comprehensive examination to the submission of my PhD thesis. I would like to acknowledge all the DC members for pointing out my mistakes in a constructive and optimistic manner.

I am very grateful to Professor Prasad V. Bharatam, Ms. Kriti Mehta, and Ms. Mehak Sood from the Department of Chemistry, National Institute of Pharmaceutical Education and Research, Mohali, for their collaboration in the DFT energy calculation for the proposed mechanisms. I also want to thank Professor S. S. Ghosh and his research scholar, Pijush Kanti Khanra, from the Bioscience and Bioengineering Department, for their fruitful collaboration in biological studies. I would like to express my gratitude to all the teachers who have guided me on this academic journey since my early years. Their teachings have paved the way for my growth and achievements in all dimensions of my life.

I would like to thank the Department of Chemistry, IITG, for providing access to various instrument facilities, including 400 MHz and 500 MHz NMR spectrometers and a single-crystal XRD instrument.

I am also grateful to the Central Instrumental Facility, IITG, for providing access to instrument facilities, particularly the 600 MHz NMR and HRMS.

I am also grateful to NECBH for providing access to the 400 MHz NMR facility.

I thank the University Grants Commission (UGC) for the financial support for my research fellowship and contingency grant, and the DST for providing a research grant to my thesis supervisor.

I would like to express my heartfelt thanks to Professor Chandan K. Jana for helping with the reaction mechanism and to all other faculty members who have mentored me during my coursework. I would like to thank all the research scholars of the Department of Chemistry at IITG for providing a conducive research environment.

I am sincerely thankful to all my Seniors and Juniors from my laboratory, Dr. Karuna Mahato Dr. Md. Belal, Dr. Saghir Ali, Dr. Santa Mondal, Dr. Sabina Yashmin, , Dr. Arnab Mondal, Dr. Anjela Xalxo, Dr. Ujjwal Jyoti Goswami, Dr. Simra Faraz, Mr. Mukesh Kumar, Mr. Satyajit Singh, Mr. Anil Rangnath Pawar, Mr. Eman Ali SK, Ms. Nisha Rani, Ms. Halida Khatun, Mr. Afzal, Mr. Devendra Kumar, and Mr. Chaugule Somesh Shekhar for their help both academically as well as emotionally. I would like to thank Dr. Gyani Yumnam, and Dr Sandeep Kumar for solving the single-crystal XRD data.

I express my sincere gratitude to all my friends, especially the group (YES Chuka), for their kind words about me. I also thank Dr. Hassan, Dr. Hanifa, Mr. Liyaqat, Mrs. Bilquees Fatima, Ms. Trinity Sherpa, Mr. Altaf Hussain Kawa, and Dr. Mudaser Rahman Dar. Mr. Muneeb, Mushtaq Sheikh, Mr. Nazir UD Din Mir, Mr. Zaheer Abbas, and all other friends whose names are not included for their direct and indirect assistance.

I would like to express my heartfelt regards to the technical staff and chemistry office staff, Dr. Babulal Das, Mr. Imdadul Islam, Dr. Kula Kamal Senapati, Mrs. Abhilasha M. Baruah, Mrs. Lipika Nath, Mr. Aniruddha Gogoi, Mr. Shyamal Kumar Mondal, Mr. Diganta Lal Hira, Mr. Tapu Ghosh, Ms. Sayanee Mukherjee, Mr. Nabajyoti Duttaand Mr. Michael Deka, for their constant help and cooperation.

Ultimately, my PhD journey would not have been possible without the support of my family and relatives. Their unconditional love and affections continuously boost my concentration and focus unidirectionally towards my research work. I would like to express my gratitude to my respected father, Mr Mohd Hussain, and my beloved mother, Mrs Nargis Banoo, for their unconditional love, support, and all their sacrifices in bringing me up. I would like to thank my elder brother, Mr. Mohd Mehdi, my elder sisters, Mrs. Rubaba Batool, and Mrs. Soqura Banoo, my younger sisters, Mrs. Syeeda Banoo and Ms. Zainab Banoo, who

always inspired and kept believing in me in all ups and downs, their unconditional sacrifices and moral support throughout my life. I also thank all my cousins for being helpful throughout my PhD journey.

I would like to extend my sincere thanks to Ms Sikhamoni Begam and her family for their love and constant emotional support throughout my PhD program. My heartfelt thanks to Mrs Khairun Begom for constantly reminding me of auspicious days and events, and for making me feel at home.

*Last but not least, I would like to thank Allah the Almighty for blessing my life with so much love and wonder (**Indeed, hardship often comes with ease**).*

GENERAL REMARKS

The present investigations were carried out at the Department of Chemistry, Indian Institute.of Technology Guwahati, Guwahati -781 039, Assam, India, during the period from July 2021 to 10th September 2025 as a doctoral student under the supervision of Prof. Abu T. Khan.

The analytical samples were routinely dried in vacuo at 50 °C. In TLC experiments, silica gel G (SRL) or silica gel GF 254 (SRL) was employed as the adsorbent. Column Chromatography was carried out with silica gel (60-120 mesh, Merck or SRL), for Purifications of the reaction mixture.

After purification, the solvent was usually removed in a rotavapor using Büchi R-114V and Büchi R-300 instrument. Melting points were determined on a Büchi melting point apparatus. IR spectra were recorded on a Perkin-Elmer Spectrum Two Instrument. $CDCl_3$ and DMSO-d6 were used for recording the NMR spectrum.

^{1}H spectra were recorded on Bruker 400 MHz, Bruker 500 MHz, and Bruker 600 MHz spectrometers using TMS as an internal standard. Similarly, ^{13}C NMR spectra were recorded on Bruker 100 MHz, 125 MHz, and 150 MHz spectrometers, with TMS as the internal reference. Chemical shifts (δ scale) are reported in parts per million (ppm). ^{1}H NMR spectra are reported in the order: multiplicity, no of protons, and coupling constant (J value) in hertz (Hz); signals were characterized as s (singlet), d (doublet),t (triplet), m (multiplet), brs (broad singlet), dd (doublet of doublet), dq (doublet of quartet), dt (doublet of triplet) and ddt (doublet of doublet of triplet).

HRMS were recorded using the instrument named Agilent 64546 LC/Q-TOF (Ultra-High-Performance Liquid Chromatography-Quadrupole Time-of-Flight-High-Resolution Mass Spectrometer) in ESI (TOF) mode. Crystal data were collected with a Bruker Smart Apex-II CCD diffractometer using graphite monochromated Mo Kα radiation (λ = 0.71073 Å) at 296 K.

ABBRE*VIA*TION

ACN	Acetonitrile
AcOH	Acetic acid
ADMET	Absorption, Distribution, Metabolism, Excretion, and Toxicity
AIBN	Azobisisobutyronitrile
AMES	Salmonella/Microsome Mutagenicity Assay
aq.	Aqueous
BBB	Blood-Brain Barrier
BHCs	Bis-Heterocycles
β-CD	β-cyclodextrin
Bu	Butyl
CCDC	Cambridge Crystallographic Data Centre
CNR1	Cannabinoid Receptor
CREB1	CAMP-responsive element binding protein 1
CYP 450	Cytochrome P450
DMF	*N, N*-Dimethyl Formamide
DMSO	Dimethyl Sulfoxide
DCM	Dichloromethane
DABCO	1,4-diazabicyclo[2.2.2]octane
DFT	Density functional theory
DMA	*N, N*-Dimethyl Acetamide
DCF	2′,7′-dichlorofluorescein
DNA	Deoxyribonucleic acid
DCFDA	2′,7′-dichlorofluorescein diacetate
Et	Ethyl
g	Gram
GPCRs	G protein-coupled receptors

GBBR	Groebke–Blackburn–Bienaymé reaction
h	Hours
HRMS	High-resolution mass spectrometer
HOMO	Highest occupied molecular orbital
HBTM-2	Homobenzotetramisole
IMCR	Isocyanide-based multicomponent reactions
$In(OTf)_3$	Indium(III)Triflate
IC_{50}	Half-maximal inhibitory concentration
IR	Infrared
KEGG	Kyoto Encyclopedia of Genes and Genomes
LUMO	Lowest occupied molecular orbital
MCR	Multicomponent reaction
MAPK	Mitogen-activated protein kinase
MDA-MB-231	M D Anderson - Metastatic Breast - 231
m-CPBA	*meta*-Chloroperoxybenzoic acid
mg	Milligram
µg	Microgram
mL	Milli litre
mp	Melting points
µM	Micro molar
MS	Molecular sieves
MTT	3-[4,5-dimethylthiazol-2-yl]-2,5 diphenyl tetrazolium bromide
NMR	Nuclear Magnetic Resonance
NBO	Non-Bonding Orbitals
NADPH	Nicotinamide Adenine Dinucleotide Phosphate Hydrogen
OSCs	Organosulfur Compounds
ORTEP	Oak Ridge Thermal-Ellipsoid Plot Program

OCT2	Organic cation transporter 2
PDA	2,6-Pyridinedicarboxylic acid
Ph	Phenyl
ppm	Parts per million
p-TSA	*Para*-Toluene sulfonic acid
Py	Pyridine
PI3K	*Phosphatidylinositol 3-kinase*
RB	Round-bottomed flask
RCSB	Research Collaboratory for Structural Bioinformatics
ROS	Reactive oxygen species
rt	Room temperature
S_N2	Substitution Nucleophilic Bimolecular
VEs	Vinyl ethers

Content of the Thesis

Chapter I

Brief introduction about elemental sulfur, organosulfur compounds, 4-hydroxycoumarin and reactivity of 4-hydroxydithiocoumarin

1.0 Introduction to Sulfur:

Sulfur is one of the most abundant elements on the planet. In the periodic table, it belongs to the chalcogens family due to its variable valence, which allows it to exist in different forms with varying chemical compositions. Such as it can exist in the form of elemental sulfur, metal sulfides, sulfate, and organosulfur compounds.[1] The name sulfur is derived either from the Sanskrit 'sulvere' or the Latin 'sulfonium'. Elemental sulfur is a yellow crystalline solid, found in the Earth's crust, mostly near volcanic regions. It is used in industries to manufacture sulfuric acid (H_2SO_4) and is an essential component in fertilisers, batteries, petroleum refining, agriculture, medicine, and the rubber industry. Since elemental sulfur is highly reactive, it easily reacts with metals to form metal sulfides, and can exist in the form of ores such as Iron Sulfide (FeS_2 – Pyrite), Zinc Sulfide (ZnS – Sphalerite), Copper Sulfides (Cu_2S, CuS – Chalcocite, Covellite), and Molybdenum Disulfide (MoS_2).[2,3] When these metal sulfides undergo oxidation, they are converted to sulfate (SO_4^{2-}), which plants absorb from soil and convert to sulfide, bringing organo-sulfur into living organisms. Once sulfide (H_2S) is formed, it is incorporated into amino acids such as cysteine (Cys). Cysteine is a precursor to other organosulfur compounds, such as methionine and glutathione.

The naturally occurring organosulfur compounds include amino acids such as cysteine, methionine, and glutathione, as well as being part of vitamin B1, insulin, oxytocin hormones, and nitrogenase enzymes. Some of them are shown in **Figure 1 (a)**. Organosulfur Compounds (OSCs) are found in plants. The Allium and Brassica (Cruciferous) genera, including onion, garlic, broccoli, cabbage, and cauliflower, are good sources of natural organosulfur compounds.[4,5] Traditionally, we are consuming all these vegetables, and studies say that they are beneficial for heart diseases, tumours (such as oesophageal, gastric, colorectal, breast, lung, skin, and prostate cancers), and immunological processes, among others, especially due to the biological action of the sulfur-containing metabolic by-products.[6-8] In addition, OSC may have an essential role in preventing inflammation. There are many non-natural organosulfur compounds that are biologically active and play a crucial role in our day-to-day lives; a few of them are shown in **Figure 1(b)**. Among the non-naturally occurring OSC, 4-hydroxydithiocoumarin and 4-hydroxythiocoumarin are part of the investigation of this

thesis, specifically 4-hydroxydithiocoumarin, as they bear a similar molecular structure to 4-hydroxycoumarin.

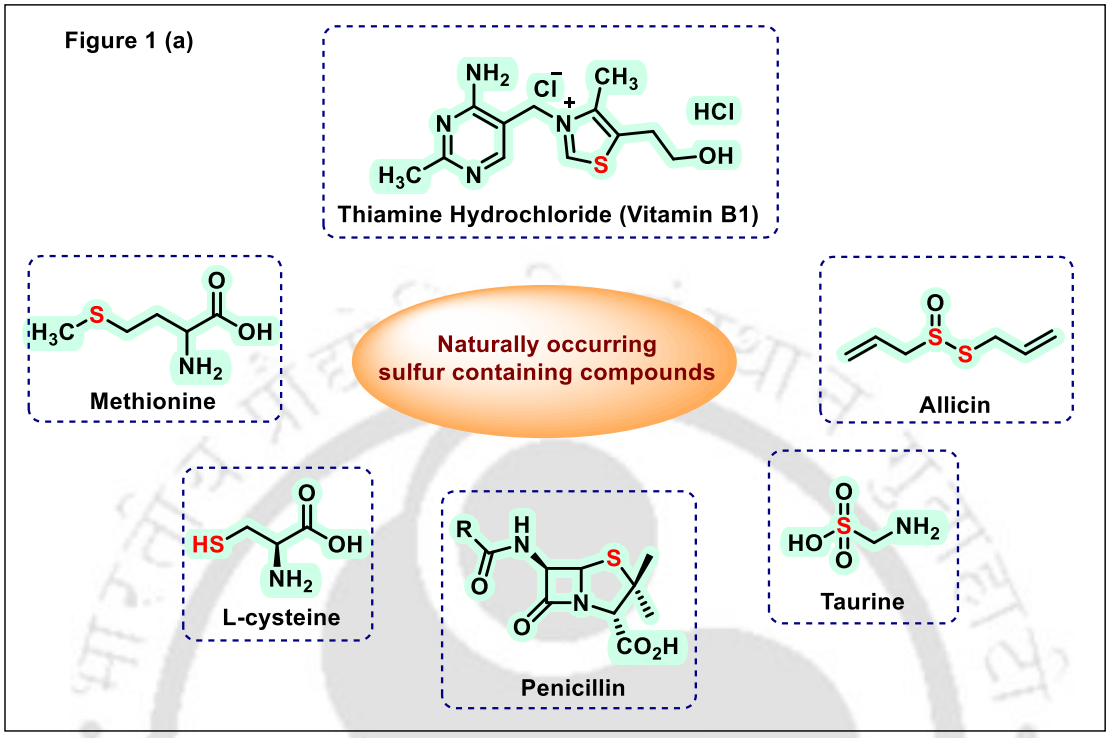

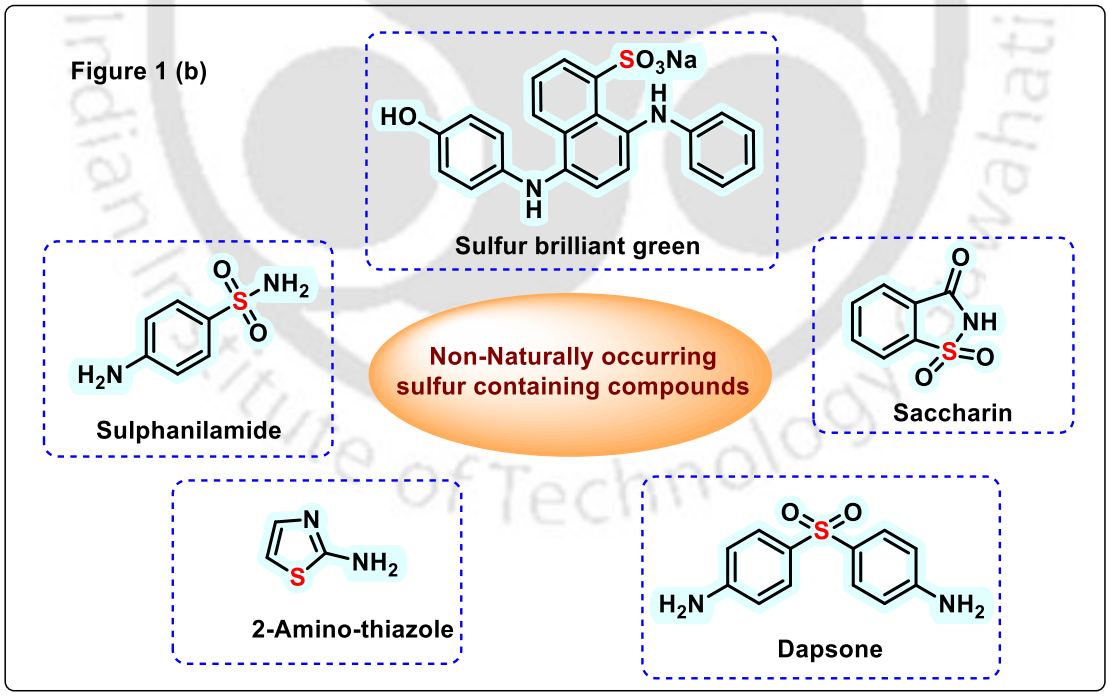

Figure 1. (a) Some important and biologically active naturally and **(b)** non-naturally occurring OSCs.

1.1 4-Hydroxycoumarin

Coumarin, a natural product first isolated from Tonka beans, and its hydroxy derivatives are renowned for their profound medicinal properties.[9] The derivative of coumarin, such as 4-hydroxycoumarin, is one of the fascinating heterocyclic molecules, as its derivatives play a vital role in the pharmaceutical area. The well-known drugs include warfarin, bromadiolone, brodifacoum, and flocoumafen.[10] They are used as potent blood thinners (anticoagulants). Additionally, 4-hydroxycoumarin derivatives exhibit broad-spectrum medicinal properties, including analgesic, anti-inflammatory, antipyretic, antibacterial, antiviral, and anticancer activities, as illustrated in **Figure 2.**[11a-c.] Due to the inherent biological activities of 4-hydroxycoumarin derivatives, researchers are still interested in exploring their reactivity and in synthesising more novel scaffolds. The biological activities, such as antiproliferative properties against cancerous cells, are retained in many derivatives of 4-hydroxythiocoumarins, which motivates our interest in exploring the reactivity of the thio-analogue of 4-hydroxycoumarin (4-hydroxydithiocoumarin) to synthesise novel organosulfur compounds (OSC).[12-14] The literature found that many novel organosulfur heterocycles are synthesised using 4-hydroxydithiocoumarin as a key precursor. For more details, refer to section **1.3.**

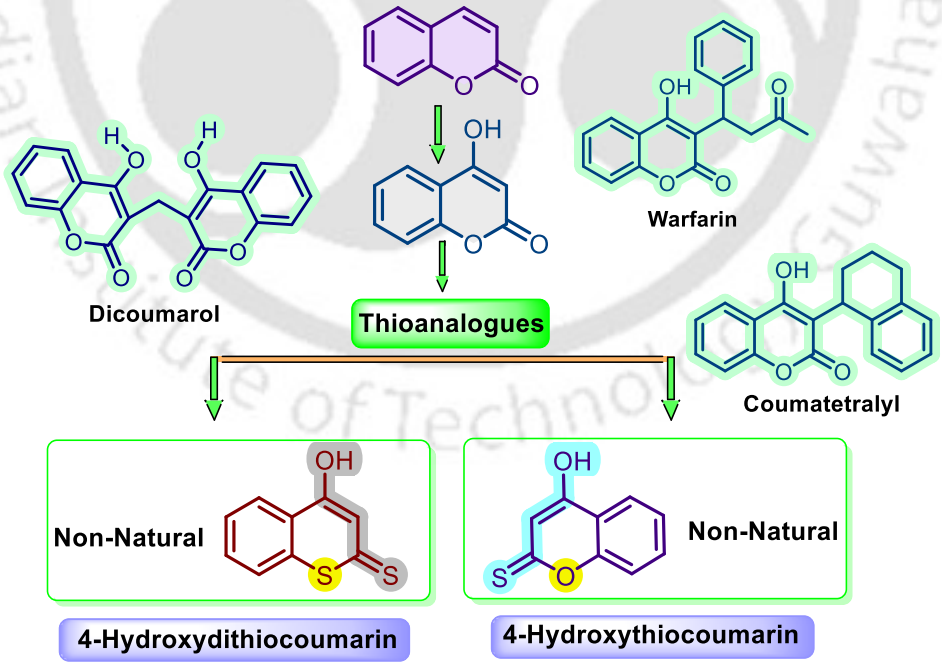

Figure 2. A flowchart of coumarin, 4-hydroxycoumarin, and their thio-analogues

1.2 Historical Background and Synthesis of 4-Hydroxydithiocoumarin

4-Hydroxydithiocoumarin is a non-natural organosulfur compound, and in 1987, Anderson-McKay and Liepa first reported the synthesis of 4-hydroxydithiocoumarin[15] from 2′-chloroacetophenone and carbon disulfide, in the presence of a base, sodium hydride in DMF at 15 °C. The reaction proceeds *via* nucleophilic addition to generate a dithio acid anion, which, upon heating at 125–130 °C, undergoes aromatic nucleophilic substitution to yield 4-hydroxydithiocoumarin as illustrated in **Scheme 1**. Six different derivatives of 4-hydroxidithiocoumarin were prepared by following the same procedure, and the general procedure is described at the end of this chapter, **Scheme 22.**

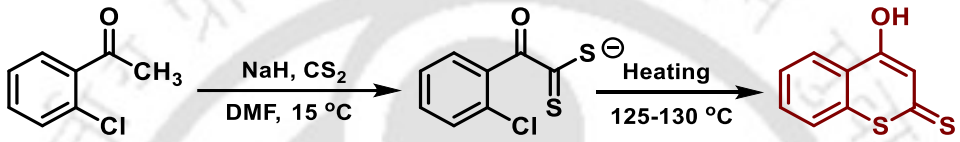

Scheme 1. Synthesis of 4-hydroxydithiocoumarin

In the same literature, they further demonstrated that 4-hydroxydithiocoumarin can be converted into 2-mercapto-1-thiochromone in the presence of HCl and acetic acid with H_2O_2, and that this transformation is reversible; 2-mercapto-1-thiochromone can be reconverted into 4-hydroxydithiocoumarin by dissolving it in a methanolic solution of NaOH followed by acidification with 5 M HCl, as shown in **Scheme 2**.

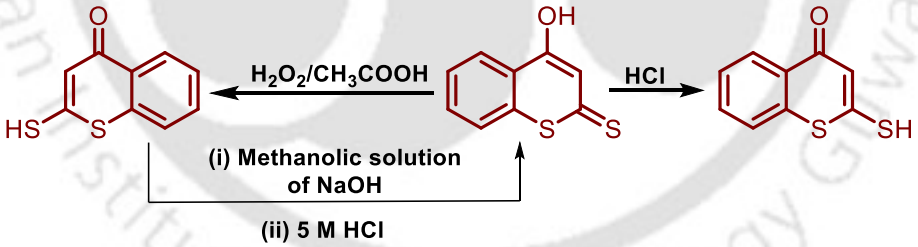

Scheme 2. The conversion of 4-hydroxydithiocoumarin to 2-mercapto-1-thiochromone

Continuing with the same article, they investigated the reactivity pattern of 4-hydroxydithiocoumarin by heating it with acetic anhydride, which afforded the *O*- and *S*-acylated products in a ratio of 2.2:1.0, respectively, as shown in **Scheme 3a**. When the same reaction was carried out with 2-mercapto-1-thiochromone, *O*- and *S*-acylated products were obtained in a 1:1 ratio, subsequently decomposing back to 4-hydroxydithiocoumarin, as shown in **Scheme 3b**. So far, they conclude from this observation that 4-hydroxydithiocoumarin is involved in the reaction, either through the oxygen or through the sulfur end.

Scheme. 3a

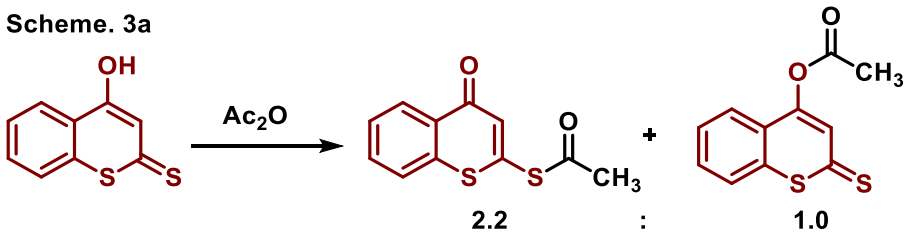

Scheme. 3b

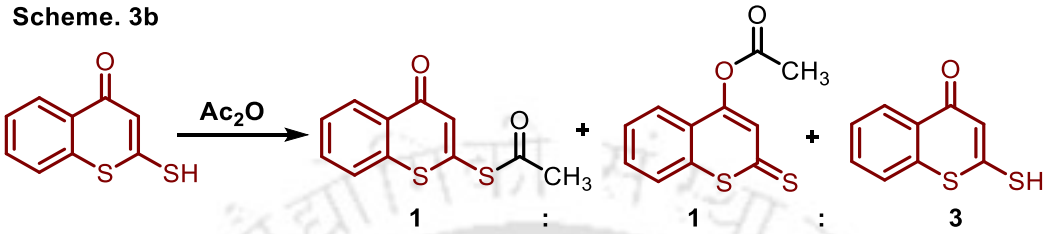

Scheme 3. (a) Reaction of 4-hydroxydithiocoumarin with (Ac_2O). (b) (2-mercapto-1-thiochromone) with Ac_2O

Notably, 4-hydroxydithiocoumarin exists in three possible resonating structures, each exposing a distinct nucleophilic reactive site. This structural feature enhances its reactivity, allowing transformations at three possible positions, as depicted in **Scheme 4**. Leveraging these reactive sites, numerous novel organosulfur compounds (OSCs) have been synthesised via various reactions and mechanisms, as discussed in detail in **Section 1.3**.

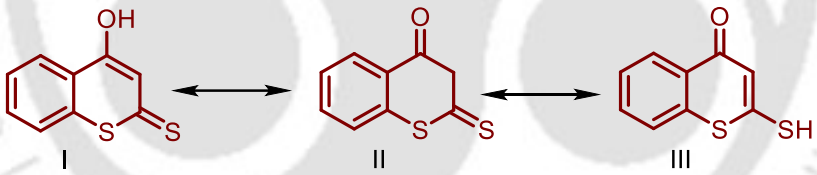

Scheme 4. Three resonating structures of 4-hydroxydithiocoumarin expose its reactive sites

Reactivity Modulation in 4-Hydroxydithiocoumarin: Exploring the Synthetic Potential of Its Ambident Nucleophilic Centres

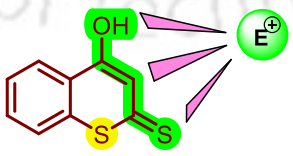

1.2 Exploration of the Reactivity of 4-hydroxydithiocoumarin

In most cases, the C3 and thiocarbonyl (C=S) centres of 4-hydroxydithiocoumarin actively participate in chemical transformations, whereas the hydroxyl group plays a secondary role without direct involvement in the reaction pathway. So far, only a single report has specifically described the direct participation of the 4-hydroxy position: the

O-acylation reaction reported by Anderson and McKay.[15] So accordingly, we have arranged the reactivity of 4-hydroxydithiocoumarin in two subclasses, depending upon the involvement of specific reactive centres, C3 and thiocarbonyl (C=S), as discussed in detail in sections **1.3.1** and **1.3.2**, respectively.

1.3.1 Reactivity of 4-Hydroxydithiocoumarin selectively at the C3 position: A Mechanistic Perspective

In 1991, Majumdar *et al.* first reported the regioselective cyclisation of 4-hydroxydithiocoumarins with propargyl bromide.[16] The motivation behind this protocol was to investigate the reactive site of 4-hydroxydithiocoumarin towards alkylation, whether it gives *O*-alkylation, *S*-alkylation or C3 alkylation product. Where they achieved two novel benzothiopyran derivatives:2-methyl-4*H*-thieno[2,3-*b*] benzothiopyran-4-one and thiopyrano [2,3-*b*]benzothiopyran-5(4*H*)-one, as represented in **Scheme 5**.

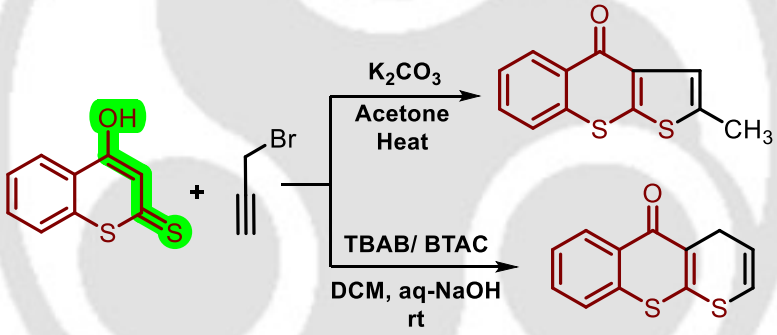

Scheme 5. Synthesis of two novel benzothiopyran derivatives: from 4-hydroxydithiocoumarin

Specifically, the study highlights a key difference in the reaction pathway depending on the conditions used. The classical alkylation at the C3 positions favoured the formation of 2-methyl-4*H*-thieno[2,3-*b*]benzothiopyran-4-one.

In contrast, the phase transfer catalysis conditions led to the formation of the distinct thiopyrano[2,3-*b*]benzothiopyran-5(4*H*)-one *via* [1,3*H*] shift in allenyl intermediate, and this intermediate is also generated by classical *S*-alkylation, followed by [3,3] sigmatropic shift as shown in **Scheme 6**.

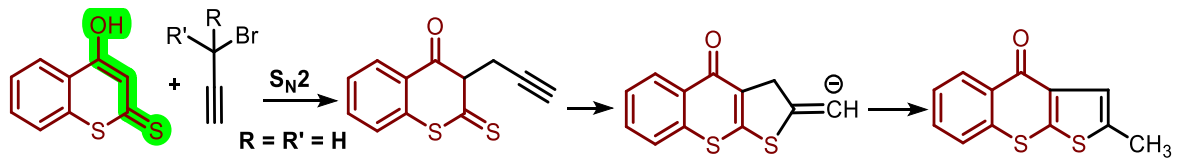

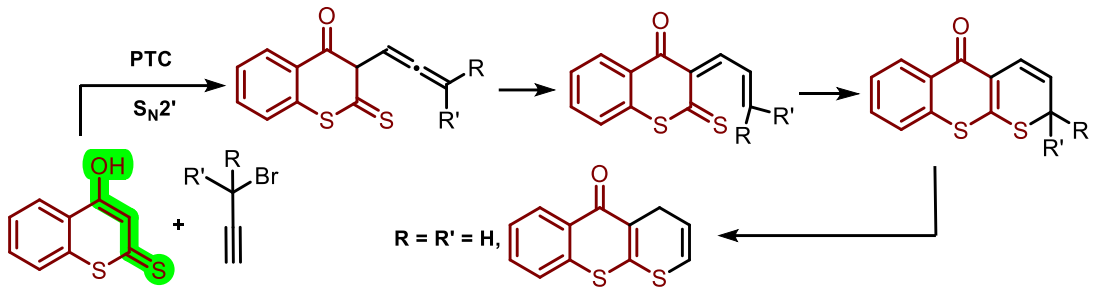

Scheme 6. The possible mechanistic pathway for the formation of products

Majumdar also reported the reaction of 4-hydroxydithiocoumarin with 2,3-dichloroalkyl-1-ene, where they obtained a cyclized product, and the formation is justified by the S_N2 mechanism *via* alkylation at the C3 position of 4-hydroxydithiocoumarin followed by cyclisation, [17] as shown in **Scheme 7**.

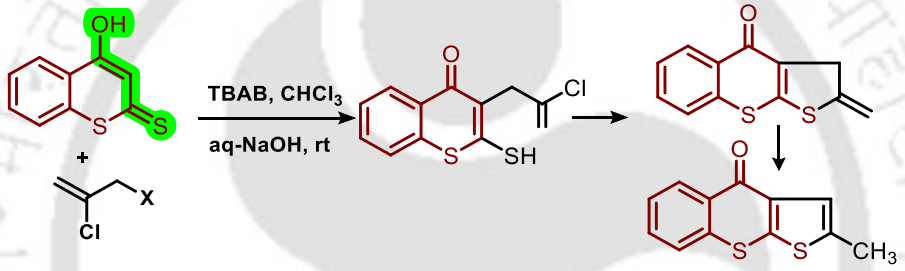

Scheme 7. Reaction of 4-hydroxydithiocoumarin with 2,3-dichloroalkyl-1-ene

In 2010, Moghaddam *et al*. developed a highly efficient and catalyst-free method for the synthesis of novel heteropoly cyclic compounds through a domino Knoevenagel-hetero-Diels-Alder reaction of *O*-acrylated salicylaldehyde with 4-hydroxydithiocoumarin in an aqueous medium.[18a] The salicylaldehyde derivative (bearing an *O*-acrylate) undergoes Knoevenagel condensation with **4**-hydroxydithiocoumarin at the C3 position, which generates an alkylidene (1,3-heterodiene) intermediate *in situ via* water removal. The resulting *in situ* generated hetero-diene then engages in an intramolecular hetero-Diels–Alder reaction with the alkene/dienophile (the *O*-acylated side chain) to forge the thiopyran ring, completing formation of the pentacyclic product as shown in **Scheme 8**. A similar investigation is also reported by Majumdar, who used *O*-propargyl salicylaldehyde in place of *O*-acrylated salicylaldehyde. [18b]

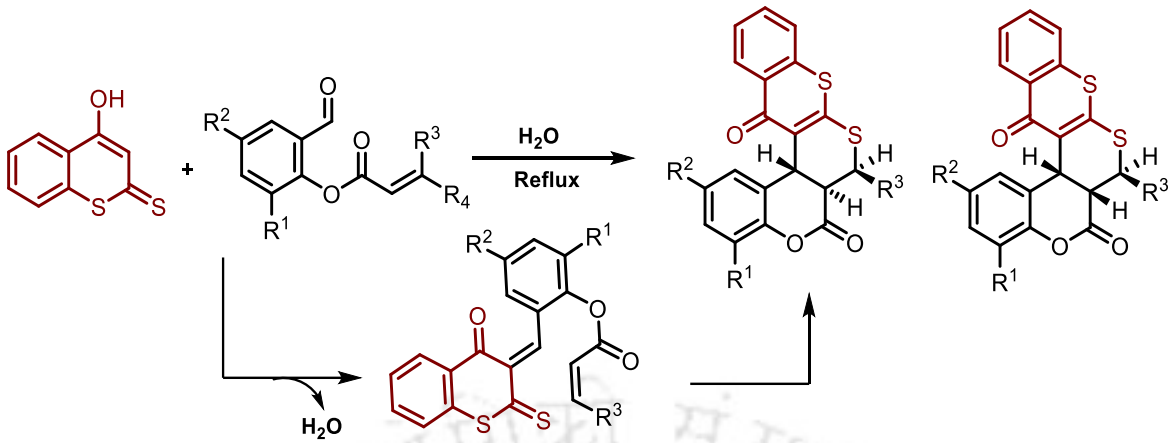

Scheme 8. Hetero Diels Alder reaction of 4-hydroxydithiocoumarin with *O*-acrylated salicylaldehyde

Consistently exploring the reactivity of 4-hydroxydithiocoumarin, Majumdar *et al.* established a three-component reaction for synthesising thiopyrano[2,3-*b*]thiochromene-3-carbonitrile derivatives.[19] This protocol utilised a multicomponent approach, condensing 4-hydroxydithiocoumarin, various aldehydes, and malononitrile in water at 100°C. This method offers a distinct, potentially more environmentally friendly route to synthesise functionalized thiopyrano compounds, diverging from the previously mentioned Sigmatropic rearrangement-based approach by using different reactants and reaction conditions. The reaction is initiated *via* Knoevenagel condensation between the arylaldehyde and malononitrile, which then undergoes Michael addition with 4-hydroxydithiocoumarin, selectively at the C3 position, followed by ring-closing S-alkylation, furnishing the desired product as shown in **Scheme 9**.

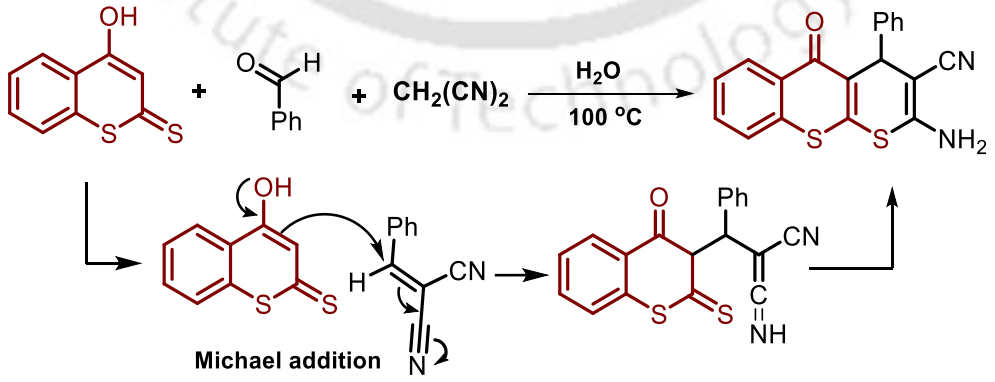

Scheme 9. Synthesis of thiopyrano[2,3-*b*]thiochromene-3-carbonitrile derivatives

To gain a deeper understanding of the reactivity behaviour of 4-hydroxydithiocoumarin, from 2012 to 2017, our research group extensively explored the reactivity of 4-hydroxydithiocoumarin using aryl aldehydes, secondary amines, thiophenols, and β-nitrostyrene. The synthesis of phenyl-thiopyrano derivatives was achieved *via* pseudo-three-component reaction. The organo-catalysis (L-Proline) directs the reaction through imine-controlled Knoevenagel/aldol–Michael followed by *S*-annulation to yield thiopyrano-bis(thiochromenes) [20] as shown in **Scheme 10**.

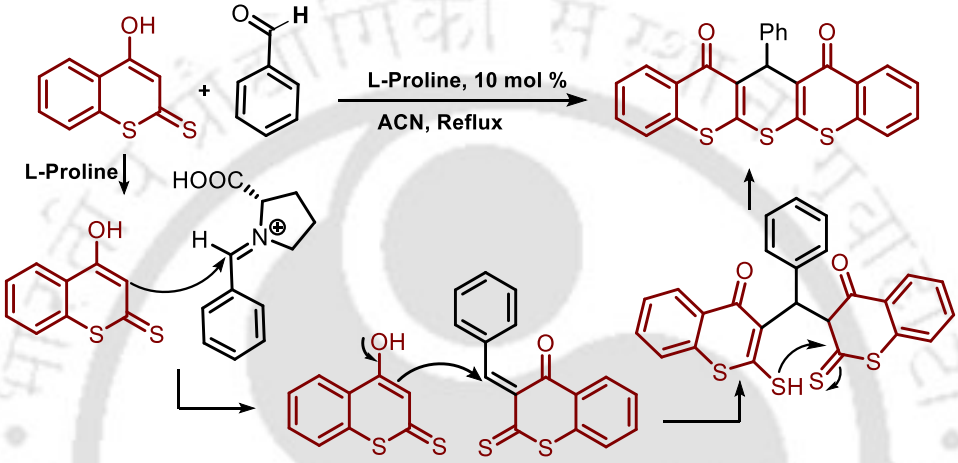

Scheme 10. Synthesis of penta-cyclic phenyl-thiopyrano derivatives from 4-hydroxydithiocoumarin

Similarly, the synthesis of phenyl-3,4-dihydro-2*H*,5*H*-thiochromeno[3,2-*e*][1,3]thiazin-5-one was achieved *via* pseudo-four-component reaction in the presence of amine/ammonium acetate and Lewis-acid catalysis $Yb(OTf)_3$. [21] In this case, also the reaction proceeds through the formation of a Knoevenagel intermediate at the C3 position of 4-hydroxydithiocoumarin, followed by concomitant regioselective hetero-Diels-Alder reactions to form the anticipated product, which is presented in **Scheme 11**.

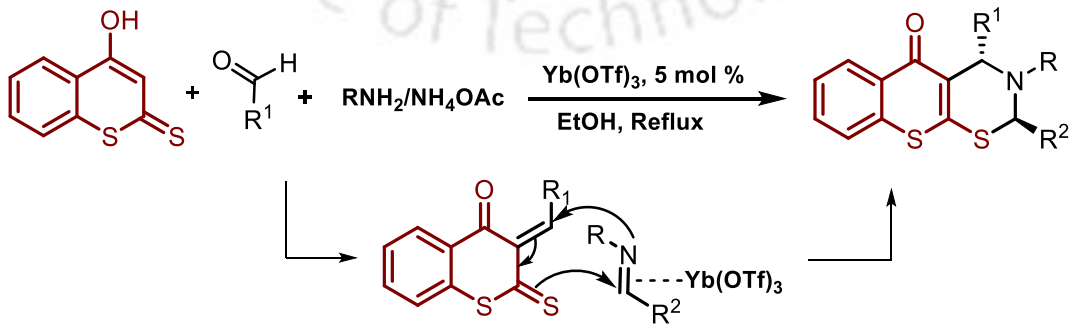

Scheme 11. Synthesis of phenyl-3,4-dihydro-2*H*,5*H*-thiochromeno[3,2-*e*][1,3]thiazin-5-one

In the year 2017, the reaction of 4-hydroxydithiocoumarin with β-nitrostyrene was investigated for the synthesis of oxime derivatives. The reaction proceeds *via* 1,4 Michael addition at the C3 position of 4-hydroxydithiocoumarin, followed by cyclization to form the final desired oxime derivatives, as shown in Scheme **12**.[22]

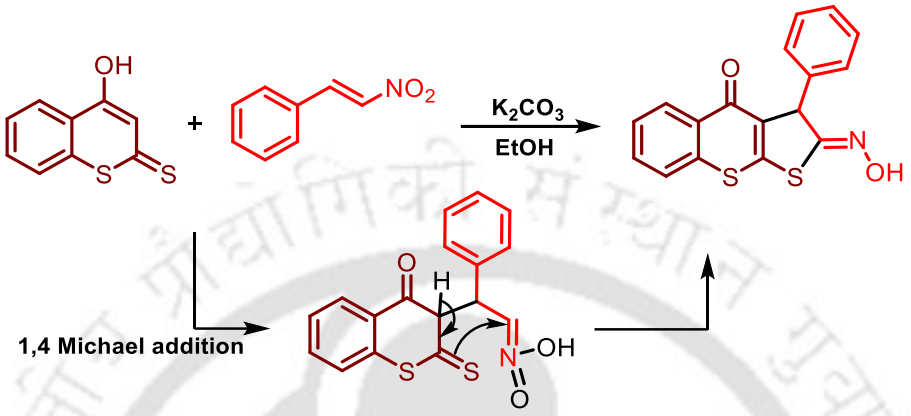

Scheme 12. Synthesis of oxime derivatives from 4-hydroxydithiocoumarin

In one of their investigations, Khan *et al.* made an interesting observation that 4-hydroxydithiocoumarin can also act as a sulfur donor. In the presence of CuO nanoparticles, 4-hydroxydithiocoumarin exhibits an unconventional sulfur transfer.[12] Here, in this case, the reaction initiates *via* activation of the C3 position of 4-hydroxydithiocoumarin to give a Knoevenagel intermediate, followed by the sulfur transfer from another unit of 4-hydroxydithiocoumarin to furnish the desired product, as shown in **Scheme 13.**

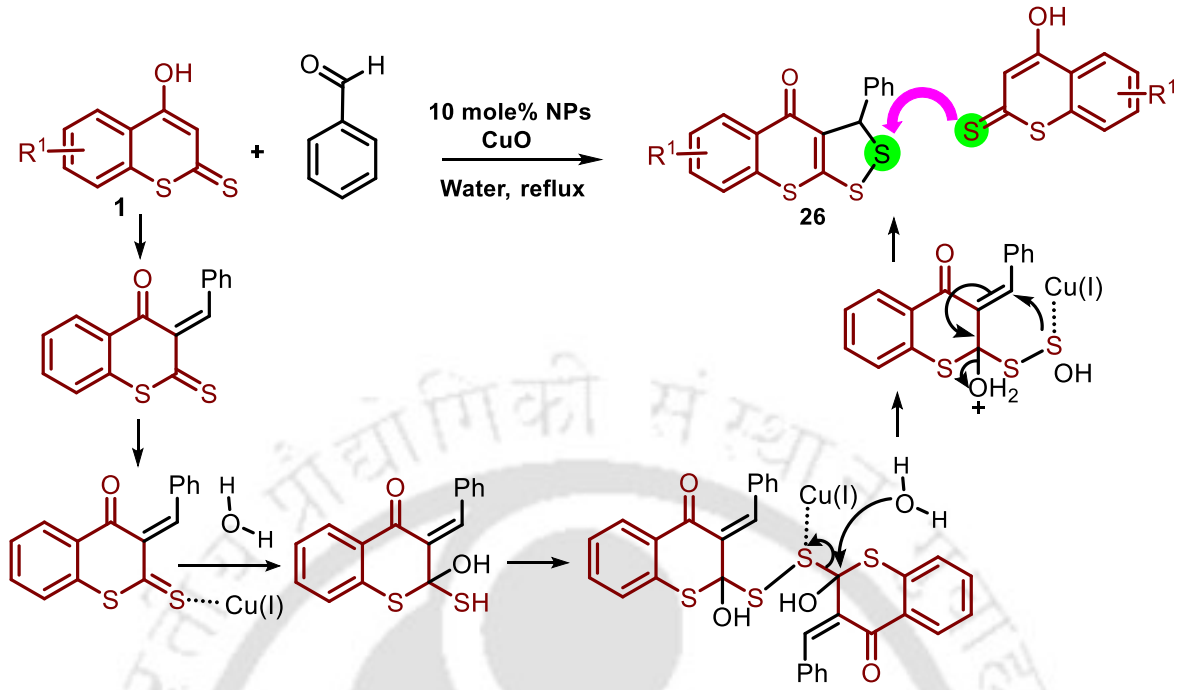

Scheme 13. Reaction of 4-hydroxydithiocoumarin with arylaldehyde for the synthesis of alkyl-dithiol-thiochromenones

The above-mentioned studies clearly emphasised that the C3 position of 4-hydroxydithiocoumarin is the major reactive site in organic transformations. This reactivity leads to the synthesis of diverse heterocyclic frameworks, including benzothiopyran, thiopyrano, thiochromene, and oxime derivatives. Even in sulfur-transfer processes, the reaction initiates through C3 activation, emphasising its central role. Collectively, these studies confirm that while the hydroxyl and thiocarbonyl groups influence the electronic environment, the C3 carbon remains the dominant site controlling the regioselectivity and structural diversity of the resulting products under such reaction conditions.

However, under certain other reaction conditions, the thiocarbonyl (C=S) is selectively involved in the organic transformation; a few examples are illustrated in Section **1.3.2**, along with the detailed mechanism.

1.3.2 Reactivity of 4-hydroxydithiocoumarin selectively at the thiocarbonyl (C=S) position: A Mechanistic Perspective

In the year 1992, Majumdar et al. synthesised 4-(aryloxymethyl)thiopyrano[2,3-*b*][1] benzothiopyran-5(2*H*)-ones by reacting 4-hydroxydithiocoumarin with 1-aryloxy-4-chloro-2-ynes *via* selective S-alkylation of 4-hydroxydithiocoumarin, followed by a classical S_N2 reaction mechanism.[23] Heating the isolated product in chlorobenzene gives a thiopyrano ring, and the transformation proceeds through an initial [3,3] sigmatropic rearrangement followed by a [1,5] proton shift, as shown in **Scheme 14**.

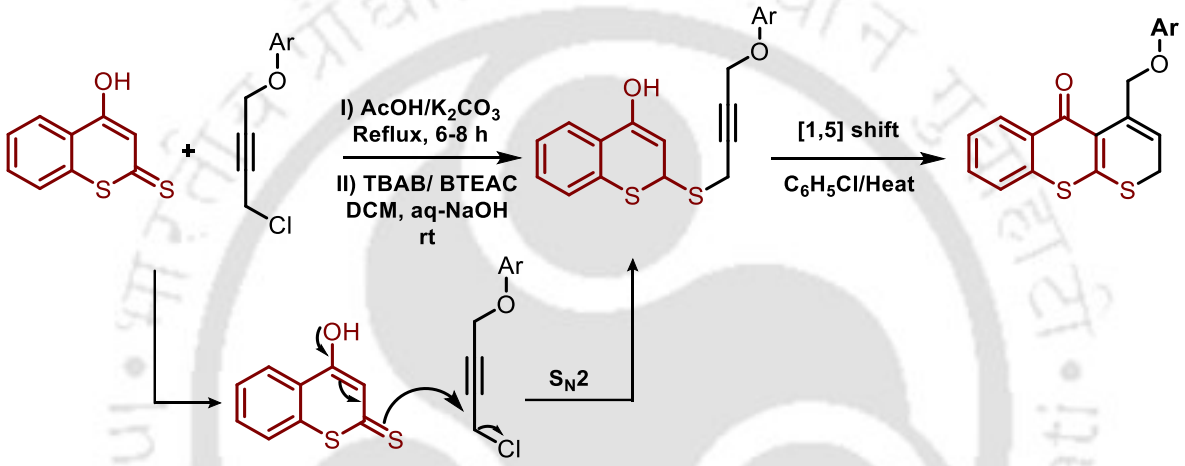

Scheme 14. Reaction of 4-hydroxydithiocoumarin with 1-aryloxy-4-chloro-2-yens

Majumdar *et al.* (2004) offered an easy access to the regioselective synthesis of 3-(aryloxyacetyl)-2,3-dihydrothieno[2,3-*b*][1]benzothiopyran-4-ones *via* tandem cyclization.[18] The authors reported that on subjecting 2-[4-aryloxybut-2-ynyl thio][1]benzothiopyran-4-one with *m*-chloroperoxybenzoic acid (*m*-CPBA) in chloroform at 0-5ºC, it furnished sulfoxide.

This transformation proceeds through an initial [2,3]-sigmatropic rearrangement of sulfoxides, followed by a subsequent [3,3]-sigmatropic rearrangement step to furnish 3-(aryloxyacetyl)-2,3-dihydrothieno[2,3-*b*][1]benzothiopyran-4-ones[24] as shown in **Scheme 7b.**

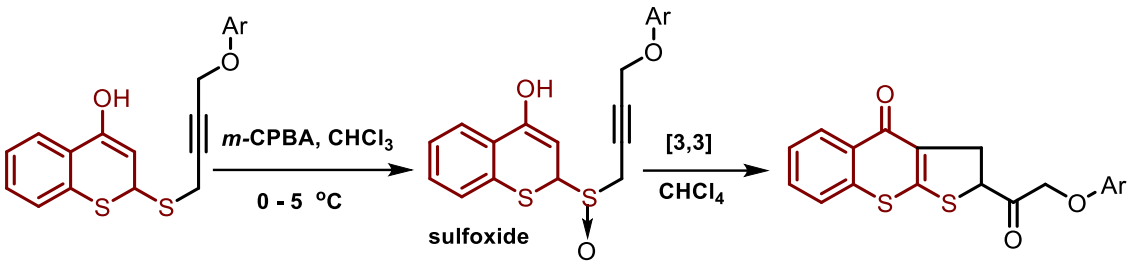

Scheme 17b. Synthesis of 3-(Aryloxyacetyl)-2,3-dihydrothieno[2,3-*b*][1]benzothiopyran-4-ones

Majumdar *et al.* investigated in 2002 a reaction between allylic halides and 4-hydroxydithiocoumarin under phase-transfer-catalysed conditions, in which they observed an S-alkylated product formed via a simple S_N2 mechanism (19, Scheme 15).

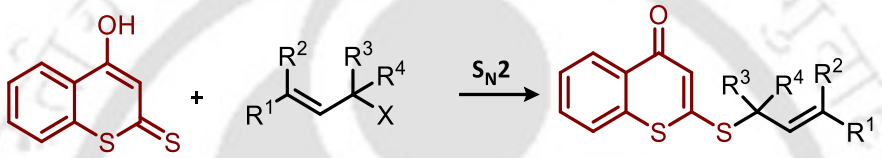

Scheme 15. Reaction of 4-hydroxydithiocoumarin with allylic halide

Karuna Mahato, in one of their research articles, elucidated the reactivity profile of 4-hydroxydithiocoumarin, demonstrating its ability to undergo oxidative cross-coupling reaction for the formation of S–C, S–S, and S–N bonds in the presence of iodine and *tert*-butyl hydrogen peroxide (TBHP) as shown in **Scheme 16**.[25] In this case they have selectively utilised the C=S bond of 4-hydroxydithicoumarin to synthesis various organosulfur derivatives. The reaction is initiated by the generation of a radical from TBHP, which converts the 4-hydroxydithiocoumarin into a radical species. This radical subsequently delocalizes to sulfur and reacts with molecular iodine to form an S-I bond. The formation of the S-I bond enhances sulfur's electrophilicity, thereby promoting cross-coupling reactions to furnish the corresponding C-S, C-N, and S-S coupled products selectively.

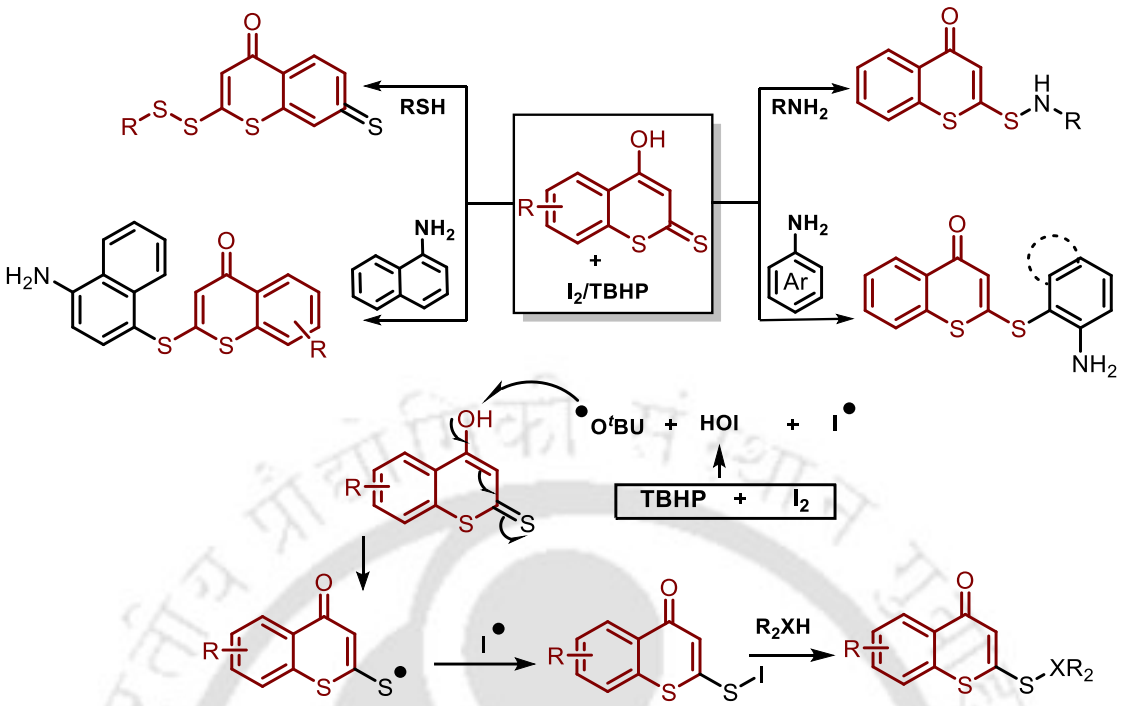

Scheme 16. Oxidative addition reaction of 4-hydroxydithiocoumarin in the presence of I_2/TBHP

From 2017 to 2021, our laboratory continuously investigated the reactivity of 4-hydroxydithiocoumarin, primarily focusing on developing novel sulfur-containing scaffolds and exploring their potential biological applications. In most cases, copper catalysts are used to selectively form S–C bonds, laying the foundation for a new methodology for diverse synthetic transformations. Building on this strategy, our research group further established a new method that enabled synthesising a novel series of indole derivatives, using DMSO as a solvent and in the presence of I_2 and CuBr, as shown in **Scheme 17**.[14] The reaction is initiated by the generation of a radical at the hydroxyl group of 4-hydroxydithiocoumarin, which subsequently delocalizes toward the C=S centre. The desired products are formed via the radical pathway described earlier in **Scheme 16**. The corresponding sulfone derivatives of the 4-hydroxydithiocoumarin–indole conjugates also exhibited significant biological activity against breast cancer cells.

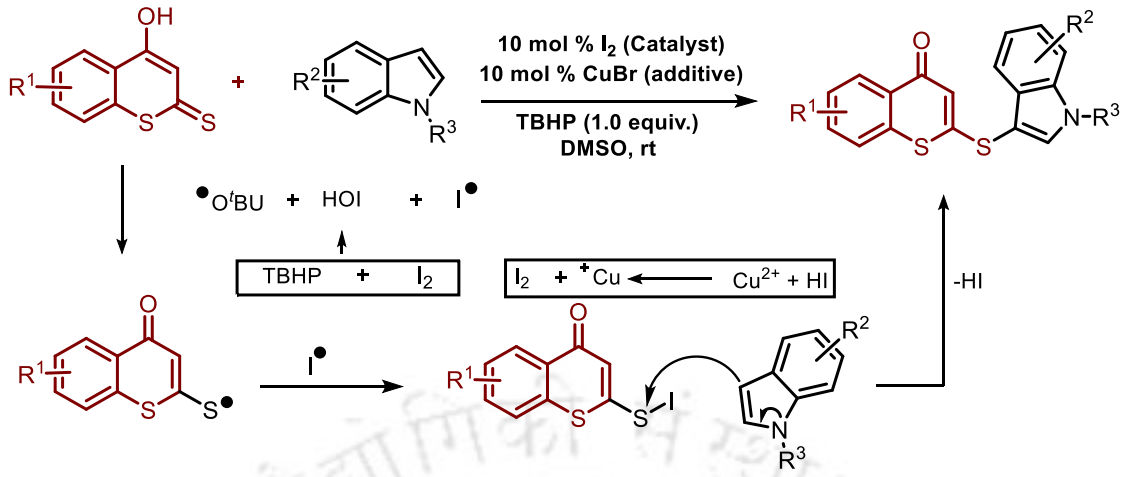

Scheme 17. Synthesis of 3-sulfenyindole derivatives from 4-hydroxydithiocoumarin

Expanding the scope of the work, Khan *et al*. reported the synthesis of α-thiocarbonyl derivatives through a cross-dehydrogenative coupling reaction between 4-hydroxydithiocoumarin and 1,3-dicarbonyl compounds, forming a C-S bond in the presence of KI and TBHP. [26] The reaction in this case also proceeds through a radical mechanism as described in Schemes **16 and 17**. This study highlighted the versatility of 4-hydroxydithiocoumarin in accessing structurally significant sulfur-based scaffolds, as shown in **Scheme 18**.

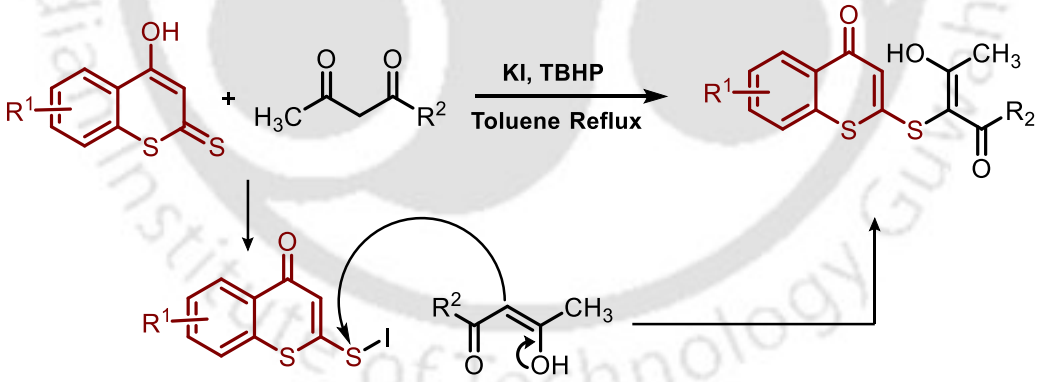

Scheme 18. Synthesis of α-thiocarbonyl derivatives from 4-hydroxydithiocoumarin

In another investigation, our group explored the reactivity of 4-hydroxydithiocoumarin with styrene and phenylacetylene under CuI catalysis for a hydrothiolation reaction, leading to the regioselective formation of Markovnikov products, specifically thioethers and vinyl sulfides.

The reaction is initiated by the formation of Copper (I)thiolate species, which undergo an insertion *syn*-addition reaction. This subsequently undergoes protonation, yielding

the final product, as shown in **Scheme 19**. These findings further broadened the synthetic utility of the scaffold toward valuable organosulfur compounds.[27]

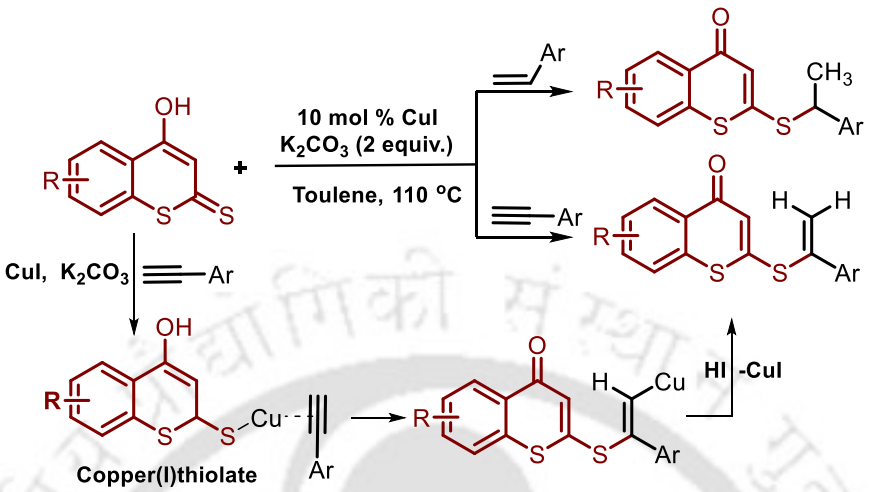

Scheme 19. Synthesis of thioethers and vinyl sulfides from 4-hydroxydithiocoumarin

Further extending the synthetic applications, our group has demonstrated the preparation of β-hydroxysulfides and β-aminosulfides by utilising 4-hydroxydithiocoumarin with epoxides and *N*-tosyl aziridines, respectively, as shown in **Scheme 20**. This approach also provided access to heterocyclic frameworks such as 2,3-dihydro-1,4-oxathiin and 2,3-dihydro-1,4-thiazine derivatives, showcasing the remarkable adaptability of 4-hydroxydithiocoumarin as a key building block in sulfur-based organic synthesis.[28] The ytterbium triflate activates the epoxy ring by accepting the lone pair, which facilitates the hydrothiolation reaction with 4-hydroxydithiocoumarin selectively at the position where the more stable carbocation can form. The resulting hydrothiolation products were further cyclized using CuI in DMF.

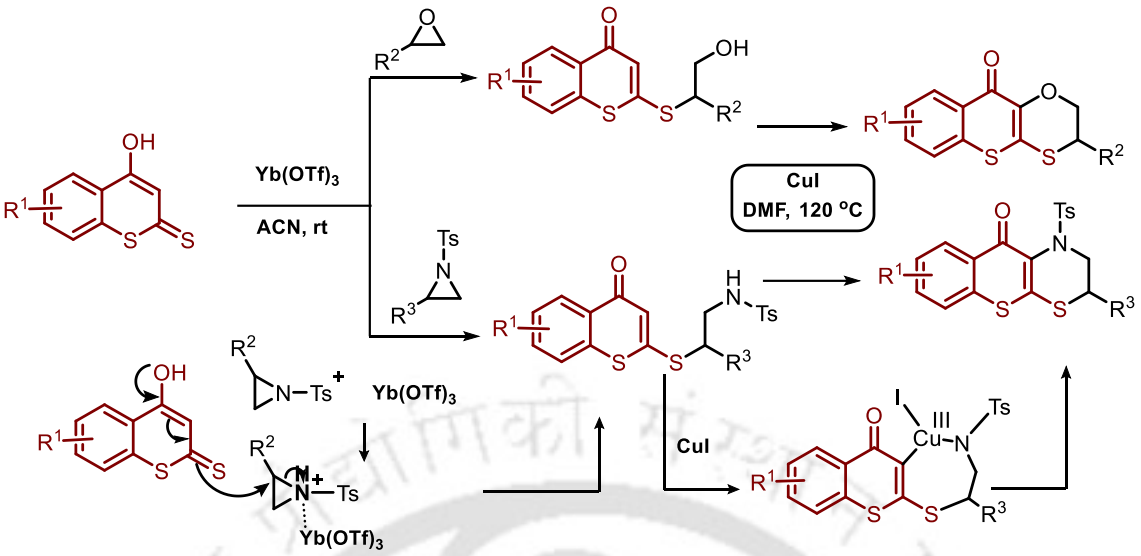

Scheme 20. Ring-opening reaction of epoxide/tosyl aziridines with 4-hydroxydithiocoumarin

Along this line, the synthesis of 1,4-oxathiin derivatives was achieved from 4-hydroxydithiocoumarin, aryl acetylenes, and DMSO in the presence of K_2CO_3 and CuI. The reaction proceeded *via* oxygenation at the C3 position of 4-hydroxydithiocoumarin, followed by cross-dehydrogenative coupling at the C=S position and finally cyclisation. Importantly, DMSO played a dual role, acting both as the solvent and as the oxygen donor, thereby facilitating the transformation, [13] as presented in **Scheme 21**. These oxathiine derivatives show potential antiproliferative activity against cancerous cells.

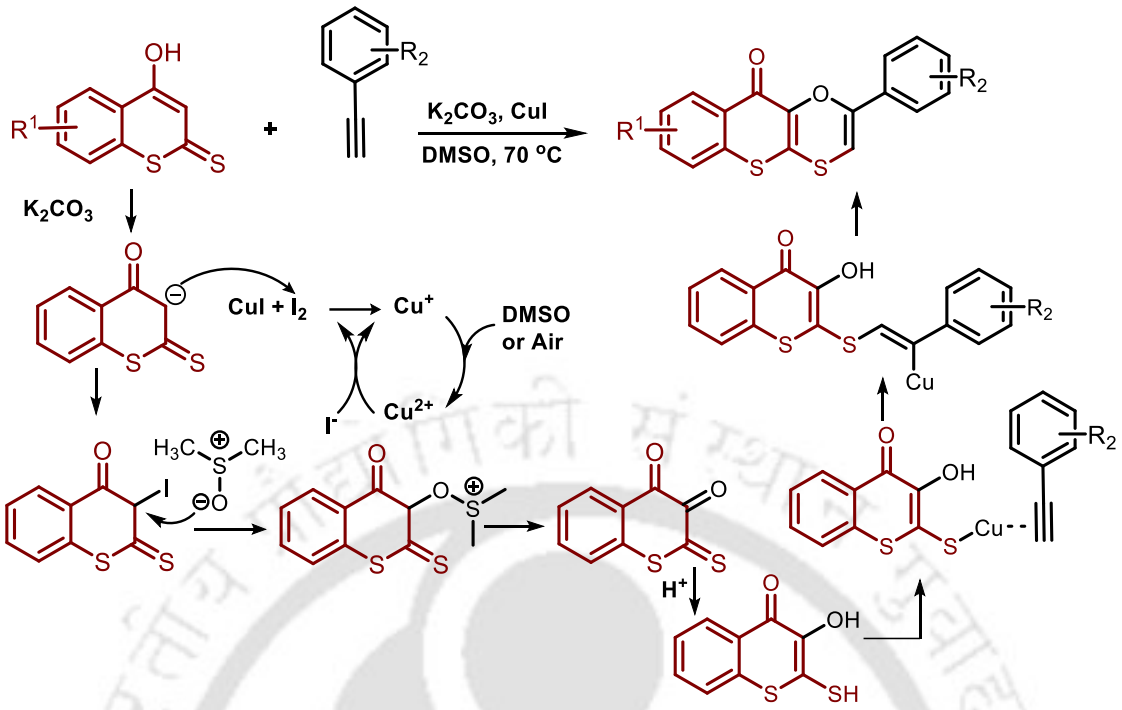

Scheme 21. Cross-dehydrogenative C-S coupling reaction of 4-hydroxydithiocoumarin.

Analysing the above-mentioned studies, we can emphasise that the thiocarbonyl (C=S) group of 4-hydroxydithiocoumarin also serves as the primary reactive site in sulfur-centred reactions. It shows high reactivity in S-alkylation, oxidative coupling, and radical reactions, especially when using halogens, peroxides, or metal catalysts (CuI). The selectivity at the sulfur atom may arise due to its high electron density and ability to stabilise radicals, leading to the formation of C–S, S–S, and S–N bonds. This makes 4-hydroxydithiocoumarin a versatile building block for the synthesis of sulfur-containing compounds.

In conclusion, we can infer that 4-hydroxydithiocoumarin has two main reactive sites: C3 and the thiocarbonyl (C=S) bond, and the reaction type depends on the conditions and reagents used. Earlier work highlighted the C3 carbon as the main reactive site, participating in Knoevenagel condensations, Michael additions, and cyclisation to build various heterocyclic structures. On the other hand, the thiocarbonyl (C=S) group plays a key role in S-alkylation, oxidative coupling, and radical reactions, especially in the presence of halogens, peroxides, or metal catalysts. Continuing these outlets in our thesis work, we have scrutinised 4-hydroxydithiocoumarin with cinnamaldehyde, vinyl ethers, isocyanide, arylaldehydes, and synthesised many novel sulfur-containing heterocycles *via* selective exploitation of the C3 position of 4-hydroxydithiocoumarin.

1.4 Inspiration behind my thesis work:

Collectively, these studies highlight the broad reactivity of 4-hydroxydithiocoumarin and establish it as a valuable synthetic precursor for the construction of sulfur-rich heterocycles and functional scaffolds with significant biological potential.

The introduction briefly outlined the inherent biological activities of 4-hydroxycoumarin derivatives. This biological activity is retained in a series of analogous 4-hydroxythiocoumarins and 4-hydroxydithiocoumarin derivatives, which piqued our interest in exploring the reactivity of 4-hydroxydithiocoumarin. Considering the three nucleophilic reactive sites of 4-hydroxydithiocoumarin, we accomplish two-component, cascade, pseudo-three-component, and pseudo-five-component reactions. Different electrophiles, such as unsaturated arylaldehyde, amphoteric nucleophile isocyanide, electron-rich olefin (vinyl ethers), arylaldehydes, and ammonium acetate, were used for the synthesis of novel organo-sulfur compounds. The thesis focuses primarily on developing new methodologies for constructing novel organosulfur frameworks using 4-hydroxydithiocoumarin as a key precursor.

1.5 General procedure for the synthesis of 4-hydroxydithiocoumarin derivatives:

For my thesis work, at the very beginning, 4-hydroxydithiocoumarin derivatives were synthesised in our lab by following the previously reported method.[15]

In a 100 mL round-bottomed flask, 2′-chloroacetophenone (15 mmol, 1.94 mL) was dissolved in DMF (10 mL). Sodium hydride (NaH in 60% oil dispersed) (45 mmol, 1.07 g) was added gradually with constant stirring, maintaining a temperature of 15-20 °C. Immediately after the addition of NaH, 30 mmol (1.81 mL) of CS_2 was introduced dropwise, and the reaction mixture was stirred for 2 hours at 15–20 °C. Excess sodium hydride was quenched with a few drops of methanol, after which the temperature was raised to 130 °C and stirring was continued for an additional two hours. After completion, the reaction mixture was then concentrated under reduced pressure using a rotary evaporator. Acetic acid (2 mL) was added, and the mixture was extracted with ethyl acetate and brine in a 1:8 ratio. The aqueous phase was separated and acidified with concentrated HCl, and the resulting precipitate was collected by filtration through a Büchner funnel. The solid was dried under vacuum at room temperature.

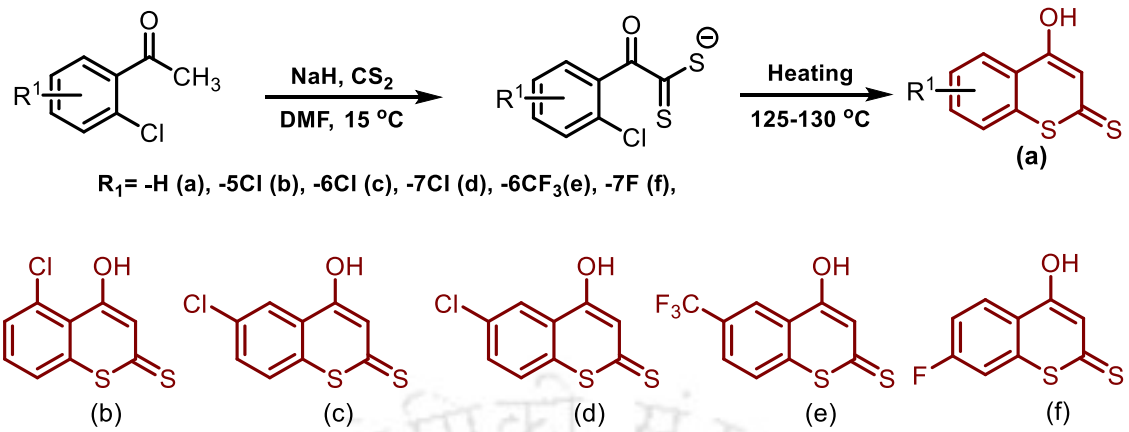

Scheme 22. Synthesis of 4-hydroxydithiocoumarin derivatives

1.6 General procedure for the synthesis of 4-hydroxythiocoumarin derivatives:

L. Costantino and his co-worker reported the synthesis of 4-Hydroxy-2H-chromene-2-thione using Potassium tertiary butoxide, 2'-hydroxyacetophenone, and carbon disulfide. [29] Later, Anjela Xalxo and Ujjwal Jyoti Goswami from our research group modified the existing scheme slightly to increase the yield by employing 30 mol% 18-crown-6 ether. We follow the modified version to synthesise the 4-Hydroxy-2*H*-chromene-2-thione derivatives.[30] In the beginning, potassium *tert*-butoxide (15 mmol) and 18-crown-6 ether (1.5 mmol) were taken in 7 mL of anhydrous THF in a pre-dried round-bottomed flask. The mixture is purged with N_2 and cooled to 0 °C in an ice bath. Then, 2-hydroxyacetophenone (5 mmol) is added dropwise to the above solution, followed by the addition of carbon disulfide (5 mmol), which forms a thick yellow precipitate. The reaction is stirred at 0-15 °C for 1 hour, then brought to room temperature and continued stirring for 16 h.The reaction was quenched by adding 5 mL of water, and then the aqueous layer was washed with ethyl acetate (2 × 5 mL). The aqueous layer was then acidified with 10% H_2SO_4 until the pH was adjusted to 4-5, and the mixture was stirred for an additional 16 hours. A yellow precipitate is formed, collected by vacuum filtration, and washed several times with petroleum ether to obtain the desired product, a yellow solid.

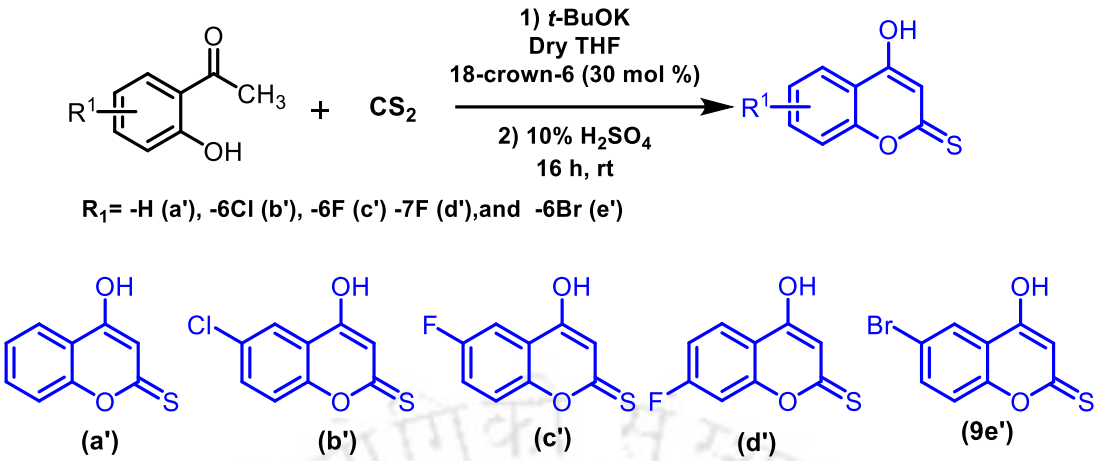

Scheme 23. Synthesis of 4-hydroxythiocoumarin derivative

References:

1. A. Kamyshny, *Cogent Arts Humanit.*, 2025, **12**, 2507988.
2. J. G. Wagenfeld, K. Al-Ali, S. Almheiri, A. F. Slavens and N. Calvet, *Waste Manag.*, 2019, **95**, 78-89.
3. A. G. R. Toledo, D. Bevilaqua, S. Panda, and A. Akcil, *Miner. Eng.*, 2023, **204**, 108409.
4. L. F. Lara, J. Medrano-Macías, F. Pérez-Labrada, E. Rivas-Martínez, E. García-Enciso, S. González-Morales, A. J. Maldonado, F. Rincón-Sánchez and A. Benavides-Mendoza, *Molecules*, 2019, **24**, 2282.
5. Melino, S. Sabelli, and R. Paci, M *Amino Acids* 2011, ***41*,** 103-112.
6. Antony, M. L. Singh, and S. V. Singh, *Indian J. Exp. Biol.*, 2011, ***49*,** 805-809.
7. Ohkubo, S. Dalla *Via*, L. Grancara, S. Kanamori, Y. García-Argáez, A. N. Canettieri, G. Arcari, P. Toninello, and A. Agostinelli, *Int. J. Oncol.*, 2018, ***53***, 1257-1268.
8. Fuentes, F. Paredes-González, and X. Kong, *Curr. Pharm. Rep.*, 2015, ***1***, 179-196.
9. J. L. Abernethy, *J. Chem. Educ.*, 1969, **46**, 561-563.
10. S. M. M. Nakayama, A. Morita, Y. Ikenaka, H. Mizukawa and M. Ishizuka. *J. Vet. Med. Sci.*, 2019, **81**, 298-313.
11. (a) L. Xue, R. K. Singla, S. He, S. Arrasate, H. González-Díaz, L. Miao and B. Shen, *Phytomedicine*, 2024, **128**, 155479. (b) B. Puri and A. Hall, *Phytochemical dictionary: a handbook of bioactive compounds from plants*, CRC Press, 1998. (c) Advances in Structure and Activity Relationship of Coumarin Derivatives, Santhosh Penta, 2015.
12. K. Mahato, S. Mondal, A. Ali, P. R. Bagdi, A. T. Khan, N. Arora and S. S. Ghosh, *New J. Chem.*, 2023, **47**, 1954-1961.
13. S. Mondal, S. Yashmin, R. Ali, R. Soundaram, S. S. Ghosh and A. T. Khan, *Org. Biomol. Chem.*, 2021, **19**, 5818-826.
14. S. Mondal, K. Mahato, N. Arora, D. Kankane, U. P. Singh, S. Ali, A. H. Khan, S. S. Ghosh and A. T. Khan, *Org. Biomol. Chem.*, 2020, **18**, 4104-4113.
15. J. E. Andersonmckay and A. J. Liepa, *Aust. J. Chem.*, 1987, **40**, 1179-1190.
16. K. C. Majumdar, A. T. Khan and S. Saha, *Synlett*, 1991, 595-596.

17. K. C. Majumdar and A. Bandyopadhyay, *Monatshefte, Fr Chem. Chem. Mon.*, 2004, **135**, 581-587.
18. (a) F. M. Moghaddam, M. Kiamehr, M. R. Khodabakhshi, Z. Mirjafary, S. Fathi and H. Saeidian, *Tetrahedron*, 2010, **66**, 8615–8622. (b) K. C. Majumdar, A. Taher, and S. Poran, *Synthesis*, 2010, **23**, 4043-4050.
19. K. C. Majumdar, S. Poran, and T. Ghosh, *RSC, Adv.*, 2012, **2**, 1144-1152.
20. K. Mahato, P. R. Bagdi and A. T. Khan, *Synthesis*, 2014, **25**, 2438-2441.
21. K. Mahato, P. R. Bagdi and A. T. Khan, *RSC Adv.*, 2015, ***5***, 48104-48111.
22. K. Mahato, P. R. Bagdi, A. T. Khan, *Org. Biomol. Chem.*, 2017, ***15***, 5625-5634.
23. K. C. Majumdar, A. T. Khan and S. Sana, *Synth. Commun.*, 1992, **22**, 901-912.
24. K. C. Majumdar, A. Bandyopadhyay, and S. K. Ghosh, *Synth. Commun.*, 2004, **34**, 2159-2167.
25. K. Mahato, N. Arora,P. R. Bagdi, R. Gattu, S. S. Ghosh and A. T. Khan, *Chem. Commun.*, 2018, ***54***, 1513-1516.
26. S. Mondal and A. T. Khan, Synthesis, 2022, **54**, 4521-4528
27. Mondal, S. Yashmin and A. T. Khan, *Org. Biomol. Chem.*, 2021,**19,** 9223-9230.
28. S. Mondal, S. Sarkar, S. S. Ghosh and A. T. Khan, *Eur. J. Org. Chem.*, 2022, **2022**, e202200355.
29. L. Costantino, A. D. Corso, G. Rastelli, J. M. Petrash and U. Mura, *Eur. J. Med. Chem*., 2001, **36**, 697.
30. A. Xalxo, U. J. Goswami, S. Sarkar, T. Kandasamy, K. Mehta, S. S. Ghosh, P. V. Bharatam and A. T. Khan, *Bioorg. Chem*., 2023, **141**, 106900.

Chapter II

Reactivity study of 4-hydroxydithiocoumarin with cinnamaldehyde derivatives: L-proline catalysed synthesis of 2-aryl-2*H*, 5*H*-thiopyrano[2,3-*b*] thiochromen-5-one's derivatives

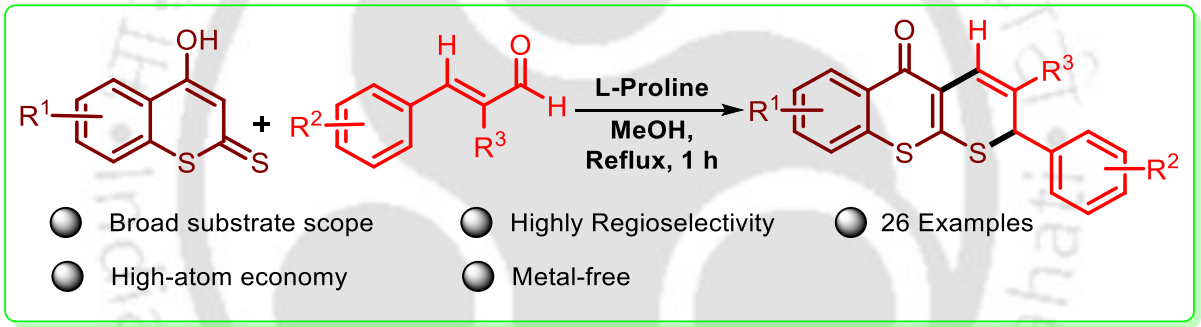

Org. Biomol. Chem. 2024, ***22****,1426–1433.*

2.0 Introduction:

Sulfur-containing heterocyclic compounds exhibit immense biological importance, and they also serve as a valuable precursor for drug design.[1a-c] Among the organosulfur compounds, thiochromone and thiopyran exhibit various biological activities,[2a-c] as the former is utilised in the synthesis of drugs in medicinal chemistry.[3] Considering the various biological activities of thiopyran derivatives, such as anti-inflammatory, anti-bacterial, anti-hyperplasia, anti-psychiatric, analgesic, and anti-cancer,[2a-b] the synthetic organic chemists have put forward efforts for developing new methodologies for the synthesis of different thiopyrano derivatives, and some of them are described in this chapter.

2.1 Synthesis of thiopyrano derivatives:

M. Minakawa *et al.* reported the synthesis of thiopyran derivatives from aromatic thiols and diols in the presence of 5 mol% $Sc(OTf)_3$ as a catalyst, as shown in **Scheme 1**.[4] The arylthiol provides thiyl radical through homolysis of a diaryldisulfide on heating. The thiyl radical interacts with the C=C of an allylic alcohol and forms a C-S bond, followed by dehydration. The $Sc(OTf)_3$-catalysed dehydrative cyclisations of aromatic thiols and diols provided the corresponding thiopyran derivatives, featuring the formation of C–C bonds.

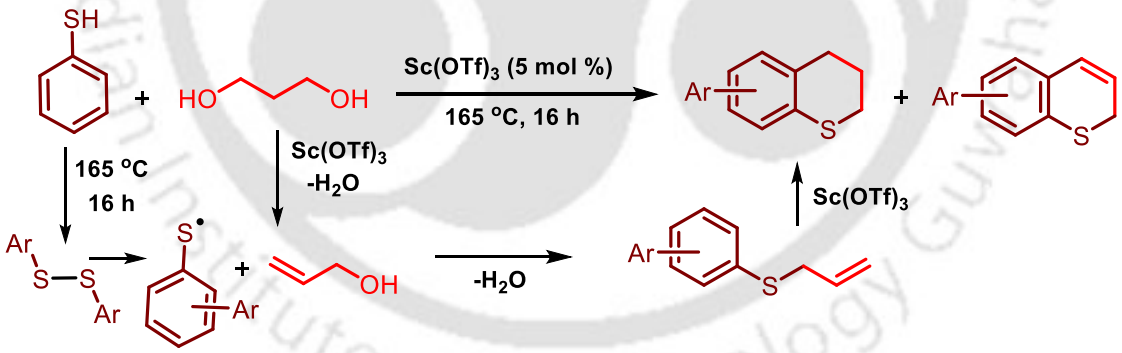

Scheme 1. Synthesis of thiopyran derivative from thiophenol and dioles

In 2006, Wang and Cordova synthesized chiral thiochromene derivatives by employing 2-mercapto benzaldehyde and cinnamaldehyde in the presence of a chiral organocatalyst and benzoic acid as an additive in toluene at room temperature, as depicted in **Scheme 2**. Initially, the chiral organocatalyst reacts with the aldehyde functionality of cinnamaldehyde to form an iminium intermediate, which undergoes a tandem Michael-aldol reaction addition with the nucleophilic thiophenol aldehyde, which subsequently undergoes a dehydration reaction to furnish the chiral thiochromene with good to high enantioselectivities.[5]

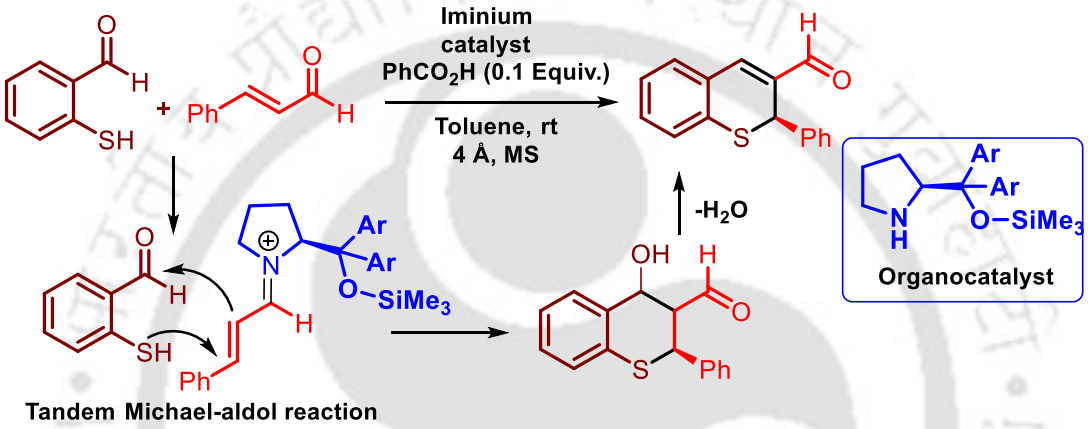

Scheme 2. Synthesis of chiral thiochromene derivatives *via* tandem Michael-aldol reaction

In the successive year, Giovanni Palmisano *et al.* achieved the synthesis of thiopyrano derivatives[6] using 4-hydroxy-2*H*-chromene-2-thione and α,β-unsaturated aldehyde in the presence of **Yb**(OTf)$_3$ as shown in **Scheme 3**. The reaction proceeds initially *via* the activation of an α,β-unsaturated aldehyde by Yb(OTf)3, followed by the formation of a Knoevenagel intermediate.

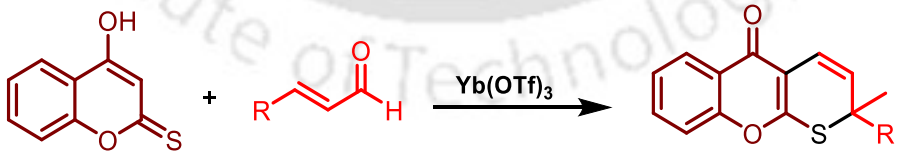

Scheme 3. Synthesis of thiochromene derivatives from 4-hydroxy-2*H*-chromene-2-thione

In 2016, Nicholas A. Ahlemeyer and Vladimir-B-Birman developed a reagent-free methodology for synthesising thiochromene derivatives using α,β-unsaturated thioesters in the presence of an acyl transfer catalyst (HBTM-2) as presented in **Scheme 4**. They observed that amidine-based catalysts, particularly homobenzotetramisole (HBTM-2)

and its analogs, provide thiochromene derivatives with high enantioselectivity and yields.[7]

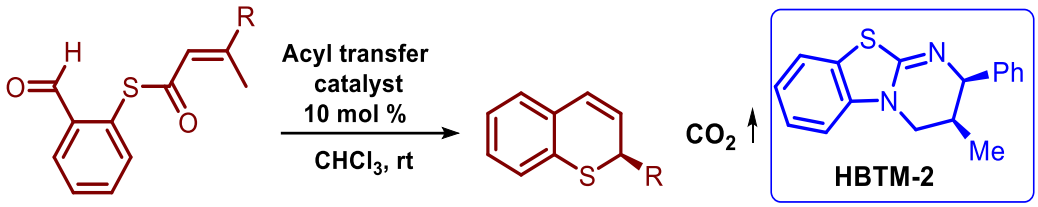

Scheme 4. Synthesis of chiral thiochromen derivatives *via* acyl transfer catalyst

Although the strategies mentioned above made significant progress in the synthesis of thiochromone and thiopyran heterocycles, they often relied on expensive or sensitive metal catalysts, non-recyclable reagents, and non-green solvents. Such limitations affect the cost, scalability, and overall sustainability of these reactions. In continuation of these studies, we developed a simple, environmentally friendly method for the synthesis of thiopyrano derivatives using 4-hydroxydithiocoumarin and cinnamaldehyde. The reaction was carried out in methanol with 20 mol% L-proline as the catalyst, providing an efficient and environmentally friendly alternative to metal-catalysed methods.

Our research group has demonstrated the usefulness of 4-hydroxydithiocoumarin as a key starting material for the synthesis of new molecules by exploring its reactivity with various reactants and conducting biological studies, which have been recently reviewed.[8] Earlier, we have noted that the reaction of 4-hydroxydithiocoumarin and aromatic aldehyde using 10 mol% L-Proline catalyst provided a pentacyclic molecule through the Knoevenagel reaction *via* a pseudo-three-component reaction. Whereas the reaction with *β*-nitrostyrene provides an unusual oxime product *via* a 1,4-Michael addition reaction, as discussed in Chapter I, **Schemes 10** and **12**, respectively.

The aim of the present study is to investigate whether the aldehyde group of cinnamaldehyde will behave similarly to aromatic aldehyde in the formation of a pentacyclic product. In addition, we intend to examine the reactivity of cinnamaldehyde and 4-hydroxydithiocoumarin, which is comparable to that of β-nitrostyrene. Interestingly, the reactivity of cinnamaldehyde differed from that of aromatic aldehydes and *β*-nitrostyrene. If the reaction pattern follows a 1,4 Michael addition, as seen in the case of β-nitrostyrene, then we may expect compound F. However, if it follows the case of an aromatic aldehyde, we expect compound **E,** which we didn't observe during our experiments, as shown in **Scheme 5**.

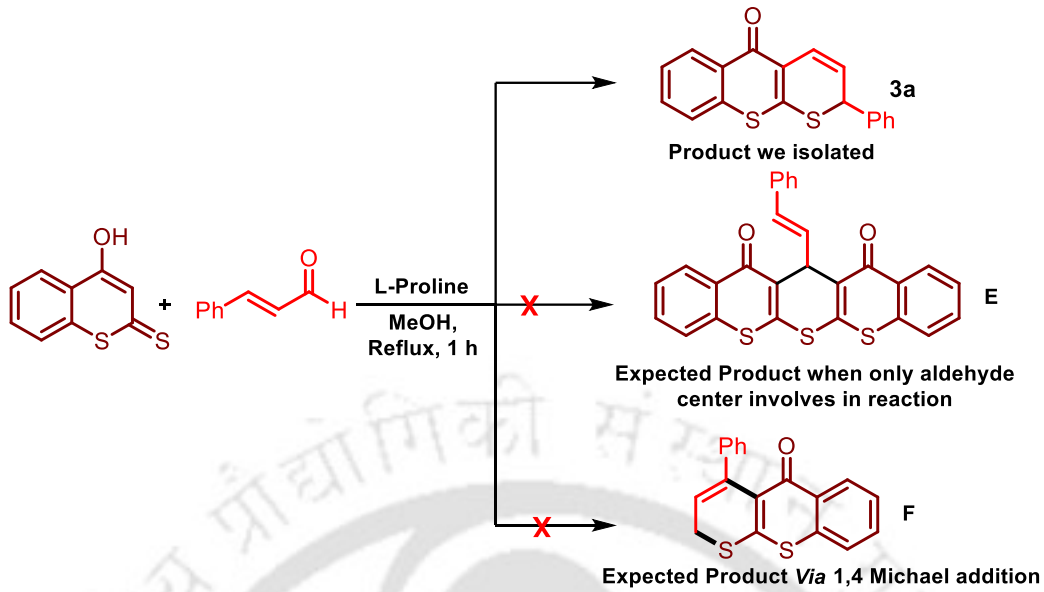

Scheme 5. Reaction of 4-hydroxydithiocoumain with cinnamaldehyde for the formation of different possible products.

As a result, a different kind of product formation was observed, which is elaborated in this chapter. Therefore, we investigated the reactivity pattern of 4-hydroxydithiocoumarin with α,β-unsaturated aldehydes using L-Proline as an organocatalyst. Because of its versatile catalytic properties, L-Proline has recently been used in various organic syntheses, particularly in MCRs,[11a,b] as an asymmetric catalyst in an aldol reaction,[12] and Mannich reaction,[13] with excellent enantioselectivity,[14a-c,] regioselectivity,[15] and chemoselectivity.[16]

2.3 Results and Discussion:

In this chapter, we discuss the synthesis of 2-aryl-2*H*,5*H*-thiopyrano[2,3-*b*] thiochromen-5-one's derivatives from 4-hydroxydithiocoumarins and cinnamaldehyde derivatives.

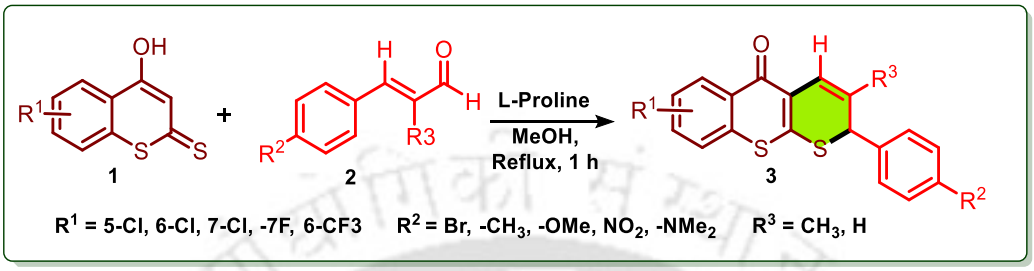

Scheme 6. (**a**) Reaction of 4-hydroxydithiocoumain with cinnamaldehydes

In the present study, various 4-hydroxydithiocoumarins were prepared following previously reported procedures, as shown in Chapter I, **Scheme 22**. We have chosen 4-hydroxydithiocoumarin (**1a**) and 4-methoxycinnamaldehyde (**2a**) as model substrates to optimise reaction conditions. Initially, a mixture of 0.20 mmol of 4-hydroxydithiocoumarin and 0.20 mmol of 4-methoxycinnamaldehyde was stirred at room temperature in methanol in the absence of catalysts (Table 1, entry 1). Then, the reaction mixture was continued by adding 5 mol% L-proline at room temperature, which yielded a product (**3a**) in 5% yield (**Table 1, entry 2**). To find favourable conditions, the catalyst loading was increased to 10 mol% while keeping the reaction at room temperature, and the yield increased from 5% to 20% (**Table 1, entry 3**). With the catalyst amount held constant, the reactions were examined at 50°C and under reflux. The yields were 32% and 50%, respectively (**Table 1, entries 4** and **5)**. Next, the catalyst loading was increased by 15-20%, and the yield was found to be maximum at 20 mol% catalyst under reflux conditions (**Table 1, entries 6** and **7**). Further increase in the amount of catalyst did not significantly affect the yield (**Table 1, entry 8**).To determine the suitability of alternative solvents, the reactions were examined in ethanol, water, and toluene. In the case of ethanol, which is a (polar protic solvent), it yields 59 % **(Table 1, entry 9)**. Whereas in the case of toluene (a nonpolar aprotic solvent), the reaction did not proceed at all **(Table 1, entry 11)**. The further increase in the amount of catalyst did not significantly affect the yield (**Table 1, entry 8**).

On the other hand, in water (a polar protic solvent), unfortunately, the reaction did not proceed at all **(Table 1, entry 10)**. To examine the efficacy of other catalysts, two reactions were carried out with 2,6-pyridine dicarboxylic *and p*-TSA under identical reaction conditions, and their results are shown in Table 1, entries 12 and 13**.**

The product **(3a)** is characterised using various spectroscopic techniques, including 1H and 13C NMR and HRMS. In the ^{1}H NMR spectrum, the product 3a exhibited a characteristic peak at δ 3.78 for three protons as a singlet for the methoxy group, and also for the C3 proton of 4-hydroxydithiocoumarin, which usually appears as a singlet at δ 7.2, vanished. This indicates that 4-methoxycinnamaldehyde has been incorporated into the final product. Furthermore, one doublet of doublet appeared at δ 4.92 (dd, J_2 = 5.5, J_1 = 1.5 Hz, 1H), for one proton of the C2 position. Another doublet of doublet appeared at δ 5.97 (dd, J_1= 5.5 Hz and J_2= 10.3 Hz, 1H) for one proton of the C3 position of the desired product **3a**. In addition to the ^{1}H NMR spectrum, the ^{13}C NMR spectrum was also recorded, which showed two signals in the aliphatic region at δ 43.8 and 55.5, corresponding to the C2 carbon and the methoxy carbon, respectively. In the aromatic region, fifteen signals were observed, among which two peaks appeared at δ 175.2 and 159.8, attributable to the carbonyl carbon (C5) and the aromatic carbon directly attached to the methoxy group, respectively. These observations further confirm the incorporation of 4-methoxycinnamaldehyde into the final product. The HRMS value 399.0521 $[M+H]^+$, which agrees with the product **3a**. ^{1}H, ^{13}C spectra and HRMS data of compound **3a** can be seen in **Figure 2.7-2.9**. To ascertain the structure of the product formation, the structure of one of the desired products, **3e**, was further confirmed by the single-XRD, having CCDC 2311036, as depicted in **Figure 2.6.** After optimising the reaction conditions, a series of cinnamaldehyde derivatives was explored to evaluate the substrate scope (Table 2). Initially, various derivatives of 4-hydroxydithiocoumarin were treated with 4-methoxycinnamaldehyde and 2-methoxycinnamaldehyde, yielding yields ranging from 80% to 92% (**3a-3i)**.

Next, (*E*)-3-(2-bromophenyl)acrylaldehyde/(*E*)-3-(4-bromophenyl)acrylaldehyde were scrutinised with 4-hydroxydithiocoumarin derivatives, and we also obtained higher yields (80-88%) (**3j-3s)**.

Table 1. Optimization Table of the reaction conditions.[a,b]

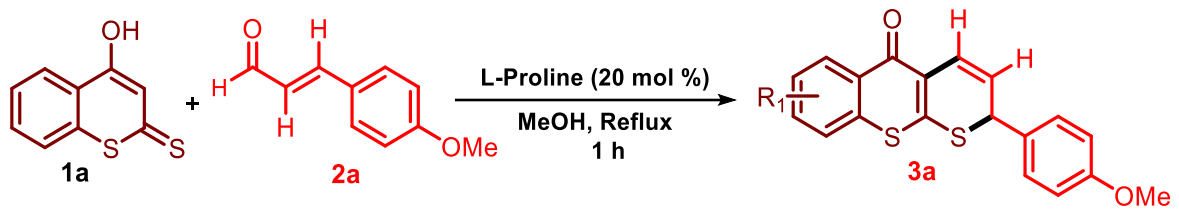

Entry	Catalyst	(Mol%)	Temp (°C)	Time (h)	Solvent	Yield (%)[b]
1	Nil	0	RT→Reflux	1	Methanol	0
2	L-Proline	5%	RT	1	Methanol	5
3	L-Proline	10%	RT	1	Methanol	20
4	L-Proline	10%	50	1	Methanol	32
5	L-Proline	10%	Reflux	1	Methanol	50
6	L-Proline	15%	Reflux	1	Methanol	73
7	**L-Proline**	**20%**	**Reflux**	**1**	**Methanol**	**92**
8	L-Proline	30%	Reflux	1	Methanol	87
9	L-Proline	20%	Reflux	1	Ethanol	59
10	L-Proline	20%	Reflux	1	Water	NR
11	L-Proline	20%	Reflux	1	Toluene	NR
12	2,6-PDA	20 %	Reflux	1	Methanol	69
13	*p*-TSA	20%	Reflux	1	Methanol	Trace

[a]All the reactions were carried out using 4-hydroxydithiocoumarin (1a, 0.2 mmol), cinnamaldehyde (2a, 0.2 mmol). bIsolated yield. RT: Room Temperature. NR: No reaction PDA: 2,6-Pyridinedi- carboxylic acid

Table 2. Substrate scope.[a,b]

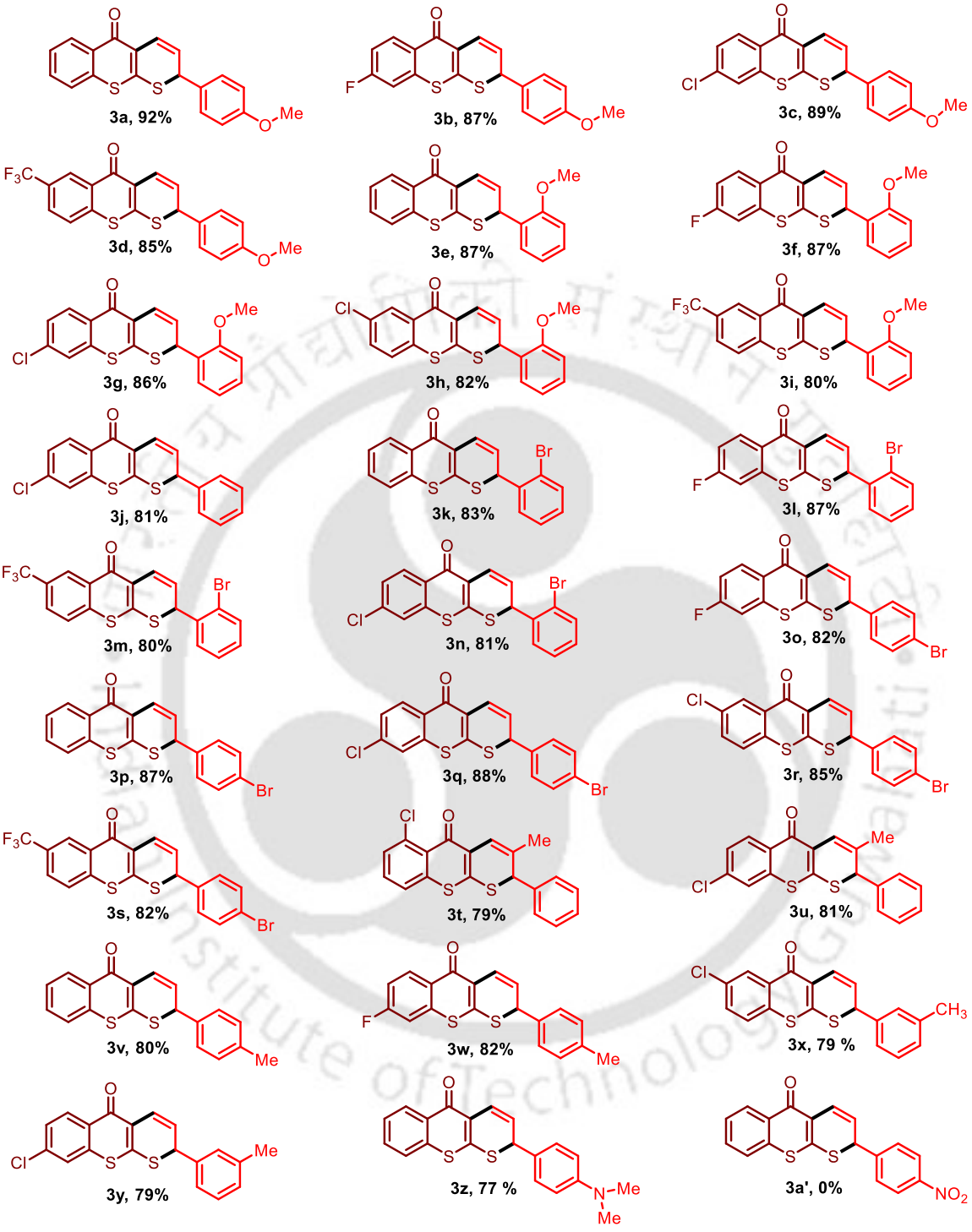

[a]All the reactions were carried out using 4-hydroxydithiocoumarin (1, 0.2 mmol), cinnamaldehyde (2, 0.2 mmol) in the presence of 20 mol% catalyst, 1 mL of methanol Solvent at reflux temperature. [b]Isolated yields.

Motivated by these results, we carried out additional reactions under the same optimized conditions, where we reacted (E)-2-methyl-3-phenylacrylaldehyde and 4-hydroxydithiocoumarin derivatives, which also yielded a good yield (79-80%) (**3t-3u).** Another reaction was carried out between *(E)*-3-(*m*-tolyl)acrylaldehyde/*(E)*-3-(*p*-tolyl)acrylaldehyde with 4-hydroxydithiocoumarin derivatives, which also gives a fairly good yield (79-82%) (**3v-3y)**. Finally, we performed the reaction of 4-hydroxydithiocoumarin with 4-dimethylaminocinnamaldehyde and 4-nitrocinnamaldehyde/2-nitrocinnamaldehyde. In the formal case, we obtained the product with 77% yield (**3z**), whereas no product was obtained with nitro cinnamaldehyde.

From the above observation, we can conclude that the 4-hydroxydithiocoumarin derivatives show excellent reactivity towards cinnamaldehyde, particularly those with electron-donating substituents on the aryl moiety. On the other hand, 4-hydroxydithiocoumarin does not react with cinnamaldehyde, which possesses an electron-withdrawing group, as in the case of 4-nitrocinnamaldehyde.

2.3 The possible reaction mechanism

The plausible reaction mechanism proposed for this reaction is based on a literature survey,[7] intermediates, and isolated products, as shown in **Scheme 8**. As we know, amino acids always exist in zwitterionic form, where they carry a negative charge on the carboxylic group by losing one proton and a positive charge on the amine group by gaining one proton. Here, in the proposed mechanism, L-Proline abstracts the acidic proton of 4-hydroxydithiocoumarin, resulting in the formation of intermediate **1b.** In a basic medium, 4-hydroxydithiocoumarin exists in three tautomeric forms as shown in **Scheme 9**. Here, the reaction may proceed via two possible mechanisms, **I** or **II**. Pathway **I,** where cinnamaldehyde reacts with L-Proline to give an intermediate iminium ion **A,** which was detected in HRMS. Pathway **II** follows the thia-Michael addition reaction, where 4-hydroxydithiocoumarin **1b** undergoes a 1,4-addition reaction with cinnamaldehyde **2** to give rise to the product **E,** but no such product was obtained

during the experiment. Therefore, we conclude that the reaction proceeds via pathway I *via* the iminium ion. Where the two intermediates **A** and **1b** react and give a Knoevenagel product intermediate **C** *via* intermediate **B** (Mannich intermediate) and release L-Proline. Ultimately, the intermediate C undergoes an electrocyclic ring-closing reaction to yield **3** as the desired product.

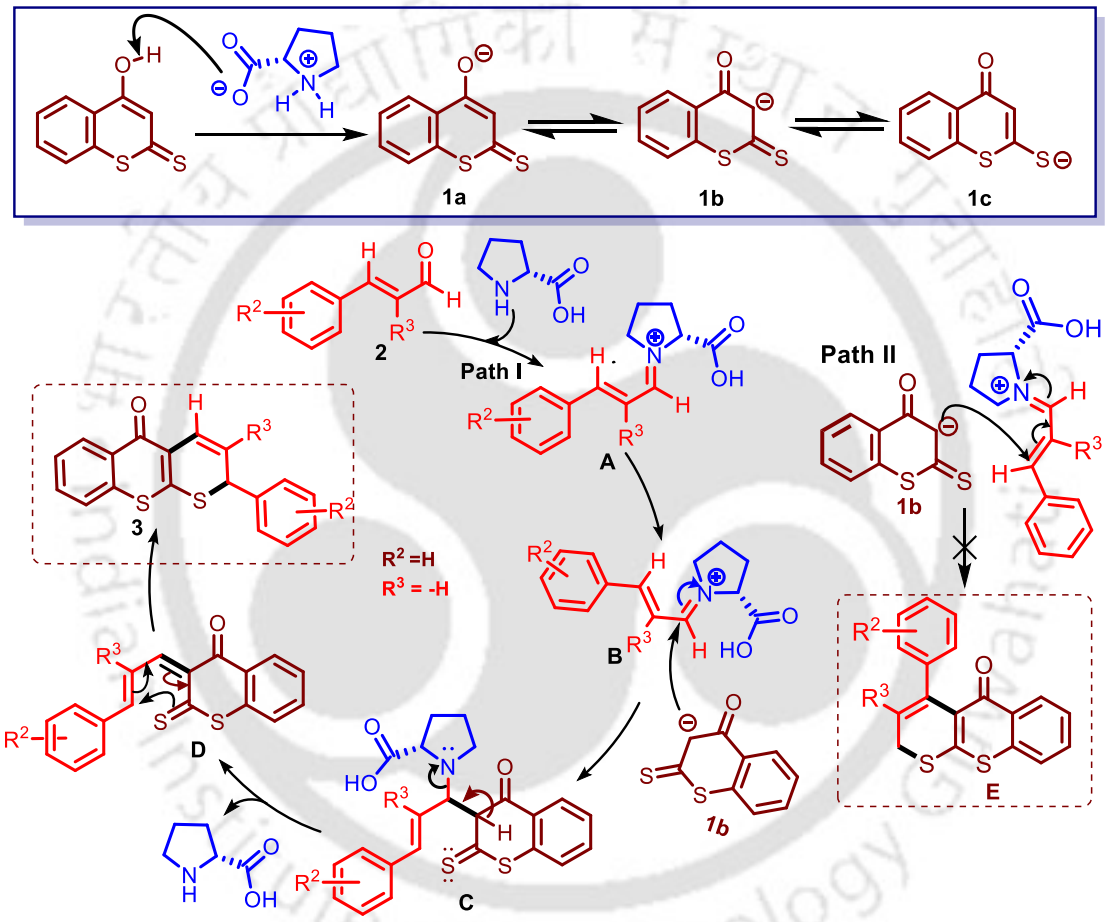

Scheme 8. Reaction mechanism for the formation of thiopyrano derivatives

Conclusions

We developed a practicable method for the synthesis of 2-aryl-2*H*,5*H*-thiopyrano[2,3-*b*]thiochromen-5-one derivatives using 4-hydroxydithiocoumarin and cinnamaldehyde in the presence of L-Proline in methanol under reflux conditions. Notably, it is observed that the reactivity of α-β-unsaturated aldehyde is different from aromatic aldehyde as well as β-nitrostyrene. The features, including good atom economy, the use of a green catalyst (L-Proline), mild reaction conditions, and reduced time consumption, make it very practical. The present method proceeds *via* the Mannich reaction, followed by annulation and electrocyclic ring closure.

2.4 Experimental Section

A general procedure for the synthesis of 2-phenyl-2*H*,5*H*-thiopyrano[2,3-*b*]thiochromen-5-one derivatives (3)

A mixture of 4-hydroxydithiocoumarin **1** (0.39 g, 0.20 mmol) and cinnamaldehyde **2** (25 µL, 0.20 mmol) was taken in 1 mL of methanol in a 10 mL two-neck round-bottomed flask. Subsequently, the organocatalyst L-proline (4.6 mg, 0.02 mmol) was added to the reaction mixture. The flask was then fitted with a reflux condenser and placed in a preheated oil bath at 80 °C with constant stirring. The reaction was completed after 1 h, as monitored by TLC. Methanol was then removed under reduced pressure using a rotary evaporator, and the crude residue was extracted with ethyl acetate (2 × 10 mL) and washed with water (2 × 5 mL). Then, the organic layer was dried over anhydrous sodium sulfate (Na_2SO_4). Finally, the organic layer is concentrated in a rotatory evaporator, and the crude residue is purified through silica gel column chromatography (mesh 60-120). The desired product was eluted with an ethyl acetate/hexane mixture (1:9). A similar procedure was followed in all other cases. The optical rotation was found to be zero, so chiral HPLC was not done to isolate the products.

2.5 Characterization

(S)-2-(4-Methoxyphenyl)-2*H*,5*H*-thiopyrano[2,3-*b*]thiochromen-5-one (3a). A

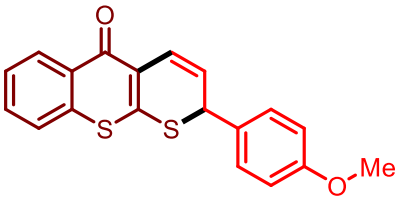

light-yellow solid (62 mg, 92 %) mp 104-105 ºC; ^{1}H NMR (500 MHz, $CDCl_3$) δ 8.52 (dd, *J* = 8.0, 1.4 Hz, 1H), 7.53 (td, *J* = 7.6, 1.6 Hz, 1H), 7.49 (dd, *J* = 8.0, 1.2 Hz, 1H), 7.43 – 7.41 (m, 1H), 7.31 – 7.27 (m, 3H), 6.87 – 6.83 (m, 2H), 5.97 (dd, *J* = 10.3, 5.5 Hz, 1H), 4.92 (dd, *J* = 5.5, 1.5 Hz, 1H), 3.78 (s, 3H). ^{13}C NMR (125 MHz,$CDCl_3$-*d*) δ 175.2, 159.8, 145.9, 136.3, 131.6, 131.4, 129.6, 129.2 (2C), 127.7, 125.8, 125.4, 124.0, 121.8, 114.4 (2C), 55.4, 43.8. IR(KBr)ν_{max}/cm^{1}, 2925 (C–H), 1603 (C=O), HRMS (ESI):m/z $[M+H]^+$ calcd for $C_{19}H_{14}O_2S_2$ 399.0508 $[M+H]^+$; found 399.0521

(S)-8-Fluoro-2-(4-methoxyphenyl)-2*H*,5*H*-thiopyrano[2,3-*b*]thiochromen-5-one

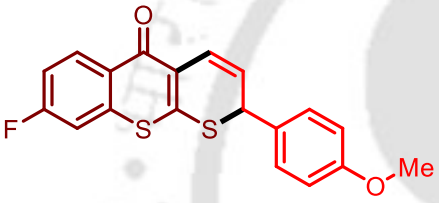

(3b). An orange solid (61 mg, 87 %) mp 175 ºC; ^{1}H NMR (500 MHz, $CDCl_3$) δ 8.53 (dd, *J* = 8.6, 6.1 Hz, 1H), 7.30 – 7.26 (m, 3H), 7.19 (td, *J* = 8.1, 2.1 Hz, 1H), 7.13 – 7.10 (m, 1H), 6.85 (d, *J* = 8.1 Hz, 2H), 5.97 (dd, *J* = 10.6, 5.9 Hz, 1H), 4.92 (d, *J* = 5.7 Hz, 1H), 3.78 (s, 3H). ^{13}C NMR (125 MHz, $CDCl_3$) δ 174.3, 163.9(d, *J* = 254.7 Hz), 159.8, 145.4, 138.3 (d, *J* = 9.5 Hz), 132.6 (d, *J* = 9.7 Hz), 131.4, 129.2, 127.9 (d, *J* = 2.3 Hz), 125.8, 123.8, 121.9, 116.2 (d, *J* = 22 Hz) 114.4, 111.4 (d, *J* = 24 Hz) 55.4, 43.9. IR(KBr)ν_{max}/cm^{1}, 2923 (C-H), 1608 (C=O), HRMS (ESI) calcd for $C_{19}H_{13}FO_2S_2$; 357.0414 $[M+H]^+$; found 357.0414.

(S)-8-Chloro-2-(4-Methoxyphenyl)-2*H*,5*H*-thiopyrano[2,3-*b*]thiochromen-5-one

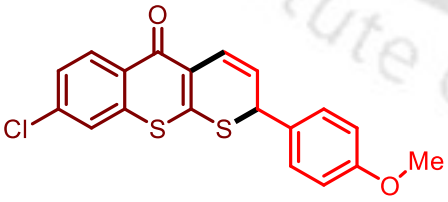

(3c). A light-yellow solid (66 mg, 89 %) mp 174 ºC; ^{1}H NMR (400 MHz, $CDCl_3$) δ 8.47 – 8.43 (m, 1H), 7.44 (d, *J* = 7.9 Hz, 2H), 7.31 – 7.26 (m, 3H), 6.86 (d, *J* = 8.7 Hz, 2H), 5.98 (dd, *J* = 10.3, 5.5 Hz, 1H), 4.94 (dd, *J* = 5.5, 1.5 Hz, 1H), 3.79 (s, 3H). ^{13}C NMR (126 MHz, $CDCl_3$) δ 174.4, 159.9, 145.6, 138.1, 137.6, 131.4, 131.2, 129.7, 129.2 (2C), 128.3, 125.9, 124.7, 123.8, 122.1, 114.5 (2C), 55.4, 43.9. IR(KBr)ν_{max}/cm^{1}, 2923 (C–H), 1610 (C=O), HRMS (ESI) calcd for $C_{19}H_{13}ClO_2S_2$ 373.0118 $[M+H]^+$; found 373.0118.

(S)-2-(4-Methoxyphenyl)-7-(trifluoromethyl)-2*H*,5*H*-thiopyrano[2,3-*b*]thiochromen-5-one (3d). 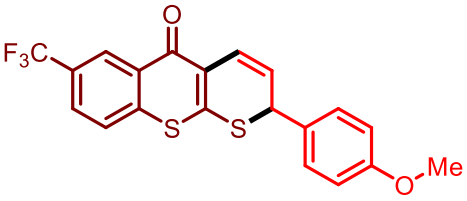

A light-yellow solid (69 mg, 85 %) mp 157 ºC; ^{1}H NMR (500 MHz, $CDCl_3$) δ 8.78 (s, 1H), 7.72 (d, *J* = 8.3 Hz, 1H), 7.52 (d, *J* = 8.4 Hz, 1H), 7.29 – 7.26 (m, 3H), 6.85 (d, *J* = 8.6 Hz, 2H), 5.99 (dd, *J* = 10.2, 5.5 Hz, 1H), 4.94 (d, *J* = 5.1 Hz, 1H), 3.77 (s, 3H). ^{13}C NMR (125 MHz, $CDCl_3$) δ 174.1, 159.9, 146.1, 139.8, 131.3, 131.2, 129.9 (q, *J* = 33 Hz), 129.2, 127.2 (q, *J* = 3.2 Hz), 126.9 (q, *J* = 4 Hz), 126.3, 126.0, 123.6, 123.0 (q, *J* = 270.8 Hz), 122.3, 114.5, 55.4, 43.9. IR(KBr)ν_{max}/cm^{1}, 2925 (C–H), 1626 (C=O), HRMS (ESI) calcd for $C_{20}H_{14}F_3O_2S_2$ 407.0382 $[M+H]^+$; found 407.0370.

(S)-2-(2-Methoxyphenyl)-2*H*,5*H*-thiopyrano[2,3-*b*]thiochromen-5-one (3e). 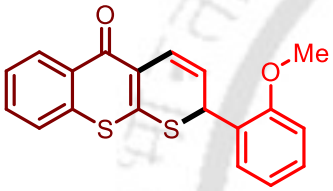

A dark brown solid (58 mg yield-87 %) mp 180 ºC; ^{1}H NMR (500 MHz, $CDCl_3$) δ 8.52 (dd, *J* = 7.8, 1.7 Hz, 1H), 7.50 (dtd, *J* = 15.2, 7.2, 5.7 Hz, 2H), 7.44 – 7.36 (m, 2H), 7.31 (dd, *J* = 7.6, 1.8 Hz, 1H), 7.24 (d, *J* = 1.8 Hz, 1H), 6.93 – 6.85 (m, 2H), 5.92 (dd, *J* = 10.3, 6.3 Hz, 1H), 5.32 (dd, *J* = 6.2, 1.1 Hz, 1H), 3.90 (s, 3H). ^{13}C NMR (125 MHz, $CDCl_3$) δ 175.3, 155.9, 146.4, 136.5, 131.4, 131.3, 129.6, 129.5, 129.3, 127.6, 127.4, 125.6, 125.3, 124.6, 120.9, 120.5, 110.8, 55.7, 36.8. IR(KBr)ν_{max}/cm^{1}, 2924 (C–H), 1602 (C=O), HRMS (ESI): calcd for $C_{19}H_{14}O_2S_2$ 399.0508 $[M+H]^+$; found399.0522.

(S)-8-Fluoro-2-(2-methoxyphenyl)-2*H*,5*H*-thiopyrano[2,3-*b*] thiochromen-5-one (3f). 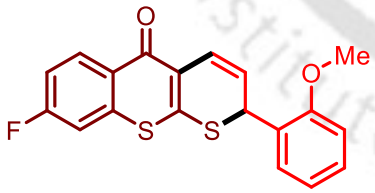

A yellow solid (61 mg -87 %) mp 191 ºC; ^{1}H NMR (500 MHz, $CDCl_3$) δ 8.54 (dd, *J* = 9.0, 5.8 Hz, 1H), 7.38 (d, *J* = 10.2 Hz, 1H), 7.32 – 7.27 (m, 2H), 7.19 (td, *J* = 8.5, 2.5 Hz, 1H), 7.11 (dd, *J* = 8.3, 2.4 Hz, 1H), 6.93 – 6.88 (m, 2H), 5.93 (dd, *J* = 10.3, 6.3 Hz, 1H), 5.35 – 5.31 (m, 1H), 3.91 (s, 3H). ^{13}C NMR (125 MHz, $CDCl_3$) δ 174.4, 163.9 (d, *J* = 254.5 Hz), 155.9, 146.2, 138.4 (d, *J* = 9.6 Hz), 132.4 (d, *J* = 9.5 Hz), 129.6, 129.2, 127.9 (d, *J* = 2.3 Hz), 127.2, 125.5, 124.4, 120.9, 120.7, 116.0 (d, *J* = 22.1 Hz) 111.3 (d, *J* = 22 Hz), 110.8, 55.7, 36.8. IR(KBr)ν_{max}/cm^{1}, 2925(C–H), 1603(C=O), HRMS (ESI) calcd for $C_{19}H_{14}FO_2S_2$ 357.0414 $[M+H]^+$; found 357.0414.

(S)-8-Chloro-2-(2-methoxyphenyl)-2*H*,5*H*-thiopyrano[2,3-*b*] thiochromen-5-one

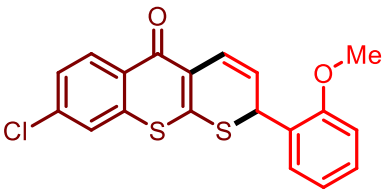

(3g). A light-yellow solid (63 mg, 86 %) mp 171 ºC; ^{1}H NMR (500 MHz, $CDCl_3$) δ 8.44 (d, *J* = 8.6 Hz, 1H), 7.44 – 7.40 (m, 2H), 7.35 (d, *J* = 10.3 Hz, 1H), 7.30 – 7.26 (m, 2H), 6.92 – 6.87 (m, 2H), 5.92 (dd, *J* = 10.3, 6.3 Hz, 1H), 5.32 (d, *J* = 6.3 Hz, 1H), 3.90 (s, 3H). ^{13}C NMR (125 MHz, $CDCl_3$) δ 174.5, 155.9, 146.5, 138.0, 137.8, 131.1, 129.7, 129.6, 129.2, 128.2, 127.2, 125.6, 124.7, 124.4, 120.9, 120.8, 110.8, 55.7, 36.8.IR(KBr)ν_{max}/cm^{1}, 2925(C–H), 1603(C=O), HRMS (ESI) calcd for $C_{19}H_{14}ClO_2S_2$ 373.0118 $[M+H]^+$; found 373.0112.

(S)-7-Chloro-2-(2-methoxyphenyl)-2*H*,5*H*-thiopyrano[2,3-*b*] thiochromen-5-one

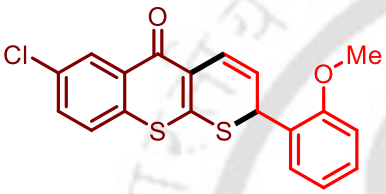

(3h). A brown solid (53 mg, 82 %) mp 178 ºC; ^{1}H NMR (500 MHz, $CDCl_3$) δ 8.44 (d, *J* = 8.6 Hz, 1H), 7.44 – 7.40 (m, 2H), 7.35 (d, *J* = 10.3 Hz, 1H), 7.30 – 7.26 (m, 2H), 6.92 – 6.87 (m, 2H), 5.92 (dd, *J* = 10.3, 6.3 Hz, 1H), 5.32 (d, *J* = 6.3 Hz, 1H), 3.90 (s, 3H).^{13}C NMR (126 MHz, $CDCl_3$) δ 174.5, 155.9, 146.5, 138.0, 137.8, 131.1, 129.7, 129.6, 129.2, 128.2, 127.2, 125.6, 124.7, 124.4, 120.9, 120.8, 110.8, 55.7, 36.8. IR(KBr)ν_{max}/cm^{1}, 2923(C–H), 1607(C=O), HRMS (ESI) calcd for $C_{19}H_{14}ClO_2S_2$ 373.0118 $[M+H]^+$; found 373.0119.

(S)-2-(2-Methoxyphenyl)-7-(trifluoromethyl)-2*H*,5*H*-thiopyrano[2,3-*b*]thiochro-men-5-one (3i).

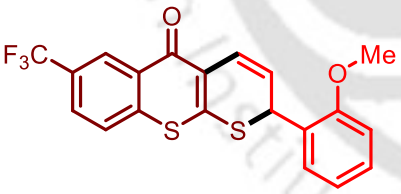

A crystalline yellow (64 mg, 80 %) mp 194 ºC; ^{1}H NMR (400 MHz, $CDCl_3$) δ 8.81 – 8.79 (m, 1H), 7.75 – 7.70 (m, 1H), 7.52 (d, *J* = 8.4 Hz, 1H), 7.38 (d, *J* = 10.3 Hz, 1H), 7.32 – 7.27 (m, 2H), 6.94 – 6.87 (m, 2H), 5.95 (dd, *J* = 10.3, 6.3 Hz, 1H), 5.35 (d, *J* = 6.2 Hz, 1H), 3.91 (s, 3H).^{13}C NMR (125 MHz, $CDCl_3$) δ 174.2, 155.8, 147.1, 140.0, 131.3, 129.8 (q, *J* = 33.4 Hz), 129.7, 129.2, 127.2 (q, *J* = 3.3 Hz), 127.0, 126.9 (q, *J* = 3.9 Hz), 126.2, 125.7, 124.3, 123.6 (q, *J* = 270.8 Hz), 121.0, 120.9, 110.8, 55.7, 36.9. IR(KBr)ν_{max}/cm^{1}, 2923(C–H), 1629(C=O), HRMS (ESI) calcd for $C_{20}H_{14}CF_3O_2S_2$ 407.0382 $[M+H]^+$; found 407.0370.

(S)-8-Chloro-2-phenyl-2*H*,5*H*-thiopyrano[2,3-*b*]thiochromen-5-one (3j). An orange solid (55 mg, 81 %) mp 164 ºC; ^{1}H NMR (500 MHz, $CDCl_3$) δ 8.43 (d, *J* = 8.6 Hz, 1H), 7.45 – 7.40 (m, 2H), 7.36 (t, *J* = 8.7 Hz, 4H), 7.32 – 7.30 (m, 1H), 7.29 – 7.26 (m, 1H), 5.99 (dd, *J* = 10.2, 5.4 Hz, 1H), 4.96 (d, *J* = 5.5 Hz, 1H). ^{13}C NMR (126 MHz, $CDCl_3$) δ 174.4, 145.6, 139.4, 138.1, 137.5, 131.1, 129.6, 129.1 (2C), 128.6, 128.4, 128.0 (2C), 126.0, 124.7, 123.9, 121.8, 44.3. IR(KBr)ν_{max}/cm^{1}, 2923(C–H), 1602(C=O),HRMS (ESI) calcd for $C_{18}H_{12}ClOS_2$ 343.0013 $[M+H]^+$; found 343.0004.

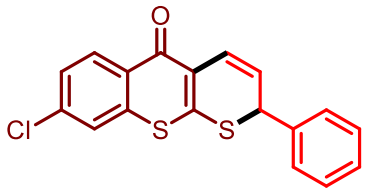

(S)-2-(2-Bromophenyl)-2*H*,5*H*-thiopyrano[2,3-*b*]thiochromen-5-one (3k). A light-yellow solid (64 mg, 83 %) mp 171 ºC; ^{1}H NMR (500 MHz, $CDCl_3$) δ 8.54 – 8.51 (m, 1H), 7.60 (d, *J* = 7.9 Hz, 1H), 7.56 – 7.48 (m, 2H), 7.47 – 7.40 (m, 3H), 7.24 (d, *J* = 7.6 Hz, 1H), 7.17 – 7.12 (m, 1H), 5.96 (dd, *J* = 10.2, 6.4 Hz, 1H), 5.29 (d, *J* = 6.5 Hz, 1H). ^{13}C NMR (125 MHz, $CDCl_3$) δ 175.27, 145.9, 137.9, 136.3, 133.4, 131.4, 131.3, 130.2, 129.8, 129.6, 128.1, 127.8, 125.6, 125.4, 125.3, 123.2, 119.9, 42.7. IR(KBr)ν_{max}/cm^{1}, 2923(C–H), 1603(C=O), HRMS (ESI) calcd for $C_{18}H_{11}BrOS_2$; 386.9507- 388.9487 $[M+H]^+$; found 386.9507-388.9487.

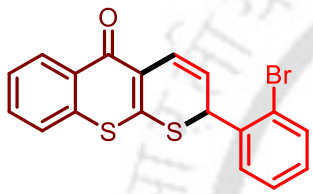

(S)-2-(2-Bromophenyl)-8-fluoro-2*H*,5*H*-thiopyrano[2,3-*b*]thio chromen-5-one (3l). A light-yellow solid (70 mg; 87 %) mp 150 ºC; ^{1}H NMR (500 MHz, $CDCl_3$) δ 8.53 (dd, *J* = 9.0, 5.8 Hz, 1H), 7.61 – 7.59 (m, 1H), 7.44 – 7.38 (m, 2H), 7.24 (d, *J* = 7.1 Hz, 1H), 7.19 (td, *J* = 8.9, 2.4 Hz, 1H), 7.14 (td, *J* = 7.8, 1.6 Hz, 1H), 7.11 (dd, *J* = 8.3, 2.4 Hz, 1H), 5.95 (dd, *J* = 10.3, 6.4 Hz, 1H), 5.29 (dd, *J* = 6.4, 1.0 Hz, 1H). ^{13}C NMR (125 MHz, $CDCl_3$) δ 174.3, 164.0 (d, *J* = 254 Hz), 145.4, 138.3 (d, *J* = 9.7 Hz), 137.8, 133.5, 132.6 (d, *J* = 9.6 Hz), 130.2, 129.9, 128.2, 127.9, 125.5, 125.1, 123.2, 120.1, 116.2 (d, *J* = 22.1 Hz), 111.4 (d, *J* = 24.4 Hz), 42.8. IR(KBr)ν_{max}/cm^{1}, 2925(C–H), 1603(C=O), HRMS (ESI): calcd for $C_{18}H_{11}BrFOS_2$ 404.9413-406.9393$[M+H]^+$; found 404.9413-404.9413.

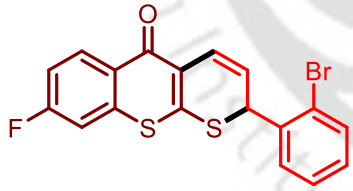

(S)-2-(2-Bromophenyl)-7-(trifluoromethyl)-2*H*,5*H*-thiopyrano[2,3-*b*]thiochrome-n-5-one (3m). 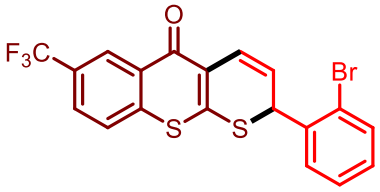

A light-yellow solid (72 mg, 80 %) mp 200 ºC; ^{1}H NMR (500 MHz, $CDCl_3$) δ 8.81 (s, 1H), 7.77 – 7.74 (m, 1H), 7.63 (d, *J* = 7.9 Hz, 1H), 7.56 (d, *J* = 8.4 Hz, 1H), 7.46 (d, *J* = 10.3 Hz, 1H), 7.43 – 7.39 (m, 1H), 7.28 (d, *J* = 6.8 Hz, 1H), 7.17 (t, *J* = 7.6 Hz, 1H), 6.00 (dd, *J* = 10.3, 6.4 Hz, 1H), 5.35 (d, *J* = 6.4 Hz, 1H).^{13}C NMR (125 MHz, $CDCl_3$) δ 174.22, 146.25, 139.91, 137.70, 133.59, 131.38, 130.28, 130.0, 130.0 (q, *J* = 33.3 Hz), 128.25, 127.48, 127.4 (q, *J* = 3.3 Hz), 127.0 (q, *J* = 3.9 Hz), 126.35, 125.82, 125.0, 123.3 (q, *J* = 3.9 Hz), 120.52, 42.93. IR(KBr)ν_{max}/cm^{1}, , 2923(C–H), 1627(C=O), HRMS (ESI) calcd for $C_{19}H_{11}BrF_3OS_2$ 454.9381 found 454.9381-456.9361[M+H]$^{+}$; found 454.9380-454.9359.

(S)-2-(2-Bromophenyl)-8-chloro-2*H*,5*H*-thiopyrano[2,3-*b*]thiochromen-5-one (3n). 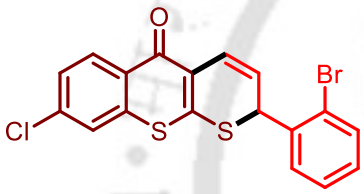

A light-yellow solid (68 mg, 81 %) mp 183 ºC; ^{1}H NMR (500 MHz, $CDCl_3$) δ 8.44 (d, *J* = 8.6 Hz, 1H), 7.61 (dd, *J* = 7.9, 1.3 Hz, 1H), 7.46 – 7.38 (m, 4H), 7.26 (d, *J* = 4.0 Hz, 1H), 7.15 (td, *J* = 7.7, 1.8 Hz, 1H), 5.96 (dd, *J* = 10.3, 6.4 Hz, 1H), 5.31 (d, *J* = 6.4 Hz, 1H). ^{13}C NMR (125 MHz, $CDCl_3$) δ 174.5, 145.7, 138.2, 137.8, 137.6, 133.5, 131.2, 130.2, 129.9, 129.6, 128.4, 128.2, 125.7, 125.0, 124.8, 123.3, 120.2, 42.8. IR(KBr)ν_{max}/cm^{1}, 2923(C–H), 1606(C=O), HRMS (ESI) calcd for $C_{18}H_{11}BrClOS_2$ 420.9118-422.9098[M+H]$^{+}$; found 420.9102-422.9080.

(S)-2-(4-Bromophenyl)-8-fluoro-2*H*,5*H*-thiopyrano[2,3-*b*]thio chromen-5-one (3o). 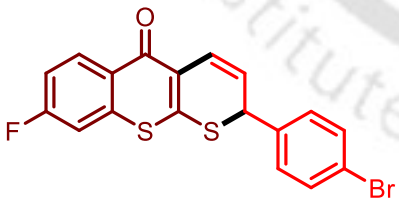

A brown solid (67 mg, 87 %) mp 159 ºC; ^{1}H NMR (500 MHz, $CDCl_3$) δ 8.52 (dd, *J* = 9.0, 5.8 Hz, 1H), 7.45 (d, *J* = 8.4 Hz, 2H), 7.31 (d, *J* = 10.2 Hz, 1H), 7.23 (d, *J* = 8.4 Hz, 2H), 7.19 (dd, *J* = 8.4, 1.8 Hz, 1H), 7.12 (dd, *J* = 8.3, 2.2 Hz, 1H), 5.97 (dd, *J* = 10.3, 5.8 Hz, 1H), 4.88 – 4.86 (m, 1H). ^{13}C NMR (125 MHz, $CDCl_3$) δ 174.32, 164.0 (d, *J* = 2.3 Hz), 144.81, 138.48, 138.1 (d, *J* = 9.6 Hz), 132.77, 132.6 (d, *J* = 9.5 Hz), 129.63, 127.9 (d, *J* = 2.3 Hz),, 125.90, 124.42, 122.74, 120.99, 116.3 (d, *J* = 22.1 Hz),, 111.5 (d, *J* = 24.6 Hz), 43.3. IR(KBr)ν_{max}/cm^{1}, 2923 (C–H), 1605 (C=O), HRMS (ESI) calcd for $C_{18}H_{11}BrFOS_2$ 404.9413-406.9393[M+H]$^{+}$; found 404.9413-404.9393.

(S)-2-(4-Bromophenyl)-2*H*,5*H*-thiopyrano[2,3-*b*]thio chromen-5-one (3p). A light orange solid (66 mg, 82 %) mp 143 ºC.[1]H NMR (500 MHz, $CDCl_3$) δ 8.52 (dd, *J* = 8.0, 1.7 Hz, 1H), 7.55 (td, *J* = 7.7, 1.4 Hz, 1H), 7.52 – 7.48 (m, 1H), 7.44 (td, *J* = 6.3, 1.6 Hz, 3H), 7.34 (dd, *J* = 10.3, 1.4 Hz, 1H), 7.24 (d, *J* = 8.4 Hz, 2H), 5.98 (dd, *J* = 10.2, 5.8 Hz, 1H), 4.89 – 4.85 (m, 1H). [13]C NMR (125 MHz, $CDCl_3$) δ 175.1, 145.3, 138.6, 136.1, 132.2 (2C), 131.5, 131.3, 129.6, 129.6 (2C), 127.8, 125.8, 125.4, 124.5, 122.6, 120.7, 43.3. IR(KBr)ν_{max}/cm[1], 2925 (C–H), 1605 (C=O), HRMS (ESI) calcd for $C_{18}H_{11}BrFOS_2$ 386.9507-388.9487$[M+H]^+$; found 386.9493-388.9469.

(S)-2-(4-Bromophenyl)-8-chloro-2*H*,5*H*-thiopyrano [2,3-*b*]thiochromen-5-one (3q). A light-yellow solid (73 mg, 88 %) mp 172 ºC; [1]H NMR (500 MHz, $CDCl_3$) δ 8.44 (d, *J* = 8.5 Hz, 1H), 7.48 – 7.42 (m, 4H), 7.30 (d, *J* = 10.3 Hz, 1H), 7.23 (d, *J* = 8.4 Hz, 2H), 5.98 (dd, *J* = 10.2, 5.8 Hz, 1H), 4.88 (d, *J* = 5.7 Hz, 1H).[13]C NMR (125 MHz, $CDCL_3$) δ 174.4, 145.0, 138.4, 138.3, 137.4, 132.2 (2C), 131.2, 129.6 (2C), 129.6, 128.5, 126.0, 124.8, 124.3, 122.7, 121.1, 43.4. IR(KBr)ν_{max}/cm[1], 2925(C–H), 1608(C=O), HRMS (ESI) calcd for $C_{18}H_{11}BrFOS_2$ 420.9118-422.9098 $[M+H]^+$; found 420.9104-422.9079.

(S)-2-(4-Bromophenyl)-7-chloro-2*H*,5*H*-thiopyrano [2,3-*b*] thiochromen-5-one (3r). A light-yellow solid (71 mg, 85 %) mp 145 ºC; [1]H NMR (500 MHz, $CDCl_3$) δ 8.48 (d, *J* = 2.0 Hz, 1H), 7.51 (dd, *J* = 8.5, 2.2 Hz, 1H), 7.45 (d, *J* = 8.4 Hz, 3H), 7.37 (d, *J* = 8.5 Hz, 1H), 7.32 – 7.29 (m, 1H), 7.23 (d, *J* = 8.4 Hz, 3H), 5.98 (dd, *J* = 10.2, 5.8 Hz, 1H), 4.88 (d, *J* = 5.5 Hz, 1H). [13]C NMR (125 MHz, $CDCl_3$) δ 174.0, 145.6, 138.4, 134.3, 134.2, 132.4, 132.2 (2C), 131.8, 129.6 (2C), 129.2, 126.9, 125.7, 124.4, 122.7, 121.1, 43.4. IR(KBr)ν_{max}/cm[1], 2922(C–H), 1603 (C=O), HRMS (ESI) calcd for $C_{18}H_{11}BrFOS_2$ 420.9118-422.9098$[M+H]^+$;found 420.9107-422.9083.

(S)-2-(4-Bromophenyl)-7-(trifluoromethyl)-2*H*,5*H*-thiopyrano[2,3-*b*]thiochromen-5-one (3s). 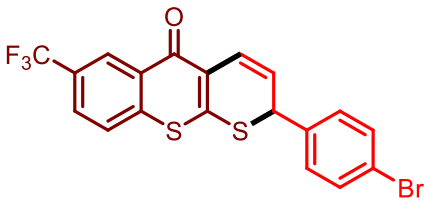

A brown solid (74 mg, 82 %) mp 181 ºC; ^{1}H NMR (500 MHz, $CDCl_3$) δ 8.81 (d, *J* = 2.1 Hz, 1H), 7.76 (dd, *J* = 8.4, 2.1 Hz, 1H), 7.56 (d, *J* = 8.4 Hz, 1H), 7.32 – 7.26 (m, 3H), 7.16 (d, *J* = 7.9 Hz, 2H), 6.02 (dd, *J* = 10.2, 5.5 Hz, 1H), 4.97 (dd, *J* = 5.4, 1.5 Hz, 1H), 2.35 (s, 3H). ^{13}C NMR (125 MHz, $CDCl_3$) δ 174.1, 146.2, 139.8, 138.7, 136.3, 130.0 (q, *J* = 33.4 Hz), 129.8 (2C), 127.9 (2C), 127.3 (q, *J* = 3.3 Hz), 127.0 (q, *J* = 3.9 Hz), 126.3, 126.1, 123.7, 123.6 (q, *J* = 270.8 Hz), 122.3, 44.2, 21.2. IR(KBr)ν_{max}/cm^{1}, 2927 (C-H), 1609 (C=O) HRMS (ESI) calcd for $C_{18}H_{11}BrFOS_2$ 454.9381-456.9359 $[M+H]^+$; found 454.9380-454.9359.

(S)-6-Chloro-3-methyl-2-phenyl-2*H*,5*H*-thiopyrano[2,3-*b*]thiochromen-5-one (3t). 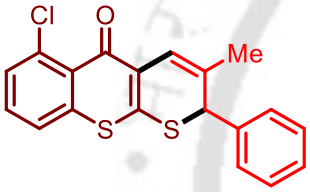

A light-yellow solid (56 mg, 79 %) mp 184 ºC; ^{1}H NMR (500 MHz, $CDCl_3$) δ 7.44 (d, *J* = 7.2 Hz, 1H), 7.28 (dd, *J* = 15.7, 7.8 Hz, 7H), 7.10 (d, *J* = 6.0 Hz, 1H), 4.49 (s, 1H), 1.98 (s, 3H). ^{13}C NMR (125 MHz, $CDCl_3$) δ 175.1, 139.1, 139.1, 138.3, 136.5, 131.4, 130.9, 130.5, 129.0 (2C), 128.4, 127.9, 127.8, 127.4 (2C), 124.5, 120.3, 47.5, 23.4. IR(KBr)ν_{max}/cm^{1}, 2923(C–H), 1607(C=O), HRMS (ESI) calcd for $C_{19}H_{13}ClOS_2$ 357.0169$[M+H]^+$; found 357.0169.

(S)-8-Chloro-3-methyl-2-phenyl-2*H*,5*H*-thiopyrano[2,3-*b*]thiochromen-5-one (3u). 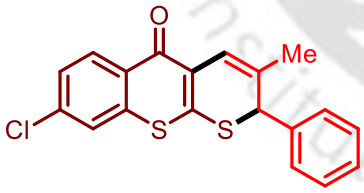

A yellow solid (57 mg, 81 %) mp 209 ºC; ^{1}H NMR(500 MHz,$CDCl_3$) δ 8.46 (d, *J* = 8.5 Hz, 1H), 7.44 – 7.40 (m, 2H), 7.30 – 7.26 (m, 5H), 7.21 – 7.18 (m, 1H), 4.52 (s, 1H), 2.01 (s, 3H).^{13}C NMR (125 MHz, $CDCl_3$) δ 174.4, 141.3, 139.1, 137.9, 137.7, 131.2, 131.2, 129.6 (2C), 129.1, 128.5, 128.2, 127.4 (2C), 126.5, 124.7, 119.9, 47.7, 23.5. IR(KBr)ν_{max}/cm^{1}, 2924 (C–H), 1605 (C=O), HRMS (ESI) calcd for $C_{19}H_{14}ClOS_2$ 357.0169 $[M+H]^+$; found 357.0169.

(S)-2-(*p*-tolyl)-2*H*,5*H*-thiopyrano[2,3-*b*]thiochromen-5-one (3v). A yellow solid (58 mg, 75 %) mp 126 ºC; ^{1}H NMR (500 MHz, $CDCl_3$) δ 8.53 (dd, *J* = 7.9, 1.7 Hz, 1H), 7.57 – 7.48 (m, 2H), 7.45 – 7.43 (m, 1H), 7.33 – 7.26 (m, 3H), 7.14 (d, *J* = 7.9 Hz, 2H), 5.98 (dd, *J* = 10.2, 5.5 Hz, 1H), 4.94 (dd, *J* = 5.5, 1.5 Hz, 1H), 2.33 (s, 3H). ^{13}C NMR (125 MHz, $CDCl_3$) δ 175.2, 145.9, 138.5, 136.7, 136.3, 131.4, 131.3, 129.7 (2C), 129.6, 127.9 (2C), 127.7, 125.9, 125.4, 124.0, 121.7, 44.1, 21.2. IR(KBr)ν_{max}/cm^{1}, 2925(C–H), 1608(C=O), HRMS (ESI) calcd for $C_{19}H_{14}OS_2$ 323.0559 $[M+H]^+$; found 323.0559.

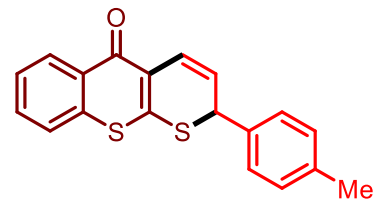

(S)-8-Fluoro-2-(*p*-tolyl)-2*H*,5*H*-thiopyrano[2,3-*b*]thiochromen-5-one (3w). A light-yellow solid (62 mg,92 %) mp 104 ºC; ^{1}H NMR (500 MHz, $CDCl_3$) δ 8.55 (dd, *J* = 9.0, 5.8 Hz, 1H), 7.29 (d, *J* = 11.4 Hz, 3H), 7.21 (td, *J* = 8.9, 2.4 Hz, 1H), 7.17 – 7.13 (m, 3H), 5.99 (dd, *J* = 10.2, 5.5 Hz, 1H), 4.95 (dd, *J* = 5.5, 1.5 Hz, 1H), 2.34 (s, 3H). ^{13}C NMR (125 MHz, $CDCl_3$) δ 174.40z, 164.0 (d, *J* = 254.6 Hz), 145.4, 138.6, 138.3 (d, *J* = 9.7 Hz), 136.52, 132.6 (d, *J* = 9.5 Hz), 129.8 (2C), 128.0, 127.9 (2C), 125.9, 123.9, 121.9, 116.2 (d, *J* = 22.1 Hz), 111.4 (d, *J* = 24.6 Hz) ,44.1, 21.2. IR(KBr)ν_{max}/cm^{1}, 2927(C–H), 1609(C=O), HRMS (ESI) calcd for $C_{19}H_{14}FOS_2$ 341.0465 $[M+H]^+$; found 357.0456.

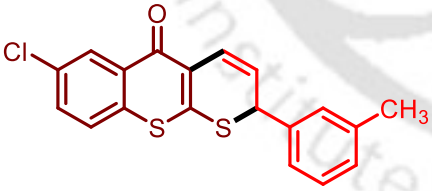

(S)-8-Chloro-2-(*m*-tolyl)-2*H*,5*H*-thiopyrano[2,3-*b*]thiochro men-5-one (3x). A light-yellow solid (55 mg, 82 %) mp 119 ºC; ^{1}H NMR (500 MHz, $CDCL_3$) δ 8.43 (d, *J* = 8.5 Hz, 1H), 7.42 (d, *J* = 8.3 Hz, 2H), 7.25 – 7.19 (m, 2H), 7.18 – 7.10 (m, 3H), 5.96 (dd, *J* = 10.3, 5.3 Hz, 1H), 4.95 (dd, *J* = 5.3, 1.6 Hz, 1H), 2.33 (s, 3H). ^{13}C NMR (125 MHz, $CDCl_3$-*d*) δ 174.4, 145.8, 139.4, 138.9, 138.1, 137.5, 131.2, 129.7, 129.5, 129.0, 128.7, 128.4, 125.9, 125.1, 124.7, 123.8, 121.9, 44.4, 21.5. IR(KBr)ν_{max}/cm^{1}, 2923(C–H), 1607(C=O), HRMS (ESI) calcd for $C_{19}H_{14}ClOS_2$ 357.0169 $[M+H]^+$; found 357.0169.

(S)-7-Chloro-2-(*m*-tolyl)-2*H*,5*H*-thiopyrano[2,3-*b*]thio chrom en-5-one (3y). A

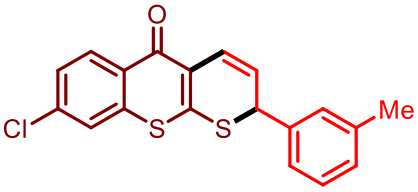

light-yellow solid (54 mg, 77 %) mp 104 ºC;^{1}H NMR (500 MHz, $CDCl_3$) δ 8.40 (d, *J* = 2.4 Hz, 1H), 7.40 (dd, *J* = 8.5, 2.4 Hz, 1H), 7.28 (s, 1H), 7.19 – 7.17 (m, 1H), 7.13 (d, *J* = 7.8 Hz, 1H), 7.09 (s, 2H), 7.03 (d, *J* = 7.5 Hz, 1H), 5.88 (dd, *J* = 10.3, 5.3 Hz, 1H), 4.87 (dd, *J* = 5.4, 1.6 Hz, 1H), 2.25 (s, 3H). ^{13}C NMR (125 MHz, $CCDl_3$) δ 173.9, 146.3, 139.3, 138.9, 134.3, 134.2, 132.4, 131.7, 129.4, 129.2, 129.0, 128.7, 126.8, 125.6, 125.1, 123.8, 122.0, 44.5, 21.5. IR(KBr)ν_{max}/cm^{1}, 2923(C–H), 1607(C=O), HRMS (ESI) calcd for $C_{19}H_{14}ClOS_2$ 357.0169[M+H]$^{+}$; found 357.0169.

(S)-2-(4-(Dimethylamino)phenyl)-2*H*,5*H*-thiopyrano[2,3-*b*]thiochromen-5-one

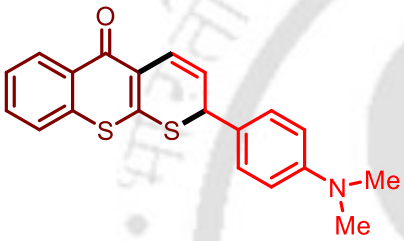

(3z). A sticky black liquid (62 mg, 92 %).^{1}H NMR (500 MHz, $CDCl_3$) δ 8.52 (d, *J* = 8.8 Hz, 1H), 7.54 (t, *J* = 6.8 Hz, 1H), 7.49 (t, *J* = 7.5 Hz, 1H), 7.43 (d, *J* = 7.9 Hz, 1H), 7.28 (d, *J* = 11.4 Hz, 1H), 7.22 (d, *J* = 8.7 Hz, 2H), 6.66 (d, *J* = 8.7 Hz, 2H), 5.97 (dd, *J* = 10.3, 5.4 Hz, 1H), 4.91 (dd, *J* = 5.5, 1.5 Hz, 1H), 2.94 (s, 6H). ^{13}C NMR (125 MHz, $CDCl_3$) δ 175.2, 150.6, 146.3, 136.5, 131.4, 131.3, 129.6, 128.9 (2C), 127.6, 126.8, 125.8, 125.4, 123.7, 122.2, 112.6, 44.5, 40.5 (2C). IR(KBr)ν_{max}/cm^{1}, 2921 (C− H), 1605(C=O), HRMS (ESI):m/z [M+H]$^{+}$ calcd for $C_{20}H_{18}NOS_2$; 352.0824 found 352.0829.

Figure 2.6. X-ray crystallographic data of compound **3e**

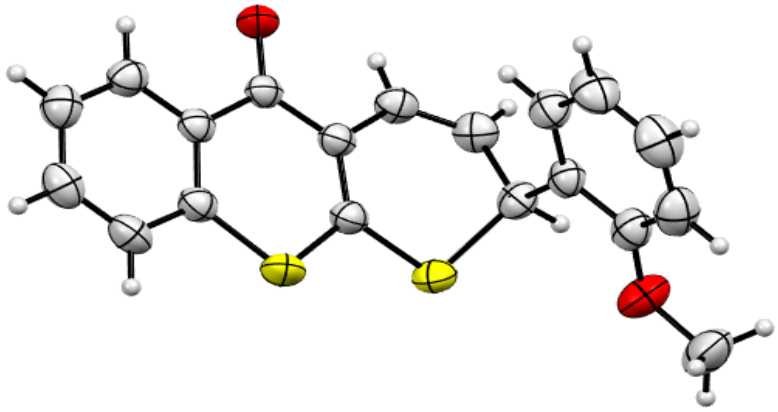

Table S1. Crystal data and structure refinement for compound **(3e)**

Entry	Identification Code	Compound 3e
01	Empirical formula	$C_{19}H_{14}O_2S_2$
02	Formula weight	338.42
03	Temperature	297 K
04	Wavelength	0.71073
07	Crystal system	Triclinic
08	Space group	P-1
09	Cell length(Å)	(a)7.6579 (10), (b)13.8840(19) (c)14.998 (2)
10	Cell angle (º)	α 87.216 (3), β 89.610 (4), γ 83.982 (3)
11	Cell volume ($Å^3$)	1584.0 (4)
12	Density	1.419
13	Absorption correction	multi-scan
15	Cell formula units Z	2
16	CCDC no	2311036

Figure 2.7 . ^{1}H NMR Compound (**3a**)

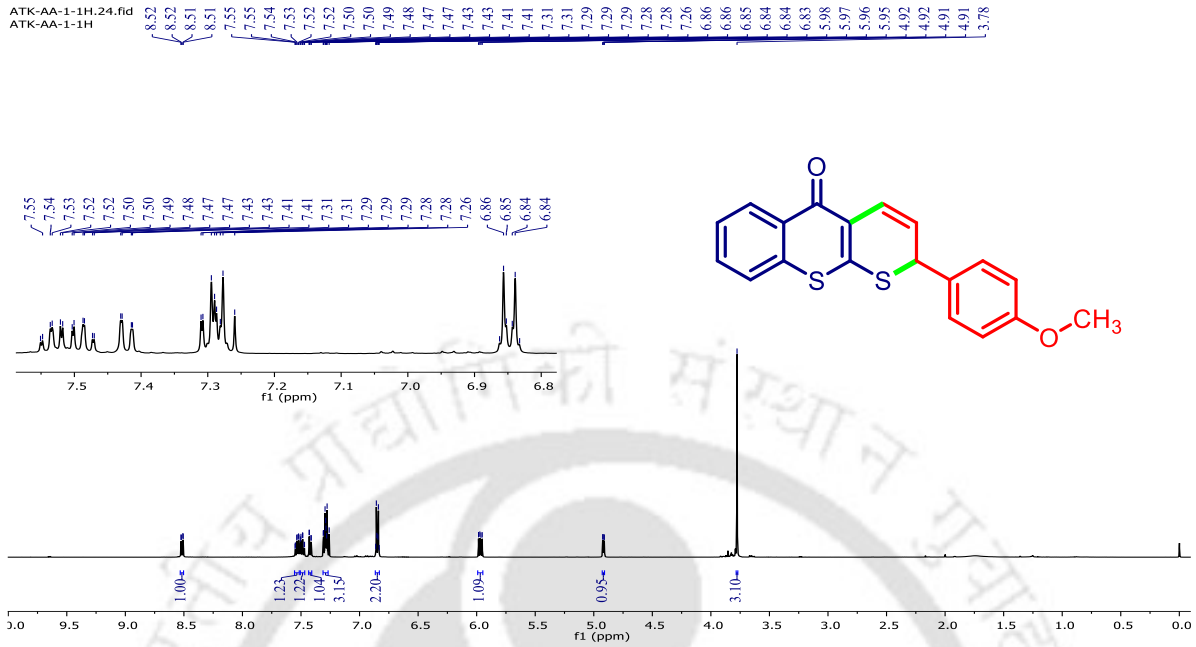

Figure 2.8. ^{13}C{^{1}H} NMR (125 MHz, CDCl3) spectrum of compound (**3a**)

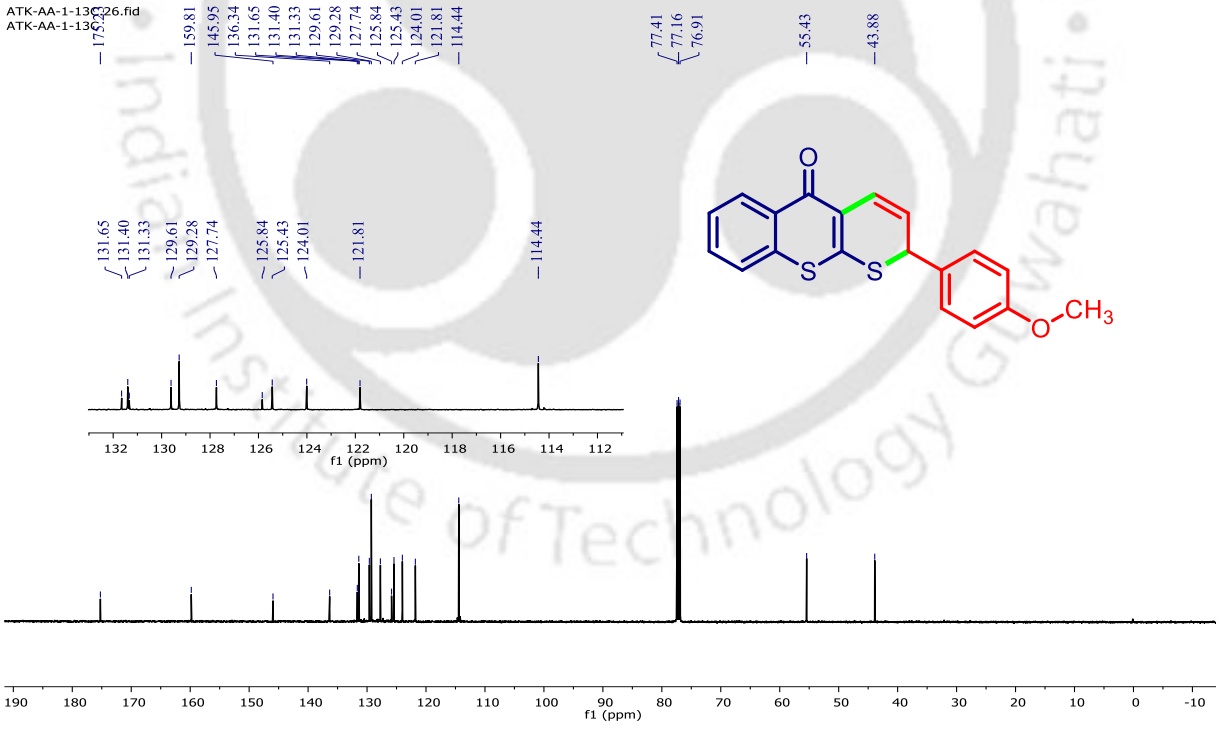

Figure 2.9. HRMS of Compound (**3a**)

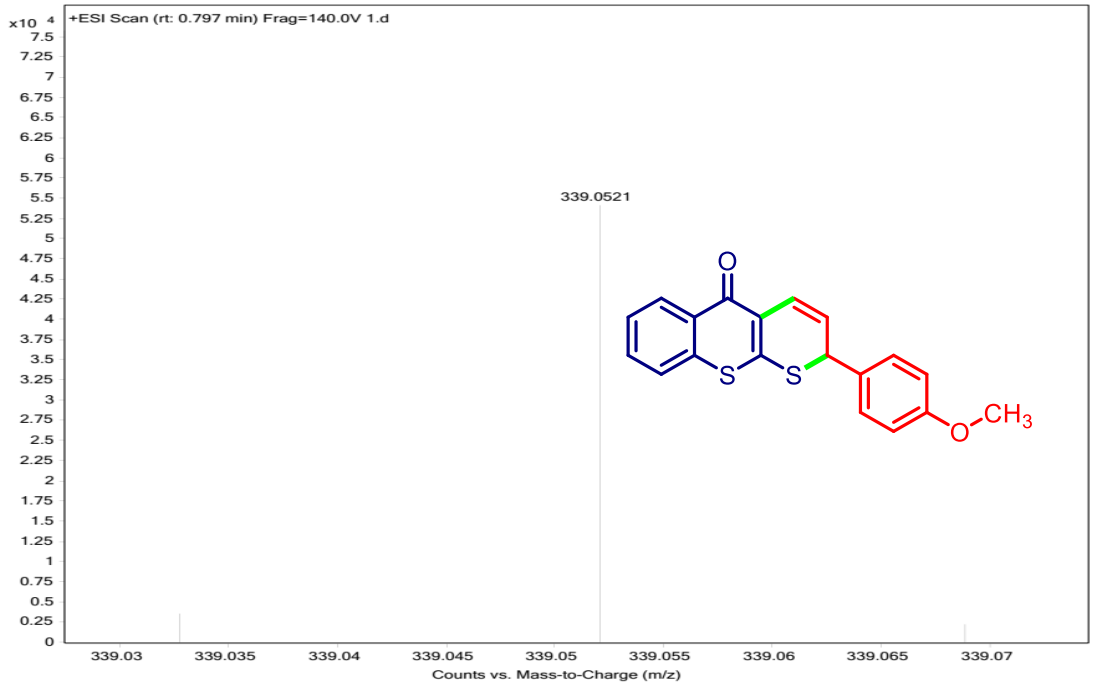

Figure 2.10. HRMS of the Intermediate (**A**)

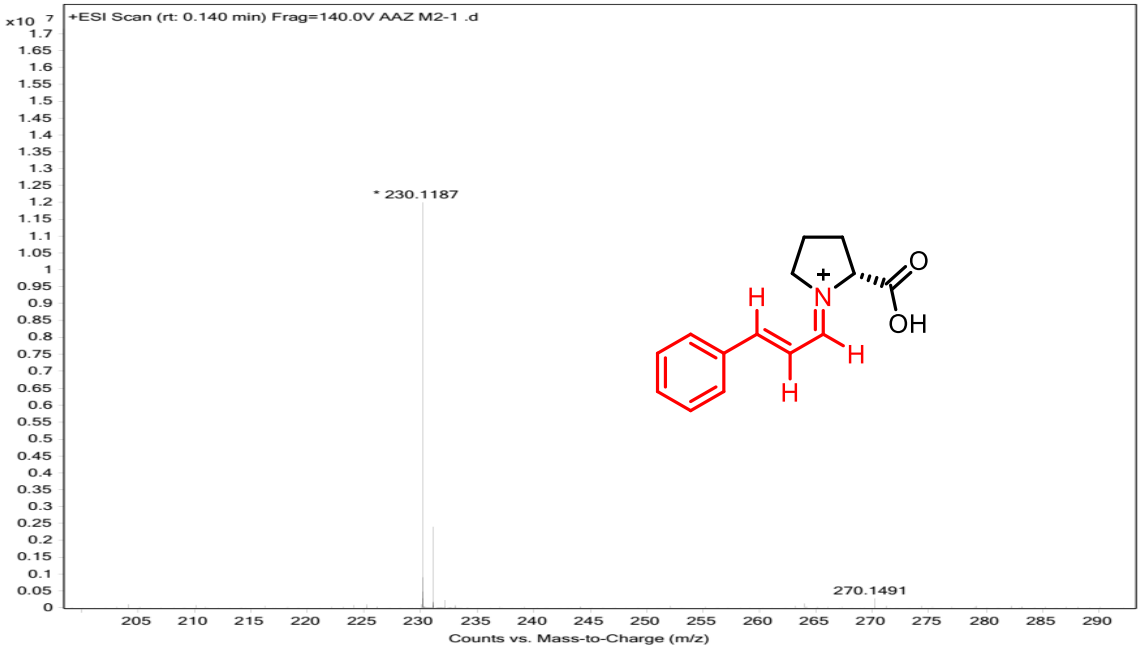

References:

1. (a) M. Mustafa and J. Y. Winum, *Expert Opin. Drug Discov.*, 2022, **17**, 501-512; (b) S. Pathania, R. K. Narang and R. K. Rawal, *Eur. J. Med. Chem.*, 2019, **180**, 486-508; (c) F. Mir, S. Shafi, M. S. Zaman, N. P. Kalia, V. S. Rajput, C. Mulakayala, N. Mulakayala, I. A. Khan and M. S. Alam, *Eur. J. Med. Chem.*, 2014, **76**, 274-283.
2. (a) R. Roy, S. Rakshit, T. Bhowmik, S. Khan, A. Ghatak and S. Bhar, *J. Org. Chem.*, 2014, **79**, 6603-6614; (b) K. Tan, S. Koh, R. P. Ee, M. Khan and M. Go, *Chem. Med. Chem.*, 2012, **7**, 1567-1579; (c) M. K. Katiyar, G. K. Dhakad, Shivani, S. Arora, S. Bhagat, T. Arora and R. Kumar, *J. Mol. Struct.*, 2022, **1263**, 133012.
3. N. G. Rule, M. R. Detty, J. E. Kaeding and J. A. Sinicropi, *J. Org. Chem.*, 1995, **60**, 1665-1673.
4. M. Minakawa, K. Minami and Y. Sato, *Synlett*, 2021, **32**, 1869-1873.
5. W. Wang, H. Li, J. Wang and L. Zu, *J. Am. Chem. Soc.*, 2006, **128**, 10354-10355.
6. G. Palmisano, L. Toma, R. Annunziata, S. Tagliapietra, A. Barge and G. Cravotto, *J. Heterocycl. Chem.*, 2007, **44**, 411-418.
7. N. A. Ahlemeyer and V. B. Birman, *Org. Lett.*, 2016, **18**, 3454-3457.
8. M. Belal, S. Mondal, S. Yashmin and A. T. Khan, *Org. Biomol. Chem.*, 2022, **20**, 715-726.
9. K. Mahato, P. Ray Bagdi and A. Khan, *Synlett*, 2014, **25**, 2438-2441.
10. K. Mahato, P. R. Bagdi and A. T. Khan, *Org. Biomol. Chem.*, 2017, **15**, 5625-5634.
11. (a) P. Gunasekaran, P. Prasanna and S. Perumal, *Tetrahedron Lett.*, 2014, **55**, 329-332; (b) J. Pandey, N. Anand and R. P. Tripathi, *Tetrahedron*, 2009, **65**, 9350-9356.
12. H. Pellissier, *Tetrahedron*, 2007, **63**, 9267-9331.
13. J. W. Yang, M. Stadler and B. List, *Angew. Chem. Int. Ed.*, 2007, **46**, 609-611.
14. (a)W. Wang, H. Li, J. Wang and L. Zu, *J. Am. Chem. Soc.*, 2006, **128**, 10354-10355; (b) N. M. H. Elnagdi and N. S. Al-Hokbany, *Molecules*, 2012, **17**, 4300-4312; (c) D. Bhattacharjee, B. Kshiar and B. Myrboh, *RSC Adv.*, 2016, **6**, 95944-95950.
15. A. Di Salvo, M. V. Spanedda, M. Ourévitch, B. Crousse and D. Bonnet-Delpon, *Synthesis*, 2003, 2231-2235.
16. K. Rajender Reddy, C. V. Rajasekhar and A. Ravindra, *Synth. Commun.*, 2006, **36**, 3761-3766.

Chapter III

Reactivity study of 4-hydroxydithiocoumarin with vinyl ether and vinyl sulfide: Synthesis of 4-methyl-3,4-dihydrothiopyran and hydrothiolated derivatives

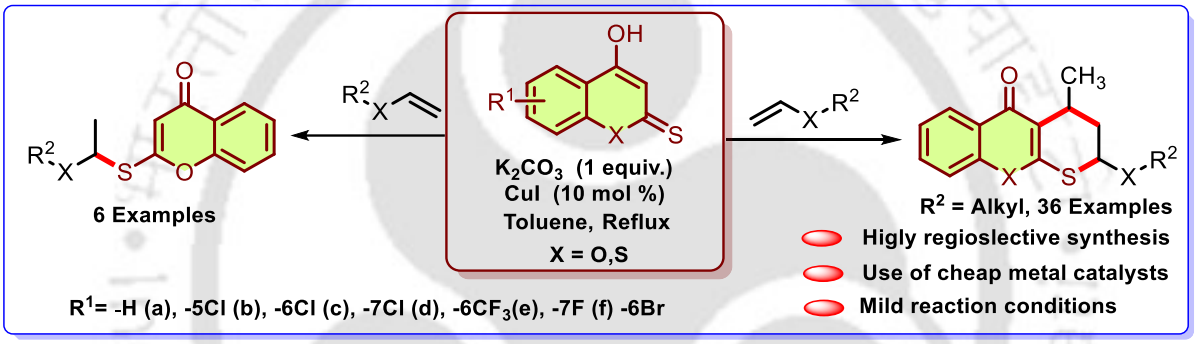

Org. Chem. Front.,2025, **12**, 6288-6300

Introduction

Results and Discussions

Expirmental

3.0 Introduction

Due to the prevalence of C-S bonds in numerous biological and pharmacological substances, there has been a continuous interest in developing mild and effective processes for forming carbon-sulfur bonds.[1] Recently, both C-S coupling reactions and direct C-H functionalization have been established for forming the C-S bond.[2] The classical constructions of C−S bonds include either the direct coupling of organic halides with thiols or the addition of thiols to unsaturated C=C bonds, and a few of them are mentioned in this chapter **3.1.**

3.1 Reactions for the synthesis of a thioether derivative

In 2012, Riduan *et al.* established a classical route for synthesising stereoselective *Z* and *E* sulfide vinyl ethers by using phenylacetylene and thiol in DMF in the presence of CuI,[3] as presented in **Scheme 1**. The stereoselectivity is controlled by the CO_2 molecule used in conjunction with the CuI catalyst. *Z*-Vinyl ether is formed in the presence of CO_2, but in the absence of CO_2, it gives *E*-vinyl ether.

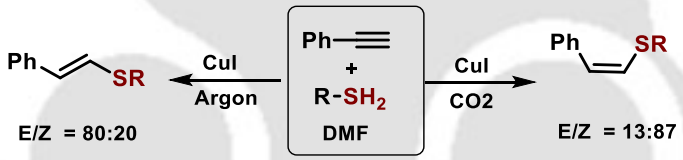

Scheme 1. CO_2 Mediated Stereoselective Copper-Catalysed Reductive Coupling of Alkynes and Thiols

Samara *et al.* demonstrated the synthesis of vinyl thioethers *via* the hydrothiolation of phenylacetylene with thiophenol in the presence of $In(OTf)_3$ as a catalyst, as shown in **Scheme 2**. Their protocol revealed two regioisomeric products: the Markovnikov and *anti*-Markovnikov products.[4] The selectivity is dependent on the substituent of the thiol: when a heteroatom-containing group was attached, the reaction afforded the Markovnikov product, whereas with alkyl or aryl substituents, the *anti*-Markovnikov product was obtained

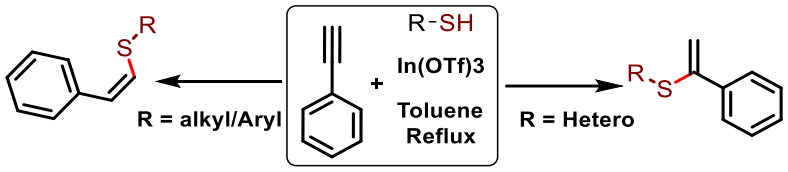

Scheme 2. Regioselective Synthesis of vinyl sulfide derivatives using phenylacetylene and thiophenol

Ding *et al.* synthesised saturated thio-ethers *via* thioalkylation of tosylated hydrazone with thiophenyl in the presence of mild base K_2CO_3 in Dioxane solvent as presented in **scheme 3.**[5]

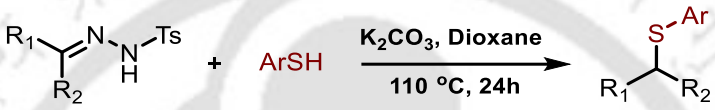

Scheme 3. Synthesis of vinyl sulfide derivatives using tosyl hydrazone and thiophenol

Fragies *et al.* (2021) reported a novel strategy for preparing thioalkyl phosphonium salts through a formal phosphine–Pummerer reaction, as shown in **Scheme 4**.[6] This approach utilizes phosphines in Pummerer-type activation with sulfoxides to generate stable thioalkyl phosphonium intermediates. These salts were then successfully utilised to pursue Wittig-type olefinations with aldehydes to synthesize vinyl sulfides.

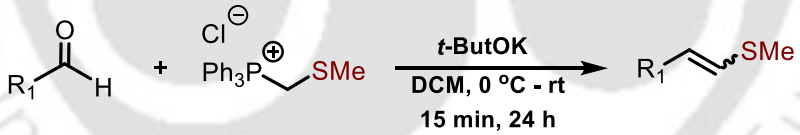

Scheme 4. Synthesis of vinyl sulfide derivatives *via* Wittig-type olefinations

Our research group recently demonstrated, in 2017, the reactivity of 4-hydroxydithiocoumarin, which behaves as a pseudo-thio moiety, with phenylacetylene, a Heteroaryl-Substituted alkyne (2-ethynylpyridine), and styrene.[7] It observed that phenylacetylene and styrene give the Markovnikov hydrothialated product in toluene in the presence of CuI. Whereas, under identical conditions, in the case of 2-ethynylpyridine, they only obtain an *anti*-Markovnikov product, as shown in **Scheme 5**.

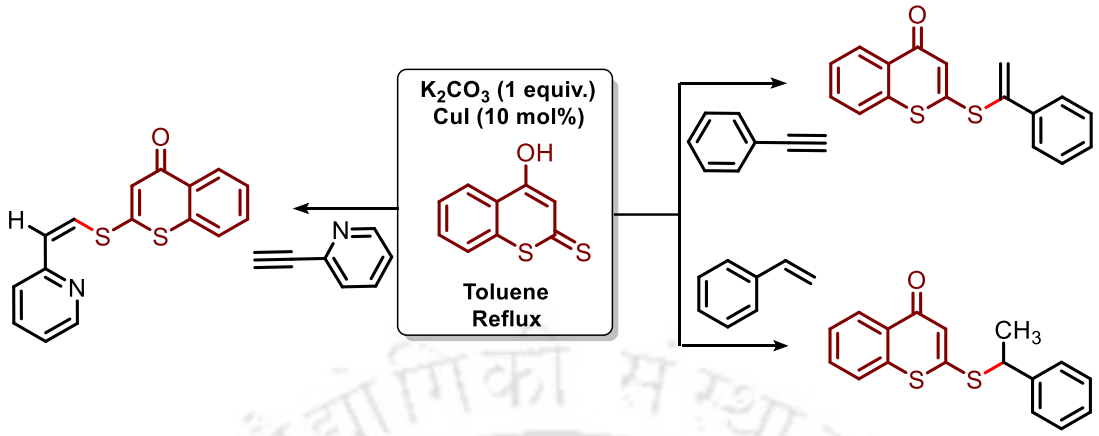

Scheme 5. Synthesis of vinyl sulfide derivatives *via* Hydrothiolation reaction using 4-hydroxydithiocoumarin.

The literature discussed above collectively describes the hydrothiolation of alkenes and alkynes, which involves the construction of a C-S bond. However, the synthesis of C-S bonds through hydrothiolation reaction and C(sp^2)-H activation is less explored with electron-rich olefins, particularly vinyl ethers (VEs).

And herein, our objective was to examine the reactivity behaviour of 4-hydroxydithiocoumarin with electron-rich alkenes (vinyl ethers) and to observe whether they exhibit similar reaction behaviour as it shows in the case of styrene in the presence of CuI. According to the literature, styrene produces only hydrothiolated products, as discussed in **Scheme 5.** Whereas, in the case of vinyl ethers, a cyclized product **3** was obtained by the incorporation of two vinyl ether units, as well as an uncyclized hydrothiolated product, as shown **in Scheme 6**. The reaction proceeds *via* the formation of a Knoevenagel intermediate at the C3 position of 4-hydroxydithiocoumain, followed by a 1,4-cycloaddition reaction, which is explained thoroughly in Section **3.2**.

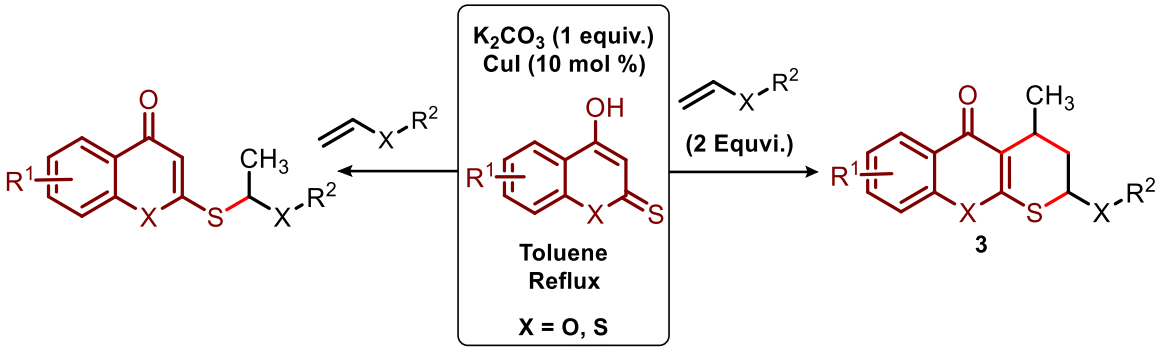

Scheme 6. Reaction of 4-hydroxydithiocoumarin with vinyl ether, styrene and phenyl acetylene

Vinyl ethers have numerous synthetic applications as monomers in polymer synthesis, [8] MCR,[9] Diels-Alder reactions,[10] and Claisen rearrangements.[11] They have also been exploited in the synthesis of natural products, new physiologically active molecules, and heterocycles.[12] Montevecchi *et al.* demonstrated the synthesis of thioether from pseudo-heterocyclic thiol and vinyl ether in the presence of AIBN.[13] In addition, Shu *et al.* reported the synthesis of pyrazole by using vinyl ether in the presence of a chiral Zr catalyst *via* C-H activation.[14] Still, the chemistry of vinyl ethers and their sulfur equivalents is under investigation and can be explored further to generate new chemistry.[15] On the other hand, organosulfur compounds are abundant in nature and significantly impact medicinal chemistry.[16] Among various organosulfur compounds, thiopyran derivatives exhibit a wide variety of biological activities, such as antimicrobial,[17] antitumor,[18] anticancer,[19] and antiviral activity. [19]

3.2 Results and Discussion

In continuation of our previous experience, here in this chapter, we report the synthesis of 4-methyl-3,4-dihydrothiopyran and 4-methyl thiopyran derivatives from 4-hydroxydithiocoumarin/4-hydroxy-2H-chromene-2-thione and vinyl ether/sulphide as presented in **Scheme 7**. The reaction proceeds in the presence of a cheap metal salt catalyst (10 mol% CuI) and a mild base (K_2CO_3) in toluene, affording the desired products in better yields with good atom economy. The reaction is highly regioselective for the C-C bond formation at the C-3 position of 4-hydroxydithiocoumarin/4-hydroxy-2H-chromene-2-thione with vinyl ether, followed by [4+2] cycloaddition of the Knoevenagel-type intermediate with another molecule of vinyl ether in the presence of CuI and results in the formation of **3a-p**, **5a-c**, and **6a-o**. However, the reaction of 4-hydroxydithiocoumarin/4-hydroxy-2*H*-chromene-2-thione with phenyl vinyl and ethyl

vinyl sulfide gives thioether through hydrothiolation **3q-s** and **7a-c,** respectively, as depicted in **Scheme 7**.

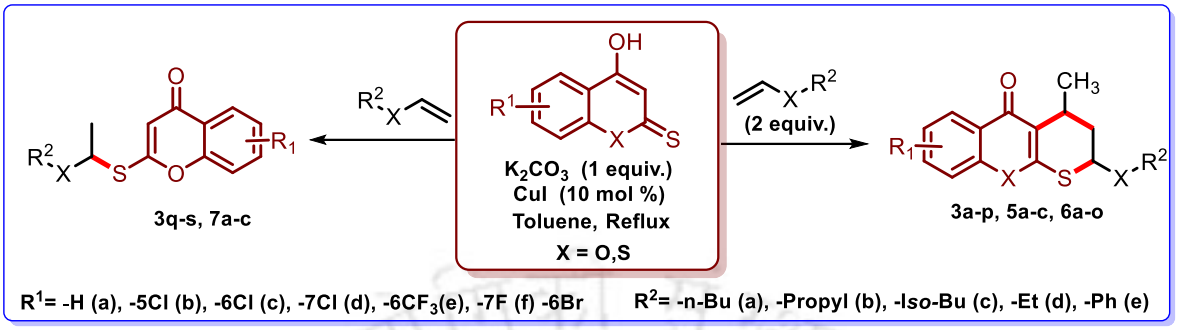

Scheme 7. Synthesis of thiopyran derivatives through a pseudo-three-component reaction

For our research investigation, various 4-hydroxydithiocoumarins **1a** and their derivatives, such as -5Cl (**b**), -6Cl (**c**), -7Cl (**d**), -6CF_3 (**e**), and -7F (**f**), were prepared using a previously reported method, which is mentioned in Chapter I, **Scheme 22**. The model substrates selected were 4-hydroxydithiocoumarin **1a** and butyl vinyl ether **2a**. The reaction was initially carried out with 4-hydroxydithiocoumarin (**1a**, 0.2 mmol) and butyl vinyl ether (2a, 0.2 mmol), using one equivalent of K2CO3 and 10 mol% of copper(I) iodide at room temperature (Table 1, entry 1). The product **3a** was isolated in a 20% yield, along with unreacted 4-hydroxydithiocoumarin, *via* column chromatography. Using ^{1}H NMR, ^{13}C NMR, and HRMS, the product was characterized as 2-butoxy-4-methyl-3,4-dihydro-2*H*,5*H*-thiopyrano[2,3-*b*]thiochromen-5-one (**3**). In ^{1}H NMR, the -CH_3 proton at the C4 position appears as a doublet at δ 1.33 ppm, J = 7.4 Hz, and the -CH_3 group attached to the ether shows a triplet at δ 0.90 ppm, J = 7.2 Hz of the anticipated product **3a**. A multiplet was observed at δ 5.16-5.15 (m, 1H), for one proton, which corresponds to the C4 proton. These characteristic peaks indicated the incorporation of vinyl ethers in the final products.

Similarly, in the ^{13}C NMR spectrum, eight signals are observed in the aliphatic region, including two at δ 70.4 and 83.2, corresponding to the carbon atom directly attached to oxygen. Furthermore, nine signals are observed in the aromatic range, indicating the different carbons of 4-hydroxydithiocoumarin, and δ 176.3 specifically indicates the carbonyl carbon. ^{1}H and ^{13}C NMR spectra, as well as HRMS, are shown in **Figures 3-5**. The compounds **3c** and **5c** were further recrystallised, and single-crystal XRD data were recorded; the details of the crystal structure are depicted in Figures **1** and **2**, respectively, at the end of this chapter.

After characterising under similar reaction conditions to increase the product yield, the reaction temperature was increased to 120˚C (Table 1, entries 2-5). However, the maximum yield was obtained at 110˚C (Table 1, entry 4). After that, there was no increase in the yield at 120˚C (Table 1, entry 5). In an effort to increase the yield of the reaction, the same reaction was conducted in the presence of other bases, such as Na_2CO_3 and Cs_2CO_3. However, the outcome was unfavourable (Table 1, entries 6 and 7). Organic bases such as pyridine and DABCO were also used to optimise the reaction, but lump formation occurred immediately upon addition of the bases, and no results were obtained (Table 1, entries 8 and 9). We employed CuBr and CuCl (Table 1, entries 10 and 11) during the catalyst screening, but the yields did not improve as anticipated. The reaction was examined in various solvents, including benzene, chlorobenzene, ACN, ethanol, and DMF, to determine solvent suitability; however, the results were disappointing, except for chlorobenzene (Table 1, entries 12-16). After evaluating various reaction conditions, it was concluded that the reaction of 4-hydroxydithiocoumarin (**1a**, 0.2 mmol) with butyl vinyl ether (**2a**, 0.4 mmol) in the presence of 1.0 equiv. of K_2CO_3, 10 mol% CuI in toluene at 110˚C is the best reaction condition (Table 1, entry 4).

After establishing the optimised reaction condition, the scope and generality of the present approach were investigated using substituted 4-hydroxydithiocoumarin **1a** and a variety of vinyl ethers: n-Bu (**2a**), iso-Bu (**2b**), propyl (**2c**), Et (**2d**), and Ph (**2e**). Despite their nature, 4-hydrodithiocoumarins **1a** and -5Cl (**1b**), -6Cl (**1c**), -7Cl (**1d**), and -7F (**1f**) were allowed to react with butyl vinyl ether 2a, and the products 3a-e were isolated in yields of 76-89%. Subsequently, 4-hydroxydithiocoumarin with substituents **1b**, **1d**, **1e**, and **1f** was subjected to isobutyl vinyl ether 2b, yielding the products **3f-i** in yields ranging from 69% to 79%, as shown in Table 2. Next, products **3j** and **3k** were achieved from the reaction of 4-hydroxydithiocoumarin **1a** and 7-fluoro-4-hydroxydithiocoumarin **1f** with propyl vinyl ether **2c**, yielding 83% and 89%, respectively. We executed the same reactions with ethyl vinyl ether **2d** and 4-hydroxydithiocoumarin derivatives **1a**, **1b**, **1c**, **1d**, and **1f**, obtaining product **3l-p** in yields ranging from 76% to 90%. However, when we performed the same reaction with 4-hydroxydithiocoumarin and phenyl vinyl ether **2e**, we isolated product **3q** in 63% yield, which was different from the earlier product. In this case, we found the product

without cyclisation, indicating that only one equivalent of phenyl vinyl ether reacted with 4-hydroxydithiocoumarin (**3q-s**, Table 5). ^{1}H and ^{13}C NMR, and HRMS, confirmed the anticipated product's structure. We also carried out the reaction of 6-chloro-4-hydroxydithiocoumarin and 6-trifluoromethyl-4-hydroxydithiocoumarin with phenyl vinyl ether, and the isolated yields of **3r** and **3s** were 59% and 70%, respectively.

Motivated by the successful results, we further investigated the generality of the procedure, scrutinising the reaction between 4-hydroxydithiocoumarin derivatives **1a**, **1b**, **1c**, **1d**, and **1e** and ethyl vinyl sulfide 4, which yielded products **5a-e** in yields ranging from 73% to 89%. The results are presented in Table 3.

Table 1. Optimisation of the reaction conditions [a,b]

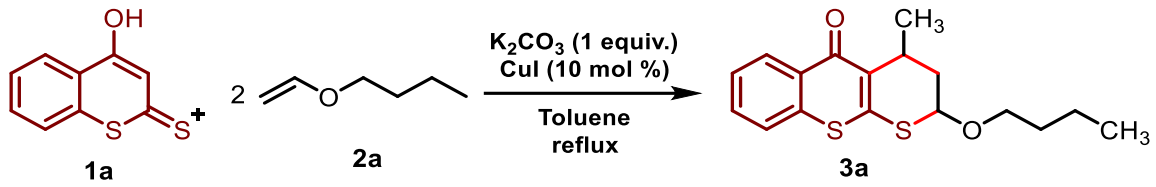

Entry	Base (1 equiv.)	Catalyst (10mol%)	Temp(°C)	Time (h)	Solvent	Yield [b] (%)
1[c]	K_2CO_3	CuI	RT	4	Toluene	20
2	K_2CO_3	CuI	60	1	Toluene	23
3	K_2CO_3	CuI	90	1	Toluene	40
4	**K_2CO_3**	**CuI**	**110**	**1**	**Toluene**	**83**
5	K_2CO_3	CuI	120	1	Toluene	80
6	Na_2CO_3	CuI	110	1	Toluene	23
7	Cs_2CO_3	CuI	110	1	Toluene	32
8	Py	CuI	110	1	Toluene	-
9	DABCO	CuI	110		Toluene	-
10	K_2CO_3	CuBr	110	1	Toluene	35
11	K_2CO_3	CuCl	110	1	Toluene	45
12	K_2CO_3	CuI	110	1	Benzene	58
13	K_2CO_3	CuI	110	1	PhCl	60
14	K_2CO_3	CuI	110	1	ACN	trace
15	K_2CO_3	CuI	110	1	Ethanol	trace

[a]All the reactions were carried out using 4-hydroxydithiocoumarin (**1a,** 0.2 mmol), vinyl butyl ether (**2a,** 0.4 mmol) in the presence of 10 mol% catalyst,1 equiv. of base in 1 ml of solvent at 110 °C. [b] Isolated yield. (Py) = Pyridine, DABCO = (1,4-diazabicyclo[2.2.2]octane).

Table 2. Substrate scope of substituted 4-hydroxydithiocoumarin with vinyl ether [a,b]

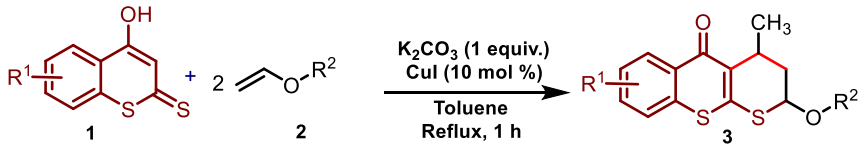

R^1= -H (a), -5Cl (b), -6Cl (c), -7Cl (d), -6CF_3(e), -7F (f), R^2= -*n*-Bu (2a), -Propyl (2b), -*Iso*-Bu (2c), -Et (2d), -Ph (2e)

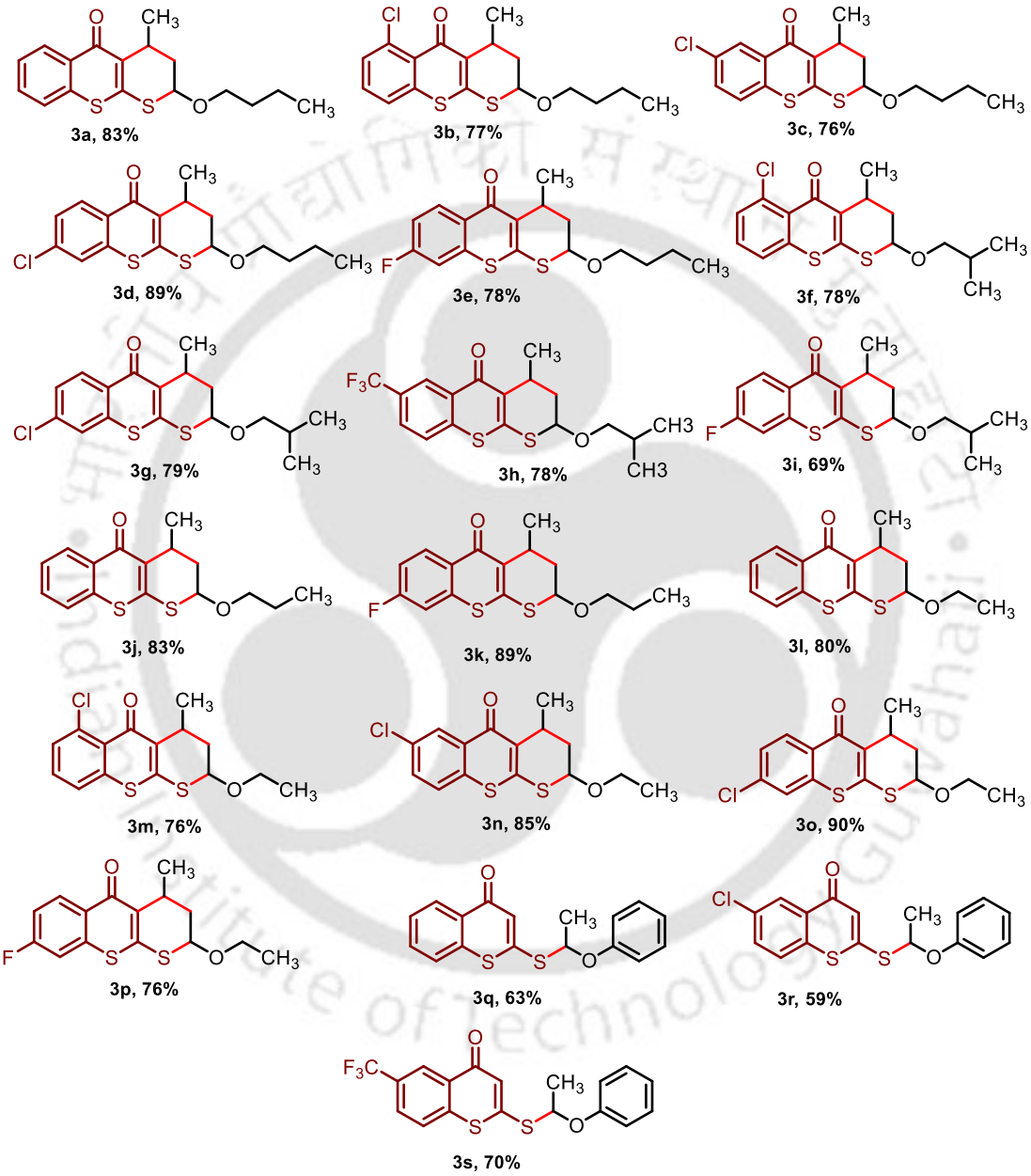

[a]All the reactions were carried out using 4-hydroxydithiocoumarin (1a-f, 0.2 mmol), and vinyl ether (2a-e, 0.4 mmol) in the presence of 10 mol% CuI, 1 equiv. K_2CO_3 in 1 ml of Toluene at 110 °C. [b]Isolated yield.

After synthesising the products **3a-s** and **5a-e**, encouraged by these successful results, we conceived that 4-hydroxy-2*H*-chromene-2-thione could be explored as it shares a similar structure with 4-hydroxydithiocoumarin. Accordingly, a similar reaction was also carried out between 4-hydroxy-2H-chromene-2-thione 1a′ and butyl vinyl ether 2a, resulting in the formation of the final product 6a, which was subsequently confirmed by NMR. In ^{1}H NMR, the proton at the C-4 position appears as a doublet at δ 1.41 ppm, *J* = 7.2 Hz, and the -CH_3 attached to the ether shows a triplet at δ 0.91 ppm, *J* =7.4 Hz **6a**. To check the reaction vulnerability, 4-hydroxy-2*H*-chromene-2-thione derivatives such as **1a′**, **1b′**, **1d′** and **1e′** were subjected to vinyl ether **2a** and yielded products (**6a-d**) in 71-80%. Optimistically, 4-hydroxythiocoumarin derivatives **1a′, 1b′**, **1c′** and **1e′** were reacted with Isobutyl vinyl ether **2b**, giving products **6e-h** (70-90%). Propyl vinyl **2c** and ethyl vinyl ether **2d** were also reacted with differently substituted 4-hydroxy-2*H*-chromene-2-thiones, such as **1a′, 1b′, 1e′,** and **1f′,** and yielded the products **6j-o**. We also found hydrothiolation products in the case of ethyl vinyl sulfide **4** reaction with 4-hydroxy-2*H*-chromene-2-thione, which yielded (83-85%). That means only one equivalent of vinyl sulfide was consumed in the reaction to form the uncyclized product (**7a-c**). The results are shown in Tables 4 and 5.

Table 3. Substrate scopes of substituted 4-hydroxydithiocoumarin with ethyl vinyl sulfide[a,b]

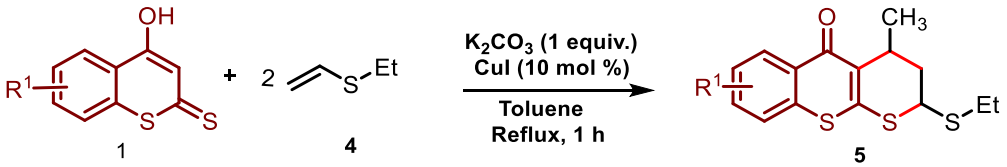

R[1]= -H (a), -5Cl (b), -6Cl (c), -7Cl (d), -6CF$_3$(e)

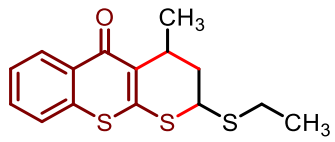

5a, 82 %

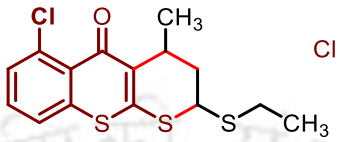

5b, 83%

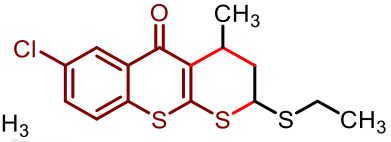

5c, 89%

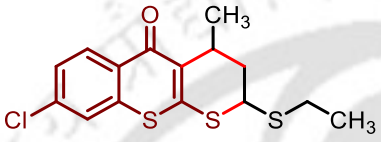

5d, 85 %

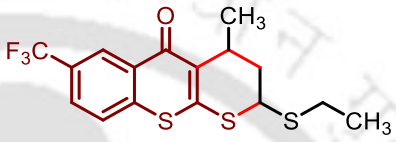

5e, 73%

[a]All the reactions were carried out using 4-hydroxydithiocoumarin (1a-e, 0.2 mmol), ethyl vinyl sulfide (4, 0.4 mmol) in the presence of 10 mol% CuI, 1 equiv. K_2CO_3 in 1 ml of toluene at 110 °C. [b] Isolated yield.

Table 4. Substrate scopes of substituted 4-hydroxy-2*H*-chromene-2-thione with vinyl ether [a,b]

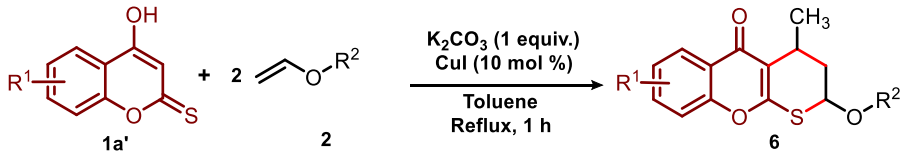

R^1= -H (a'), -6Cl (b'), -6F (c') -7F (d'), -6Br (e'), R^2= -*n*-Bu (2a),-*Iso*-Bu (2b), -Prop (2c), -Et (2d)

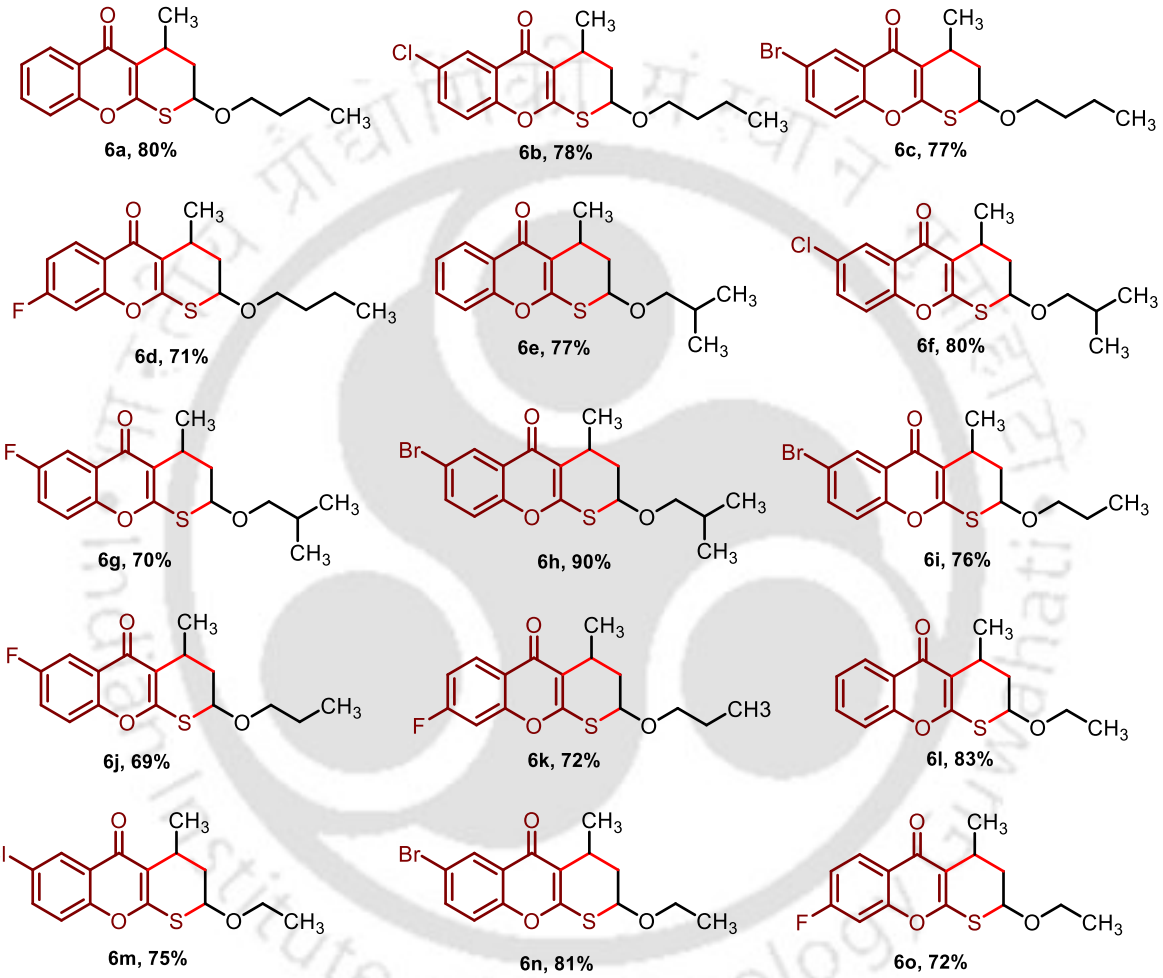

[a]All the reactions were carried out using 4-hydroxy-2*H*-chromene-2-thione (1a′, 0.2 mmol), vinyl ethers (2a, 0.4 mmol) in presence of 10 mol% CuI, 1 equiv. K_2CO_3 in 1 ml of toluene at 110 ˚C.
[b] Isolated yield.

Table 5. Substrate scopes of substituted 4-hydroxy-2*H*-chromene-2-thione with ethyl vinyl sulfide [a,b]

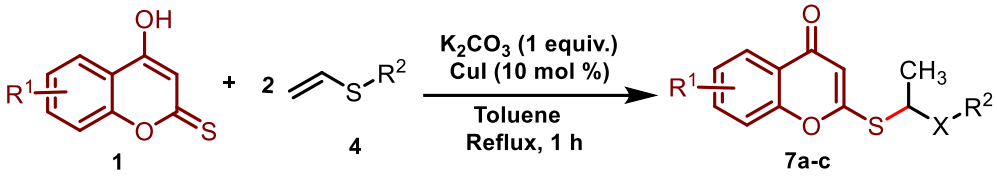

R^1= -H (a'), -6Cl (b'), -6F (c') -7F (d'), -6Br (e'), R^2 = -Et,

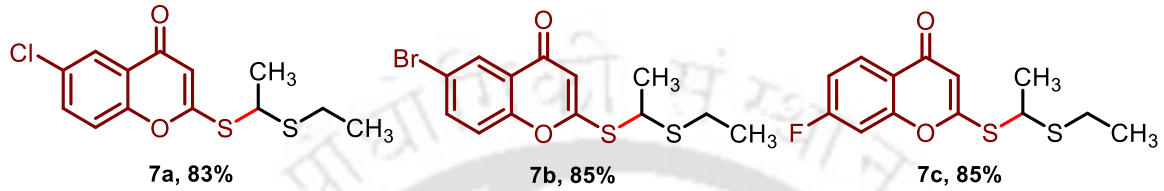

[a]All the reactions were carried out using 4-hydroxydithiocoumarin/4-hydroxy-2H-chromene-2-thione (1a, 0.2 mmol), phenyl vinyl ether ethyl vinyl sulfide (4a, 0.4 mmol) in presence of 10 mol% CuI, 1 equiv. K_2CO_3 in 1 ml of toluene at 110 ˚C. [b] Isolated yield.

3.3 Possible Reaction Mechanism

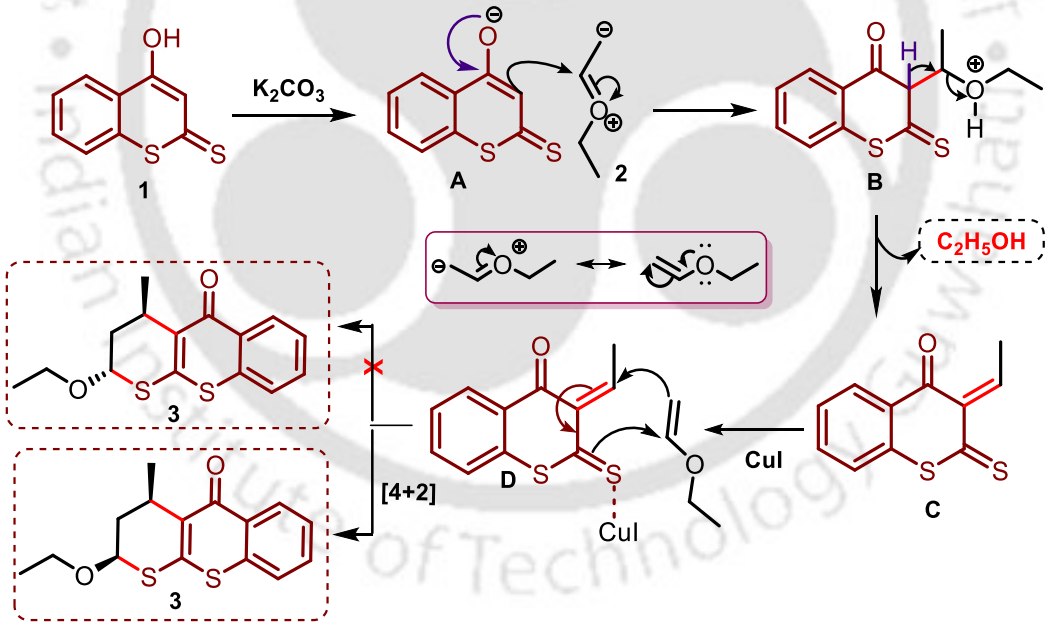

Scheme 8. Schematic diagram of reaction mechanism

The proposed mechanism is based on the previously reported literature and the isolated products obtained from the experiment. In the very first step, K_2CO_3 abstracts the acidic proton from the 4-hydroxy position, resulting in the formation of an anionic species **A**, which further reacts with the electron-rich olefin **2** (vinyl ether)[20] to give intermediate **B**. It gets converted into a Knoevenagel-type intermediate **C** through the elimination of

ethanol. Finally, the intermediate **C** undergoes [4+2] cycloaddition with the electron-rich olefin (vinyl ether) in the presence of CuI through the addition to afford the final desired product **3** as shown in **Scheme 8**.

Conclusion:

In the current protocol, we present a novel one-step route to thiopyrans *via* a pseudo-three-component reaction. The reaction is highly regioselective for the C-C bond formation at the C-3 position of 4-hydroxydithiocoumarin/4-hydroxy-2H-chromene-2-thione with vinyl ether, followed by [4+2] cycloaddition of the Knoevenagel-type intermediate with another molecule of vinyl ether in the presence of CuI. The use of a less expensive Cu(I) salt, gentle reaction conditions, high yields, excellent regioselectivity, a shorter reaction time, good atom economy, and a broad substrate scope make this approach highly practical. Interestingly, we found that 4-hydroxydithiocoumarin/4-hydroxy-2H-chromene-2-thione exhibits different reactivity towards vinyl ether than towards styrene.

During the reaction, both 4-hydroxydithiocoumarin and 4-hydroxy-2H-chromene-2-thione showed similar reactivity toward vinyl ether. However, with ethyl vinyl sulfide, their reactivity differed: 4-hydroxy-2H-chromene-2-thione reacted with 1 equivalent of vinyl ether, while 4-hydroxydithiocoumarin reacted with 2 equivalents.

During the course of the reaction, it was observed that both 4-hydroxydithiocoumarins and 4-hydroxy-2*H*-chromene-2-thione showed similar reactivity with vinyl ether. However, with ethyl vinyl sulfide, their reactivity differed: 4-hydroxy-2H-chromene-2 reacts with 1 equivalent of vinyl ether, while 4-hydroxydithiocoumarin reacts with 2 equivalents of vinyl ether. A similar reactivity was observed in the reaction between 4-hydroxydithiocoumarin and phenyl vinyl ether, where again, only one equivalent of the vinyl ether was consumed.

3.5 Experimental section:

General procedure for synthesising 4-methyl-3,4-dihydrothiopyran derivatives from 4-hydroxydithiocoumarin and 4-hydroxy-2*H*-chromene-2-thione

To a 10-mL round-bottom flask, a mixture of 4-hydroxydithiocoumarin/4-hydroxy-2*H*-chromene-2-thione (0.20 mmol) and alkyl vinyl ether (0.40 mmol) in 1mL toluene (1 equiv.) K_2CO_3 and (10 mol% CuI) were added one after another. The mixture was refluxed in an oil bath with constant stirring, and the reaction progress was monitored by TLC. After the reaction was completed, the mixture was extracted with ethyl acetate. The mixture was dried using anhydrous Na_2SO_4 and then concentrated using a rotary evaporator. It was then purified by column chromatography using silica gel 60-120 mesh and a solvent mixture of ethyl acetate/hexane (2.5:97.5). Melting points were determined using a melting point apparatus. ^1H and ^{13}C NMR spectra were recorded on 400 and 500 MHz NMR spectrometers. TMS was used as an internal reference; chemical shifts (δ scale) are reported in parts per million(ppm).

3.6 Characterization Table:

2-Butoxy-4-methyl-3,4-dihydro-2*H*,5*H*-thiopyrano[2,3-*b*]thiochromen-5-one(3a):

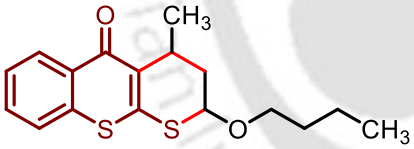

A yellow viscous liquid (53 mg, Yield -83%) ^1H NMR (500 MHz, $CDCl_3$) δ 8.46 (dd, *J* = 8.0, 1.5 Hz, 1H), 7.52 – 7.48 (m, 1H), 7.46 – 7.42 (m, 1H), 7.40 (dd, *J* = 7.9, 1.4 Hz, 1H), 5.16 (t, *J* = 3.3 Hz, 1H), 3.84 – 3.79 (m, 1H), 3.71 – 3.68 (m, 1H), 3.42 – 3.28 (dt, *J* = 8.9, 6.2 Hz, 1H), 2.45 (dt, *J* = 14.3, 3.1 Hz, 1H), 2.17 – 2.12 (m, 1H), 1.63 – 1.56 (m, 2H), 1.39 (q, *J* = 7.1, 6.3 Hz, 2H), 1.32 (d, *J* = 7.2 Hz, 3H), 0.92 (t, *J* = 7.4 Hz, 3H); $^{13}C\{^1H\}$ NMR (125 MHz, $CDCl_3$) δ 176.3, 145.6, 136.6, 132.0, 130.9, 130.7, 129.4, 127.1, 124.8, 83.2, 70.4, 35.6, 31.6, 26.3, 19.4, 18.8, 13.8. IR (KBr)ν_{max} /cm^{-1} 2930 (C–H), 1620 (C=O), 1248 (C–O); HRMS (ESI): m/z [M+H^+] calcd for $C_{17}H_{21}O_2S_2$ 321.0977; Found 321.1002.

2-Butoxy-6-chloro-4-methyl-3,4-dihydro-2*H*,5*H*-thiopyrano[2,3-*b*]thiochromen-5-one (3b):

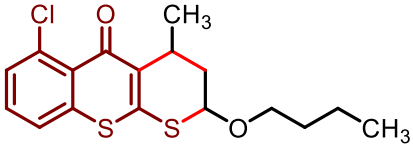

A light yellow liquid (54 mg, Yield-77%)^1H NMR (400 MHz, $CDCl_3$) δ 7.45 (dd, *J* = 7.0, 2.0 Hz, 1H), 7.37 – 7.31 (m, 2H), 5.15 (t, *J* = 3.3 Hz, 1H), 3.81

(dt, *J* = 8.9, 6.6 Hz, 1H), 3.70 – 3.65 (m, 1H), 3.44 – 3.38 (m, 1H), 2.43 (dt, *J* = 14.3, 3.6 Hz, 1H), 2.18 – 2.13 (m, 1H), 1.59 – 1.53 (m, 2H), 1.44 – 1.36 (m, 2H), 1.31 (d, *J* = 7.2 Hz, 3H), 0.92 (t, *J* = 7.4 Hz, 3H); $^{13}C\{^{1}H\}$ NMR (100 MHz, $CDCl_3$) δ 176.4, 142.5, 139.2, 136.1, 133.3, 131.0, 130.4, 127.4, 124.0, 83.0, 70.5, 36.0, 31.5, 26.8, 19.4, 19.0, 13.9. IR(KBr)ν_{max} /cm^{-1} 2930 (C− H),1620 (C=O),1272 (C− O); HRMS (ESI): m/z [M+H^+] calcd for $C_{17}H_{20}ClO_2S_2$ 355.0588; found:355.0582.

2-Butoxy-7-chloro-4-methyl-3,4-dihydro-2*H*,5*H*-thiopyarno[2,3-*b*]thiochromen-5-one (3c): A light yellow crystal, (53 mg, Yield-76%) mp 105 °C,^{1}H NMR (400 MHz, $CDCl_3$) δ 8.45 (d, *J* = 2.3 Hz, 1H), 7.47 (dd, *J* = 8.6, 2.4 Hz, 1H), 7.36 (d, *J* = 8.6 Hz, 1H), 5.17 (td, *J* = 3.2, 0.8 Hz, 1H), 3.82 (dt, *J* = 8.9, 6.6 Hz, 1H), 3.70 – 3.65 (m, 1H), 3.43 – 3.38 (m, 1H), 2.46 (dt, *J* = 14.3, 3.0 Hz, 1H), 2.17-2.11 (m, 1H), 1.64 – 1.60 (m, 2H), 1.43 – 1.36 (m, 2H), 1.31 (d, *J* = 7.2 Hz, 3H), 0.92 (t, *J* = 7.4 Hz, 3H); $^{13}C\{^{1}H\}$ NMR (100 MHz, $CDCl_3$) δ 175.2, 146.1, 134.7, 133.5, 131.9, 131.7, 131.3, 129.0, 126.3, 83.3, 70.4, 35.4, 31.5, 26.3, 19.4, 18.8, 13.9. IR(KBr)ν_{max}/cm^{-1} 2925 (C−H), 1610 (C=O), 1260 (C−O); HRMS (ESI): m/z [M+H^+] calcd for $C_{17}H_{20}ClO_2S_2$ 355.0588 found 355.0612.

2-Butoxy-8-chloro-4-methyl-3,4-dihydro-2*H*,5*H*-thiopyrano[2,3-*b*]thiochrome-5-one (3d): A yellow viscous liquid (63 mg, Yield-89%) ^{1}H NMR (500 MHz, $CDCl_3$) δ 8.40 (d, *J* = 8.5 Hz, 1H), 7.41 – 7.38 (m, 2H), 5.17 (t, *J* = 3.3 Hz, 1H), 3.84 – 3.80 (m, 1H), 3.68-3.65 (m, 1H), 3.43-3.38 (m, 1H), 2.46 (dt, *J* = 14.3, 3.0 Hz, 1H), 2.16-2.12 (m, 1H), 1.63 – 1.59 (m, 2H), 1.42 – 1.37 (m, 2H), 1.31 (d, *J* = 5 Hz, 3H), 0.92 (t, *J* = 7.4 Hz, 3H); $^{13}C\{^{1}H\}$ NMR (100 MHz, $CDCl_3$) δ 175.6, 145.6, 137.9, 137.6, 132.2, 131.1, 129.0, 127.8, 124.1, 83.3, 70.5, 35.4, 31.5, 26.2, 19.4, 18.8, 13.9. IR(KBr)ν_{max} cm^{1} /cm^{-1} 2925 (C−H), 1621 (C=O), 1243 (C−O); HRMS (ESI): m/z [M+H^+] calcd for $C_{17}H_{20}ClO_2S_2$ 355.0588 found 355.0605.

2-Butoxy-8-fluoro-4-methyl-3,4-dihydro-2*H*,5*H*-thiopyrano[2,3-*b*]thiochrome-5-one (3e): A colourless solid (52 mg, Yield-78%); mp 111 ºC, 1H NMR (400 MHz, CDCl3) δ 8.49 (dd, J = 9.0, 5.9 Hz, 1H), 7.15 (ddd, J = 9.0, 8.1, 2.5 Hz, 1H), 7.11 (dd, J = 8.4, 2.4 Hz, 1H), 5.19 – 5.15 (m, 1H), 3.82 (dt, J = 8.9, 6.5 Hz, 1H), 3.71

– 3.63 (m, 1H), 3.41 (dt, J = 8.9, 6.2 Hz, 1H), 2.46 (dt, J = 14.4, 3.0 Hz, 1H), 2.14 (ddd, J = 14.4, 5.2, 3.5 Hz, 1H), 1.67 – 1.60 (m, 2H), 1.40 (dtd, J = 14.3, 7.4, 1.4 Hz, 2H), 1.32 (d, J = 7.2 Hz, 3H), 0.92 (t, J = 7.4 Hz, 3H); 13C{1H} NMR (100 MHz, CDCl3) δ 175.5, 163.7 (d, J = 253 Hz) 145.3, 138.6 (d, J = 9.7 Hz), 132.5 (d, J = 9.5 Hz),132.0, 127.3, 115.7 (d, J = 22 Hz), 110.7 (d, J = 24 Hz), 83.2, 70.4, 35.5, 31.5, 26.2, 19.4, 18.8, 13.9; IR(KBr)νmax/cm-1 2926 (C−H), 1619 (C=O), 1242 (C−O); HRMS (ESI): m/z [M+H$^+$] calcd for $C_{17}H_{20}FO_2S_2$ 339.0883 found 339.0874.

6-Chloro-2-isobutoxy-4-methyl-3,4-dihydro-2*H*,5*H*-thiopyrano[2,3-*b*]thiochrom-

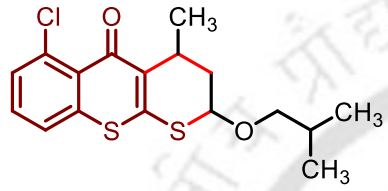

en-5-one (3f): A yellow viscous liquid (55 mg, Yield-78%)1H NMR (400 MHz, CDCl3) δ 7.44 (dd, J = 7.1, 2.0 Hz, 1H), 7.36 – 7.29 (m, 2H), 5.13 (t, J = 3.2 Hz, 1H), 3.73 – 3.64 (m, 1H), 3.57 (dd, J = 8.6, 6.7 Hz, 1H), 3.18 (dd, J = 8.6, 6.1 Hz, 1H), 2.44 (dt, J = 14.3, 3.5 Hz, 1H), 2.16 – 2.12 (m, 1H), 1.87 (dq, J = 12.1, 6.0, 5.5 Hz, 1H), 1.31 (d, J = 7.2 Hz, 3H), 0.92 (d, J = 6.7 Hz, 6H); 13C{1H} NMR (100 MHz, CDCl3) δ 176.3, 142.6, 139.2, 136.1, 133.2, 131.0, 130.4, 127.3, 123.9, 83.2, 77.4, 35.9, 28.5, 26.6, 19.4, 19.3, 19.1. IR(KBr)νmax/cm-12924 (C−H), 1623 (C=O), 1244 (C− O); HRMS (ESI): m/z [M+Na+] calcd for $C_{17}H_{20}ClO_2S_2$ 355.0588 found 355.0609.

8-Chloro-2-*iso*butoxy-4-methyl-3,4-dihydro-2*H*,5*H*-thiopyrano[2,3-*b*]thiochrom-

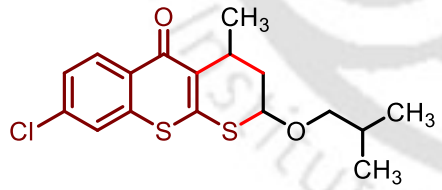

en-5-one (3g): A yellow solid (56 mg, Yield-79%). mp 154 ºC, ^{1}H NMR (500 MHz, $CDCl_3$) δ 8.39 (d, *J* = 8.6 Hz, 1H), 7.40 (d, *J* = 11.1 Hz, 2H), 5.16 (s, 1H), 3.68 (dd, *J* = 9.1, 4.8 Hz, 1H), 3.62 – 3.57 (m, 1H), 3.19 (dd, *J* = 8.3, 6.3 Hz, 1H), 2.47 (d, *J* = 14.3 Hz, 1H), 2.14 (dt, *J* = 14.3, 4.2 Hz, 1H), 1.90 (dt, *J* = 13.1, 6.6 Hz, 1H), 1.33 (d, *J* = 7.2 Hz, 3H), 0.93 (d, *J* = 6.7 Hz, 6H); ^{13}C{^{1}H} NMR (100 MHz, $CDCl_3$) δ 176.4, 142.5, 139.2, 136.2, 133.3, 131.1, 130.9, 127.4, 124.0, 83.2, 77.5, 35.9, 28.5, 26.7, 19.4 (2C), 19.1; IR(KBr)ν_{max}/cm^{-1} 2924 (C−H), 1611 (C=O), 1272 (C−O); HRMS (ESI): m/z [M+H$^+$] calcd for $C_{17}H_{20}ClO_2S_2$ 355.0588 found 355.0590.

2-Isobutoxy-4methyl-7-(trifluoromethyl)-3,4-dihydro-2*H*,5*H*-thiopyrano[2,3-*b*] thiochromen-5-one (3h): 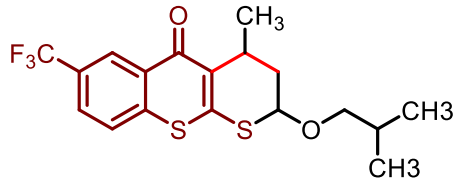

A yellow solid (60 mg, Yield-78%) mp 144 ºC 1H NMR (500 MHz, CDCL3) δ 8.76 – 8.73 (m, 1H), 7.71 (dd, J = 8.4, 2.1 Hz, 1H), 7.53 (d, J = 8.4 Hz, 1H), 5.17 (t, J = 3.2 Hz, 1H), 3.69 (ddd, J = 7.7, 5.1, 2.8 Hz, 1H), 3.59 (dd, J = 8.6, 6.6 Hz, 1H), 3.20 (dd, J = 8.5, 6.1 Hz, 1H), 2.49 (dt, J = 14.3, 3.0 Hz, 1H), 2.17-2.12 (m, 1H), 1.93 – 1.87 (m, 1H), 1.34 (d, J = 7.2 Hz, 3H), 0.93 (d, J = 6.7 Hz, 6H); 13C{1H} NMR (125 MHz, CDCl3) δ 175.3, 147.5, 146.2, 140.2, 132.4, 130.6, 129.5 (q, J = 33 Hz), 126.9 (q, J = 3.2 Hz), 125.7, 123.7 (q, J = 270 Hz), 83.5, 77.5, 35.3, 28.5, 26.2, 19.4, 19.3, 18.8. IR(KBr)νmax/cm-1 2925 (C−H), 1603 (C=O), 1262 (C−O); HRMS (ESI): m/z [M+H$^+$] calcd for $C_{18}H_{20}F_3O_2S_2$ 389.866 found 389.0866.

8-Fluoro-2-*iso*butoxy-4-methyl-3,4-dihydro2*H*,5*H*-thiopyrano[2,3-*b*]thiochromen-5-one (3i): 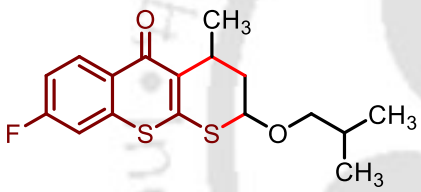

A light yellow liquid, (46 mg, Yield-69%)^{1}H NMR (500 MHz, $CDCl_3$) δ 8.48 (dd, *J* = 9.0, 5.9 Hz, 1H), 7.15 (td, *J* = 8.5, 2.5 Hz, 1H), 7.10 (dd, *J* = 8.5, 2.5 Hz, 1H), 5.15 (t, *J* = 3.2 Hz, 1H), 3.71-3.57 (m, 1H), 3.59 (dd, *J* = 8.6, 6.7 Hz, 1H), 3.19 (dd, *J* = 8.5, 6.1 Hz, 1H), 2.47 (dt, *J* = 14.4, 3.0 Hz, 1H), 2.14 (ddd, *J* = 14.4, 5.2, 3.6 Hz, 1H), 1.93-1.85 (m, 1H), 1.33 (d, *J* = 7.2 Hz, 3H), 0.93 (d, *J* = 6.7 Hz, 6H); ^{13}C{^{1}H} NMR (100 MHz, $CDCl_3$) δ 175.4, 163.7 (d, *J* = 253.8 Hz), 145.4, 138.7 (d, *J* = 9.7 Hz), 132.6 (d, *J* = 9.6 Hz), 131.9, 127.3 (d, *J* = 2.3 Hz), 115.7 (d, *J* = 2.2 Hz), 110.8 (d, *J* = 24.5 Hz), 83.4, 35.4, 28.5, 26.1, 19.4, 19.4 (2C), 18.8. IR(KBr)ν_{max}/cm^{-1} 2927 (C− H), 1623 (C=O),1244 (C− O) HRMS (ESI): m/z [M+H$^+$] calcd for $C_{17}H_{20}FO_2S_2$ 339.0883; found 339.0876.

4-Methyl-2-propoxy-3,4-dihydro-2*H*,5*H*-thiopyrano[2,3-b]thiochromen-5-one(3j) : 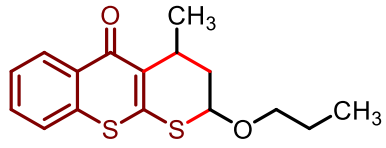

A dark yellow liquid, (50 mg, Yield-83%) ^{1}H NMR (500 MHz, $CDCl_3$) δ 8.47 (dd, *J* = 8.0, 1.2 Hz, 1H), 7.53 – 7.49 (m, 1H), 7.47 – 7.40 (m, 2H), 5.17 (t, *J* = 3.0 Hz, 1H), 3.78 (dt, *J* = 8.7, 6.6 Hz, 1H), 3.73 – 3.68 (m, 1H), 3.38 (dt, *J* = 8.7, 6.3 Hz, 1H), 2.47 (dt, *J* = 14.3, 3.0 Hz, 1H), 2.18 – 2.13 (m, 1H), 1.64 (dt, *J* = 13.9, 6.9 Hz, 2H), 1.33 (d, *J* = 7.2 Hz, 3H), 0.95 (t, *J* = 7.4 Hz, 3H). ^{13}C{^{1}H} NMR (125 MHz, $CDCl_3$) δ 176.3, 145.6, 136.6, 132.0, 131.0, 130.7, 129.4, 127.2, 124.8,

83.2, 72.3, 35.6, 26.3, 22.9, 18.8, 10.8. IR(KBr)ν_{max}/cm^{-1} 2927 (C−H), 1623 (C=O), 1244 (C−O); HRMS (ESI): m/z [M+H$^+$] calcd for $C_{16}H_{19}O_2S_2$ 307.0821 found 307.0821.

8-Fluoro-4-methyl-2-propoxy-3,4-dihydro-2*H*,5*H*-thiopyarno[2,3-*b*]thiochromen-5-one (3k): A yellow solid (58 mg, Yield-89%). mp 154 ºC,^{1}H NMR (400 MHz, $CDCl_3$) δ 8.48 (dd, *J* = 9.0, 5.9 Hz, 1H), 7.15 (td, *J* = 8.6, 2.5 Hz, 1H), 7.10 (dd, *J* = 8.5, 2.4 Hz, 1H), 5.17 (t, *J* = 3.1 Hz, 1H), 3.80 – 3.74 (m, 1H), 3.69 – 3.65 (m, 1H), 3.40 – 3.35 (m, 1H), 2.47 (dt, *J* = 14.3, 3.0 Hz, 1H), 2.17 – 2.11 (m, 1H), 1.64 – 1.61 (m, 2H), 1.32 (d, *J* = 7.2 Hz, 3H), 0.94 (t, *J* = 7.4 Hz, 3H); ^{13}C{^{1}H} NMR (100 MHz, $CDCl_3$) δ 175.5, 163.7 (d, *J* = 253.8 Hz), 145.4, 138.6 (d, *J* = 9.7 Hz), 132.5 (d, *J* = 9.5 Hz), 131.9, 127.3, 115.7 (d, *J* = 22.2 Hz), 110.7 (d, *J* = 24.6 Hz), 83.2, 72.3, 35.5, 26.2, 22.8, 18.8, 10.8. IR(KBr)ν_{max}/cm^{-1} 2926 (C−H), 1615 (C=O), 1251 (C−O) HRMS (ESI): m/z [M+H$^+$] calcd for $C_{16}H_{18}FO_2S_2$ 325.0727 found 325.728.

2-Ethoxy-4-methyl-3,4-dihydro-2*H*,5*H*-thiopyrano[2,3-*b*]thio chromen-5-one (3l): A Brown liquid; (46 mg, Yield-80%)^{1}H NMR (500 MHz, $CDCl_3$) δ 8.47 (dd, *J* = 8.0, 1.6 Hz, 1H), 7.51 (td, *J* = 7.5, 1.6 Hz, 1H), 7.47 – 7.44 (m, 1H), 7.43 – 7.41 (m, 1H), 5.18 (t, *J* = 3.3 Hz, 1H), 3.91 – 3.85(m, 1H), 3.72 – 3.67 (m, 1H), 3.46 (dq, *J* = 8.9, 7.0 Hz, 1H), 2.46 (dt, *J* = 14.3, 3.1 Hz, 1H), 2.19 – 2.14 (m, 1H), 1.33 (d, *J* = 7.2 Hz, 3H), 1.25 (t, *J* = 7.1 Hz, 3H); ^{13}C{^{1}H} NMR (125 MHz, $CDCl_3$) δ 176.3, 145.5, 136.6, 132.0, 131.0, 130.6, 129.4, 127.2, 124.8, 82.8, 66.0, 35.6, 26.3, 18.8, 15.0. IR(KBr)ν_{max}, /cm^{-1} 2929 (C−H), 1611 (C=O), 1241 (C−O); HRMS (ESI): m/z [M+H$^+$] calcd for $C_{15}H_{17}O_2S_2$ 293.0664 found 293.0664.

6-Chloro-2-ethoxy-4-methyl-3,4-dihydro-2*H*,5*H*-thiopyrano[2,3-*b*] thiochromen-5-one (3m): A white solid (49 mg, Yield-76%); mp 87 ºC,^{1}H NMR (400 MHz, $CDCl_3$) δ 7.45 (dd, *J* = 7.0, 2.0 Hz, 1H), 7.37 – 7.30 (m, 2H), 5.16 (t, *J* = 3.4 Hz, 1H), 3.86 (dq, *J* = 9.0, 7.0 Hz, 1H), 3.72 – 3.64 (m, 1H), 3.47 (dq, *J* = 9.0, 7.0 Hz, 1H), 2.43 (dt, *J* = 14.3, 3.8 Hz, 1H), 2.20 – 2.14 (m, 1H), 1.31 (d, *J* = 7.1 Hz, 3H), 1.25 (s, 3H); ^{13}C{^{1}H} NMR (100 MHz, $CDCl_3$) δ 175.1, 145.9, 134.6, 133.4, 131.8, 131.6, 131.2, 128.9, 126.1, 82.8, 66.0, 35.3, 26.2, 18.6, 14.9. IR(KBr)ν_{max}/cm^{-1}2926 (C−H), 1619 (C=O), 1273 (C−O) HRMS (ESI) m/z [M+H$^+$] calcd for $C_{15}H_{16}ClO_2S_2$ 327.0275 found 327.0275.

7-Chloro-2-ethoxy-4-methyl-3,4-dihydro-2*H*,5*H*-thiopyrano [2,3-*b*] thiochromen-5-one (3n): 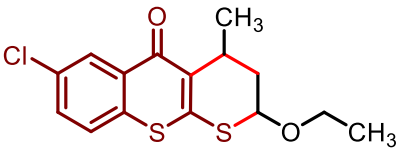
A brown solid (55 mg, Yield-85%); mp 110 ºC,^{1}H NMR (400 MHz, $CDCl_3$) δ 8.45 (d, *J* = 2.3 Hz, 1H), 7.47 (dd, *J* = 8.6, 2.4 Hz, 1H), 7.36 (d, *J* = 8.7 Hz, 1H), 5.18 (td, *J* = 3.3, 0.8 Hz, 1H), 3.91-3.84 (m, 1H), 3.71 – 3.63 (m, 1H), 3.50 – 3.42 (m, 1H), 2.46 (dt, *J* = 14.4, 3.1 Hz, 1H), 2.18 – 2.12 (m, 1H), 1.32 (d, *J* = 7.2 Hz, 3H), 1.25 (t, *J* = 7.0 Hz, 3H); ^{13}C{^{1}H} NMR (100 MHz, $CDCl_3$) δ 175.2, 146.0, 134.7, 133.5, 131.9, 131.7, 131.3, 129.0, 126.3, 82.9, 66.1, 35.5, 26.3, 18.7, 15.0. IR(KBr)ν_{max}/cm^{-1}

2924 (C− H), 1614 (C=O),1251 (C− O); HRMS (ESI) m/z [M+H^{+}] calcd for $C_{15}H_{16}ClO_2S_2$ 327.0275 found 327.0279.

8-Chloro-2ethoxy-4-methyl-3,4-dihydro-2H,5H-thiopyrano[2,3-b]thiochromen-5-one (3o): 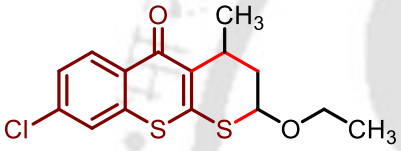
An orange solid (58 mg, Yield-90%); mp 113 ºC,1H NMR (400 MHz, CDCl3) δ 8.39 (dd, J = 8.5, 0.7 Hz, 1H), 7.42 – 7.38 (m, 2H), 5.18 (t, J = 3.4 Hz, 1H), 3.92 – 3.84 (m, 1H), 3.70 – 3.62 (m, 1H), 3.46 (dq, J = 9.0, 7.0 Hz, 1H), 2.46 (dt, J = 14.4, 3.1 Hz, 1H), 2.17 – 2.12 (m, 1H), 1.32 (d, J = 7.2 Hz, 3H), 1.25 (t, J = 7.0 Hz, 3H); 13C{1H} NMR (100 MHz, CDCl3) δ 175.6, 145.5, 137.9, 137.6, 132.1, 131.1, 129.0, 127.8, 124.1, 82.9, 66.1, 35.5, 26.3, 18.8, 15.0. IR(KBr)νmax/cm-1 2929 (C−H), 1612 (C=O), 1296 (C–O), HRMS (ESI):m/z [M+H+] calcd for $C_{15}H_{16}ClO_2S_2$ 327.0275 found 327.0294.

2-Ethoxy-8-fluoro-4-methyl-3,4-dihydro-2*H*,5*H*-thiopyrano [2,3-*b*]thiochromen-5-one (3p): 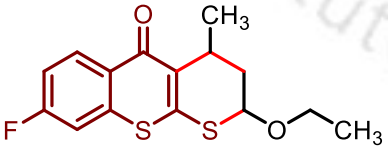
A yellow soild (47 mg, Yield-76%); mp 87 ºC, ^{1}H NMR (500 MHz, $CDCl_3$) δ 8.48 (dd, *J* = 9.0, 5.9 Hz, 1H), 7.17 – 7.13 (m, 1H), 7.10 (dd, *J* = 8.4, 2.5 Hz, 1H), 5.18 (t, *J* = 3.3 Hz, 1H), 3.88 (dq, *J* = 8.9, 7.0 Hz, 1H), 3.69 – 3.63 (m, 1H), 3.46 (dq, *J* = 8.9, 7.0 Hz, 1H), 2.46 (dt, *J* = 14.4, 3.1 Hz, 1H), 2.17 – 2.12 (m, 1H), 1.32 (d, *J* = 7.2 Hz, 3H), 1.25 (t, *J* = 7.0 Hz, 3H); ^{13}C{^{1}H} NMR (100 MHz, $CDCl_3$) δ 175.5, 163.8 (d, *J* = 253.8 Hz), 145.2, 138.6 (d, *J* = 9.7 Hz), 132.6 (d, *J* = 9.7 Hz), 131.9, 127.3 (d, *J* = 2.5 Hz), 115.7 (d, *J* = 22.1 Hz), 110.8 (d, *J* = 24.6 Hz), 82.8, 66.1, 35.5, 26.2, 18.8, 15.0; IR(KBr)ν_{max} /cm^{-1} 2958 (C−H),1612 (C=O),1296 (C−O), HRMS (ESI) m/z [M+H^{+}] calcd for $C_{15}H_{16}FO_2S_2$ 311.0570 found 311.0596.

2-((1-Phenoxyethyl)thio)-4*H*-thiochromen-4-one (3q): A yellow liquid (39 mg, Yield-63%) ^{1}H NMR (500 MHz, $CDCl_3$) δ 8.48 (d, *J* = 8.0 Hz, 1H), 7.59 (t, *J* = 7.3 Hz, 1H), 7.53 (t, *J* = 6.9 Hz, 2H), 7.31 (t, *J* = 7.8 Hz, 2H), 7.17 (s, 1H), 7.05 (t, *J* = 7.5 Hz, 3H), 5.86 (q, *J* = 6.2 Hz, 1H), 1.88 (d, *J* = 6.2 Hz, 3H); ^{13}C{^{1}H} NMR (125 MHz, $CDCl_3$) δ 179.5, 156.0, 147.6, 139.2, 131.8, 131.0, 130.9, 129.7, 128.9, 128.0, 125.7, 123.1, 117.4, 82.6, 22.6. IR(KBr)ν_{max}, 2992 (C−H), 1609 (C=O), 1292 (C−O), HRMS (ESI) m/z [M+H$^+$] calcd for $C_{19}H_{15}O_2S_2$ 315.0508; found315. 0508.

7-Chloro-2-((1-phenoxyethyl)thio)-4H-thiochromen-4-one (3r): A dark brown viscous liquid (41 mg, Yield-59%)^{1}H NMR (500 MHz, $CDCl_3$) δ 8.45 (s, 1H), 7.56 – 7.54 (m, 1H), 7.45 (d, *J* = 8.6 Hz, 1H), 7.31 (t, *J* = 7.8 Hz, 2H), 7.16 (s, 1H), 7.04 (t, *J* = 6.9 Hz, 3H), 5.86 (q, *J* = 6.3 Hz, 1H), 1.87 (d, *J* = 6.2 Hz, 3H); ^{13}C{^{1}H} NMR (125 MHz, $CDCl_3$) δ 178.2, 155.9, 148.3, 137.2, 134.5, 132.1, 131.9, 130.4, 129.7, 128.4, 127.0, 123.2, 117.4, 82.7, 22.5. IR(KBr)ν_{max}, 2995 (C−H), 1608 (C=O), 1292 (C−O), HRMS (ESI) m/z [M+H$^+$] calcd for $C_{19}H_{14}ClO_2S_2$ 373.0118 found 373.0101.

2-((1-Phenoxyethyl)thio)-6-(trifluoromethyl)-4H-thiochromen-4-one (3s): An orange dense liquid (53 mg, Yield-70%) ^{1}H NMR (400 MHz, $CDCl_3$) δ 8.74 (s, 1H), 7.79 (dd, *J* = 8.5, 1.8 Hz, 1H), 7.63 (d, *J* = 8.4 Hz, 1H), 7.35 – 7.29 (m, 2H), 7.19 (s, 1H), 7.08 – 7.03 (m, 3H), 5.87 (q, *J* = 6.2 Hz, 1H), 1.88 (d, *J* = 6.3 Hz, 3H); ^{13}C{^{1}H} NMR (100 MHz, $CDCl_3$) δ 178.3, 155.9, 148.4, 142.6, 130.9, 130.3 (q, *J* = 33.9 Hz), 129.8, 127.8 (q, *J* = 3.3 Hz), 126.6, 126.4 (q, *J* = 4.0 Hz), 123.5 (q, *J* = 270.9 Hz), 123.3, 117.5, 82.8, 22.5; IR(KBr)ν_{max},/cm^{-1}2927 (C−H),1629 (C=O),1278 (C−O), HRMS (ESI) m/z [M+H$^+$] calcd for $C_{20}H_{14}F_3O_2S_2$ 383.0382 found 383.0363.

2-(Ethylthio)-4-methyl-3,4-dihydro-2*H*,5*H*-thiopyrano[2,3-*b*]thio chromen-5-one (5a): A brown liquid (50 mg, Yield-82%) ^{1}H NMR (400 MHz, $CDCl_3$) δ 8.41 (d, *J* = 6.9 Hz, 1H), 7.55 – 7.51 (m, 1H), 7.48 – 7.41 (m, 2H), 4.31 (dd, *J* = 10.1, 3.4 Hz, 1H), 3.68 (q, *J* = 7.3 Hz, 1H), 2.82-2.75 (m, 2H), 2.71 – 2.65 (m, 1H), 2.18 – 2.10 (m, 1H), 1.34 (t, *J* = 8.0 Hz, 3H), 1.29 (d, *J* = 6.8 Hz, 3H); ^{13}C{^{1}H} NMR (100 MHz, $CDCl_3$) δ 177.5, 146.9, 136.2, 132.6, 131.4, 131.2, 129.3, 127.4, 124.9, 48.4, 41.5, 31.0, 26.6,

20.3, 14.9; IR(KBr)ν_{max}/cm^{-1} 2924 (C−H), 1621 (C=O), 1429 (C−S); HRMS (ESI) m/z [M+H$^+$] calcd for $C_{15}H_{17}OS_3$ 309.0436; found 309.0436.

6-Chloro-2-(ethylthio)-4-methyl-3,4-dihydro-2*H*,5*H*-thiopyrano[2,3-*b*]thiochro-

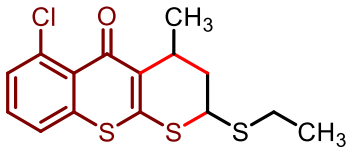

men-5-one (5b): A pale yellow solid (56 mg, Yield-83%); mp 93 ºC,^{1}H NMR (400 MHz, $CDCl_3$) δ 7.45 (dd, *J* = 7.4, 1.7 Hz, 1H), 7.38 – 7.31 (m, 2H), 4.32 (dd, *J* = 11.2, 2.5 Hz, 1H), 3.62 (dt, *J* = 10.0, 6.8 Hz, 1H), 2.82 – 2.72 (m, 2H), 2.67 – 2.61 (m, 1H), 2.11 – 2.02 (m, 1H), 1.33 (t, *J* = 7.4 Hz, 3H), 1.25 (d, *J* = 6.7 Hz, 3H); ^{13}C{^{1}H} NMR (100 MHz, $CDCl_3$) δ 178.8, 142.7, 138.3, 135.0, 133.3, 130.8, 130.5, 128.9, 123.9, 47.6, 42.0, 32.4, 26.1, 19.9, 15.0; IR(KBr)ν_{max}/cm^{-1} 2924 (C−H), 1621 (C=O), 1269 (C−O), 1429 (S−C), HRMS (ESI) m/z [M+H$^+$] calcd $C_{15}H_{16}ClOS_3$ 343.0046; found 343.0059.

7-Chloro-2-(ethylthio)-4-methyl-3,4-dihydro-2*H*,5*H*-thiopyrano[2,3-b]thiochro-

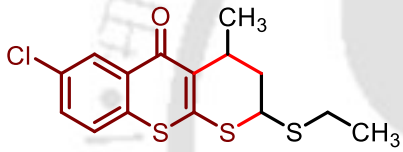

men-5-one (5c): A yellow liquid (61 mg, Yield-89%) ^{1}H NMR (400 MHz, $CDCl_3$) δ 8.38 (d, *J* = 2.3 Hz, 1H), 7.49 (dd, *J* = 8.5, 2.4 Hz, 1H), 7.37 (d, *J* = 8.5 Hz, 1H), 4.31 (dd, *J* = 10.1, 3.4 Hz, 1H), 3.66 (q, *J* = 7.2 Hz, 1H), 2.78 (dq, *J* = 7.4, 3.9 Hz, 2H), 2.71 – 2.64 (m, 1H), 2.14 (ddd, *J* = 14.0, 10.1, 7.9 Hz, 1H), 1.34 (d, *J* = 7.4 Hz, 3H), 1.28 (d, *J* = 6.8 Hz, 3H); ^{13}C{^{1}H} NMR (100 MHz, $CDCL_3$) δ 176.3, 147.4, 134.3, 133.8, 132.6, 132.5, 131.5, 128.9, 126.3, 48.5, 41.4, 31.1, 26.6, 20.2, 14.9. IR(KBr)ν_{max}/cm^{-1} 2925 (C−H), 1618 (C=O), 1382 (C−S), HRMS (ESI) m/z [M+H$^+$] calcd for $C_{15}H_{16}ClOS_3$ 343.0046; found: 343.0057.

8-Chloro-2-(ethylthio)-4-methyl-3,4-dihydro-2*H*,5*H*-thiopyra-no[2,3-*b*]thiochro-

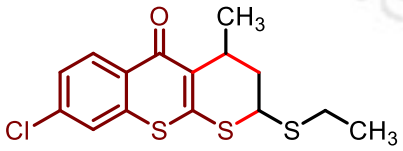

men-5-one (5d): An orange solid (58 mg, Yield-85%); mp 131 ºC, ^{1}H NMR (500 MHz, $CDCl_3$) δ 8.33 (d, *J* = 8.6 Hz, 1H), 7.40 (d, *J* = 8.1 Hz, 2H), 4.31 (dd, *J* = 9.9, 3.0 Hz, 1H), 3.65 (q, *J* = 7.1 Hz, 1H), 2.79 – 2.77 (m, 2H), 2.69-2.64 (m, 1H), 2.17 – 2.11 (m, 1H), 1.34 (t, *J* = 7.4 Hz, 3H), 1.29 (d, *J* = 6.8 Hz, 3H); ^{13}C{^{1}H} NMR (100 MHz, $CDCl_3$) δ 176.7, 146.8, 137.9, 137.5, 132.8, 130.9, 129.8, 128.0, 124.2, 48.6, 41.3, 31.0, 26.6, 20.2, 14.9: IR(KBr)ν_{max}/cm^{-1} 2925 (C−H), 1618 (C=O), 1382 (C−S), HRMS (ESI) m/z [M+H$^+$] calcd for $C_{15}H_{16}ClOS_3$ 343.0046 found 343.0071.

2-(Ethylthio)-4-methyl-7-(trifluoromethyl)-3,4-dihydro-2*H*,5*H*-thiopyrano[2,3b] thiochromene-5-one (5e): A brown liquid (55 mg, Yield-73%) 1H NMR (400 MHz, CDCl3) δ 8.68 (s, 1H), 7.73 (dd, J = 8.4, 1.9 Hz, 1H), 7.54 (d, J = 8.4 Hz, 1H), 4.33 (dd, J = 10.0, 3.4 Hz, 1H), 3.71 – 3.62 (m, 1H), 2.83 – 2.74 (m, 2H), 2.72 – 2.65 (m, 1H), 2.20 – 2.12 (m, 1H), 1.34 (t, J = 7.4 Hz, 3H), 1.30 (d, J = 6.8 Hz, 3H); 13C{1H} NMR (100 MHz, CDCl3) δ 176.4, 147.4, 139.8, 133.0, 131.4,129.7 (q, J = 33 Hz),127.2 (q, J = 3 Hz) 126.7(q, J=4 Hz), 125.7,123.7 (q, J = 270 Hz) 48.6, 41.2, 31.0, 26.6, 20.1, 14.8. IR(KBr)νmax/cm-12926 (C−H),1625 (C=O),1454 (C−S) HRMS (ESI) m/z [M+H+] calcd for $C_{16}H_{16}F_3OS_3$; 377.0310; found 377.0338

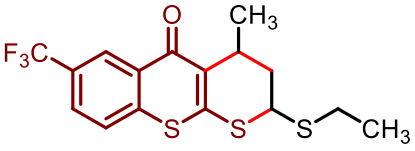

2-Butoxy-4-methyl-3,4dihydro-2*H*,5*H*-thiopyrano[2,3-*b*] chromen-5-one (6a): A brown, liquid (48 mg, Yield-80%) 1H NMR (400 MHz, CDCl3) δ 8.18 (dd, J = 8.3, 1.6 Hz, 1H), 7.61 – 7.56 (m, 1H), 7.37 – 7.32 (m, 2H), 5.25 (t, J = 3.5 Hz, 1H), 3.88-3.83, (m, 1H), 3.55 – 3.47 (m, 1H), 3.43-3.38, (m, 1H), 2.42-2.37 (m, 1H), 2.14-2.08, (m, 1H), 1.61 – 1.56 (m, 2H), 1.45 – 1.40 (m, 2H), 1.39 (d, J = 7.2 Hz, 3H), 0.92 (t, J = 7.4 Hz, 3H). 13C{1H} NMR (100 MHz, CDCl3) δ 174.2, 162.2, 156.3, 133.0, 126.1, 124.8, 123.5, 120.5, 117.2, 84.5, 70.4, 35.0, 31.5, 25.4, 19.5, 19.4, 13.9.IR(KBr)νmax/cm-1 2950 (C− H),1603(C=O), 1264(C− O),HRMS (ESI):m/z [M+H]+ calcd for $C_{17}H_{21}O_3S$, 305.1206; found; 305.1205.

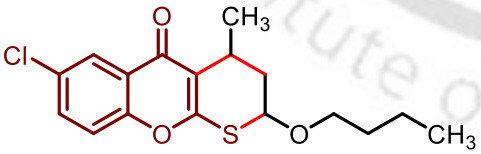

2-Butoxy-7-chloro-4-methyl-3,4-dihydro-2*H*,5*H*-thiopyrano [2,3-*b*]chromen-5-one (6b): A golden yellow, liquid (52 mg, Yield-78%) ^{1}H NMR (400 MHz, $CDCl_3$) δ 8.12 (d, *J* = 2.6 Hz, 1H), 7.51 (dd, *J* = 8.9, 2.6 Hz, 1H), 7.29 (dd, *J* = 8.9, 1.9 Hz, 1H), 5.25 (t, *J* = 3.0 Hz, 1H), 3.84 (dt, *J* = 8.8, 6.5 Hz, 1H), 3.50 – 3.44 (m, 1H), 3.39 (dt, *J* = 8.9, 6.2 Hz, 1H), 2.39 (dt, *J* = 14.3, 3.0 Hz, 1H), 2.11 – 2.06, (m, 1H), 1.62 –1.54 (m, 2H), 1.42 – 1.37 (m, 2H) 1.36 (d, *J* = 7.2 Hz, 3H), 0.89 (t, *J* = 7.4 Hz, 3H). ^{13}C{^{1}H} NMR (100 MHz, $CDCl_3$) δ 172.9, 162.8, 154.5, 133.1, 130.6, 125.5, 124.4, 120.6, 118.9, 84.5, 70.5, 34.9, 31.5, 25.4, 19.4 (2C), 13.8. IR(KBr)ν_{max}/cm^{-1} 2930(C−H), 1603(C=O), 1255 (C−O), HRMS (ESI):m/z [M+H]$^+$ calcd for $C_{17}H_{20}ClO_3S$, 339.0816; found:339.0816.

7-Bromo-2-butoxy-4-methyl-3,4-dihydro-2*H*,5*H*-thiopyrano [2,3-*b*]chromen-5-one (6c): A brown, liquid (58 mg, Yield-77%) ^{1}H NMR (500 MHz, $CDCl_3$) δ 8.29 (s, 1H), 7.66 (d, *J* = 8.7 Hz, 1H), 7.24 (d, *J* = 8.9 Hz, 1H), 5.25 (s, 1H), 3.85 (q, *J* = 6.9 Hz, 1H), 3.52 – 3.45 (m, 1H), 3.40 (q, *J* = 7.8, 7.1 Hz, 1H), 2.40 (dt, *J* = 14.5, 3.0 Hz, 1H), 2.12 – 2.09 (m, 1H), 1.63 – 1.61(m, 2H), 1.42 – 1.39 (m, 2H), 1.37 (d, *J* = 7.3 Hz, 3H), 0.92 (t, *J* = 7.4 Hz, 3H). ^{13}C{^{1}H} NMR (100 MHz, $CDCl_3$) δ 174.2, 162.2, 156.3, 133.0, 126.1, 124.8, 123.5, 120.5, 117.2, 84.5, 70.4, 35.0, 31.5, 25.4, 19.5, 19.4, 13.9. IR(KBr)ν_{max}/cm^{-1} 2985(C−H),1605(C=O),1262 (C−O), HRMS (ESI):m/z $[M+H]^+$ calcd for$C_{17}H_{20}BrO_3S$, 383.0311;found:383.0312, 385.0294.

2-Butoxy-8-fluoro-4-methyl-3,4dihydro-2*H*,5*H*-thiopyrano [2,3-*b*]chromene-5-one (6d): A brown, liquid (45 mg Yield-71%) ^{1}H NMR (500 MHz, $CDCl_3$) δ 8.17 (dd, *J* = 8.9, 6.4 Hz, 1H), 7.08 – 7.00 (m, 2H), 5.24 (t, *J* = 3.1 Hz, 1H), 3.84 (dt, *J* = 8.6, 6.6 Hz, 1H), 3.52 – 3.43 (m, 1H), 3.39 (dt, *J* = 8.8, 6.2 Hz, 1H), 2.39 (dt, *J* = 14.3, 2.9 Hz, 1H), 2.11-2.09 (m, 1H), 1.58 (dt, *J* = 13.3, 6.6 Hz, 2H), 1.45-1.38 (m, 2H), 1.37 (d, *J* = 7.1 Hz, 3H), 0.91 (t, *J* = 7.4 Hz, 3H). ^{13}C{^{1}H} NMR (125 MHz, $CDCl_3$) δ 173.3, 165.2(d, *J* = 253 Hz), 162.5, 157.0 (d, *J* = 13 Hz), 128.5(d, *J* = 10 Hz), 120.5, 120.3(d, *J* = 2.3 Hz), 113.5 (d, *J* = 22 Hz), 104.0 (d, *J* = 27 Hz), 84.5, 70.5, 34.9, 31.5, 25.4, 19.5, 19.4, 13.8; IR(KBr)ν_{max}/cm^{-1} 2992(C−H), 1603(C=O), 1264(C–O), HRMS (ESI):m/z $[M+H]^+$ calcd for $C_{17}H_{20}FO_3S$, 323.1112;found:323.1112.

2-*Iso*butoxy-4-methyl-3,4-dihydro-2*H*,5*H*-thiopyrano[2,3-*b*] chromen-5-one (6e): A yellow, liquid (46 mg, Yield-77%) ^{1}H NMR (500 MHz, $CDCl_3$) δ 8.19 – 8.16 (m, 1H), 7.59-7.56 (m, 1H), 7.35-7.32 (m, 2H), 5.24 (t, *J* = 3.2 Hz, 1H), 3.63 (dd, *J* = 8.6, 6.6 Hz, 1H), 3.51 (td, *J* = 7.6, 4.0 Hz, 1H), 3.17 (dd, *J* = 8.5, 6.1 Hz, 1H), 2.41 (dt, *J* = 14.3, 2.9 Hz, 1H), 2.13 – 2.08 (m, 1H), 1.93 – 1.85 (m, 1H), 1.39 (d, *J* = 7.2 Hz, 3H), 0.92 (dd, *J* = 6.8, 1.8 Hz, 6H). ^{13}C{^{1}H} NMR (125 MHz, $CDCl_3$) δ 174.2, 162.2, 156.3, 132.9, 126.1, 124.8, 123.5, 120.5, 117.2, 84.6, 77.4, 34.9, 28.5, 25.3, 19.6, 19.4, 19.4. IR(KBr)ν_{max}/cm^{-1}2925 (C−H),1603(C=O),1260 (C−O), HRMS (ESI):m/z $[M+H]^+$ calcd for $C_{17}H_{21}O_3S$, 305.1206; found; 305.1206.

7-Chloro-2-*iso*butoxy-4-methyl-3,4-dihydro-2*H*,5*H*-thiopyrano [2,3-*b*]chromen-5-one (6f): A brown, liquid (54 mg, Yield-80%) ^{1}H NMR (400 MHz, $CDCl_3$δ) 8.13 (d, *J* = 2.6 Hz, 1H), 7.52 (dd, *J* = 8.9, 2.6 Hz, 1H), 7.31 (s, 1H), 5.25 (t, *J* = 3.0 Hz, 1H), 3.63 (dd, *J* = 8.5, 6.6 Hz, 1H), 3.51 – 3.45 (m, 1H), 3.18 (dd, *J* = 8.5, 6.1 Hz, 1H), 2.41 (dt, *J* = 14.3, 2.9 Hz, 1H), 2.12 – 2.06 (m, 1H), 1.93 – 1.84 (m, 1H), 1.38 (d, *J* = 7.2 Hz, 3H), 0.92 (dd, *J* = 6.6, 1.9 Hz, 6H). ^{13}C{^{1}H} NMR (100 MHz, $CDCl_3$) δ 173.0, 162.8, 154.5, 133.1, 130.6, 125.5, 124.4, 120.6, 119.0, 84.7, 34.8, 28.5, 25.4, 19.5, 19.4 (2C), 19.3.IR(KBr)ν_{max}/cm^{-1} 2975(C−H),1604(C=O), 1263 (C-O), HRMS (ESI):m/z [M+H]$^{+}$ calcd for $C_{17}H_{20}ClO_3S$, 339.0816; found:339.0817.

7-Fluoro-2-*iso*butoxy-4-methyl-3,4-dihydro-2*H*,5*H*-thiopyrano [2,3-*b*]chromen-5-one (6g):A brown, liquid (45 mg, Yield-70%) ^{1}H NMR (500 MHz, $CDCl_3$) δ 7.81 (dd, *J* = 8.3, 3.0 Hz, 1H), 7.35 (dd, *J* = 9.1, 4.2 Hz, 1H), 7.30 (dt, *J* = 9.1, 4.5 Hz, 1H), 5.25 (t, *J* = 2.9 Hz, 1H), 3.63 (dd, *J* = 8.5, 6.6 Hz, 1H), 3.51 – 3.48 (m, 1H), 3.18 (dd, *J* = 8.5, 6.1 Hz, 1H), 2.44 – 2.39 (m, 1H), 2.1 – 2.07 (m, 1H), 1.89 (dt, *J* = 13.2, 6.6 Hz, 1H), 1.39 (d, *J* = 7.2 Hz, 3H), 0.92 (dd, *J* = 6.7, 2.4 Hz, 6H). ^{13}C{^{1}H} NMR (125 MHz, $CDCl_3$) δ 173.3 (d, *J* = 2.5 Hz), 162.8, 159.3 (d, *J* = 243.7 Hz), 152.4 (d, *J* = 2.5 Hz), 124.6 (d, *J* = 7.5 Hz), 121.0 (d, *J* = 25 Hz), 120.07, 119.1 (d, *J* = 7.5 Hz), 111.0 (d, *J* = 23.7 Hz) 84.7, 77.5, 34.9, 28.5, 25.4, 19.6, 19.4, 19.4; IR(KBr)ν_{max}/cm^{-1} 2759(C− H), 1604(C=O), 1265(C− O) HRMS (ESI):m/z [M+H]$^{+}$ calcd for, $C_{17}H_{20}FO_3S$,323.1112; found: 323.1112.

7-Bromo-2-*iso*butoxy-4-methyl-3,4-dihydro-2*H*,5*H*-thiopyran o[2,3-*b*]chromen-5-one (6h): A brown, liquid (68 mg, Yield-90%) ^{1}H NMR (500 MHz, $CDCl_3$)δ 8.29 (d, *J* = 10.1 Hz, 1H), 7.68 – 7.63 (m, 1H), 7.24 – 7.23 (m, 1H), 5.24 (dd, *J* = 7.9, 4.8 Hz, 1H), 3.62 (dt, *J* = 10.0, 5.0 Hz, 1H), 3.51 – 3.45 (m, 1H), 3.18 (dt, *J* = 10.0, 5.0 Hz, 1H), 2.44 – 2.39 (m, 1H), 2.13 – 2.07 (m, 1H), 1.92 – 1.83 (m, 1H), 1.38 (d, *J* = 7.2 Hz, 3H), 0.92 (d, *J* = 2.7 Hz, 6H). ^{13}C{^{1}H} NMR (100 MHz, $CDCl_3$) δ173.0, 162.8, 154.5, 133.1, 130.6, 125.5, 124.4, 120.6, 119.0,

84.7, 34.8, 28.5, 25.4, 19.5, 19.4 (2C), 19.3. IR(KBr)ν_{max}/cm^{-1} 2985(C−H),1605(C=O),1262 (C− O), HRMS (ESI):m/z $[M+H]^+$ calcd for$C_{17}H_{20}BrO_3S$, 383.0311;found:383.0311, 383.0292.

7-Bromo-4-methyl-2-propoxy-3,4-dihydroxy-2*H*,5*H*-thio pyrano[2,3-*b*]chromen-5-one (6i): A brown, solid (59 mg, Yield-76%), mp 99 ºC ^{1}H NMR (500 MHz, $CDCl_3$) δ 8.29 (d, *J* = 2.4 Hz, 1H), 7.66 (dd, *J* = 8.8, 2.4 Hz, 1H), 7.24 (d, *J* = 8.9 Hz, 1H), 5.26 (t, *J* = 3.1 Hz, 1H), 3.83 – 3.77 (m, 1H), 3.52 – 3.45 (m, 1H), 3.37 (dt, *J* = 8.7, 6.3 Hz, 1H), 2.40 (dt, *J* = 14.3, 2.9 Hz, 1H), 2.12 – 2.07 (m, 1H), 1.67 – 1.62 (m, 2H), 1.37 (d, *J* = 7.2 Hz, 3H), 0.93 (d, *J* = 7.4 Hz, 3H). $^{13}C\{^1H\}$ NMR (125 MHz, $CDCl_3$) δ 172.8, 162.8, 155.0, 135.9, 128.8, 124.8, 120.7, 119.2, 118.0, 84.5, 72.4, 34.9, 25.5, 22.8, 19.5, 10.8. IR(KBr)ν_{max}/cm^{-1} 2975(C−H),1603(C=O), 1263(C− O), HRMS (ESI):m/z $[M+H]^+$ calcd for $C_{16}H_{18}BrO_3S$,369.0155; found: 369.0155, 371.0135.

7-Fluoro-4-methyl-2-propoxy-3,4-dihydro-2*H*,5*H*-thiopyrano [2,3-*b*]chromen-5-one (6j): A yellow, liquid (42 mg, Yield-69%) ^{1}H NMR (400 MHz, $CDCl_3$) δ 8.48 (dd, *J* = 9.0, 5.9 Hz, 1H), 7.18 – 7.09 (m, 2H), 5.17 (t, *J* = 3.2 Hz, 1H), 3.77 (dt, *J* = 8.7, 6.6 Hz, 1H), 3.71 – 3.63 (m, 1H), 3.37 (dt, *J* = 8.8, 6.2 Hz, 1H), 2.47 (dt, *J* = 14.3, 3.0 Hz, 1H), 2.18 – 2.11 (m, 1H), 1.68 – 1.61 (m, 2H), 1.32 (d, *J* = 7.2 Hz, 3H), 0.94 (t, *J* = 7.4 Hz, 3H). $^{13}C\{^1H\}$ NMR (100 MHz, $CDCl_3$) δ 175.5, 163.7 (d, *J* =253 Hz), 145.3, 138.6(d, J = 9.7 Hz), 132.5 (d, *J* = 9.5 Hz), 127.2(d, *J* = 2.3 Hz), 131.9, 115.7 (d, *J* = 22.2 Hz), 110.7 (d, *J* = 24 Hz), 83.2, 72.3, 35.5, 26.2, 22.8, 18.8, 10.8. δ IR(KBr)ν_{max}/cm^{-1}2995(C−H),1606(C=O), 1264(C−O), HRMS (ESI):m/z $[M+H]^+$ calcd for $C_{16}H_{18}FO_3S$, 309.0955; found: 309.0957.

8-Fluoro-4-methyl-2-propoxy-3,4-dihydro-2*H*,5*H*-thiopyrano [2,3-*b*]chromen-5-one (6k): A golden yellow, liquid (44.5 mg Yield-72%) 1H NMR (500 MHz, CDCl3) δ 7.81 (dd, J = 8.3, 3.0 Hz, 1H), 7.37 – 7.28 (m, 2H), 5.26 (t, J = 3.3 Hz, 1H), 3.80 (dt, J = 8.8, 6.6 Hz, 1H), 3.54 – 3.46 (m, 1H), 3.37 (dt, J = 8.7, 6.3 Hz, 1H),

2.41 (dt, J = 14.4, 2.9 Hz, 1H), 2.1 – 2.09 (m, 1H), 1.64 – 1.61 (m, 2H), 1.38 (d, J = 7.2 Hz, 3H), 0.94 (t, J = 7.4 Hz, 3H) 13C{1H} NMR (125 MHz, Chloroform-d) δ173.4 (d, J = 2.1 Hz), 162.8, 160.3 (d, J = 244 Hz) 152.5, 124.6 (d, J = 7 Hz) 121.0 (d, J = 25 Hz), 120.09, 119.3 (d, J = 7 Hz), 111.0 (d, J =23 Hz), 84.5, 72.3, 34.9, 25.4, 22.8, 19.5, 10.8. IR(KBr)νmax/cm-12995(C− H),1606(C=O), 1264(C− O),HRMS (ESI):m/z [M+H]+ calcd for $C_{16}H_{18}FO_3S$, 309.0955; found: 309.0957.

2-Ethoxy-4-methyl-3,4-dihydro-2*H*,5*H*-thiopyrano[2,3-*b*]chromen-5-one (6l): A

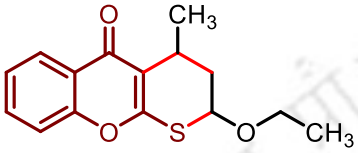

brown, liquid (45 mg, Yield-83%) ^{1}H NMR (500 MHz, $CDCl_3$) δ 8.17 (dd, *J* = 8.1, 1.6 Hz, 1H), 7.60 – 7.56, (m, 1H), 7.36 – 7.32 (m, 2H), 5.26 (t, *J* = 3.0 Hz, 1H), 3.94-3.88, (m, 1H), 3.52 – 3.44 (m, 2H), 2.43 – 2.38 (m, 1H), 2.14 – 2.09, (m, 1H), 1.39 (d, *J* = 7.2 Hz, 3H), 1.24 (t, *J* = 7.0 Hz, 3H). ^{13}C{^{1}H} NMR (125 MHz, $CDCl_3$) δ 174.2, 162.1, 156.2, 133.0, 126.1, 124.8, 123.5, 120.5, 117.2, 84.1, 66.0, 35.0, 25.4, 19.5, 15.0. IR(KBr)ν_{max}/cm^{-1} 2930, (C− H),1605(C=O),1254 (C− O), HRMS (ESI):m/z [M+H]$^+$ calcd for $C_{15}H_{17}O_3S$, 277.0893; found: 277.0893.

7-Chloro-2-ethoxy-4-methyl-3,4-dihydro-2*H*,5*H*-thiopyrano [2,3-*b*]chromen-5-one

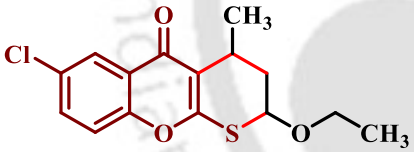

(6m): A brown, solid (46 mg, Yield-75%) mp 120 ºC, ^{1}H NMR (500 MHz, $CDCl_3$) δ 8.13 (d, *J* = 2.6 Hz, 1H), 7.52 (dd, *J* = 8.9, 2.6 Hz, 1H), 7.30 (d, *J* = 8.9 Hz, 1H), 5.26 (t, *J* = 3.1 Hz, 1H), 3.92 – 3.88 (m, 1H), 3.49 – 3.44 (m, 2H), 2.42 – 2.38 (m, 1H), 2.13 – 2.08 (m, 1H), 1.38 (d, *J* = 7.2 Hz, 3H), 1.25 (t, *J* =7.4Hz, 3H). ^{13}C{^{1}H} NMR (125 MHz, $CDCl_3$) δ 173.0, 162.7, 154.5, 133.1, 130.6, 125.5, 124.4, 120.6, 118.9, 84.1, 66.1, 34.9, 25.5, 19.4, 15.0. IR(KBr)ν_{max}/cm^{-1} 2928(C− H),1603(C=O),1258 (C− O), HRMS (ESI):m/z [M+H]$^+$ calcd for $C_{15}H_{16}ClO_3S$, 311.0503; found; 311.0503.

7-Bromo-2-ethoxy-4-methyl-3,4-dihydro-2*H*,5*H*-thiopyrano[2,3-*b*] chromen-5-one

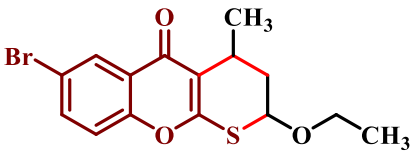

(6n): A Brown, solid (57 mg, Yield-81%) mp 126 ºC ^{1}H NMR (500 MHz, $CDCl_3$) δ 8.29 (d, *J* = 2.4 Hz, 1H), 7.66 (dd, *J* = 8.8, 2.4 Hz, 1H), 7.24 (d, *J* = 8.9 Hz, 1H), 5.26 (t, *J* = 3.0 Hz, 1H), 3.93 – 3.87 (m, 1H), 3.49 – 3.44 (m, 2H), 2.40 (dt, *J* = 14.3, 3.0 Hz, 1H), 2.13-2.08 (m, 1H), 1.37 (d, *J* = 7.2

Hz, 3H), 1.25 (t, *J* = 7.0 Hz, 3H). $^{13}C\{^{1}H\}$ NMR (125 MHz, $CDCl_3$) δ 172.8, 162.7, 155.0, 135.9, 128.7, 124.8, 120.7, 119.2, 118.0, 84.1, 66.1, 34.9, 25.5, 19.4, 15.0. IR(KBr)ν_{max}/cm^{-1} 2976(C−H),1605(C=O),1258(C−O), HRMS (ESI):m/z $[M+H]^+$ calcd for $C_{15}H_{16}BrO_3S$,354.9998; found:354.9998, 356.9980.

2-Ethoxy-8-fluoro-4-methyl-3,4-dihydro-2*H*,5*H*-thiopyrano[2,3-*b*] chromen-5-one

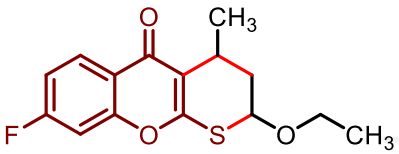

(6o): A brown, liquid (42 mg, Yield-72%) ^{1}H NMR (500 MHz, $CDCl_3$) δ 8.18 (dd, *J* = 8.8, 6.4 Hz, 1H), 7.09 – 7.01 (m, 2H), 5.26 (t, *J* = 3.0 Hz, 1H), 3.91 (td, *J* = 7.1, 1.7 Hz, 1H), 3.50 – 3.43 (m, 2H), 2.40 (dt, *J* = 14.3, 3.2 Hz, 1H), 2.12 – 2.08 (m, 1H), 1.38 (d, *J* = 7.2 Hz, 3H), 1.26 (d, *t* = 7.1 Hz, 3H). $^{13}C\{^{1}H\}$ NMR (125 MHz, $CDCl_3$) δ 173.4, 165.2 (d, *J* = 252.2 Hz) 162.4, 157.1, 128.5 (d, *J* = 10 Hz), 120.5, 120.3 (d, J = 2.5 Hz), 113.5 (d, *J* = 22.2 Hz), 104.0 (d, *J* = 25.3 Hz), 84.1, 66.1, 35.0, 25.4, 19.5, 15.0; IR(KBr)ν_{max}/cm^{-1} 2952 (C−H),1603(C=O),1264 (C−O), HRMS (ESI):m/z $[M+H]^+$ calcd for $C_{15}H_{16}FO_3S$, 295.0799; found: 295.0799.

7-Chloro-2-((1-ethylthio)ethyl)thio)-4H-chromene-4-one (7a): A light yellow, solid

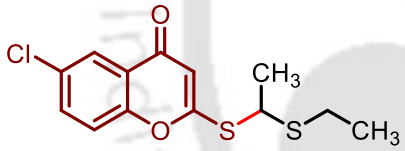

(50 mg, Yield-83%) mp 143 0C, 1H NMR (500 MHz, CDCl3) δ 8.09 (d, J = 2.6 Hz, 1H), 7.56 (dd, J = 8.8, 2.6 Hz, 1H), 7.36 (d, J = 8.9 Hz, 1H), 6.35 (s, 1H), 4.65 (q, J = 6.9 Hz, 1H), 2.82 – 2.69 (m, 2H), 1.77 (d, J = 7.0 Hz, 3H), 1.29 (t, J = 7.4 Hz, 3H). 13C{1H} NMR (125 MHz, CDCl3) δ 174.9, 167.2, 155.3, 133.7, 131.4, 125.4, 124.7, 119.1, 111.1, 47.0, 25.9, 23.5, 14.4. IR(KBr)νmax/cm-12925(C−H),1606(C=O), 1432 (C−S), HRMS (ESI):m/z [M+H]+ calcd for $C_{13}H_{14}ClO_2S_2$ 301.0118; found 301.0118.

6-Bromo-2-((1-(ethylthio)ethyl)thio)-4H-chromene-4-one (7b): A golden yellow, liquid (58 mg, yield - 85%)

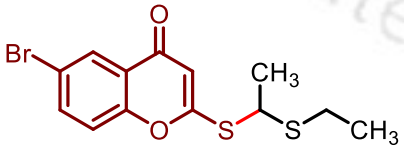

1H NMR (400 MHz, CDCl3) δ 8.27 (d, J = 2.5 Hz, 1H), 7.72 (dd, J = 8.9, 2.5 Hz, 1H), 7.30 (d, J = 8.8 Hz, 1H), 6.36 (s, 1H), 4.66 (q, J = 6.9 Hz, 1H), 2.85 – 2.67 (m, 2H), 1.78 (d, J = 6.9 Hz, 3H), 1.30 (t, J = 7.4 Hz, 3H). 13C{1H} NMR (100 MHz, CDCl3) δ 174.8, 167.2, 155.7, 136.6, 128.7, 125.1, 119.4, 119.0, 111.2, 47.0, 25.9, 23.5, 14.4. IR(KBr)νmax/cm-1 2926(C−H),1606(C=O), (C− S)1425, HRMS (ESI):m/z [M+H]+ calcd for,$C_{13}H_{14}BrO_2S_2$, 344.9613;found: 344.9613, 346.9591.

2-((1-(Ethylthio)ethyl)thio)-6-fluoro-4*H*-chromen-4-one (7c): A light orange, liquid

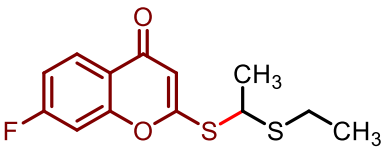

(48 mg, Yield-85%) ^{1}H NMR (500 MHz, $CDCl_3$) δ 7.81 (dd, *J* = 8.1, 2.5 Hz, 1H), 7.43 (dd, *J* = 9.1, 4.1 Hz, 1H), 7.39 – 7.35 (m, 1H), 6.37 (s, 1H), 4.67 (q, *J* = 6.8 Hz, 1H), 2.78 (ddt, *J* = 34.6, 12.7, 7.1 Hz, 2H), 1.80 (d, *J* = 6.9 Hz, 3H), 1.32 (t, *J* = 7.4 Hz, 3H). ^{13}C{^{1}H} NMR (100 MHz, $CDCl_3$) δ 175.4 (d, *J* = 2.68 Hz), 167.2, 159.7 (d, *J* = 245 Hz),153.2, 121.7(d, *J* = 25 Hz), 119.6, 119.5, 111.1 (d, *J* = 23 Hz) 110.7, 47.0, 25.9, 23.6, 14.4; IR(KBr)ν_{max}/cm^{-1} 2969(C−H),1615(C=O),1424(C−S), HRMS (ESI):m/z [M+H]$^{+}$ calcd for $C_{13}H_{14}FO_2S_2$,285.0414; found:285.0411.

Figure 1. ORTEP Diagram of compound **3c**

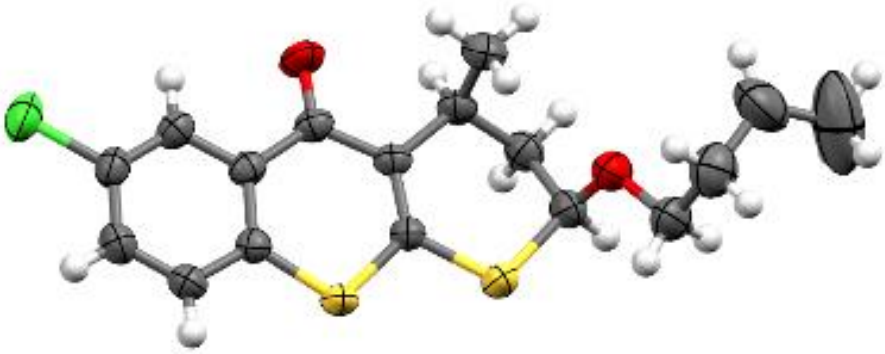

Table 6. Crystal data and structure refinement for compound 3(c).

Entry	Identification Code	Compound 3c
01	Empirical formula	$C_{17}H_{18}ClO_2S_2$
02	Formula weight	370.961
03	Temperature	297 K
04	Wavelength	0.71073
05	Crystal system	Triclinic
06	Space group	P -1
07	Cell length	a 7.8588 (8) b 10.3914 (8) c 11.7530 (8)
08	Cell angle	α 113.777 (2) β 97.924 (2) γ 96.258 (2)
09	Cell volume	855.48 (12)
10	Density	1.374
11	Completeness to theta	99.14
12	Index ranges	-15<=h<=15, -6<=k<=6, -20<=l<=19
13	Theta range	2.2- 26.3
14	Cell formula units Z	12
15	CCDC no	2311054

Figure 2. ORTEP Diagram of compound **5d**

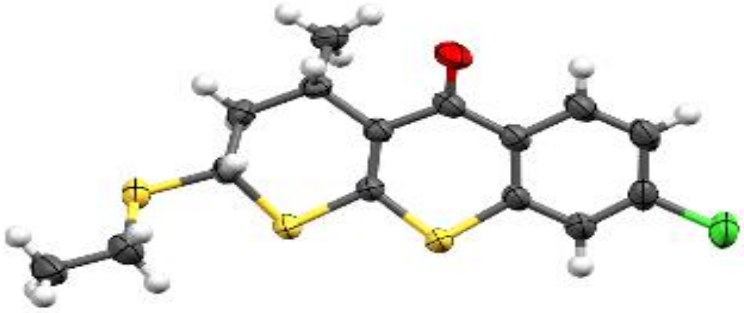

Table 7. Crystal data and structure refinement for compound 5(d).

Entry	Identification Code	Compound 5d
01	Empirical formula	$C_{15}H_{15}ClOS_3$
02	Formula weight	342.90
03	Temperature	296 K
04	Wavelength	0.71073
05	Crystal system	Triclinic
06	Space group	P 21/c
07	Cell length	a 10.9013 (4) b 4.3678 (2) c 32.5560 (13)
09	Cell angle	A 90 β 93.691 (1) γ 90
10	Cell volume	1546.93 (11)
11	Density	1.472
12	Completeness to theta	99.3
13	Index ranges	-15<=h<=15, -6<=k<=6, -20<=l<=19
14	Theta range	1.254- 25.964
15	Cell formula units Z	4
16	CCDC no	2311048

Figure 3. ^{1}H NMR (500 MHz, $CDCl_3$) spectrum of compound 3a

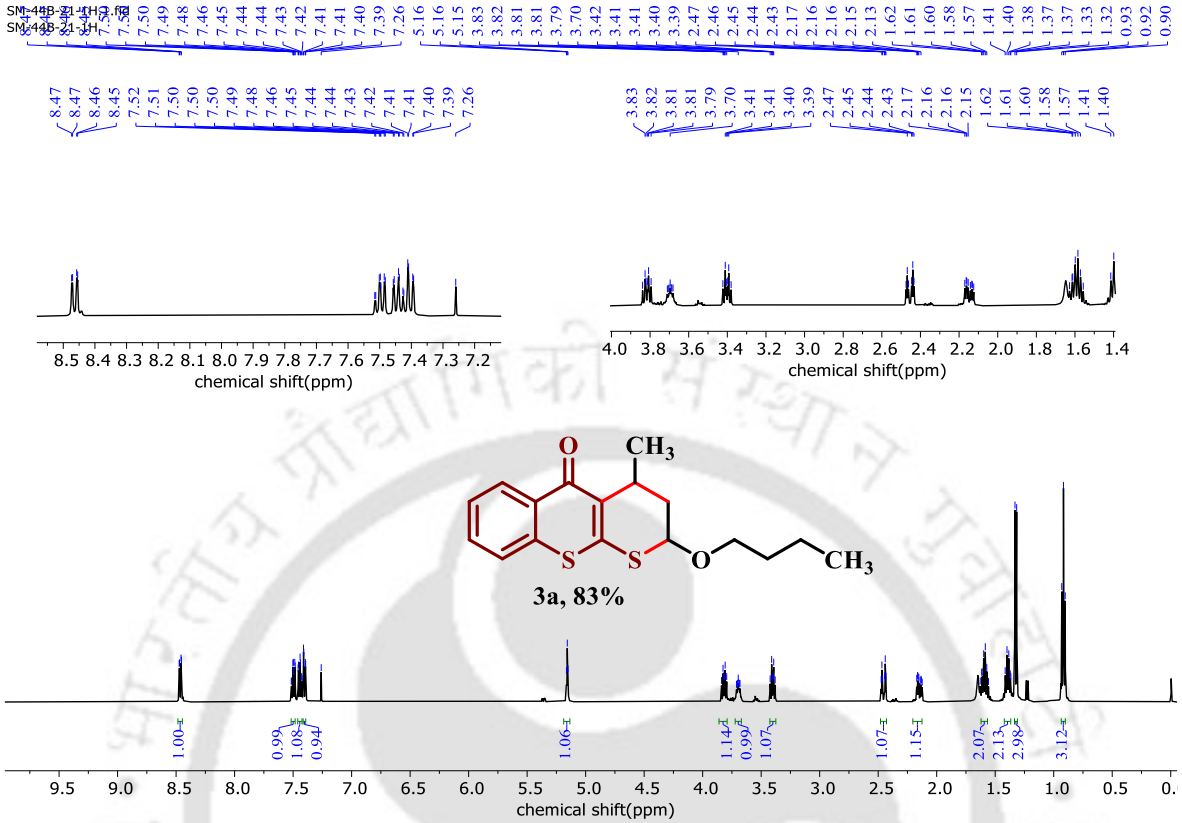

Figure 4. $^{13}C\{^{1}H\}$ NMR (125 MHz, CDCl3) spectrum of compound 3a

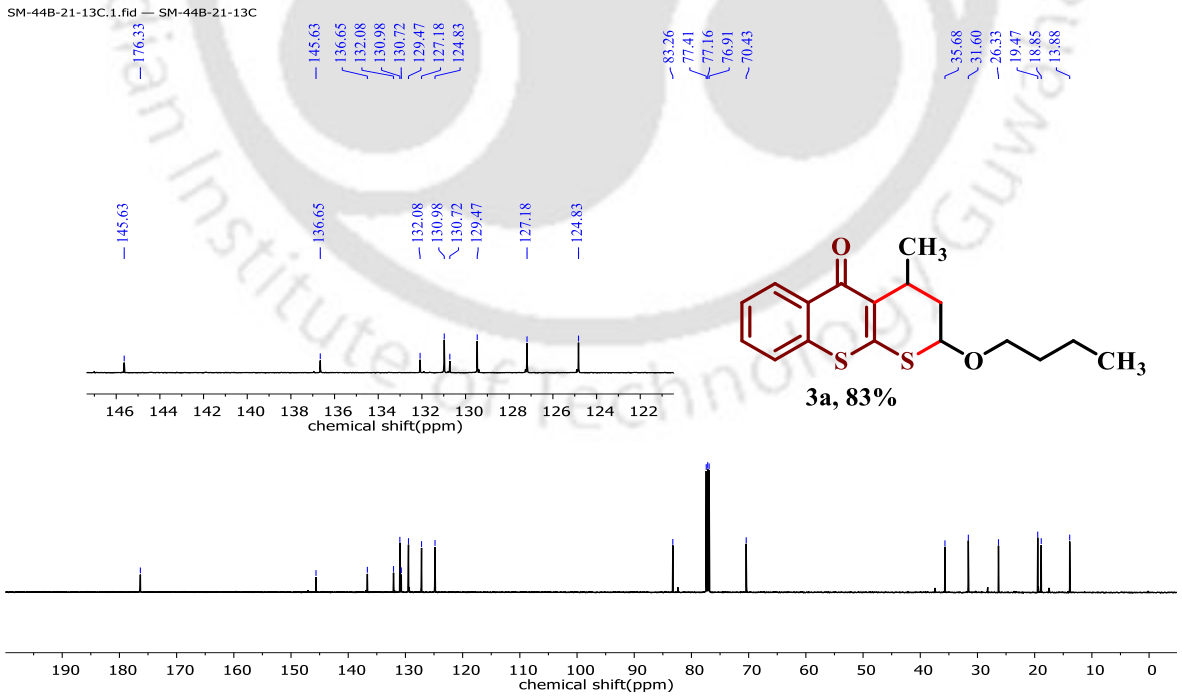

Figure 5. HRMS of compound 3a

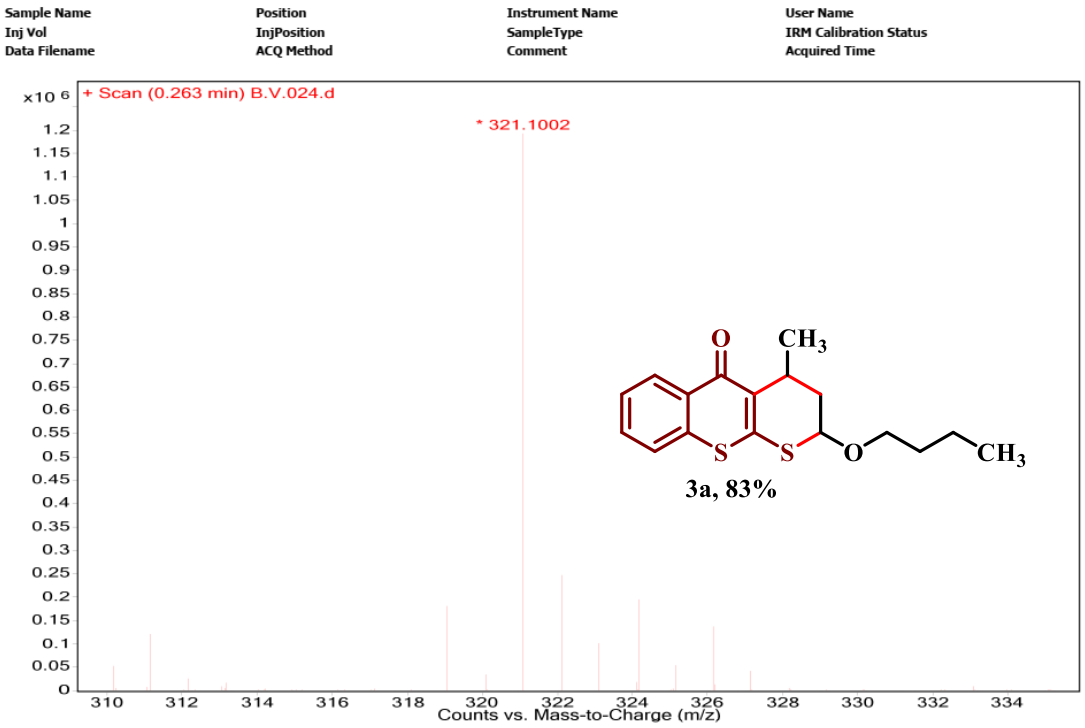

Reference:

1 X.-B. Xu, J. Liu, J.-J. Zhang, Y.-W. Wang and Y. Peng, *Org. Lett.*, 2013, **15**, 550-553.

2 S. M. Chinchkar, J. D. Patil, S. N. Korade, G. S. Gokavi, R. V. Shejawal and D. M. Pore, *Lett. Org. Chem.* 2017, **14,** 1570-1786.

3 S. Nurhanna Riduan, J. Y. Ying and Y. Zhang, *Org. Lett.*, 2012, **14**, 1780-1783.

4 R. Samar, N. Rajesh and D. Prajapati, *Chem. Commun.*, 2012, **48**, 4014-4016.

5 Q. Ding, B. Cao, J. Yuang, X. Liu, and Y. Peng, *Org. Biomol. Chem.*, 2011, **9**, 748-751.

6 M. fragies, J. L. Deobald, S. Dharavath, J. Scoot and J. Magolan, *Org. Lett.*, 2021, **23**, 4548-4552.

7 S. Mondal, S. Yashmin and Abu T. Khan, *Org. Biomol. Chem.*, 2021, **19**, 9223-9230.

8 X. Lin, J. Li, J. Zhang, S. Liu, X. Lin, X. Pan, J. Zhu and X. Zhu, *Polym. Chem.*, 2021, **12**, 983-990.

9 L. Ouyang, L. Zhan, J. Li, Q. Zhang, C. Qi, W. Wu and H. Jiang, *Org. Lett.*, 2018, **20**, 550–553.

10 A. Juranovič, K. Kranjc, S. Polanc, F. Perdih and M. Kočevar, *Monatshefte Fü, Chem. - Chem. Mon.*, 2012, **143**, 771-777.

11 X. Wei, J. C. Lorenz, S. Kapadia, A. Saha, N. Haddad, C. A. Busacca and C. H. Senanayake. *J. Org. Chem.*, 2007, **72**, 4250-4253.

12 M. Yu, R. R. Schrock and A. H. Hoveyda, *Angew. Chem. Int. Ed.*, 2015, **54**, 215-220.

13 P. C. Montevecchi and M. L. Navacchia, *J. Org. Chem.* 1995, **60**, 6455-6459.

14 Y. Yamashita and S. Kobayashi, *J. Am. Chem. Soc.*, 2004, **126**, 11279–11282.

15 M. S. Ledovskaya, V. V. Voronin, K. S. Rodygin and V. P. Ananikov, *Org. Chem. Front.*, 2020, **7**, 638-647.

16 M. Belal, S. Mondal, S. Yashmin, and A. T. Khan, *Org. Biomol. Chem.*, 2022, **20**, 715-726.

17 M. Aghajani, S. Asghari, G. F. Pasha, and M. Mohseni, *Res. Chem. Intermed.* 2020, **46**, 1841-1855.

18 C. Ji, S. Wang, S. Chen, S. He, Y. Jiang, Z. Miao, J. Li, and C. Sheng, *Bioorg. Med. Chem.* 2017, **25**, 5268-5277.

19 A. Lozynskyi, S. Golota, B. Zimenkovsky, D. Atamanyuk, A. Gzella, and R. Lesyk, *Phosphorus Sulfur Silicon Relat. Elem.*, 2016, **191**, 1245-1249.

20 R. Bihovsky, M.U. Kumar, S. Ding and A. Goyal, J. Org. Chem., 1989, 54, 4291-4293.

Chapter IV

Reactivity study of 4-hydroxydithiocoumarin with Isocyanide: Regioselective Synthesis of *(E)*-3-((alkylamino)methylene)-2thioxothiochroman 4-one Derivatives and their Regioselective Cycloaddition with Alkynes

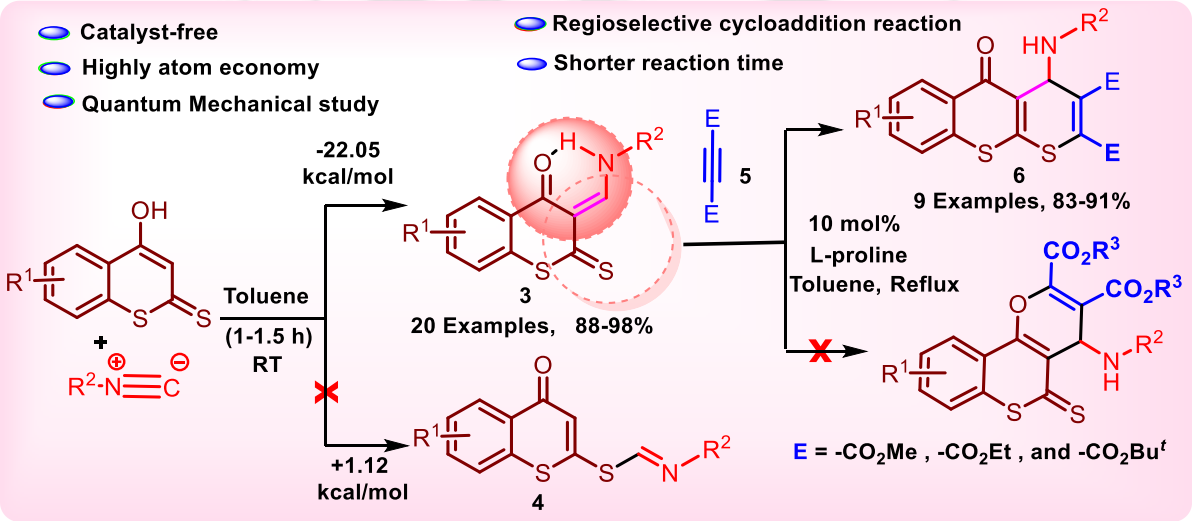

J. Org. Chem., 2025, **90**, 8857–8868.

4.0 Introduction:

Organosulfur compounds are being investigated in various research areas because of their remarkable biological and pharmaceutical importance, as well as their utility in diverse organic transformations.[1–4] Compounds derived from 4-hydroxycoumarin, such as the naturally occurring dicoumarol[5,6] and the non-natural warfarin[7,8], exhibit anticoagulant activities. The analogues of 4-hydroxycoumarin, such as 4-hydroxythiocoumarin and 4-hydroxydithiocoumarin, exhibit a structural resemblance and are utilised in various organic transformations. In the first chapter, we discussed the three-resonating structure of 4-hydroxydithiocoumarin in detail. Through DFT energy calculations, it was found that the 4-hydroxy **I** form is more energetically stable than the active methylene **II** form and its thiol **III** form, as shown in **Figure 1** below**.**

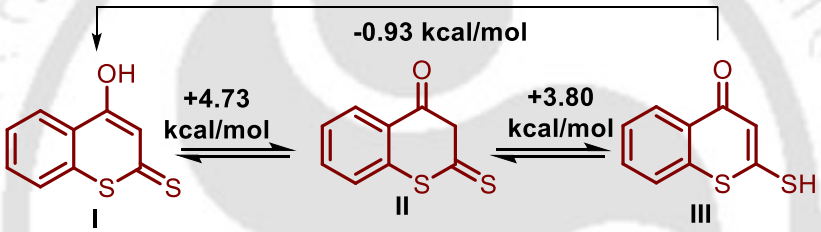

Figure 1. Three tautomeric forms of 4-hydroxycoumarin. The structure (I) is the most stable form. The calculations were carried out using the B3LYP/6-31+G(d,p) level of DFT. All the energy values are estimated using the free energy (G) values. The relative energies of the reaction path are provided in kcal/mol.

It is well known in the literature that many of the reactants act as either an electrophile or a nucleophile, depending upon the other reactant. For example, *meta*-chloroperbenzoic acid *(m*-CPBA) acts as an electrophile[9] in the epoxidation of olefins. On the other hand, it also acts as a nucleophile[10] in Baeyer-Villiger oxidation of cyclic ketones. Based on this fact, our aim is to investigate the reaction behaviour between 4-hydroxydithiocoumarin bearing three nucleophilic centres and the isocyanide, which also acts as a nucleophile, as evidenced in the Passerini reaction.[11] In this chapter, we want to disclose that isocyanide has a dual role: it acts as a base for the deprotonation of 4-hydroxydithiocoumarin and *in situ* converts itself into an electrophile and catalyses the reaction in the forward direction. We successfully synthesised several alkyl aminomethylene (**3**) derivatives in toluene under catalyst-free conditions at room temperature. In the present work, there are two possible routes to obtain two different product types: *S*-alkylated or *C*-alkylated. Notably, we get only the C-alkylated product as described in **Scheme 1.**

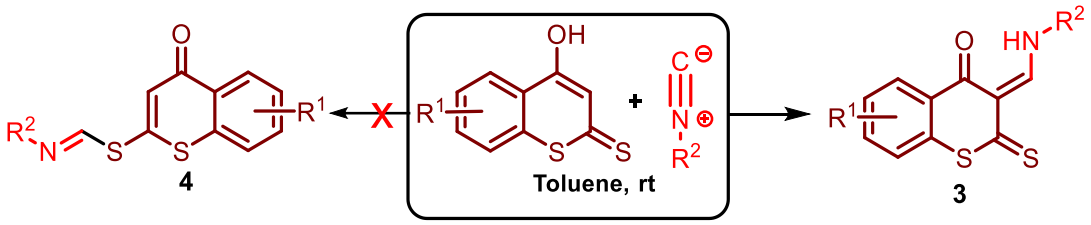

Scheme 1. Reaction of 4-hydroxydithiocoumarin with isocyanide

Since 1838, isocyanide has captured the interest of synthetic chemists because its terminal carbon atom can behave both as a nucleophile and an electrophile (α-addition).[12,13] This unique characteristic makes isocyanide a highly attractive starting material for the synthesis of new molecules. Isocyanides can also exist in two resonating forms (**Figure 2)**.

New J. Chem. 2012, **36**, 1137-1140. *Chem. Rev.* 2021, 121, **17**, 10742–10788

Figure 2. Two most important resonance forms of isocyanide account for 84% of the weight of all resonance forms

Numerous new molecules have been synthesised in the pharmaceutical industry by utilising isocyanides in various multicomponent reactions (MCRs).[14] Moreover, isocyanide-based MCRs, such as the Passerini[11] and Ugi reactions, are well documented for diversity-oriented synthesis.[15] A literature survey revealed that isocyanide has been utilised in a multi-component reaction with 4-hydroxycoumarin and vinyl acetate in the presence of DABCO,[16] resulting in a furan ring formation at the C3 position of 4-hydroxycoumarin and an aminomethylene by-product (**Scheme 2**).

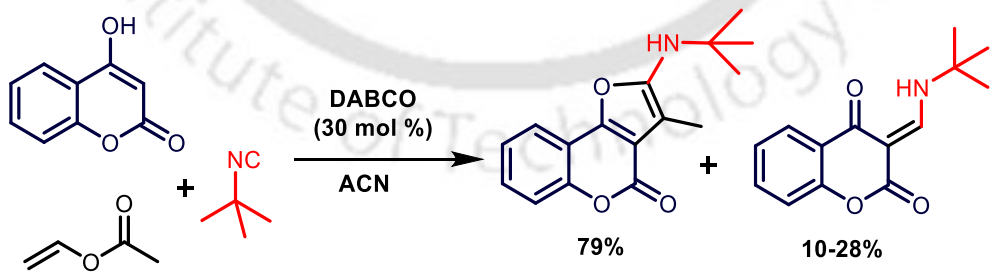

Scheme 2. Multi-component reaction of 4-hydroxycoumarin with isocyanide and vinyl acetate

Similarly, Park and Lee reported [17] almost identical (aminomethylene) products using 4-hydroxythiocoumarin, amines, and triethyl orthoformate, as shown in **Scheme 3**. A three-component synthesis of 3-aminomethylene-thiochroman-2,4-dione derivatives by the condensation reactions of amines,*α*-amino acids, and ureas, with 4-hydroxythiocoumarin,

respectively, in the presence of triethyl orthoformate using *Iso*propyl alcohol under reflux conditions.

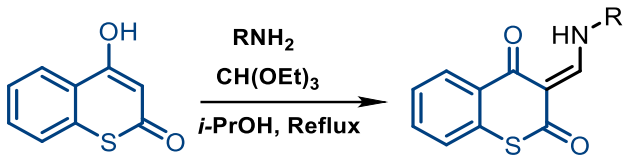

Scheme 3. Three-component synthesis of aminomethylene thiochromone derivatives using 4-hydroxycoumarin, amines, and orthoformate

V. Edmont and his co-workers also demonstrate the synthesis of aminomethylene derivatives by the reaction of pyridinone, aniline, and orthoformate in a DMF/AcOH (3:1) solvent mixture at 103 °C. The synthesised aminomethylene derivatives were further utilised for the preparation of aldehydes, demonstrating their post-synthetic applicability as shown in **Scheme 4**.[18]

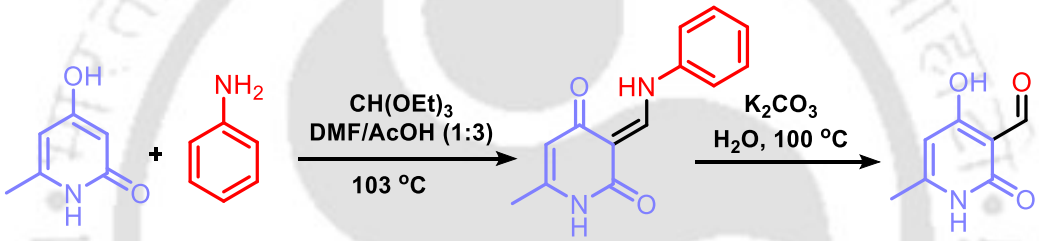

Scheme 4. Synthesis of aminomethylene derivatives, aryl amines, and orthoformate

The literature reviewed above indicates that aminomethylene compounds can also be used for post-synthetic applications. As V. Edmont *et al*. demonstrate, the utility of these versatile intermediates for the preparation of aldehydes and other functionalized heterocycles is evident. Similarly, inspired by these reports, we have demonstrated the post-synthetic applications of aminomethylene compounds **3** by employing them as a diene system in Diels-Alder reactions and in *N*-alkylation reactions followed by cyclisation, in an effort to construct novel organosulfur heterocyclic frameworks.

4.1 Results and Discussion:

In this chapter, our current work demonstrates the reaction between 4-hydroxydithiocoumarin and isocyanide, despite both serving as nucleophiles. We report the successful outcome of this reaction, as shown in **Scheme 5**. The post-synthetic application of the synthesised alkylamino derivatives **3** is also demonstrated in this chapter, sections **4.5** and **4.6**.

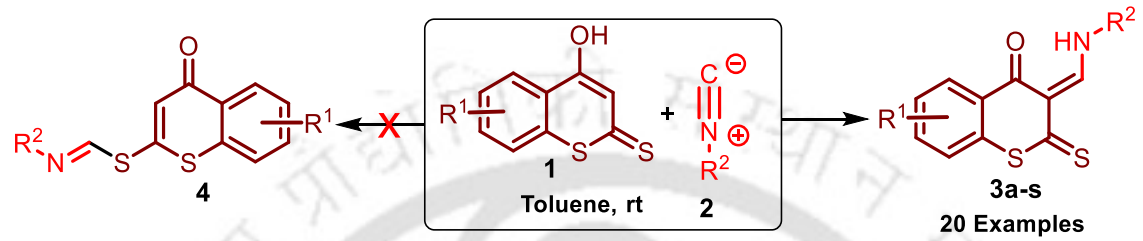

Scheme 5. Reaction between 4-hydroxydithiocoumarin and isocyanide

In the beginning, various 4-hydroxydithiocoumarins (**1a**) and their derivatives, such as 7-F (**1b**), 5-Cl (**1c**), 6-Cl (**1d**), 7-Cl (**1e**), and 6-CF_3 (**1f**) were prepared by following the reported literature mentioned in Chapter I, **Scheme 22**. For the optimisation study, the reaction was carried out by taking 4-hydroxydithiocoumarin (**1a**) (0.20 mmol) and cyclohexyl isocyanide (**2a**) (0.20 mmol) in 1 mL of water in a 10 mL round-bottomed flask. The reaction mixture was stirred at room temperature for one hour, as shown in **Table 1**, entry 1. No reaction occurred, so the same reaction was refluxed for another hour. The reaction was then attempted in ethanol, but no product was observed, as shown in **Table 1**, entry 2. Similarly, the reaction was investigated at room temperature using various polar aprotic solvents, including DMF, 1,4-dioxane, and DMA. A trace amount of product **3a** was observed as depicted in **Table 1**, entries 3-5. Later, the reaction was performed in chlorobenzene and toluene at room temperature, yielding fair results in both cases. Still, it was observed that the yield was almost quantitative in toluene, as presented in **Table 1**, entries 6 and 7. The product (**3a**) was characterised using various spectroscopic techniques, including ^{1}H and ^{13}C NMR spectra, HRMS, and single-crystal XRD. In the ^{1}H NMR spectrum of product **3a**, the characteristic peaks at δ 3.59 (s, 1H), 2.08 (d, J = 8.9 Hz, 2H), 1.90-1.83 (m, 2H), 1.58 (d, J = 14.7 Hz, 3H), 1.49-1.39 (m, 2H), and 1.36-1.26 (m, 1H) indicate that cyclohexyl isocyanide is incorporated into the final product.

One doublet proton is also observed at δ 9.48 (d, J = 14 Hz), indicating the C=CH proton adjacent to the NH group. A broad peak for NH at δ 13.10 (s, 1H) is observed in the spectrum. Similarly, in ^{13}C NMR, four signals appear in the aliphatic region, where one signal at δ 59.2 corresponds to the carbon of cyclohexyl that is directly attached to nitrogen. Whereas ten signals were observed for the aromatic carbon, two of them were very specific to the carbonyl and exocyclic carbon adjacent to nitrogen, with δ values of 178.1 and 202.1, respectively. In addition, the m/z value was 304.0824 for $[M + H]^+$, which agrees with the mass of product **3a**. Furthermore, the structure of compound **3a** was determined through single-crystal XRD. the ORTEP diagram of compound **3a**, as well as ^{1}H, ^{13}C, and HRMS data, are presented at the end of this chapter (**Figure 2-5)**.

After optimising the reaction conditions, we examined various reactions of 4-hydroxydithiocoumarin (**1a**) with substituents 7-F (**1b**), 5-Cl (**1c**), and 6-Cl (**1d**) with cyclohexyl isocyanide (**2a**) under identical conditions. The desired products **3a-d** were obtained in almost quantitative yields of 96-98%, as shown in **Table 2**. Subsequently, the reaction was scrutinised between 4-hydroxydithiocoumarin (**1a**) and various substituents, including 7-F (**1b**), 5-Cl (**1c),** 6-Cl (**1d**), 6-CF_3 (**1f**), and tert-butyl isocyanide (**2b**), yielding the desired products **3e-i** with excellent yields of 93-98%. Similarly, 4-hydroxydithiocoumarin (**1a**), having substituents 5-Cl (**1c**), 6-Cl (**1d**), 7-Cl (**1e**), and 6-CF_3 (**1f**), was subjected to 2-morpholinoethyl isocyanide, affording products **3j-n** with 88-93% yield. Finally, 4-hydroxydithiocoumarin (**1a**), having substituents 7-F (**1b**), 5-Cl (**1c**), 6-Cl (**1d**), 7-Cl (**1e**), and 6-CF_3 (**1f**), was subjected to 1,1,3,3-tetramethylbutyl isocyanide (**2d**), yielding products **3o-t**.

Table 1. Optimisation Table of the reaction conditions.[a,b]

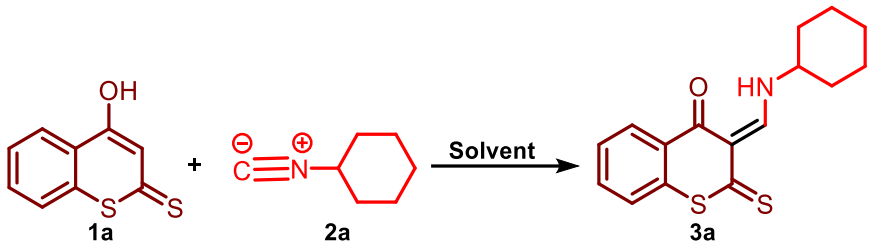

Entry	Temp (°C)	Time (h)	Solvent	Yield (%)[b]
1	RT	1-2	Water	NR
2	RT	1-2	Ethanol	NR
3	RT	1	DMF	trace
4	RT	1	1-4 Dioxane	trace
5	RT	1	DMA	trace
6	RT	1	Chlorobenzene	68
7	**RT**	**1**	**Toluene**	**98**

[a]All the reactions were carried out using 4-hydroxydithiocoumarin (1a, 0.2 mmol), cyclohexyl isocyanide (2a, 0.2 mmol). [b] Isolated yield. RT: Room Temperature, NR: No reaction. DMF = N, N-dimethyl formamide, DMA = N, N-dimethyl acetamide.

Table 2. Substrate Scope

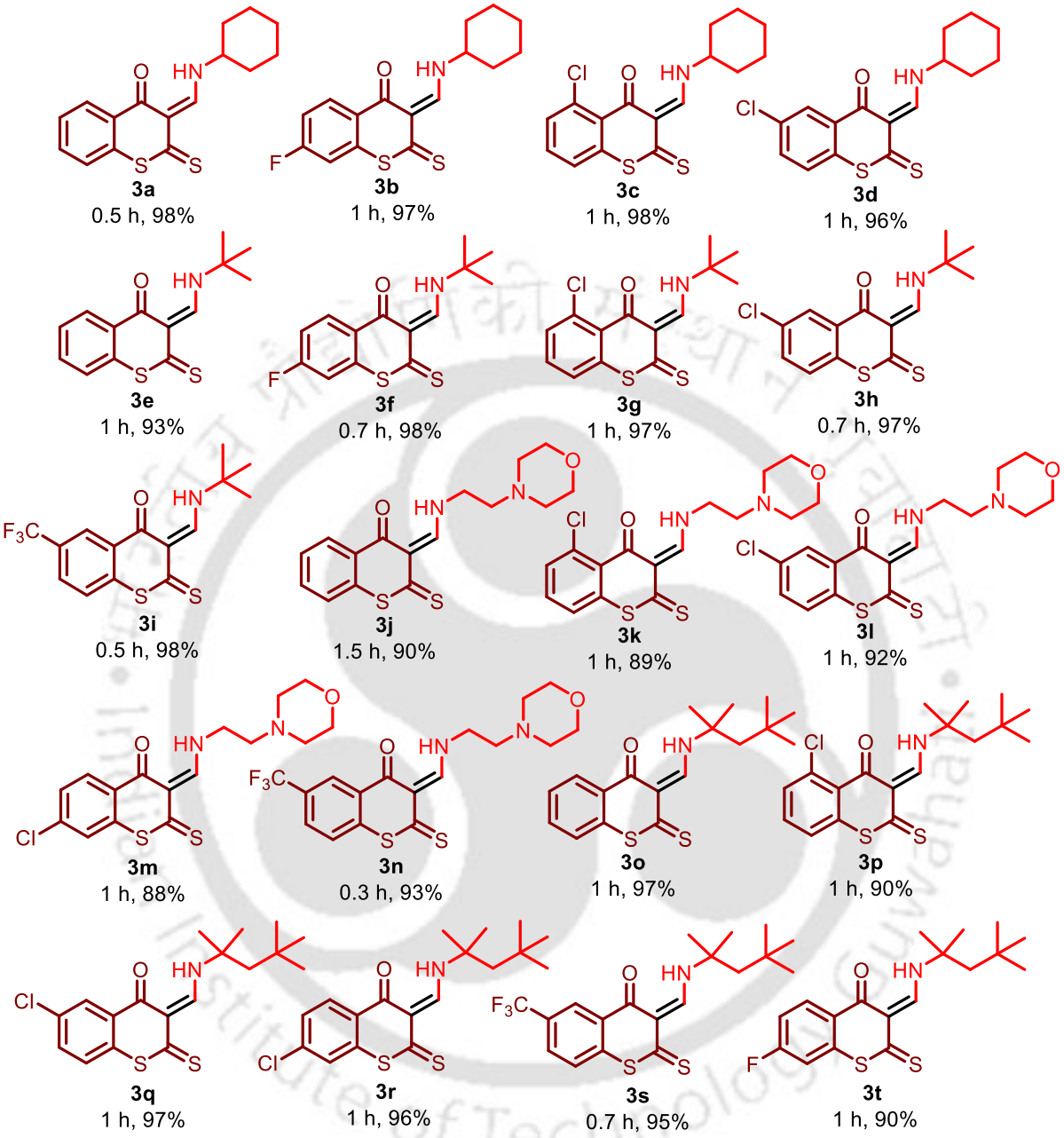

[a]All the reactions were carried out using 4-hydroxydithiocoumarin derivatives (1a-f, 0.2 mmol), isocyanide derivatives (2a-d, 0.2 mmol) in toluene at room temperature. [b] Isolated yield.

4.2 Plausible Reaction Mechanism

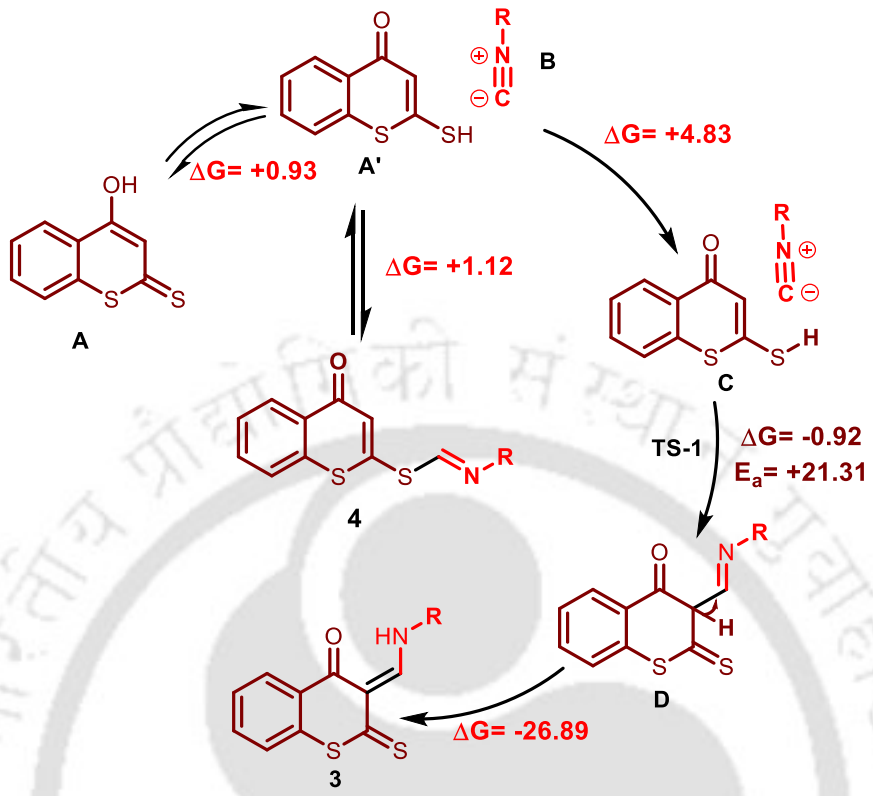

Scheme 6. Reaction Mechanism for the formation of compound 3e

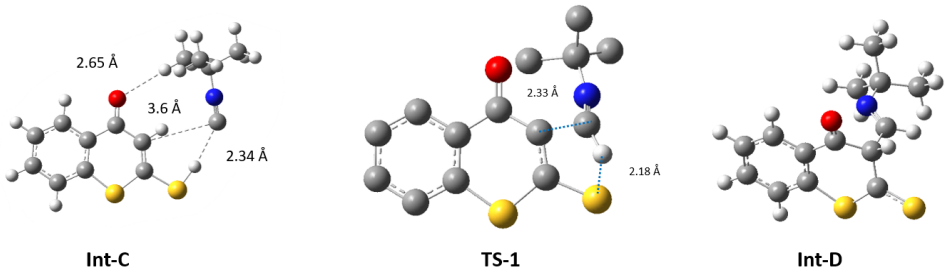

Figure 2. 3D structures of Int-C, intermediate Int-D and TS-1 (provided without hydrogen atoms)

The proposed reaction mechanism is based on isolated products, the previously reported literature, and DFT calculations.[19,20] A plausible reaction mechanism for the regioselective formation of **3** (instead of compound **4**) has been proposed, based on clues from the energy profile of the reaction evaluated using the DFT method B3LYP/6-31+G(d,p) with Gaussian software. **Scheme 6** shows the proposed mechanism and energy requirements at each step. The 4-hydroxythiocoumarin can exist in the two preferred states, enol (**A**) or thienol (**A′**). As shown in **Scheme 6,** two products can be expected from this work. Product **3** is thermodynamically

more favoured by 22.05 kcal/mol, whereas product **4** is an endergonic product by 1.12 kcal/mol. Thus, the regioselectivity in this reaction originates from the thermodynamic stability of the product. The **TS-1** for this formation is with C----C 2.33 Å, in which the nucleophilic carbon centre attacks the electrophilic carbon of isocyanide. IRC calculations have confirmed that the identified transition state lies along the path connecting the substrates and the product. This IRC study and the vibrational motions in **TS-1** clearly indicate that the reaction originates from **A′**. A complex intermediate, **C,** forms between A′ and B, with an endergonic free energy of 4.83 kcal/mol. Intermediate **D** is marginally more stable than the complex intermediate **C** by 0.92 kcal/mol. The barrier for C----C bond formation and simultaneous hydrogen transfer from the S-H group of **A′** is 21.3 kcal/mol. Intermediate **D** undergoes tautomerization to give **3** and is highly exergonic with a ΔG° of 26.89 kcal/mol. The 3D structure of the transition state (**S1**) clearly shows C---C bond formation and hydrogen migration (**Figure 2**).

It is noteworthy that the present protocol can be performed on a 1 mmol scale, and the successful results are shown below.

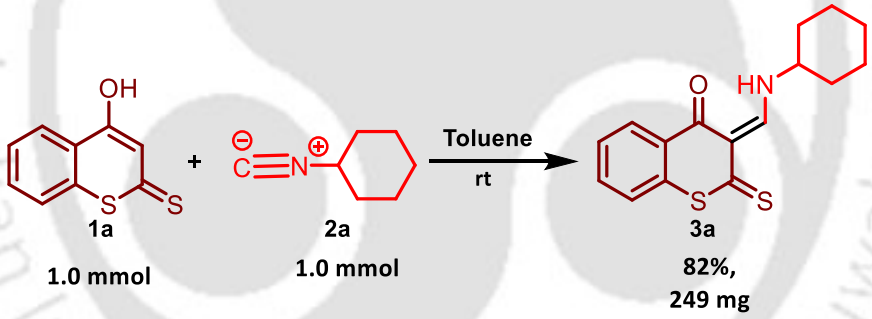

Large-scale reaction for the synthesis of **3a**

4.3 Post-synthetic Applications

Regioselective Cycloaddition reaction of (*E*)-3-((cyclohexylamino)methylene)-2-thioxo-thiochrom an-4-one derivatives with acetylene dicarboxylates

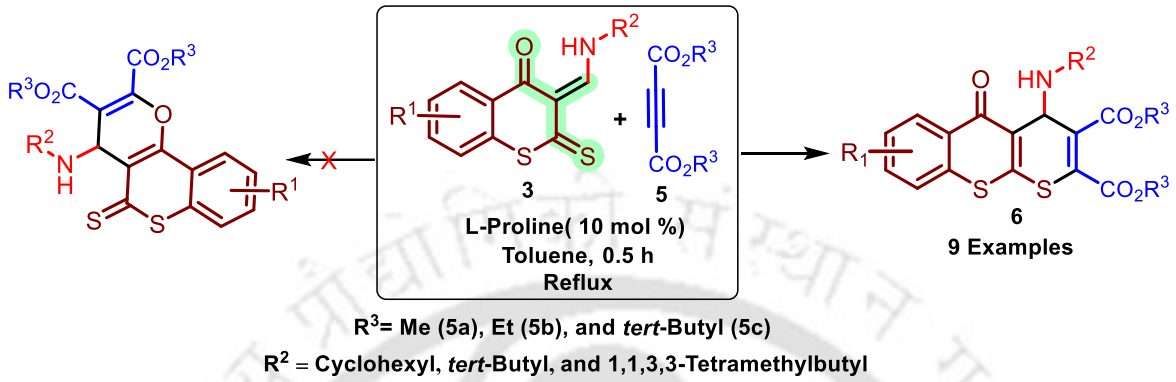

Scheme 7. L-Proline-catalysed cycloaddition reaction of the synthesised compound 3 with alkynes

After synthesising product **3** and being encouraged by these successful results, we considered exploring it further for cycloaddition reactions. As product **3** exhibits two diene systems through which it can undergo a Diels-Alder reaction at two possible sites (i.e., *via* sulphur or oxygen), as shown in **Scheme 7**, we wanted to investigate whether compound **3** undergoes a cycloaddition reaction and, if so, which site is involved in the reaction. It was noted in the literature[21] that Moghaddam and his co-workers reported a regioselective domino Knoevenagel-hetero-Diels-Alder reaction of 4-hydroxydithiocoumarin and *O*-acrylated salicylaldehyde derivatives in water as solvent. With this goal in mind, the cycloaddition reaction was examined with substrate **3a** and methylacetylene dicarboxylate **5a** in the presence of 10 mol% L-proline catalyst under reflux conditions in toluene.

The expected product**, 6aa,** was isolated in an 86% yield. The product (**6aa**) was characterised using various spectroscopic techniques, including ^{1}H and ^{13}C NMR, HRMS, and XRD, as shown in **Figure 3**. The ^{1}H NMR spectrum of product **6aa**, with characteristic peaks at δ 3.86 (s, 3H) and δ 3.84 (s, 3H), confirms that acetylene dimethyl dicarboxylate is incorporated into the final product. The peaks at δ 2.55 – 2.49 (m, 1H), 1.81 (t, J = 15.1 Hz, 2 H), 1.63 (d, J = 12.9 Hz, 2 H), 1.50 (d, J = 12.3 Hz, 1 H), 1.22 – 1.11 (m, 2 H), 1.08 (d, J = 12.2 Hz, 1 H), and 1.02 – 0.95 (m, 2 H), corresponding to 11 protons, indicate that cyclohexyl isocyanide is incorporated into the final product, as observed in the spectra. Additionally, the m/z value of 446.1083 for [M + H]+ is consistent with the mass of product **6aa**. The IR spectrum of the

product showed a characteristic absorption at 3344 cm^{-1}, indicating the presence of an N-H bond. For further confirmation of the structures, we have performed single-crystal XRD of compound 6fb, and the crystal details are shown in **Figure 6**. Additionally, the ^{1}H, ^{13}C, and HRMS spectra of compound **6aa** are presented in **Figures 7-9** at the end of this chapter.

Initially, optimisation was done by varying the solvent, catalyst amount, and temperature. For the experiments, we used **3a** (0.15 mmol) and **5a** (0.15 mmol) in a 10 mL round-bottom flask with 1 mL of toluene, stirring for three hours at room temperature. A trace amount of product **6aa** was observed in **Table 3**, entry 1. Then, the same reaction was refluxed for 2 hours, and the yield increased by up to 30% (Table 3, entry 2). When 10 mol% L-proline was introduced under the same reaction conditions, the reaction proceeded rapidly, yielding 86% (Table 3, entry 3). Encouraged by the good results, the catalyst amount was further optimised. Increasing the catalyst amount to 20 mol% did not improve yield, whereas decreasing it negatively affected yield, as shown in **Table 3**, entries 4 and 5. After optimising the catalyst, we tested different solvents (polar aprotic chlorobenzene and DMF, as well as polar protic solvents methanol and water), but positive results were observed only with chlorobenzene (Table 3, entries 6-9). In conclusion, the conditions described in **Table 3**, entry **3**, provided the best results for this reaction. The same reaction conditions were also carried out at room temperature, where we observed that the reaction took longer and yielded less amount of product (**Table 3**, entry **10**). When we used K_2CO_3 instead of L-proline, we obtained the same yield (85%), but the reaction took longer.

Table 3. Optimisation table of the reaction conditions[a-b]

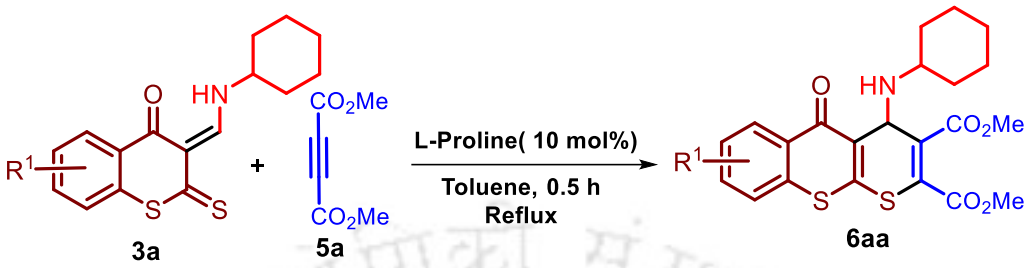

Entry	Temp (°C)	Time (h)	Catalyst (L-proline) mol%	Solvent	Yield (%)[b]
1	RT	3	Nil	Toluene	Trace
2	110	1-3	Nil	Toluene	30
3	**110**	**0.5**	**10**	**Toluene**	**86**
4	110	1	20	Toluene	85
5	110	1	5	Toluene	67
6	132	1	10	Chlorobenzene	68
7	110	1	10	DMF	Trace
8	64	1	10	Methanol	NR
9	100	1	10	Water	NR
10	RT	3	10	Toluene	50
11	110	2	K_2CO_3 (1 equiv.)	Toluene	85

[a]All the reactions were carried out using (3a, 0.15 mmol), (5a, 0.15 mmol)in presence of 10 mol% (L-proline). [b] Isolated yield. RT: Room Temperature, NR: No Reaction. DMF = N, N-dimethylformamide.

To examine the substrate scope, we initially reacted **3a** with acetylene dimethyl dicarboxylate **5a** in the presence of an organic catalyst (L-Proline, 10 mol%) in toluene at 110 °C for 0.5 hours, yielding the regioselective cycloadduct 6aa, with the cycloaddition occurring at the sulfur site. Similarly, when **3c**, **3d**, **3e**, **3g**, **3h**, **3s**, **3t** were subjected to different acetylene dicarboxylates **5a**, **5b**, and **5c**, we obtained regioselective cycloadducts **6bc-ic** with yields ranging from 83-91% and are presented in **Table 4**.

Table 4. Substrate scope for the cycloaddition reaction.

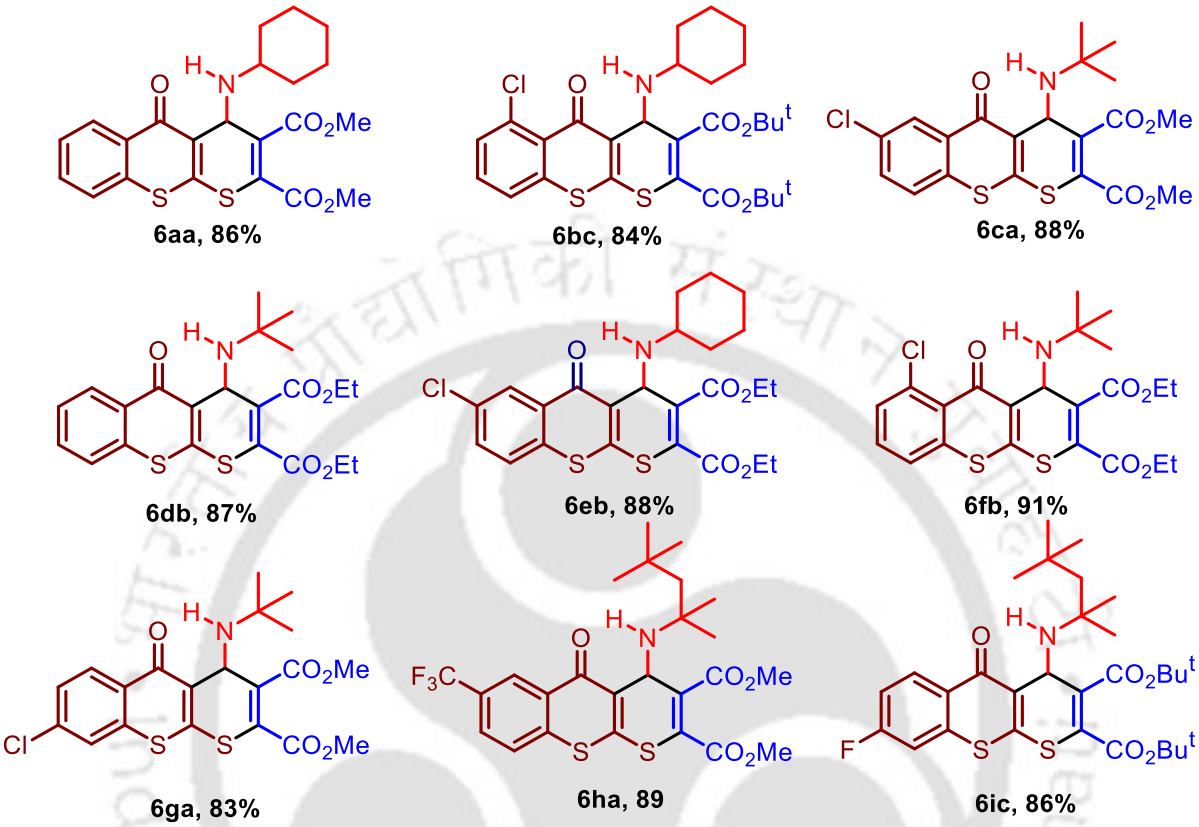

[a] All the reactions were carried out using (E)-3-((alkylamino)methylene)-2-thioxothiochroman-4-one derivatives (0.15 mmol), acetylene dicarboxylate (0.15 mmol) in the presence of L-proline (10 mol %). [b] Isolated yields. Reflux, toluene used as a solvent.

To understand the energetics of the reaction reported in **Scheme 7**, quantum-chemical calculations have been performed using model molecules **3u** and **5d**. The formation of **6** is an exergonic process by 4.76 kcal/mol. It follows a Diels-Alder reaction path, forming concerted C---C and C---S bonds. A plausible reaction mechanism involving L-Proline has been proposed, drawing on clues from earlier L-proline-catalysed cycloaddition reactions.[22,23] The first step involves the formation of an imine complex**, C1,** which is endergonic by 24.1 kcal/mol, as suggested by earlier DFT studies on L-Proline-catalysed reactions.[24] Second step involves a [4+2] cycloaddition reaction to form intermediate complex **C2** with an energy barrier (*via* **TS-2**) of 33.5 kcal/mol. In the final step, **C2** is hydrolysed to give the desired product 6jd with an energy release of 29.4 kcal/mol (Scheme 8). NBO analysis of **C1** showed that the energy of HOMO increases marginally upon iminium ion formation and facilitates the Diels-Alder reaction (**Figure 13**).

A plausible reaction mechanism for the formation of cycloadducts

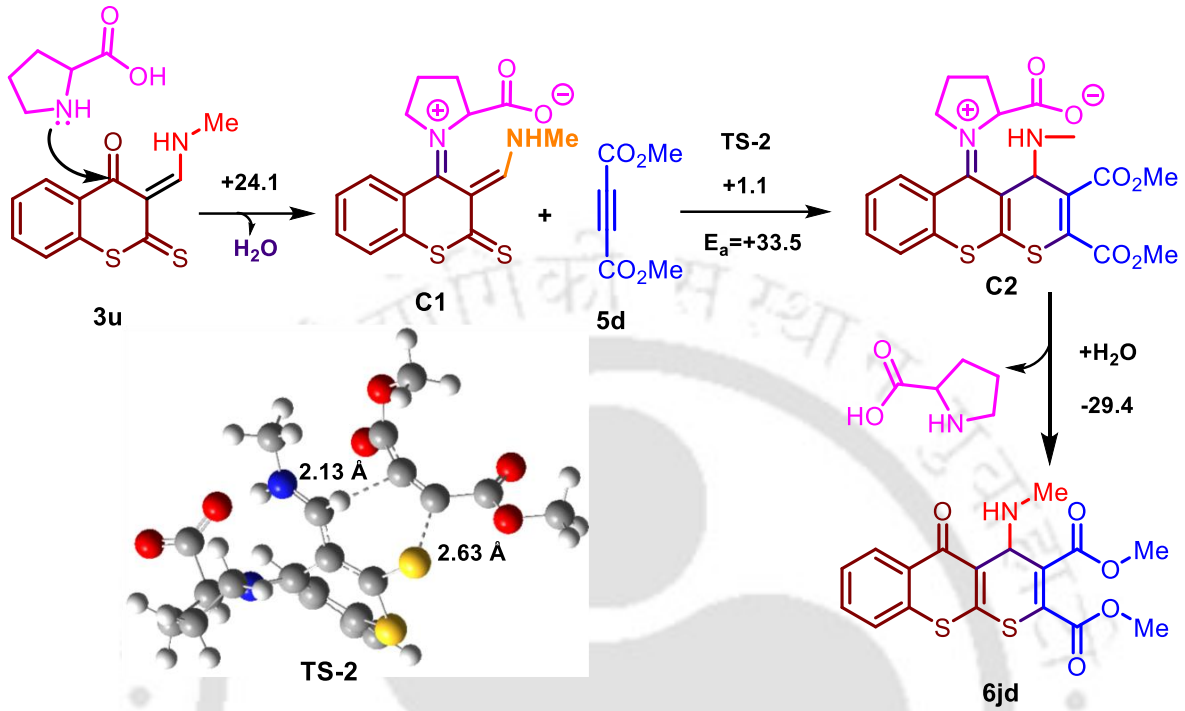

Scheme 8. Plausible mechanism of formation of 6jd in the presence of L-Proline. The calculations were carried out using B3LYP/6-31+G(d,p) level of DFT. All energy values are estimated from free energy (G) values. The relative energies of the reaction path are provided in kilocalories per mole (kcal/mol).

However, in the case of 3j-n (morpholine) derivatives, no cycloadduct was observed under the same conditions Scheme 9. We believe that the [4+2] addition reaction fails due to the morpholine group's orientation or bulkiness.

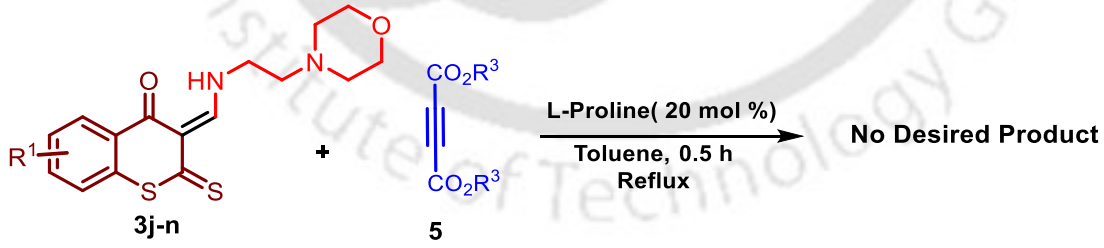

Scheme 9. No reaction cycloaddition occurs with morpholine derivatives

N-alkylation followed by Cycloaddition reaction of (E)-3-((cyclohexylamino)methylene)-2-thioxo-thiochroman-4-one derivatives with propargyl-bromide 7

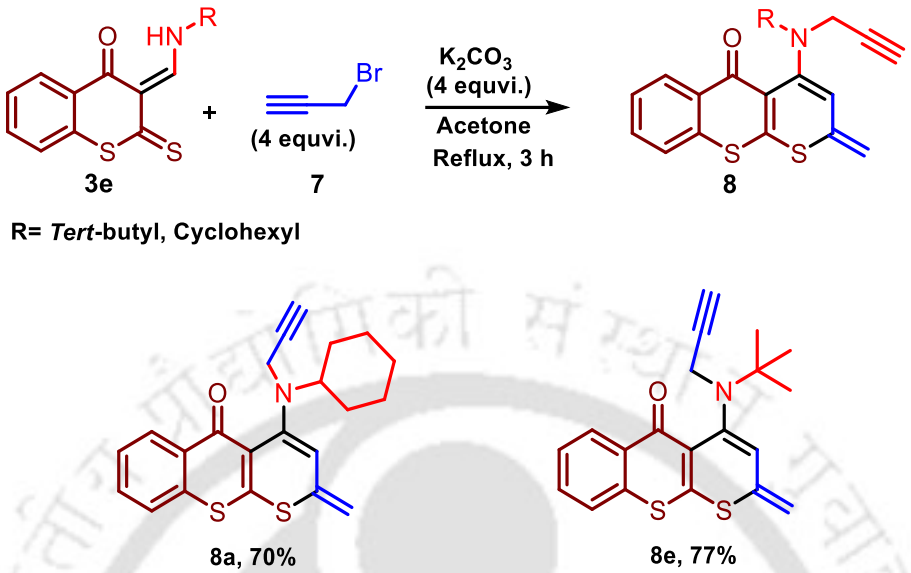

Scheme 10. [a] The reactions were carried out using "(*E*)-3-((cyclohexylamino)methylene)-2-thioxothiochroman-4-one derivatives" (0.15 mmol), propargyl bromide (0.6 mmol). [b] Isolated yield. Reflux, acetone as solvent.

It is well known that propargyl bromide is a good alkylating agent. We subjected product **3e** to propargyl bromide **7** to check whether product **3e** undergoes alkylation at the secondary amine position or not. Interestingly, we obtained an *N*-alkylated product followed by a cycloaddition product **8e**, where two molecules of propargyl bromide **7** were consumed, as shown in **Scheme 10**. Spectroscopic techniques and mass spectrometry confirmed the identity of the product as **8e**. In the proton NMR, the characteristic peak at δ 2.29 (s, 1H) indicates the propargyl sp hybridised proton, and at δ 3.84 (d, J = 17.0 Hz, 1H) and 3.66 (d, J = 17.1 Hz, 1H), these two peaks represent the two protons of propargyl bromide that are adjacent to the nitrogen. At δ 6.25 (s, 1H) and 6.00 (s, 1H), these two peaks represent the exocyclic double-bond protons. In addition, the m/z value of 354.0981 for $[M + H]^+$ agrees with the mass of product **8e** 354.0984. The ^{1}H, ^{13}C, and HRMS spectral data of the compound **8e** are shown in Figures **10-12**. Similarly, when the compound **3a** was subjected to propargyl bromide, it gave rise to compound **8a**. Propargyl bromide **7** is used in an excess amount due to its volatile nature.To explore the energy profile of the mechanism, a quantum chemical analysis of each step of the mechanism, as shown in **Scheme 11**, using **3a** leading to **8a**, has been performed at the B3LYP/6-31+(d,p) level. Two possible mechanisms can be suggested for this reaction: the first

involves the use of a mild base, K_2CO_3, and the other occurs in the absence of a base. The quantum chemical study indicated that this reaction, in the absence of a base, is endergonic by 11.65 kcal/mol. However, the energy released during this overall reaction in the presence of the base K_2CO_3 is -43.42 kcal/mol, indicating a highly exergonic process. Hence, the DFT study supports the mechanism involving K_2CO_3, which first abstracts the acidic NH proton of **3a**, forming the intermediate G, which is exergonic by 7.09 kcal/mol. Intermediate **G** then undergoes an S_N2 reaction with propargyl bromide 7, leading to N-C bond formation (an endergonic process), and intermediate **H** is formed by the release of KBr, endergonic by 4.58 kcal/mol. In intermediate **H**, the nitrogen lone pair electron is delocalized towards the sulfur end as a result of the sulfur-carbon π bond attacking the electrophilic center of the second propargyl bromide, giving rise to intermediate I *via* a cycloaddition reaction, which is

Plausible Reaction Mechanism of the formation of compound 8a.

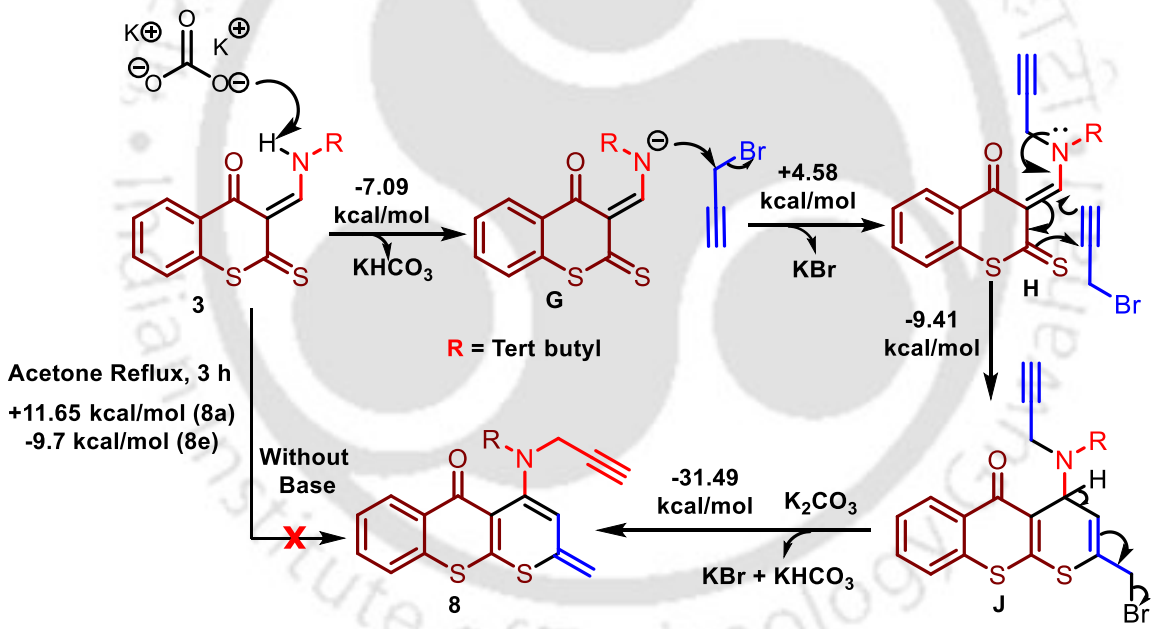

Scheme 11. The calculations were carried out using B3LYP/6-31+G(d,p) level of DFT. All energy values are estimated from free energy (G) values. The relative energies of the reaction path are provided in kcal/mol.

exergonic by 9.41 kcal/mol. K_2CO_3 abstracts the proton, and $KHCO_3$, along with KBr, is released to give the final product **8a** with an exocyclic double bond. The final step of the reaction is highly exergonic, characterised by an energy change of -31.49 kcal/mol. Experimentally, the reaction did not occur in the absence of a base. DFT studies confirmed the importance of a mild base, as the reaction is endergonic by 11.65 kcal/mol in its absence. Similarly, a DFT calculation for 8e also shows that the reaction is exergonic.

4.4 Conclusions

In conclusion, the reaction between 4-hydroxydithiocoumarin and isocyanide successfully provided regioselectively substituted (E)-3-aminomethylene-2-thioxothiochroman-4-one derivatives **(3).** This catalyst-free, highly atom-economical reaction proceeded with high regioselectivity, quantitative yields, and shorter reaction time. Furthermore, the reaction of compound **3** with 1,4-acetylene dicarboxylate esters **5** produced cycloadducts **6** in good yields, also with high regioselectivity. Interestingly, when substrate **3a** was reacted with propargyl bromide in the presence of potassium carbonate in acetone, an unexpected product **8a** was formed. The quantum chemical studies justified the regioselective product formation in **3** and **6**. The key features of this work include the absence of catalysts, high atom economy, regioselectivity, quantitative yields, and shorter reaction times, making it an efficient and attractive approach for synthesising these valuable heterocyclic compounds.

4.5 Experimental section

General procedure for the synthesis of (3a-t)

A mixture of 4-hydroxydithiocoumarin, **1** (0.39 g, 0.20 mmol), and isocyanide, 2 (22.8 µL, 0.20 mmol), was prepared in 1 mL of toluene in a 10 mL round-bottomed flask. The reaction flask was then kept on a stirrer for constant stirring at room temperature. At times, the reaction was monitored by TLC. After an hour, the reaction was over. Toluene was removed from the reaction mixture in a rotatory evaporator, and the crude residue was extracted with ethyl acetate (2 × 10 mL) and washed with water (2 × 5 mL). The organic layer was dried over anhydrous sodium sulfate (Na_2SO_4). Finally, the organic layer was concentrated in a rotatory evaporator, and the crude residue was purified through silica gel column chromatography (mesh 60–120). The desired products **3a-3i and 3m-3t** were isolated during chromatographic separation by eluting with a mixture of ethyl acetate/ petroleum ether (05 : 95), whereas the compounds **3j-3n** were eluted with ethyl acetate/petroleum ether mixture (15 : 85). A similar procedure was followed in all other cases. Further, the isolated product **3a** was recrystallised using a mixture of solvents, DMSO and DCM (1:1). The isocyanides used in our thesis work such *tert*-butyl, Cyclohexyl and 2-morpholinoethyl isocyanide were purchased from Sigma-Aldrich and 1,1,3,3-tetramethylbutyl isocyanide from BLD Pharma Chemicals.

General procedure for synthesising (6aa-6ic)

A mixture of product **3a** (0.15 mmol) and acetylene dicarboxylate (0.15 mmol) was taken in 1 mL of toluene in a 10 mL round-bottomed flask. Subsequently, the organ-catalyst L-proline (1.72 mg, 0.015 mmol) was added to the reaction mixture. The reaction flask was fitted with a reflux condenser and placed in a pre-heated oil bath at 110 °C with constant stirring. The reaction was complete after thirty minutes, as monitored by TLC. Toluene was removed from the reaction mixture in a rotatory evaporator, and the crude residue was extracted with ethyl acetate (2 × 10 mL) and washed with water (2 × 5 mL). The organic layer was dried over anhydrous sodium sulfate (Na2SO4). Finally, the organic layer was concentrated in a rotatory evaporator, and the crude residue was purified through silica gel column chromatography (mesh 60–120). The desired products **6aa-6ic** were separated using a mixture of solvents, ethyl acetate/petroleum ether mixture (10:90). The isolated product **6fb** was recrystallised using a mixture of solvents, chloroform and hexane (1:1).

General procedure for synthesising (8a,8e)

A mixture of product **3a** (53 mg, 0.15 mmol) and propargyl bromide **7** (46 µL, 0.60 mmol) was taken in 1 mL of acetone in a 10 mL round-bottomed flask. Subsequently, (0.6 mmol) K_2CO_3 was added to the reaction mixture. The reaction flask was then kept on a stirrer at reflux temperature. After 3 hours, the reaction was complete, as monitored by TLC at regular intervals. Acetone was removed from the reaction mixture in a rotatory evaporator, and the crude residue was extracted with ethyl acetate (2 × 10 mL) and washed with water (2 × 5 mL). The organic layer was dried over anhydrous sodium sulfate (Na_2SO_4). Finally, the organic layer was concentrated in a rotatory evaporator, and the crude residue was purified through silica gel column chromatography (mesh 60–120). The desired product **8a** was eluted with a solvent mixture of ethyl acetate/petroleum ether (10:90). A Similar polarity of solvent system was used to separate **8e**.

Quantum chemical methods

Quantum chemical calculations were performed using the Gaussian 16 suite of programs.[25] Geometry optimization of all compounds, intermediates, and transition

states along two pathways were performed by DFT using the B3LYP method.[27,30] The basis set employed was 6-31+G(d,p). The frequency calculations were performed on all structures to verify the nature of the stationary points (minima or saddle points). IRC calculations were carried out to confirm the reaction path. NBO analysis.

4.6 Characterisation Table:

(*E*)-3-((cyclohexylamino)methylene)-2-thioxothiochroman-4-one (3a). An orange solid (59 mg, 98%), mp118-120 °C, ^{1}H NMR (500 MHz, $CDCl_3$-*d*) δ 13.10 (s, 1H), 9.48 (d, *J* = 14.0 Hz, 1H), 8.38 – 8.27 (m, 1H), 7.50 (t, *J* = 7.2 Hz, 1H), 7.38 (t, *J* = 7.6 Hz, 1H), 7.23 (d, *J* = 7.9 Hz, 1H), 3.59 (s, 1H), 2.08 (d, *J* = 8.9 Hz, 2H), 1.90 – 1.83 (m, 2H), 1.58 (d, *J* = 14.7 Hz, 3H), 1.49 – 1.39 (m, 2H), 1.36 – 1.26 (m, 1H). ^{13}C{^{1}H} NMR (125 MHz, $CDCl_3$) δ 202.1, 178.1, 160.5, 139.2, 132.8, 129.4, 128.3, 127.5, 123.1, 118.5, 59.5, 32.1, 24.5, 23.8. IR(KBr)ν_{max}/cm^{-1} 3150 (N-H), 2923(C−H),1606(C=O), HRMS (ESI):m/z $[M+H]^+$ calcd for $C_{16}H_{17}NOS_2$ 304.0824; found 304.0824.

(*E*)-3-((cyclohexylamino)methylene)-7-fluoro-2-thioxothio chro-man-4-one (3b). A yellow solid (62 mg, 97%) mp 109-110 °C, ^{1}H NMR (500 MHz, DMSO-d_6) δ 12.97 (s, 1H), 9.21 (d, *J* = 14.9 Hz, 1H), 8.30 – 8.25 (m, 1H), 7.43 (d, *J* = 8.8 Hz, 1H), 7.31 (t, *J* = 7.6 Hz, 1H), 3.81 (s, 1H), 1.96 (d, *J* = 9.6 Hz, 2H), 1.72 (d, *J* = 12.7 Hz, 2H), 1.59 – 1.51 (m, 3H), 1.37 (q, *J* = 11.7 Hz, 2H), 1.22 (d, *J* = 11.9 Hz, 1H). ^{13}C{^{1}H} NMR (125 MHz, DMSO-d_6) δ 201.7, 177.2, 164.1 (d, *J* = 252.6 Hz), 160.5, 141.8 (d, *J* = 9.9 Hz), 131.6 (d, *J* = 10.2 Hz), 126.3, 118.3, 115.3 (d, *J* = 22.5 Hz), 109.6 (d, *J* = 25.2 Hz), 59.6, 32.1, 24.5, 23.9. IR(KBr)ν_{max}/cm^{-1}3150 (N-H), 2995 (C− H),1609(C=O), HRMS (ESI):m/z $[M+H]^+$ calcd for $C_{16}H_{16}FNOS_2$ 322.0730; found 322.0730.

(*E*)-5-chloro-3-((cyclohexylamino)methylene)-2-thioxothiochro- man-4-one (3c). A yellow solid (67 mg, 98%) mp 118-120 °C**,** ^{1}H NMR (500 MHz, DMSO-d_6) δ 12.83 (s, 1H), 9.09 (d, *J* = 15.2 Hz, 1H), 7.56 – 7.52 (m, 1H), 7.49 (d, *J* = 7.2 Hz, 1H), 7.44 (d, *J* = 7.5 Hz, 1H), 3.82 (1H), 1.96 (d, *J* = 10.6 Hz, 2H), 1.78 – 1.69 (m, 2H), 1.61 – 1.51 (m, 3H), 1.37 (q, *J* = 11.4 Hz, 2H), 1.28 – 1.19 (m, 1H). ^{13}C{^{1}H} NMR (125 MHz, DMSO-d_6) δ 198.8, 177.6, 160.0, 141.7, 134.7, 132.5, 131.2, 125.8, 122.6, 119.7, 59.57, 32.0,

24.4, 23.8. IR(KBr)ν_{max}/cm^{-1}3160 (N-H), 2995 (C−H),1609(C=O), HRMS (ESI):m/z $[M+H]^+$ calcd for $C_{16}H_{16}ClNOS_2$ 338.0435; found 338.0436.

(*E*)-6-chloro-3-((cyclohexylamino)methylene)-2-thioxothio-chroman-4-one (3d). A

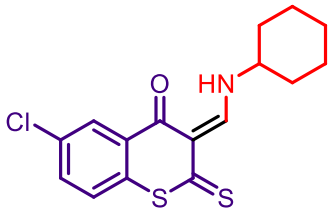

brown crystalline solid (66 mg, 96%) mp 200-202 °C, ^{1}H NMR (500 MHz, DMSO-d_6) δ 12.97 (s, 1H), 9.24 (d, *J* = 15.0 Hz, 1H), 8.15 (s, 1H), 7.71 (d, *J* = 8.4 Hz, 1H), 7.54 (d, *J* = 8.5 Hz, 1H), 3.83 (s, 1H), 1.98 (d, *J* = 11.4 Hz, 2H), 1.74 (d, *J* = 12.1 Hz, 2H), 1.63 – 1.51 (m, 3H), 1.38 (q, *J* = 11.3 Hz, 2H), 1.28 – 1.19 (m, 1H). ^{13}C{^{1}H} NMR (125 MHz, DMSO-d_6) δ201.5, 176.6, 160.5, 137.9, 132.4, 132.0, 130.8, 127.3, 125.3, 118.2, 59.6, 31.9, 24.4, 23.8 IR(KBr)ν_{max}/cm^{-1} 3153(N-H), 2992(C−H), 1603(C=O), HRMS (ESI):m/z $[M+H]^+$ calcd for $C_{16}H_{16}ClNOS_2$ 338.0435; found 338.0435

(*E*)-3-((tert-butylamino)methylene)-2-thioxothiochroman-4-one (3e). A grey crystalline

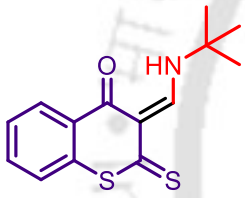

solid (42 mg, 93%) mp 126-128 °C, ^{1}H NMR (500 MHz, DMSO-d_6) δ 13.31 (s, 1H), 9.29 (s, 1H), 8.24 (d, *J* = 8.0 Hz, 1H), 7.63 (t, *J* = 7.5 Hz, 1H), 7.48 (t, *J* = 7.6 Hz, 1H), 7.45 (d, *J* = 7.9 Hz, 1H), 1.46 (s, 9H). ^{13}C{^{1}H} NMR (125 MHz, DMSO-d_6) δ 202.2, 178.2, 158.3, 139.3, 132.9, 129.4, 128.3, 127.6, 123.2, 118.1, 57.2, 28.4. 8 IR(KBr)ν_{max}/cm^{-1} 3154(N-H), 2992(C−H), 1603(C=O), HRMS (ESI):m/z $[M+H]^+$ calcd for $C_{14}H_{16}NOS_2$ 278.0668; found 278.0664.

(*E*)-3-((tert-butylamino)methylene)-7-fluoro-2-thioxothiochroman-4-one (3f). A yellow

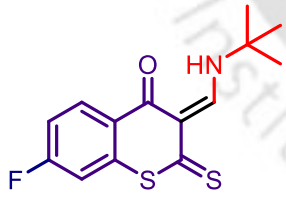

solid (63 mg, 98%) mp 184-186 °C. ^{1}H NMR (500 MHz, DMSO-d_6) δ 13.26 (d, *J* = 13.3 Hz, 1H), 9.26 (d, *J* = 15.2 Hz, 1H), 8.33 – 8.26 (m, 1H), 7.47 (d, *J* = 8.7 Hz, 1H), 7.34 (t, *J* = 8.5 Hz, 1H), 1.47 (s, 9H). ^{13}C{^{1}H} NMR (125 MHz, DMSO-d_6) δ 201.7 177.1, 164.0 (d, *J* = 252 Hz,), 158.2, 141.7 (d, *J* = 10 Hz,), 131.4 (d, *J* = 10Hz,), 126.2, 117.8, 115.2 (d, *J* = 21 Hz,), 115.17, 109.6 (d, *J* = 25 Hz,), 57, 28.2. 8 IR(KBr)ν_{max}/cm^{-1} 3159(N-H), 2993(C−H), 1606(C=O), HRMS (ESI):m/z $[M+H]^+$ calcd for $C_{14}H_{15}FNOS_2$ 296.0574; found 296.0574.

***(E)*-3-((tert-butylamino)methylene)-5-chloro-2-thioxothiochroman-4-one(3g) .** A yellow

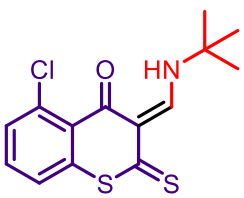

solid (66 mg, 97%) mp 126-128 °C, ^{1}H NMR (500 MHz, DMSO-d_6) δ 13.15 (s, 1H), 9.11 (d, *J* = 15.4 Hz, 1H), 7.54 (t, *J* = 7.8 Hz, 1H), 7.49 (d, *J* = 6.7 Hz, 1H), 7.43 (d, *J* = 7.7 Hz, 1H), 1.47 (s, 9H). ^{13}C{^{1}H} NMR (125 MHz, DMSO-d_6) δ 198.9, 177.6, 157.9, 141.8, 134.7, 132.5, 131.3,

125.7, 122.6, 119.2, 57.1, 28.3. IR(KBr)ν_{max}/cm^{-1} 3170 (N-H), 2990(C−H), 1601(C=O), HRMS (ESI):m/z $[M+H]^+$ calcd for $C_{14}H_{15}ClNOS_2$ 312.0278; found 312.0278.

(*E*)-3-((tert-butylamino)methylene)-7-chloro-2-thioxothiochroman-4-one(3h). A grey

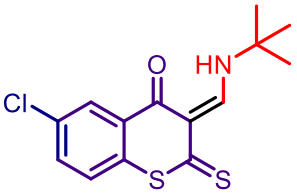

crystalline solid (60 mg, 97%) mp 127-129 °C, ^{1}H NMR (500 MHz, DMSO-d_6) δ 13.23 (d, *J* = 15.7 Hz, 1H), 9.27 (d, *J* = 15.3 Hz, 1H), 8.16 (d, *J* = 2.0 Hz, 1H), 7.71 (d, *J* = 10.6 Hz, 1H), 7.55 (d, *J* = 8.5 Hz, 1H), 1.47 (s, 9H). ^{13}C{^{1}H} NMR (125 MHz, DMSO-d_6) δ 202.1, 177.1, 158.7, 138.4, 132.9, 132.5, 131.3, 127.7, 125.8, 118.2, 57.7, 28.7. IR(KBr)ν_{max}/cm^{-1} 3160(N-H), 2993(C− H), 1605(C=O), HRMS (ESI):m/z $[M+H]^+$ calcd for $C_{14}H_{15}ClNOS_2$ 3120282; found 312.0282.

(*E*)-3-((tert-butylamino)methylene)-2-thioxo-6-(trifluoromethyl) thiochroman-4-one(3i) .

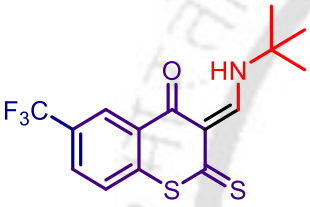

A light-yellow solid (67 mg, 98%) mp 191-193 °C, ^{1}H NMR (500 MHz, Chloroform-*d*) δ 13.32 (s, 1H), 9.49 (s, 1H), 8.57 (s, 1H), 7.68 (d, *J* = 8.2 Hz, 1H), 7.32 (d, *J* = 8.3 Hz, 1H), 1.54 (s, 9H). ^{13}C{^{1}H} NMR (125 MHz, $CDCl_3$) δ 178.3, 159.1, 144.0, 130.3, 129.3 (q, *J* = 33.2 Hz), 128.3, 128.3, 126.0, 123.7(q, *J* = 270.2 Hz), 123.5,118.6, 56.9, 29.5. IR(KBr)ν_{max}/cm^{-1} 3165(N-H), 2995 (C−H), 1606(C=O), HRMS (ESI):m/z $[M+H]^+$ calcd for $C_{15}H_{15}F_3NOS_2$ 346.0538; found 346.0538

(*E*)-3-(((2-morpholinoethyl)amino)methylene)-2-thioxothio chroman-4-one(3j). A brown

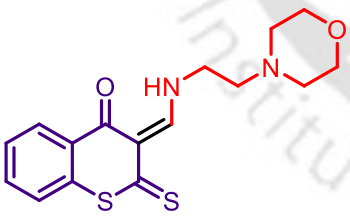

solid (66 mg, 90%) mp 87-89 °C, ^{1}H NMR (400 MHz, DMSO-d_6) δ 12.70 (s, 1H), 9.19 (d, *J* = 11.4 Hz, 1H), 8.23 (d, *J* = 7.9 Hz, 1H), 7.63 – 7.59 (m, 1H), 7.47 (d, *J* = 7.3 Hz, 1H), 7.42 (d, *J* = 7.9 Hz, 1H), 3.78 (s, 2H), 3.60 (s, 4H), 2.62 (s, 2H), 2.50 (s, 4H). ^{13}C{^{1}H} NMR (100 MHz, DMSO-d_6) δ 202.4, 178.1, 163.3, 139.3, 132.8, 129.6, 128.4, 127.5, 123.1, 118.8, 56.4, 52.9, 46.8. IR(KBr)ν_{max}/cm^{-1} 3150 (N-H), 2992 (C−H), 1610(C=O), HRMS (ESI):m/z $[M+H]^+$ calcd for $C_{16}H_{19}N_2O_2S_2$ 335.0882; found 335.0878

(*E*)-5-chloro-3-(((2-morpholinoethyl)amino)methylene)-2-thioxothiochroman-4-one(3k). A brown solid (65 mg, 89%) mp 127-129 °C, ^{1}H NMR (500 MHz, DMSO-d_6) δ 12.45 (s, 1H),

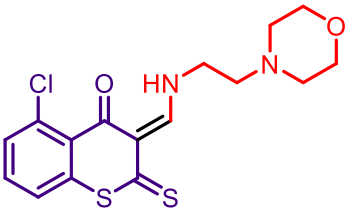

9.03 (d, J = 15.2 Hz, 1H), 7.51 (t, J = 7.8 Hz, 1H), 7.45 (d, J = 7.4 Hz, 1H), 7.40 (d, J = 7.7 Hz, 1H), 3.77 (s, 2H), 3.59 (s, 4H), 2.61 (s, 2H), 2.48 (s, 4H). ^{13}C{^{1}H} NMR (125 MHz, DMSO-d_6) δ 177.6, 162.6, 141.8, 134.6, 132.3, 131.2, 125.9, 122.5, 120.0, 66.0, 56.3, 52.7, 46.7. IR(KBr)ν_{max}/cm^{-1} 3160 (N-H), 2990(C−H), 1612(C=O), HRMS (ESI):m/z [M+H]$^{+}$ calcd for $C_{16}H_{18}ClN_2O_2S_2$ 369.0493; found 369.0493

(*E*)-6-chloro-3-(((2-morpholinoethyl)amino)methylene)-2-thioxothiochroman-4-one(3l).

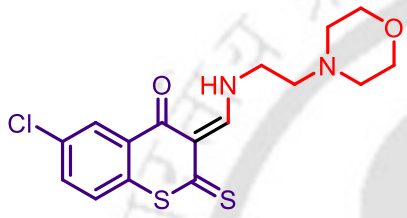

Brown liquid, (67 mg, 92%), ^{1}H NMR (500 MHz, Chloroform-d) δ 12.63 (s, 1H), 9.18 (d, J = 14.4 Hz, 1H), 8.18 (d, J = 8.4 Hz, 1H), 7.63 (s, 1H), 7.49 (d, J = 8.6 Hz, 1H), 3.84 (s, 2H), 3.64 (s, 4H), 2.74 (s, 2H), 2.60 (s, 4H). ^{13}C{^{1}H} NMR (125 MHz, Chloroform-d) δ 202.0, 177.0, 163.2, 140.9, 137.7, 130.1, 128.2, 127.3, 122.3, 118.7, 65.7, 56.1, 52.6, 46.5. IR(KBr)ν_{max}/cm^{-1} 3160 (N-H), 2990(C−H), 1612(C=O), HRMS (ESI):m/z [M+H]$^{+}$ calcd for $C_{16}H_{18}ClN_2O_2S_2$ 369.0493; found 369.0492

(*E*)-7-chloro-3-(((2-morpholinoethyl)amino)methylene)-2-thioxothiochroman-4-one

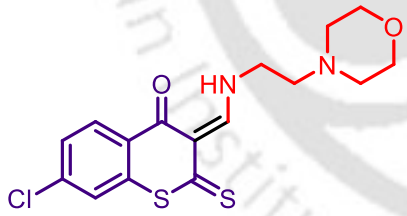

(3m). A brown solid (64 mg, 88%) mp 134-136 °C, ^{1}H NMR (500 MHz, DMSO-d_6) δ 12.65 (s, 1H), 9.17 (d, J = 14.7 Hz, 1H), 8.19 (d, J = 8.6 Hz, 1H), 7.65 – 7.62 (m, 1H), 7.49 (d, J = 10.0 Hz, 1H), 3.81 (s, 2H), 3.62 (s, 4H), 2.67 (s, 2H), 2.60 – 2.51 (m, 4H). ^{13}C{^{1}H} NMR (125 MHz, DMSO-d_6) δ 201.9, 177.0, 163.1, 141.0, 137.7, 130.1, 128.2, 127.3, 122.3, 118.6, 56.2, 52.7, 46.6. IR(KBr)ν_{max}/cm^{-1} 3155 (N-H), 2993(C−H), 1610(C=O), HRMS (ESI):m/z [M+H]$^{+}$ calcd for $C_{16}H_{18}ClN_2O_2S_2$ 369.0493; found 369.0493.

(*E*)-3-(((2-morpholinoethyl)amino)methylene)-2-thioxo-6-(trifluoromethyl)Thiochrom-an-4-one (3n). A yellow solid (74 mg, 93%) mp 137-139 °C, ^{1}H NMR (500 MHz, DMSO-d_6)

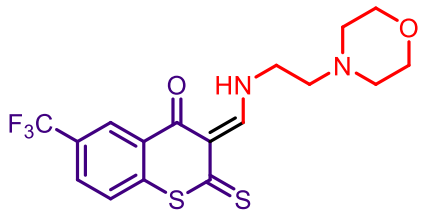

δ 12.65 (s, 1H), 9.19 (d, *J* = 14.7 Hz, 1H), 8.40 (s, 1H), 7.92 (d, *J* = 8.3 Hz, 1H), 7.68 (d, *J* = 8.3 Hz, 1H), 3.84 – 3.79 (m, 2H), 3.62 – 3.58 (m, 4H), 2.61 (s, 2H), 2.47 (s, 4H). ^{13}C{^{1}H} NMR (125 MHz, DMSO-d_6) δ 201.5, 176.5, 163.0, 143.6, 129.8, 128.7(d, *J* = 3.2 Hz), 128.5, 127.4 (d, *J* = 32.4 Hz), 124.5, 123.7 (d, *J* = 270.4 Hz), 118.7, 66.2, 56.2, 52.8, 46.9. IR(KBr)ν_{max}/cm^{-1} 3155 (N-H), 2993(C− H), 1610(C=O), HRMS (ESI):m/z [M+H]$^{+}$ calcd for $C_{17}H_{18}F_3N_2O_2S_2$ 403.0756; found 403.0757.

(*E*)-2-thioxo-3-(((2,4,4-trimethylpentan-2-yl)amino)methylene) thiochroman-4-one (3o).

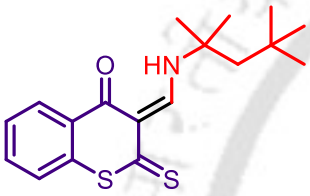

A brown sticky (64 mg, 97%), ^{1}H NMR (500 MHz, DMSO-d_6) δ 13.44 (s, 1H), 9.31 (d, *J* = 15.1 Hz, 1H), 8.24 (d, *J* = 8.0 Hz, 1H), 7.62 (d, *J* = 7.9 Hz, 1H), 7.50 – 7.44 (m, 3H), 1.78 (s, 2H), 1.52 (s, 6H), 0.95 (s, 9H). ^{13}C{^{1}H} NMR (125 MHz, DMSO-d_6) δ 202.2, 178.0, 158.4, 139.2, 132.7, 129.3, 128.2, 127.4, 123.1, 118.0, 60.1, 53.6, 31.4, 31.0, 28.3. IR(KBr)ν_{max}/cm^{-1} 3152 (N-H), 2992(C−H), 1600(C=O), HRMS (ESI):m/z [M+H]$^{+}$ calcd for $C_{18}H_{24}NOS_2$; 334.1294 found 334.1295

(*E*)-5-chloro-2-thioxo-3-(((2,4,4-trimethylpentan-2-yl)amino) methylene)thiochroman- 4-one(3p).

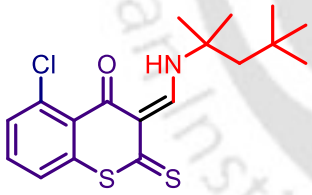

A brown solid (66 mg, 90%) mp 177-179 °C, ^{1}H NMR (500 MHz, DMSO-d_6) δ 13.25 (d, *J* = 14.7 Hz, 1H), 9.10 (d, *J* = 15.4 Hz, 1H), 7.54 (t, *J* = 7.8 Hz, 1H), 7.49 (d, *J* = 7.8 Hz, 1H), 7.43 (d, *J* = 7.8 Hz, 1H), 1.78 (s, 2H), 1.51 (s, 6H), 0.95 (s, 9H). ^{13}C{^{1}H} NMR (125 MHz, DMSO-d_6) δ 198.8, 177.7, 158.0, 141.7, 134.7, 132.5, 131.3, 125.7, 122.7, 119.3, 60.2, 53.6, 31.5, 31.1, 28.3. IR(KBr)ν_{max}/cm^{-1} 3151 (N-H), 2995(C− H), 1611(C=O), HRMS (ESI):m/z [M+H]$^{+}$ calcd for $C_{18}H_{23}ClNOS_2$; 368.0904 found 368.0903

(*E*)-6-chloro-2-thioxo-3-(((2,4,4-trimethylpentan-2-yl)amino) methylene) thiochroman-4-one(3q).

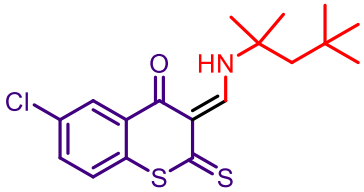

A yellow crystalline solid (71 mg, 97%) mp 99-101 °C, ^{1}H NMR (500 MHz, DMSO-d_6) δ 13.35 (d, *J* = 14.6 Hz, 1H), 9.28 (d, *J* = 15.2 Hz, 1H), 8.13 (d, *J* = 2.1 Hz, 1H), 7.68 (dd, *J* = 8.5, 2.2 Hz, 1H), 7.51 (d, *J* = 8.5 Hz, 1H), 1.78 (s, 2H), 1.52 (s, 6H), 0.96 (s, 9H). ^{13}C{^{1}H} NMR (125 MHz, DMSO-d_6) δ 201.7, 176.7, 158.4, 138.0, 132.5, 132.1, 130.7, 127.3, 125.3, 117.8, 60.3, 53.6, 31.5, 31.1, 28.2. IR(KBr)ν_{max}/cm^{-1} 3151 (N-H),

2994(C−H), 1610(C=O), HRMS (ESI):m/z $[M+H]^+$ calcd for $C_{18}H_{23}ClNOS_2$; 368.0904 found 368.0903

(*E*)-7-chloro-2-thioxo-3-(((2,4,4-trimethylpentan-2-yl)amino) methylene)thiochroman-4-one(3r). A light yellow solid (70 mg, 96%) mp 105-107 °C, ^{1}H NMR (500 MHz, DMSO-d_6) δ 13.37 (d, *J* = 14.8 Hz, 1H), 9.28 (d, *J* = 15.2 Hz, 1H), 8.22 (d, *J* = 8.6 Hz, 1H), 7.70 (d, *J* = 1.6 Hz, 1H), 7.52 (d, *J* = 10.3 Hz, 1H), 1.79 (s, 2H), 1.52 (s, 6H), 0.96 (s, 9H). ^{13}C{^{1}H} NMR (125 MHz, DMSO-d_6) δ 201.8, 177.2, 158.4, 141.0, 137.8, 130.1, 128.0, 127.5, 122.5, 118.0, 60.3, 53.6, 31.5, 31.0, 28.2. IR(KBr)ν_{max}/cm^{-1} 3150 (N-H), 2995(C−H), 1609(C=O), HRMS (ESI):m/z $[M+H]^+$ calcd for $C_{18}H_{23}ClNOS_2$; 368.0904 found 368.0904

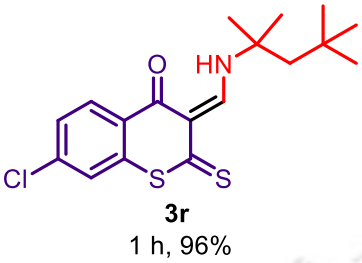

3r
1 h, 96%

(*E*)-2-thioxo-6-(trifluoromethyl)-3-(((2,4,4-trimethylpentan-2-yl) amino)methylene) thio chroman-4-one(3s). A yellow crystalline solid (76 mg, 95%) mp 105-107 °C, ^{1}H NMR (500 MHz, DMSO-d_6) δ 13.34 (d, *J* = 14.8 Hz, 1H), 9.27 (d, *J* = 15.2 Hz, 1H), 8.40 (s, 1H), 7.93 (d, *J* = 8.3 Hz, 1H), 7.69 (d, *J* = 8.3 Hz, 1H), 1.79 (s, 2H), 1.52 (s, 6H), 0.96 (s, 9H). ^{13}C{^{1}H} NMR (125 MHz, DMSO-d_6) δ 202.2, 177.2, 158.9, 144.1, 130.0, 128.9 (q, *J* = 3.7 Hz,), 128.0 (q, *J* = 32 Hz,), 125.2 (q, *J* = 2.5Hz,), 125.1, 124.1 (q, *J* = 271.2 Hz,), 118.5, 6.0.9, 54.0, 31.9, 31.5, 28.6. IR(KBr)ν_{max}/cm^{-1} 3151 (N-H), 2999(C− H), 1615(C=O), HRMS (ESI):m/z $[M+H]^+$ calcd for $C_{19}H_{23}F_3NOS_2$; 402.1168 found 402.1168

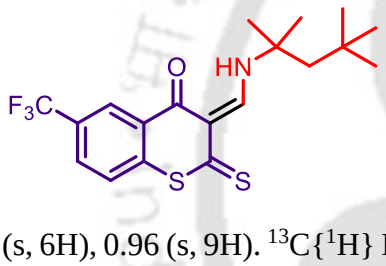

(*E*)-6-fluoro-2-thioxo-3-(((2,4,4-trimethylpentan-2-yl)amino) methylene)thiochroman-4-one(3t). A yellow crystalline (63 mg, 90%) mp 120-122 °C, ^{1}H NMR (500 MHz, DMSO-d_6) δ 13.37 (d, *J* = 14.6 Hz, 1H), 9.27 (d, *J* = 15.1 Hz, 1H), 8.28 (dd, *J* = 8.9, 5.9 Hz, 1H), 7.46 (dd, *J* = 8.9, 2.3 Hz, 1H), 7.32 (td, *J* = 8.7, 2.4 Hz, 1H), 1.78 (s, 2H), 1.51 (s, 6H), 0.95 (s, 9H). ^{13}C{^{1}H} NMR (125 MHz, DMSO-d_6) δ 201.9, 177.23, 164.1 (d, *J* = 251.2 Hz,), 158.4, 141.8 (d, *J* = 10 Hz,), 131.5 (d, *J* = 10 Hz,), 126.2(d, *J* = 10 Hz,), 117.9, 115.2

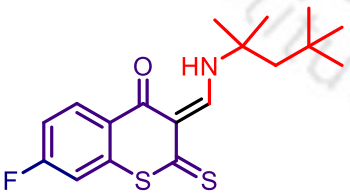

(d, *J* = 22 Hz,), 109.6 (d, *J* = 25 Hz,), 60.3, 53.6, 31.5, 31.1, 28.3. IR(KBr)ν_{max}/cm^{-1} 3166 (N-H), 2997(C−H), 1617(C=O), HRMS (ESI):m/z $[M+H]^+$ calcd for $C_{18}H_{22}FNOS_2$; 352.1205 found 352.1205

Dimethyl4-(cyclohexylamino)-5-oxo-4*H*,5*H*-thiopyrano[2,3-*b*]thiochromene-2,3-dicarb-oxylate (6aa). 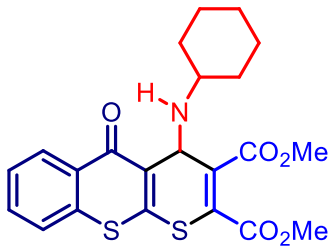 A brown solid (56 mg, 86%) mp 101-103 ^{o}C ^{1}H NMR (500 MHz, Chloroform-*d*) δ 8.46 (d, *J* = 8.0 Hz, 1H), 7.56 (t, *J* = 7.4 Hz, 1H), 7.51 – 7.44 (m, 2H), 5.76 (s, 1H), 3.85 (d, *J* = 6.4 Hz, 6H), 2.55 – 2.49 (m, 1H), 1.81 (t, *J* = 15.1 Hz, 2H), 1.63 (d, *J* = 12.9 Hz, 2H), 1.50 (d, *J* = 12.3 Hz, 1H), 1.22 – 1.11 (m, 2H), 1.08 (d, *J* = 12.2 Hz, 1H), 1.02 – 0.95 (m, 2H). ^{13}C{^{1}H} NMR (125 MHz, Chloroform-*d*) δ 176.4, 166.3, 163.2, 145.1, 136.2, 135.6, 131.9, 130.7, 129.9, 129.7, 128.2, 127.8, 125.3, 53.5, 53.4, 52.9, 48.1, 33.9, 33.7, 26.0, 25.0, 24.9. IR(KBr)ν_{max}/cm^{-1} 3344 (N-H), 2942(C− H), 1721(C=O), 1605(C=O), HRMS (ESI):m/z $[M+H]^+$ calcd for $C_{22}H_{24}NO_5S_2$; 446.1083 found 446.1083.

Di-*tert*-butyl-6-chloro-4-(cyclohexylamino)-5-oxo-4*H*,5*H*-thiopyrano[2,3-*b*]thiochromene -2,3-dicarboxylate(6bc). 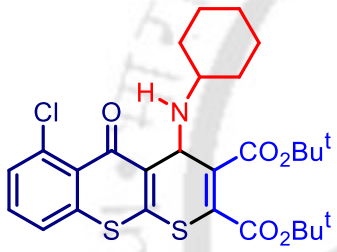 A yellow solid (45 mg, 84%) mp 73-75^{o}C, ^{1}H NMR (500 MHz, Chloroform-*d*) δ 7.51 (dd, *J* = 7.4, 1.7 Hz, 1H), 7.44 – 7.38 (m, 2H), 5.72 (s, 1H), 2.46 (ddt, *J* = 10.1, 7.4, 3.6 Hz, 1H), 1.92 (d, *J* = 12.2 Hz, 1H), 1.77 (d, *J* = 12.4 Hz, 1H), 1.67 (s, 2H), 1.57 (s, 9H), 1.54 (s, 9H), 1.21 (ddd, *J* = 25.5, 13.9, 6.0 Hz, 2H), 1.15 – 1.07 (m, 2H), 1.05 – 0.98 (m, 2H). ^{13}C{^{1}H} NMR (125 MHz, Chloroform-*d*) δ 176.3, 164.6, 161.4, 141.6, 138.0, 136.2, 135.9, 131.0, 130.7, 129.3, 129.1, 124.1, 83.9, 82.6, 52.9, 48.7, 33.5, 32.9, 27.7, 27.6, 25.7, 24.5, 24.5. IR(KBr)ν_{max}/cm^{-1} 3341 (N-H), 2965(C− H), 1725 (C=O), 1615(C=O), HRMS (ESI):m/z $[M+H]^+$ calcd for $C_{28}H_{35}ClNO_5S_2$; 564.1623 found 564.1623.

Dimethyl-4-(*tert*-butylamino)-7-chloro-5-oxo-4*H*,5*H*-thiopyrano[2,3-*b*]thiochromene-2,3-dicarbox-ylate (6ca). 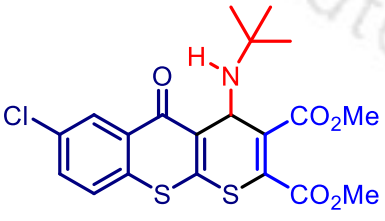 A brown solid (59 mg, 88%) mp 83-85 ^{o}C, ^{1}H NMR (500 MHz, Chloroform-*d*) δ 8.47 (d, *J* = 2.0 Hz, 1H), 7.57 (dd, *J* = 8.6, 1.8 Hz, 1H), 7.45 (d, *J* = 8.6 Hz, 1H), 5.82 (s, 1H), 3.87 (d, *J* = 3.9 Hz, 6H), 1.47 (s, 1H).1.06 (s, 9H). ^{13}C{^{1}H} NMR (125 MHz, Chloroform-*d*) δ 175.4, 165.6, 163.6, 146.1, 134.4, 133.8, 132.6, 132.3, 131.1, 130.7, 129.4, 126.9, 53.6, 52.9, 51.1, 46.2, 30.2. IR(KBr)ν_{max}/cm^{-1} 3343 (N-H), 2950(C− H), 1715 (C=O), 1613(C=O), HRMS (ESI):m/z $[M+H]^+$ calcd for $C_{20}H_{20}ClNO_5S_2$; 454.0539 found 454.0539.

Diethyl-4-(*tert*-butylamino)-5-oxo-4*H*,5*H*-thiopyrano[2,3-*b*] thiochromene-2,3-dicarboxylate (6db). 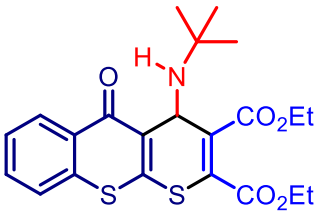

A dark brown liquid, (58 mg, 87), ^{1}H NMR (400 MHz, Chloroform-*d*) δ 8.50 (d, *J* = 9.0 Hz, 1H), 7.60 (td, *J* = 7.5, 1.5 Hz, 1H), 7.55 – 7.49 (m, 2H), 5.85 (s, 1H), 4.32 (q, *J* = 7.1 Hz, 4H), 1.37 – 1.33 (m, 6H), 1.07 (s, 9H). ^{13}C{^{1}H} NMR (125 MHz, Chloroform-*d*) δ 176.6, 165.3, 163.3, 146.0, 135.7, 131.9, 131.5, 130.8, 30.2, 129.8, 129.6, 128.2, 127.9, 125.5, 62.9, 62.1, 51.0, 46.3, 14.1, 14.0. IR(KBr)ν_{max}/cm^{-1} 3335 (N-H), 2963(C−H), 1717(C=O), 1603(C=O), HRMS (ESI):m/z [M+H]$^{+}$ calcd for $C_{22}H_{26}NO_5S_2$; 448.1242 found 448.1242.

Diethyl-6-chloro-4-(cyclohexylamino)-5-oxo-4*H*,5*H*-thiopyrano[2,3-*b*]thiochromene-2,3-dicarbo-xylate (6eb). 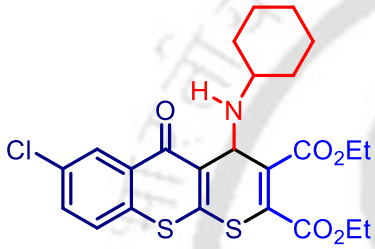

A brown liquid (66 mg, 88%), ^{1}H NMR (500 MHz, Chloroform-*d*) δ 8.43 (d, *J* = 8.6 Hz, 1H), 7.52 – 7.44 (m, 2H), 5.76 (s, 1H), 4.33 (q, *J* = 6.8 Hz, 4H), 2.59 – 2.53 (m, 1H), 1.88 (d, *J* = 12.1 Hz, 1H), 1.81 (d, *J* = 12.1 Hz, 1H), 1.69 – 1.64 (m, 2H), 1.54 (d, *J* = 12.3 Hz, 1H), 1.35 (dt, *J* = 7.1, 3.6 Hz, 6H), 1.22 – 1.15 (m, 2H), 1.14 – 1.07 (m, 1H), 1.01 (q, *J* = 11.6 Hz, 2H). ^{13}C{^{1}H} NMR (125 MHz, Chloroform-*d*) δ 175.8, 165.9, 162.7, 145.3, 138.7, 137.1, 136.6, 131.4, 129.8, 129.3, 128.7, 128.6, 124.8, 63.0, 62.2, 53.6, 48.3, 34.0, 33.7, 26.0, 25.1, 24.9, 14.1, 14.06. IR(KBr)ν_{max}/cm^{-1} 3313 (N-H), 2955(C−H), 1715 (C=O), 1603(C=O), HRMS (ESI):m/z [M+H]$^{+}$ calcd for $C_{24}H_{27}ClNO_5S_2$; 508.1014 found 508.1010.

Diethyl4-(*tert*-butylamino)-6-chloro-5-oxo-4H,5H-thiopyrano[2,3-b]thiochromene-2,3-dicarboxylate (6fb) 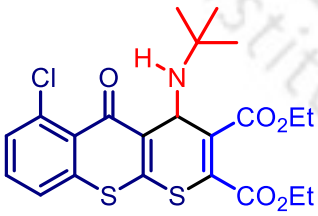

A yellow crystalline (65mg, 91%) mp 120-122 ^{o}C , ^{1}H NMR (500 MHz, Chloroform-*d*) δ 7.51 (dd, *J* = 7.2, 1.8 Hz, 1H), 7.45 – 7.39 (m, 2H), 5.69 (s, 1H), 4.32 (p, *J* = 6.9 Hz, 4H), 1.35 (dd, *J* = 10.6, 7.1 Hz, 6H), 1.04 (s, 9H). ^{13}C{^{1}H} NMR (125 MHz, Chloroform-*d*) δ 177.3, 165.4, 163.1, 142.0, 138.2, 136.0, 137.3, 131.8, 131.4, 131.2, 129.9, 128.8, 124.5, 62.9, 62.1, 51.3, 30.1, 14.1, 14.0. IR(KBr)ν_{max}/cm^{-1} 3345 (N-H), 2992 (C−H), 1727(C=O), 1601(C=O), HRMS (ESI):m/z [M+H]$^{+}$ calcd for $C_{20}H_{20}ClNO_5S_2$ 482.0857 found 4820853.

Dimethyl-4-(*tert*-butylamino)-8-chloro-5-oxo-4*H*,5*H*-thiopyrano[2,3-*b*]thiochromene-2,3-dicarbo-xylate (6ga). 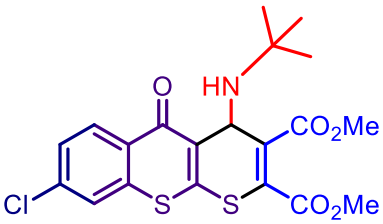

A brown viscous liquid (56 mg, 83^{1}H NMR (500 MHz, Chloroform-*d*) δ 8.43 (d, *J* = 8.6 Hz, 1H), 7.51 – 7.46 (m, 2H), 5.83 (s, 1H), 3.87 (d, *J* = 6.3 Hz, 6H), 1.80 (s, 1H), 1.06 (s, 9H). ^{13}C{^{1}H} NMR (125 MHz, Chloroform-*d*) δ 175.8, 168.3, 165.6, 163.6, 145.7, 138.7, 137.0, 131.3, 131.2, 130.8, 129.8, 128.6, 124.8, 53.6, 52.9, 51.1, 30.2. IR(KBr)ν_{max}/cm^{-1} 3343 (N-H), 2994(C− H), 1723(C=O), 1601(C=O), HRMS (ESI):m/z [M+H]$^{+}$ calcd for $C_{20}H_{20}ClNO_5S_2$ 454.0544 found 454.0544.

Dimethyl-5-oxo-7-(trifluoromethyl)-4-((2,4,4-trimethylpentan-2-yl)amino)-4*H*,5*H*-thio pyrano[2,3-*b*]thiochromene-2,3-dicarboxylate (6ha). 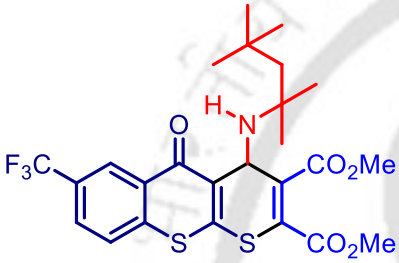

A yellow solid (72 mg, 89%) mp 116-118 ^{o}C, ^{1}H NMR (400 MHz, Chloroform-*d*),δ 8.78 (s, 1H), 7.82 (d, *J* = 10.2 Hz, 1H), 7.64 (d, *J* = 8.4 Hz, 1H), 5.85 (s, 1H), 3.88 (d, *J* = 4.6 Hz, 6H), 1.60 (s, 1H), 1.30 (d, *J* = 4.8 Hz, 2H), 1.16 (s, 3H), 1.08 (s, 3H), 0.87 (s, 9H). ^{13}C{^{1}H} NMR (150 MHz, Chloroform-*d*) δ 175.6, 165.6, 163.6, 146.1, 139.3, 131.5, 131.3, 130.3 (q, *J* = 33 Hz), 128.0, (q, *J* = 3 Hz), 127.1(q, *J* = 4.5 Hz), 126.5, 123.5, (q, *J* = 271.5 Hz), 55.7, 55.0, 53.6, 53.0, 45.8, 31.8, 29.6, 29.3. IR(KBr)ν_{max}/cm^{-1} 3353 (N-H), 2994(C− H), 1717(C=O), 1601(C=O), HRMS (ESI):m/z [M+H]$^{+}$ calcd for $C_{25}H_{28}F_3NO_5S_2$; 544.1421 found 544.1421.

Di-*tert*-butyl-8-fluoro-5-oxo-4-((2,4,4-trimethylpentan-2-yl)amino)-4*H*,5*H*-thiopyrano [2,3-*b*]thio-chromene-2,3-dicarboxylate (6ic) 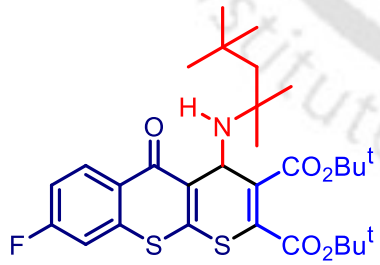

A yellow solid (67 mg, 86%) mp 101-103 ^{o}C, ^{1}H NMR (500 MHz, Chloroform-*d*) δ 8.51 (dd, *J* = 8.8, 5.8 Hz, 1H), 7.24 – 7.18 (m, 2H), 5.82 (s, 1H), 1.57 (s, 9H), 1.54 (s, 9H), 1.30 (d, *J* = 7.2 Hz, 2H), 1.17 (s, 3H), 1.10 (s, 3H), 0.86 (s, 9H). ^{13}C{^{1}H} NMR (125 MHz, Chloroform-*d*) δ 175.7, 164.3, 162.2, 145.8, 138.0, 132.8, 132.7, 131.4, 128.3, 116.3, 116.2, 111.6, 111.4, 84.2, 83.0, 55.4, 54.8, 46.2, 31.8, 31.6, 29.7, 29.5, 28.1, 28.0. IR(KBr)ν_{max}/cm^{-1} 3327 (N-H), 2996(C− H), 1726(C=O), 1604(C=O), HRMS (ESI):m/z [M+H]$^{+}$ calcd for $C_{30}H_{40}FNO_5S_2$; 578.2405 found 578.2380.

4-(*tert*-butyl(prop-2-yn-1-yl)amino)-2-methylene-2*H*,5*H*-thiopyrano[2,3-*b*]thiochromen-5-one (8e). A yellow liquid (40 mg, 77%), ^{1}H NMR (500 MHz, Chloroform-*d*) δ 8.50 (d, *J* = 7.5 Hz, 1H), 7.59 (t, *J* = 8.3 Hz, 2H), 7.55 – 7.50 (m, 1H), 7.05 (s, 1H), 6.25 (s, 1H), 6.00 (s, 1H), 3.84 (d, *J* = 17.0 Hz, 1H), 3.66 (d, *J* = 17.1 Hz, 1H), 2.29 (s, 1H), 1.51 (s, 9H). ^{13}C{^{1}H} NMR (125 MHz, Chloroform-*d*) δ 177.9, 152.3, 136.1, 131.4, 131.1, 130.8, 129.8, 127.9, 125.5, 124.8, 121.2, 113.2, 107.5, 78.2, 72.9, 57.4, 31.1, 21.0. IR(KBr)ν_{max}/cm^{-1} 2996(C−H), 1726(C=O), 1604(C=O), HRMS (ESI):m/z [M+H]$^{+}$ calcd for $C_{20}H_{19}NOS_2$; 354.0981 found 354.0984.

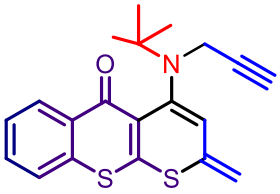

8e, 77%

4-(Cyclohexyl(prop-2-yn-1-yl)amino)-2-methylene-2*H*,5*H*-thiopyrano[2,3-*b*]thiochromen-5-one (8a)A dark brown viscous liquid (39 mg, 70%), ^{1}H NMR (500 MHz, Chloroform-*d*) δ 8.50 (d, *J* = 7.9 Hz, 1H), 7.61 (q, *J* = 8.1 Hz, 2H), 7.53 (t, *J* = 7.2 Hz, 1H), 6.94 (s, 1H), 6.29 (s, 1H), 6.07 (s, 1H), 3.83 (d, *J* = 17.1 Hz, 1H), 3.62 (d, *J* = 17.1 Hz, 1H), 3.44 (t, *J* = 11.4 Hz, 1H), 2.25 (dd, *J* = 25.4, 6.8 Hz, 2H), 2.01 (d, *J* = 13.0 Hz, 1H), 1.78 (dd, *J* = 25.9, 10.1 Hz, 2H), 1.66 (s, 1H), 1.56 (d, *J* = 12.2 Hz, 2H), 1.20 (m, , 3H). ^{13}C{^{1}H} NMR (125 MHz, Chloroform-*d*) δ 177.2, 152.9, 136.3, 131.4, 130.7, 129.7, 128.0, 127.8, 125.5, 124.7, 118.4, 110.5, 108.2, 78.2, 77.3, , 72.8, 56.4, 35.6, 34.1, 26.1, 26.0, 25.6, 21.2. HRMS (ESI):m/z [M+H]$^{+}$ calcd for $C_{22}H_{22}NOS_2$; 380.1137 found 380.1137.

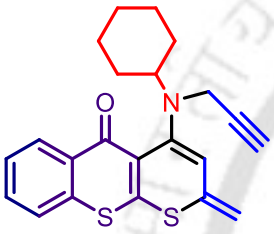

8a, 70%

Figure 2. ORTEP Diagram of compound **3a**

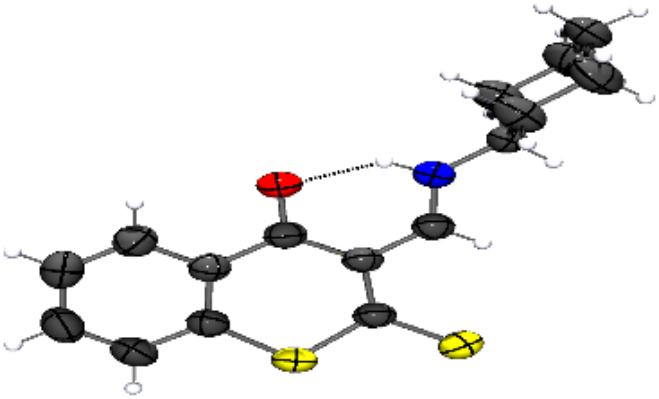

Table S1. Crystal data and structure refinement for compound **3a**

Entry	Identification Code	Compound 3a
01	Empirical formula	$C_{16}H_{17}NOS_2$
02	Formula weight	303.43
03	Temperature	295 K
04	Wavelength	0.71073
05	Crystal system	monoclinic
06	Space group	'P 1 21/c 1'
07	Cell length	a 11.9640 (5) b 6.2363 (2) c 20.3162 (8)
08	Cell angle	α 90 β 93.020 (1) γ 90
09	Cell volume	1513.71 (10)
10	Density	1.331
11	Completeness to theta	0.987
12	Index ranges	-16<=h<=16, -8<=k<=8, -27<=l<=27
13	Theta range	0.0680-0.0746
14	Cell formula units Z	4
15	CCDC no	2388159

Figure 3. ^{1}H NMR (500 MHz, $CDCl_3$) spectrum of compound 3a

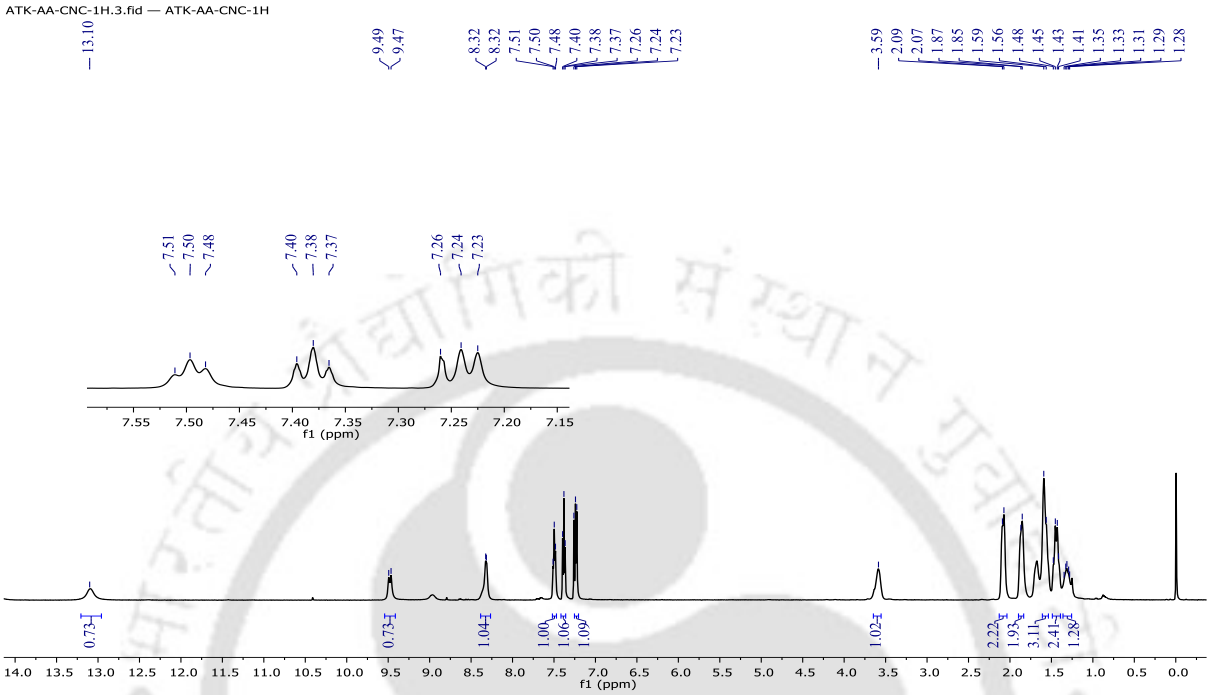

Figure 4. ^{13}C{^{1}H} NMR (125 MHz, DMSO-d_6) spectrum of compound 3a

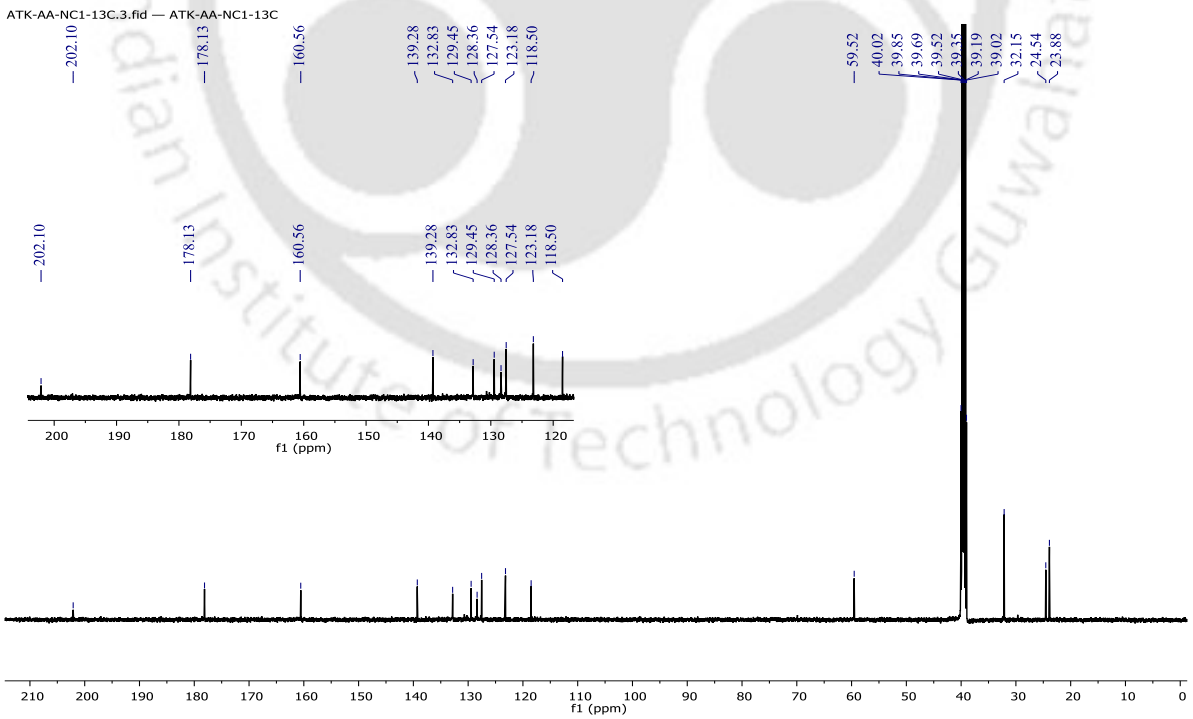

Figure 5. HRMS of compound 3a

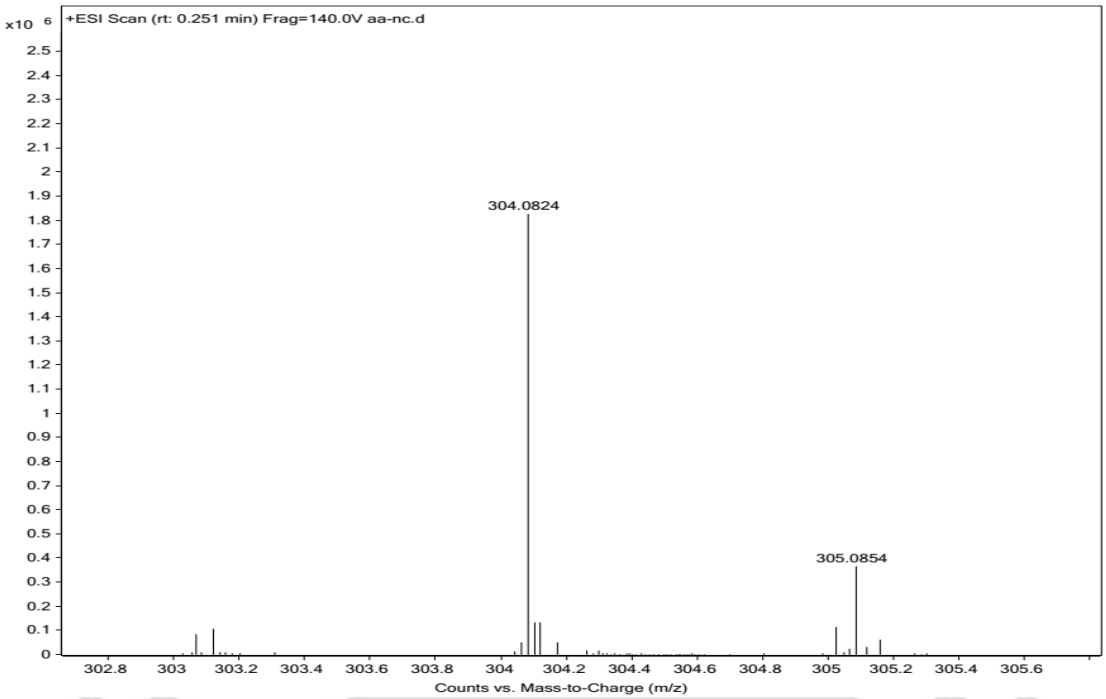

Figure 6. ORTEP Diagram of compound **6fb**

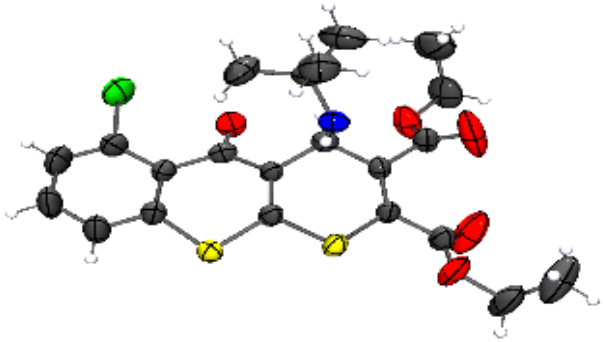

Table S1. Crystal data and structure refinement for compound (**6fb**).

Entry	Identification Code	Compound 6fb
01	Empirical formula	$C_{22}H_{24}$ Cl N O_5S_2
02	Formula weight	481.99
03	Temperature	295 K
04	Wavelength	0.71073
05	Crystal system	monoclinic
06	Space group	'P 1 21/n 1'
07	Cell length	a 11.6563 (10) b 6.0816 (5) c 32.504 (3)
08	Cell angle	α 90 β 93.888 (3) γ 90
9	Cell volume	2298.9 (3)
10	Density	1.393
11	Completeness to theta	0.897
12	Index ranges	-13<=h<=13, -7<=k<=7, -38<=l<=38
13	Theta range	2.48- 25.04
14	Cell formula units Z	4
15	CCDC no	2388163

Figure 7. ^{1}H NMR (500 MHz, $CDCl_3$) spectrum of compound **6aa**

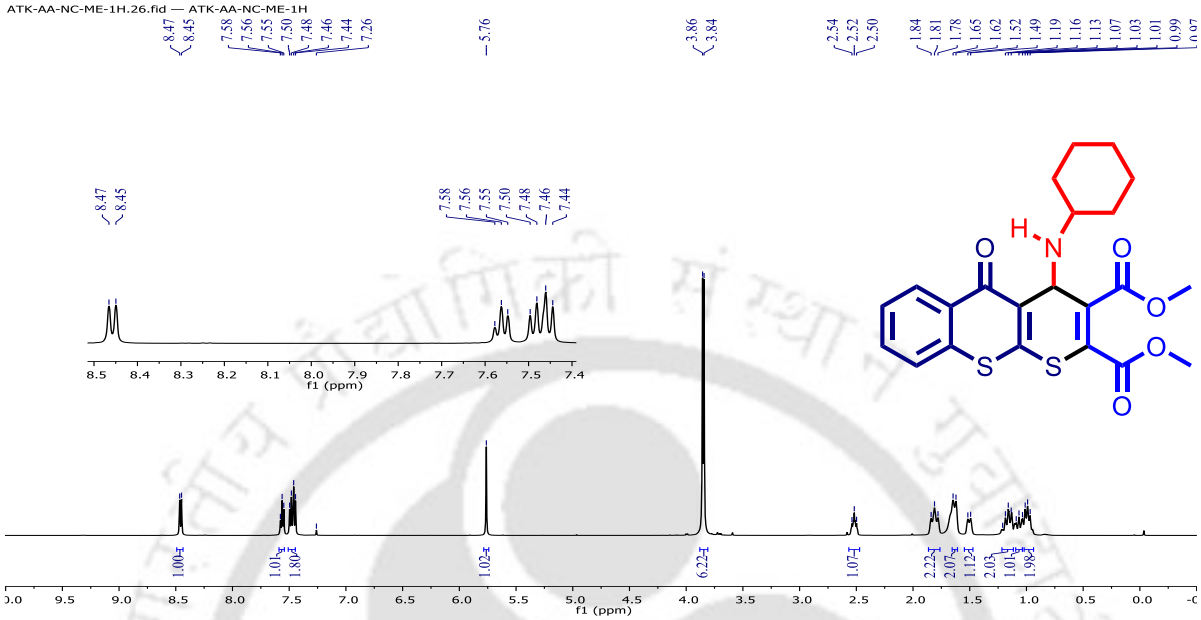

Figure 8. $^{13}C\{^{1}H\}$ NMR (125 MHz, CDCl3) spectrum of compound **6aa**.

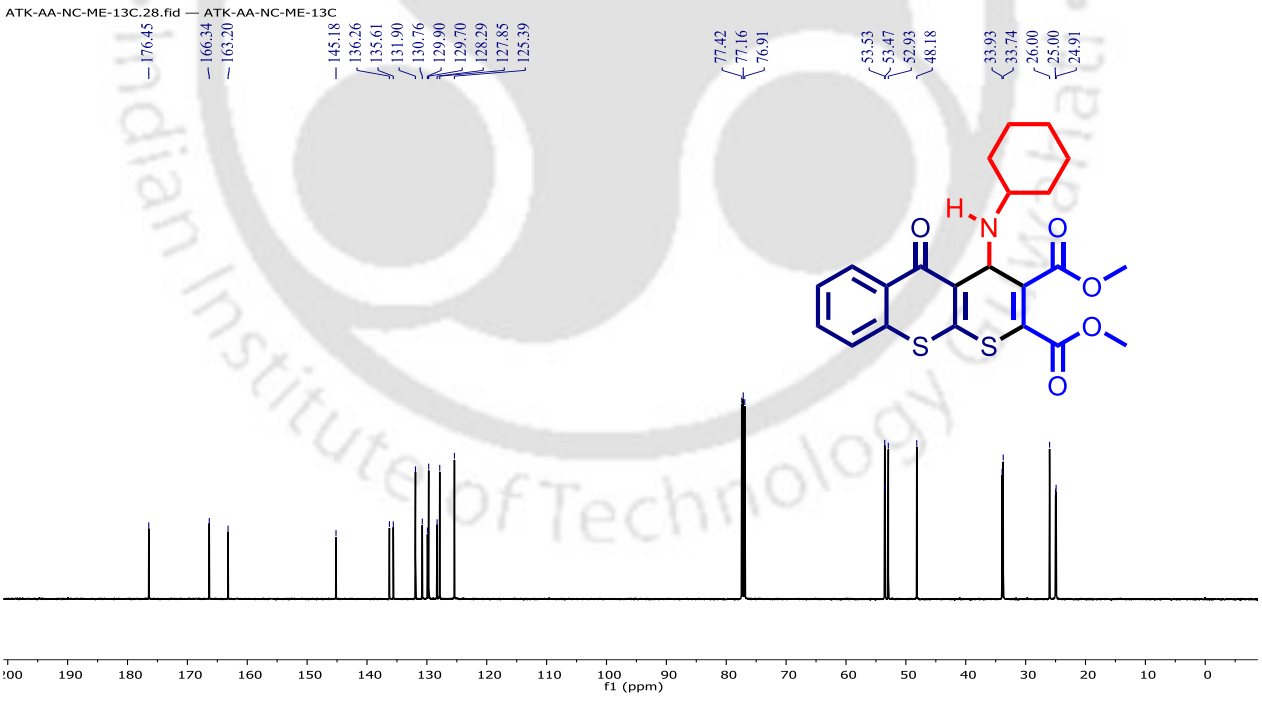

Figure 9. HRMS of Compound **6aa.**

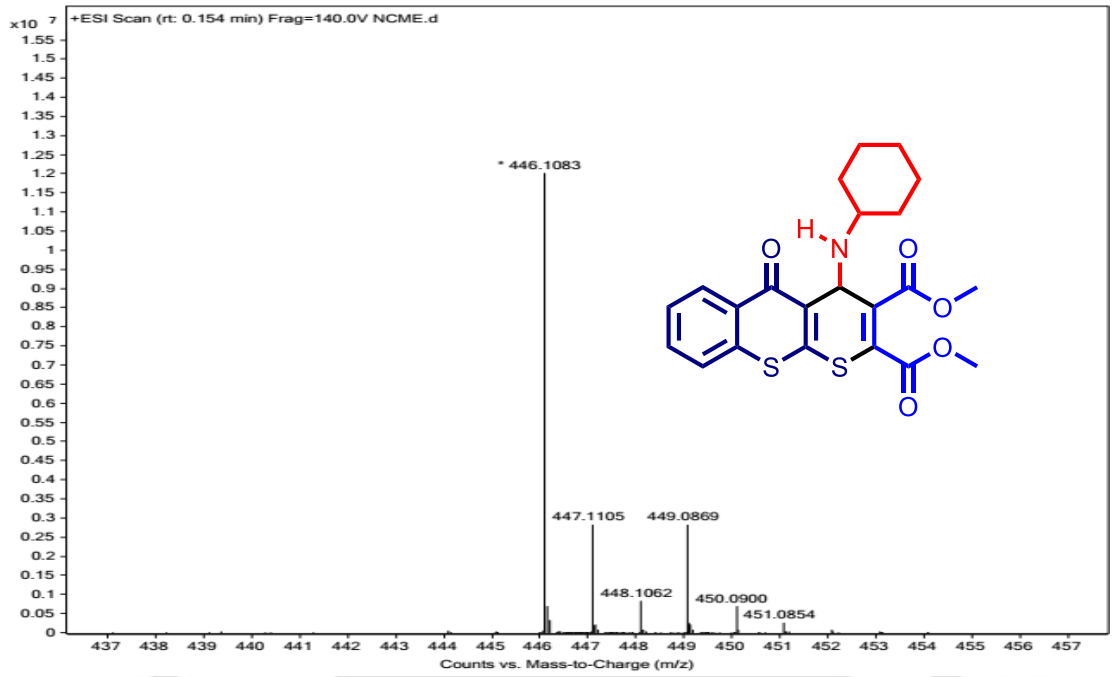

Figure 10. ^{1}H NMR (400 MHz, CDCl3) spectrum of compound **8e.**

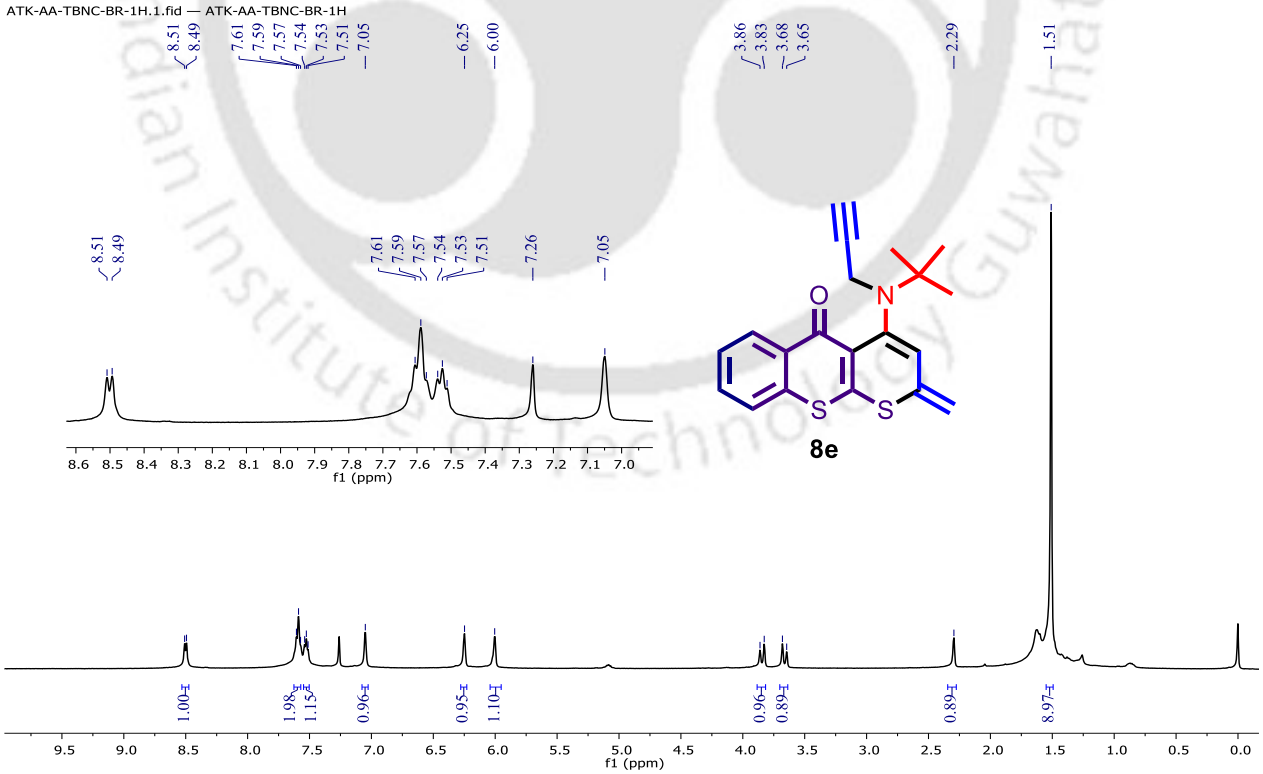

Figure 11. ^{13}C NMR (125 MHz, CDCl3) spectrum of compound **8e**

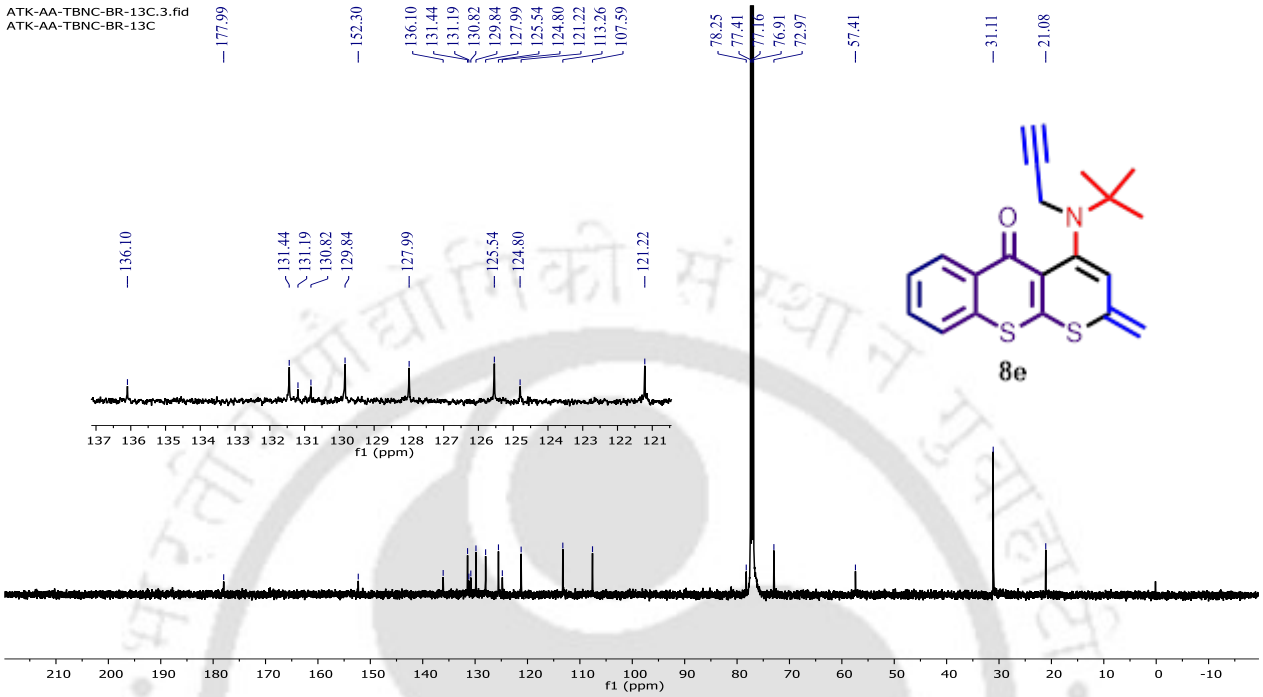

Figure 12. HRMS of compound **8e.**

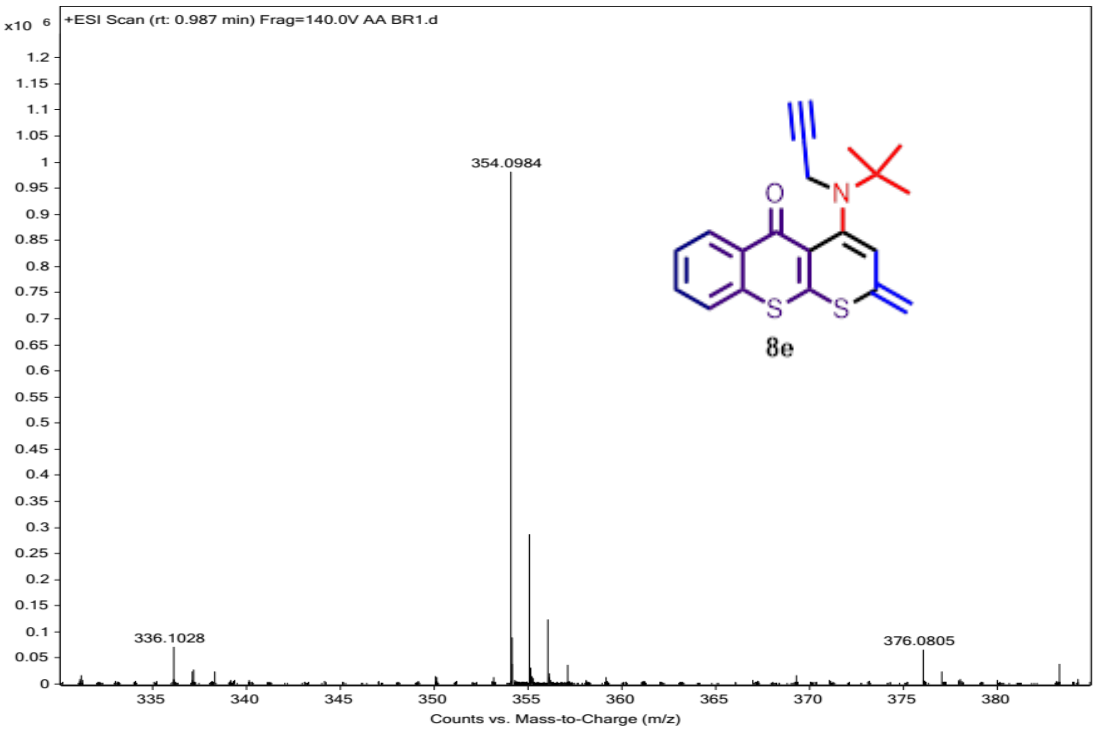

Figure 13. HOMO-LUMO energies of diene and dienophile

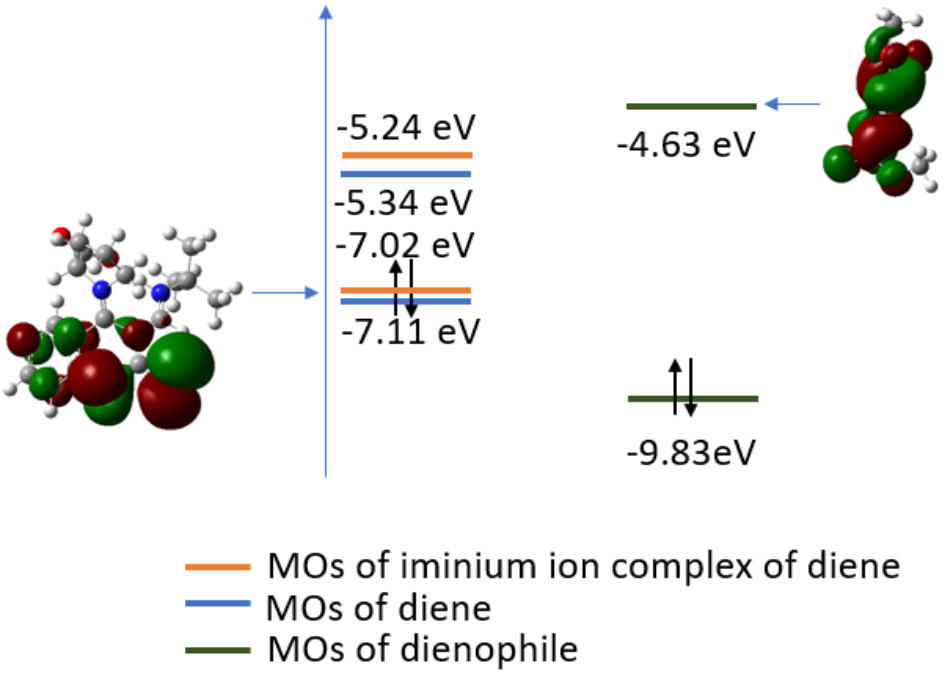

References:

1. M. Mustafa, and J. Y. Winum, *Expert Opin. on Drug Discov.*, 2022, **17**, 501-512.
2. S. Pathania, R. K. Narang, and R. K. Rawal, *Eur. J. Med. Chem*., 2019, **180,** 486-508.
3. F. Mir, S. Shafi, M. S. Zaman, N. P. Kalia, V. S. Rajput, C. Mulakayala, N. Mulakayala, I. A. Khan, and M. S. Alam, *Eur. J. Med. Chem*., 2014, **76**, 274-283.
4. I. Akbar, A. A. Ahamed, I. Arif, R. Surendra Kumar, K. Selva Raj, and A. Manilal, *J. Mex. Chem. Soc.*, 2019, **62**, 135-143.
5. C. Sun, W. Zhao, X. Wang, Y. Sun, and X. Chen, *Pharmacol. Res*., 2020, **160**, 105193.
6. H. A. Campbell, K. P. Link, ***Nutr. Rev.,* 2009,** 32, 244-246.
7. L. Xue, R. K. Singla, S. He, S. Arrasate, H. González-Díaz, L. Miao, and B. Shen, *Phytomedicine*, 2024, **128**, 155479.
8. P. S. Wells, *Ann Intern Med*., 1994, **121,** 676-683.
9. N. N. Schwartz and J. H. blumbergs. *Org. Chem.*, 1964, **29**, 7, 1976–1979
10. A. S. Demir , and A. Aybey. *Tetrahedron*, 2008, **64**, 11256–11261
11. R. Ramozzi, N. Chéron, B. Braïda, P. C. Hiberty, P. A. Fleurat-Lessard, and Valence, *New J. Chem.*, 2012, **36**, 1137.
12. A. Massarotti, F. Brunelli, S. Aprile, M. Giustiniano, and G .C. Tron, *Chem. Rev.*, 2021, **121** , 10742-10788.
13. Dömling, A. Recent Developments in Isocyanide-Based Multi-Component Reactions in Applied Chemistry. *Chem. Rev.*, 2006, **106**, 17-89.
14. L. Banfi, A. Basso, C. Lambruschini, L. Moni, and R. Riva, *Chem. Sci.*, 2021, **12**, 15445-15472.
15. E. M. M. Abdelraheem, S. Khaksar, K. Kurpiewska, J. Kalinowska-Tłuścik, S. Shaabani, and A. Dömling, *J. Org. Chem.*, 2018, **83**, 1441-1447.
16. M. Kumar, S. Bagchi, Sharma. *RSC. Adv.*, 2015, **5**, 53592-53603.
17. H. Park, and K. Lee. *Synth. Commun.*, 2004, **34**, 2053-2061.
18. V. Edmont, Stoyanov, and C. Ivanov, *Synth. Commun*., **28,** 1755-1767.
19. M. J. Frisch, G. W. Trucks, H. B. Schlegel, G. E. Scuseria, M. A. Robb, J. R. Cheeseman, G. Scalmani, V. Barone, G. A. Petersson, H. Nakatsuji, X. Li, M. Caricato, A.V Marenich, J. Bloino, B.G. Janesko, R. Gomperts, B. Mennucci, H. P.

Hratchian, J. V. Ortiz, A. F. Izmaylov, J. L. Sonnenberg, F. Williams-Young, D. Ding, F. Lipparini, F. Egidi, J. Goings, B. Peng, A. Petrone, T. Henderson, D. Ranasinghe, V. G. Zakrzewski, J. Gao, N. G. Rega, W. Liang, M. Hada, M. Ehara, K. Toyota, R. Fukuda, J. Hasegawa, M. Ishida, T. Nakajima, Y. Honda, O. Kitao, H. Nakai, T. Vreven, K. Throssell, J. A. Montgomery, J. E. Peralta, F. Ogliaro, M. J. Bearpark, J. J. Heyd, E. N. Brothers, K. N. Kudin, V. N. Staroverov, T. A. Keith, R. Kobayashi, J. Normand, K. Raghavachari, A. P. Rendell, J. C. Burant, S. S. Iyengar, J. Tomasi, M. Cossi, J. M. Millam, M. Klene, C. Adamo, R. Cammi, J. Ochterski, JR. L. Martin, K. Morokuma, O. Farkas, J. B. Foresman, and D. J. Fox. *Gaussian 16*, Revision C.01; Gaussian, Inc.: Wallingford CT, 2019.

20. R. G. Parr, and, W. Yang. *Density-Functional Theory of Atoms and Molecules*; Oxford University Press: New York, **1989**.
21. F. M. Moghaddam, M. Kiamehr, M. R. Khodabakhshi, Z. Mirjafary, S. Fathi, and H. A. Saeidian. *Tetrahedron*, 2010, **66,** 8615-8622.
22. V. Maurya, and C. Appayee, *Org. Lett.*, 2018, **20,** 4111-4115.
23. H. Shirakawa, and H. Sano, *Tetrahedron Lett.*, 2014, **55**, 4095-4097.
24. C. Lee, W. Yang, and R. G. Parr, *Phys. Rev.*, 1988, 37, 785-789.

Chapter V

Green Synthesis of 4-Hydroxydithiocoumarin-Imidazole Bis-Heterocycle Scaffold, and its Antiproliferative Study and Unusual Single XRD Pattern

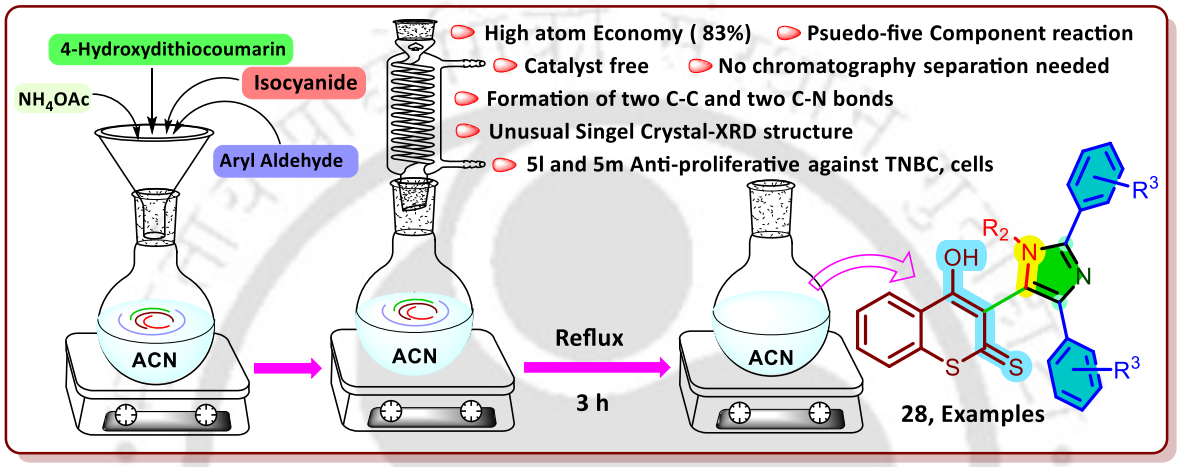

Org. Chem. Front.,2026, ***13***, 2841-2857

5.0 Introduction:

Bis-heterocycles (BHCs) are organic compounds that contain two heterocyclic moieties within a single molecule.[1] These rings can be identical or different and are often connected *via* a covalent bond, a linker, or fused.[2] The involvement of two heterocycles in a single unit enhances functional groups' overall activities and orthogonal reactivity, rather than a discrete unit.[3,4] Consequently, BHCs show a vast spectrum in medicinal chemistry, pharmaceutical, and the development of new anticancer drugs.[5-8] Owning these applications, scientists have constructed various (BHCs) *via* Multicomponent reactions (MCRs) approaches, a few of which are mentioned in section 4.1.9-11. MCRs are considered a powerful synthetic toolbox for accomplishing complex organic frameworks within a single step.[12-15] In a typical (MCR), more than two reactants are combined in a single pot to produce the desired product, incorporating all the building block moieties, enabling it to generate a wide variety of chemical entities simply by changing the starting materials. Some critical features of MCR are high atom efficiency, one-pot operation, ease of handling, creation of orthogonal reactive functional groups, and contributions to sustainability.[16,17]

5.1 Synthesis of Bis-heterocycles Imidazole derivatives *via* multicomponent reactions (MCRs)

Ghomeshi *et al*. demonstrated the synthesis of bis-heterocycles (coumarin-imidazole) [18] through a three-component reaction from 4-formylcoumarin, benzil and ammonium acetate in acetic acid medium as solvent at reflux conditions. The reaction proceeds through the condensation of benzil and 4-formylcoumarin with ammonium acetate, followed by cyclisation and oxidation to furnish the desired product as shown in **Scheme 1**.

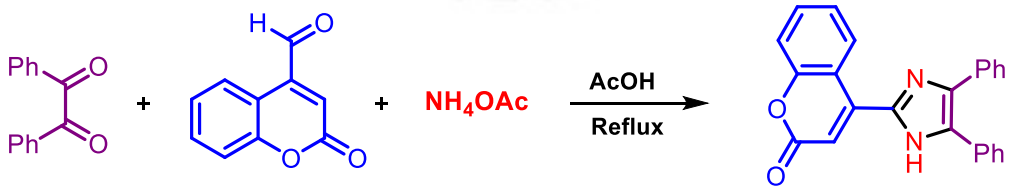

Scheme 1. Synthesis of bis-heterocycles (Coumarin-Imidazole) derivatives

In 2017, G. R. Ortíz and his co-workers reported a series of C2-bound julolidin-imidazo[1,2-*a*]pyridine benzoheterocyclic compounds (BHCs) using a microwave-assisted Groebke–Blackburn–Bienaymé reaction (GBBR).[19] The reaction involved the stepwise addition of 2,3,6,7-tetrahydro-1*H*,5*H*-pyrido[3,2,1-*ij*]quinoline-9-carbaldehyde, 2-aminopyridine derivatives, and isocyanides in anhydrous methanol, with 2-chloroacetic acid as a catalyst **Scheme 2**.

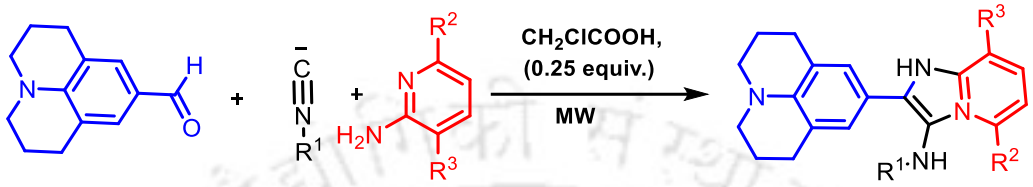

Scheme 2. Synthesis of Imidazole derivative *via* GBBR one-pot variants

Mozhgan Masoudi *et al.* synthesised a new class of bis(imidazolyl)pyrrole derivatives by reacting pyrrole or indole with aryl glyoxal monohydrates and *N*-aryl amidines in ethanol using $FeCl_3$ as a catalyst at room temperature,[20] as depicted in **Scheme 3**. The reaction proceeds via electrophilic aromatic substitution, $FeCl_3$-promoted dehydration, and cyclisation with *N*-aryl amidines, yielding the bis(imidazolyl)pyrrole product under mild conditions.

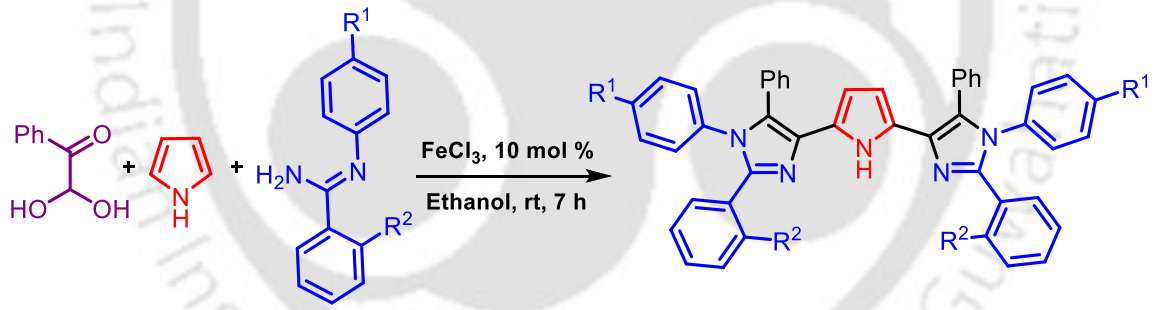

Scheme 3. Synthesis of bis-Imidazole derivative using pyrrole, aryl glyoxalmonohydrates and N-aryl amidines in the presence of $FeCl_3$

Sparks *et al.* in 2004 developed a microwave-assisted synthesis of tri-substituted imidazoles by reacting a keto-oxime and an aldehyde with NH_4OAc in AcOH at 200 °C for 20 min21, as shown in **Scheme 4**. The reaction proceeds through the formation of an *N*-hydroxyimidazole intermediate, which undergoes an *in situ* thermal reduction of the N–O bond to generate 2,4,5-triaryl-imidazoles in moderate to good yields (up to 70%).

Scheme 4. Synthesis of trisubstituted Imidazole derivative using Keto-oxime aldehyde and ammonium acetate

Wang, Y. *et al*. reported the synthesis of fused imidazole bis-heterocycles through an MCR using phenanthrene-9,10-dione, an aryl amine, and formyl-coumarin with acetic acid as the medium. The reaction was heated at 120 ºC for 12 hours, and the yields were about 50% after purification by column chromatography, as shown in **Scheme 5**.

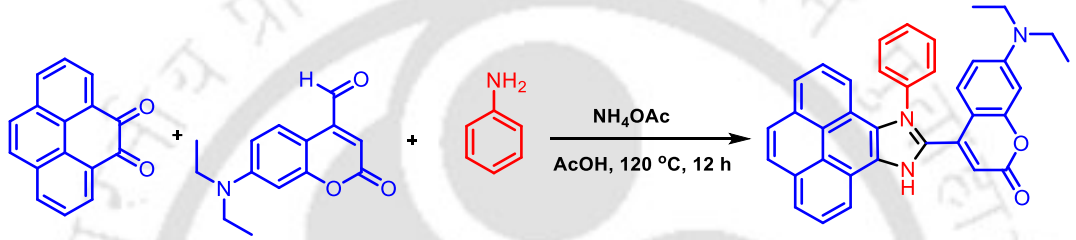

Dyes Pigments **2020**, 173, 107958.

Scheme 5. Synthesis of fused Imidazole derivative phenanthrene-9,10-dione, aryl amine, and formyl-coumarin in acetic acid

In 2020, Nipate *et al.* established an eco-friendly, multicomponent one-pot synthesis of substituted imidazole derivatives catalysed by β-cyclodextrin (β-CD), using a three-component reaction between aldehydes, isatin, and ammonium acetate in H_2O–EtOH at 80 °C. β-CD, a biodegradable and recyclable supramolecular catalyst, efficiently promoted the formation of 1,8-dihydroimidazo[2,3-*b*]indoles in high yields, as shown in **Scheme 6**. [23]

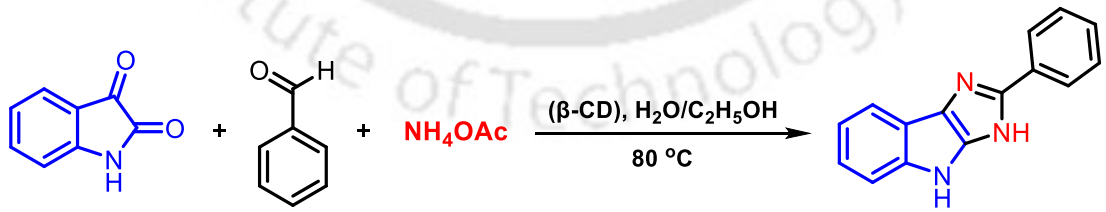

Scheme 6. Synthesis fused Imidazole derivative using aldehydes, isatin, and ammonium acetate in H_2O–EtOH at 80 °C in the presence of β-CD

In addition to the above-mentioned protocols, a substantial body of literature exists on the synthesis of imidazole derivatives using as a various reactive precursors.[24-25] In most cases, they have used an expensive catalyst to promote the reaction. Whereas, in some cases, they have used benzil, which resembles diketones, and synthesised only a fused imidazole bis-heterocyclic system. In the current study, we propose a convenient and straightforward synthetic strategy for the synthesis of highly substituted Bis-heterocycle (BHC) imidazole derivatives using 4-hydroxydithiocoumarin, *via* a pseudo-5-component reaction in a single step. The key features, such as catalyst-free, high atom economy, low E-factor, easy to handle, good yield, no column chromatography required for separations, and shorter reaction time, overcome the drawbacks reported in earlier literature and make the current protocol a very efficient and attractive procedure for synthesising tetra-substituted Bis-Imidazole derivatives. The synthesised compounds were also examined for biological applications, and we found that **5l** and **5m** showed antiproliferative activity against TNBC cells.

5.2 Results and Discussion:

As discussed in **Chapter 1**, 4-Hydroxydithiocoumarin, a thio-analogue of 4-hydroxycoumarin bearing three nucleophilic sites, serves as a versatile synthetic precursor for the construction of sulfur-containing heterocycles. Our group further summarized its reactivity profile in a 2021 review.[26] Moreover, in **chapter IV,** we explained the reactivity of 4-hydroxydithiocoumarin with another nucleophile, isocyanide, to form an alkyl amino derivative, regioselectively at the C3 position of 4-hydroxydithiocoumarin. Taking cues from earlier results, we propose a retro-synthetic analysis to construct a highly substituted imidazole-bound bis-heterocycle using 4-hydroxydithiocoumarin, as shown in **Scheme 7.**

Guided by this idea, we established the present protocol, in which we are investigating the reactivity of 4-hydroxydithiocoumarin in the MCR domains with isocyanide, arylaldehyde, and ammonium acetate. Literature reports indicate that 4-hydroxydithiocoumarin reacts with aryl aldehydes *via* a Knoevenagel intermediate to give pentacyclic products. In contrast, reactions with isocyanides typically yield alkylamino derivatives, as already discussed in Chapter I, Scheme 10, and Chapter IV, **Scheme 5,** respectively.

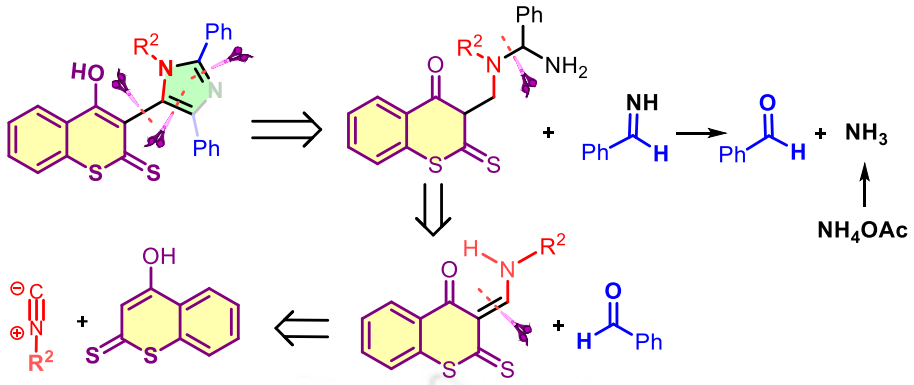

Scheme 7. Retrosynthesis analysis of 4-Hydroxydithiocoumarin-Imidazole Bis-Heterocycle Scaffold

Herein, we investigate the competitive reaction between an isocyanide and an aryl aldehyde in the presence of 4-hydroxydithiocoumarin. Notably, it is found that the isocyanide dominates the reactivity of the aryl aldehyde under our reaction conditions with 4-hydroxydithiocoumarin, directing the reaction through an alkylamino methylene intermediate and leading to the formation of an imidazole bis-heterocyclic product, as depicted in **Scheme 8**.

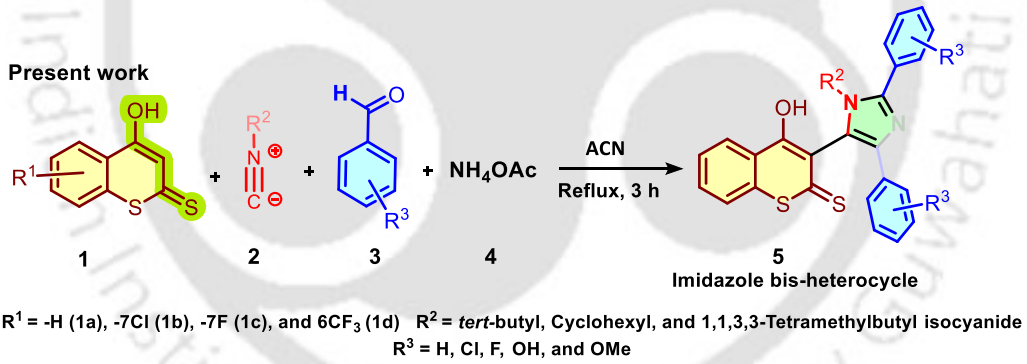

Scheme 8. Synthesis of imidazole Bis-heterocycle from 4-hydroxydithiocoumarin *via* pseudo five-component reaction

Isocyanide is also a key precursor used extensively by Ugi [27] and Paserniri [28] in MCR reactions to synthesise peptide scaffolds. In the present era, it is well-renowned by the title of (ICMR) isocyanide multicomponent reaction.

For the current study, 4-hydroxydithiocoumarins (**1a**) and their derivatives, such as 7-F (**1b**), 7-Cl (**1c**), and 6-CF_3 (**1d**), 4-hydroxydithocoumarin derivatives were prepared in our laboratory by following the previously reported procedure mentioned in **Chapter I, Scheme 20**. For the current studies, 0.20 mmol 4-hydroxydithiocoumarin **1a**, 0.20 mmol

tert-butyl isocyanide **2**, 0.40 mmol tolu-aldehyde **3**, and 0.20 mmol ammonium acetate **4** were chosen as model substrates. The reactants were added one by one, and the mixture was dissolved in 1mL of acetonitrile in a round-bottomed flask and stirred at room temperature for 24 hours (Table 1, entry 1), but no result was observed. Later, the same reaction mixture was heated at 50°C for 12 hours with constant stirring. The desired product **5b** was isolated in 30% yield, along with unreacted 4-hydroxydithiocoumarin and tolualdehyde, as shown in Table 2, entry 2.

The anticipated product is then characterized using various spectroscopic techniques, including ^{1}H and ^{13}C NMR, IR spectra, and HRMS. In the ^{1}H NMR, a singlet is observed for nine protons at $\boldsymbol{\delta}$ 1.50, which indicates the incorporation of *tert*-butyl isocyanide in the final product. Similarly, we observed two singlets for six protons at $\boldsymbol{\delta}$ 2.21 and 2.44, respectively, indicating that two units of tolualdehyde are incorporated into the final product **5b** and accounting for 14 protons in the aromatic region. In ^{13}C NMR, four signals were observed in the aliphatic range: two for the methyl groups on the benzaldehyde, and two for the tertbutyl and quaternary carbons of the isocyanide at $\boldsymbol{\delta}$ 21.0, 20.7, 30.5, and 63.6, respectively. The observed mass also agreed with the experimental mass, as recorded using HRMS (m/z $[M+H]^+$ calcd. for $C_{30}H_{29}N_2O_3S_2$, 497.1716; found, 497.1715). The ^{1}H, ^{13}C spectra and HRMS data of compound **5n** are presented in **Figures 11-13**. Single-crystal X-ray Diffraction is also reported for the synthesised compounds **5b**, **5g**, and **5o**, which are presented at the end of this chapter (Figure 8-10). The crystal structure reveals that the molecule is asymmetrical, with the oxygen atom of the 4-hydroxydithiocoumarin unit interacting with the imidazole nitrogen of a neighbouring molecule, thereby forming a helical structure via intermolecular hydrogen bonding. In addition, the crystal structure reveals that the N3 of imidazole is quaternary and carries a positive charge. In contrast, the oxygen is negatively charged and is further stabilised by another molecule, as shown in **Figure 1a-c**. The isolated compound can exist in two possible isomeric forms (**x** and **x′**) through proton transfer from the N3 position of the imidazole ring to the oxygen atom of 4-hydroxydithiocoumarin, as shown in **Figure 2**. The bond length of a carbonyl group is usually about 1.21 Å. However, in this case, from the single-crystal data, it is observed

that the carbonyl bond length is 1.25 Å, which is slightly longer than expected and may be due to enol–keto tautomerization (**x′** to **x′**); therefore, we concluded that the product exists in the solid state in the form of (**x**). Meanwhile, in DMSO solvent, it can exist in (**x′**) forms, which is justified *via* ^{1}H and ^{13}C NMR spectra.

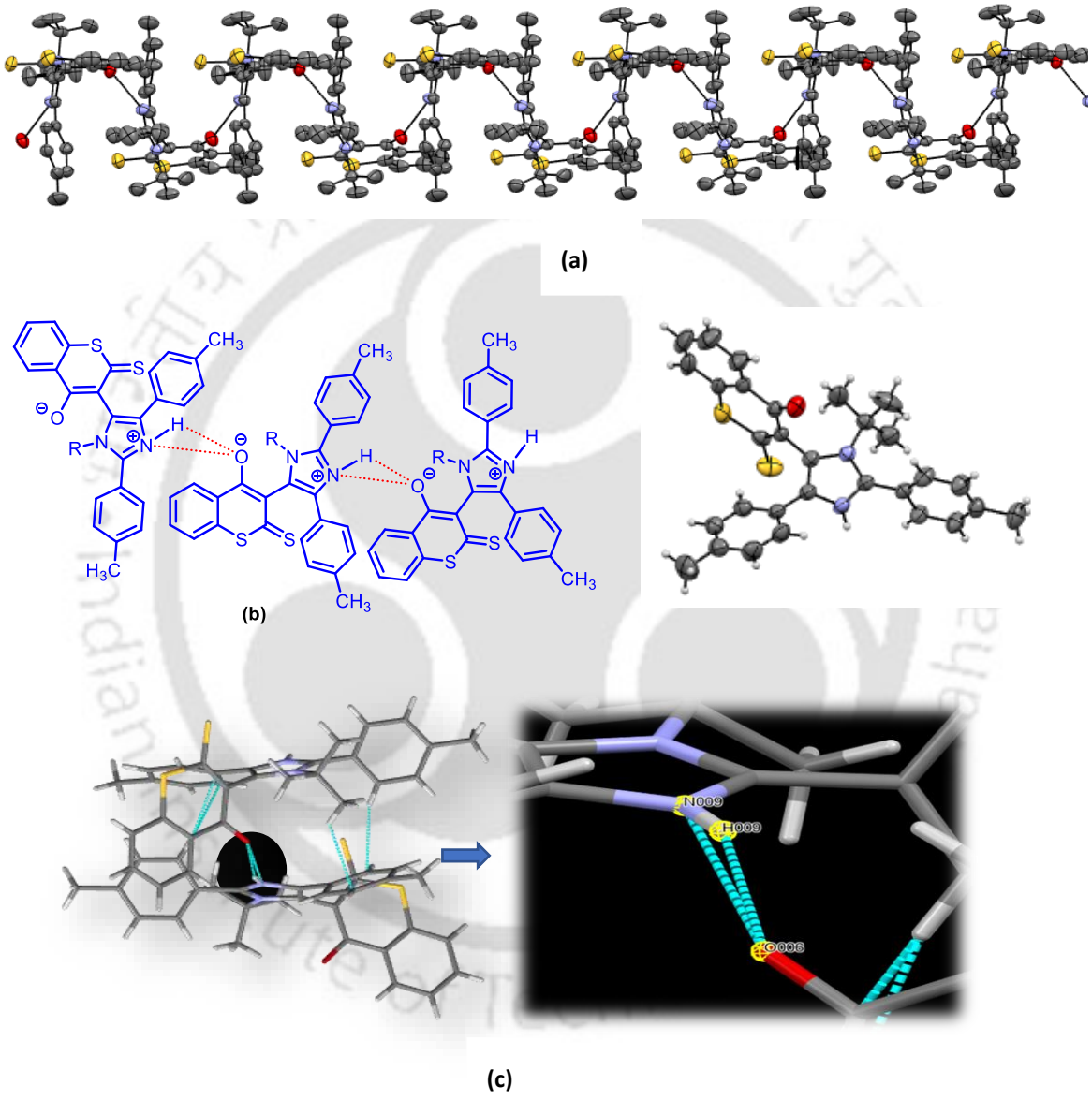

Figure 1. (a) Helical structure of the compound 5b. (b) Chem-Draw diagram showing the interaction of oxygen with the nitrogen of the imidazole of another molecule and hydrogen bonding. (c) Crystal structure of compound 5b showing interaction of nitrogen with oxygen as well as hydrogen bonding.

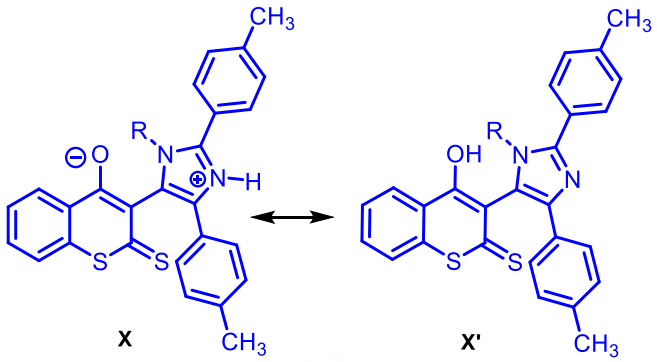

Figure 2. Two possible isomeric forms of compound 5b (x and x′)

After characterisation to determine suitable reaction conditions, we increased the temperature to the reflux point and, optimistically, obtained 80% of the desired product (Table 1, entry 3). As the temperature increases, the yield also increases. Furthermore, different polar aprotic solvents, such as DMSO, DMF, and DCM, were examined to optimise the reaction conditions, but the results were unsuccessful (Table 1, entries 4-6). Finally, the reaction was investigated in polar protic greener solvents, such as water and ethanol, but it didn't proceed (Table 1, entries 8-9). After analysing the temperature and solvent optimisation, we conclude that the best condition for this protocol is listed in **Table 1,** entry 3.

Table 1. Optimization Table and reaction conditions.[a,b]

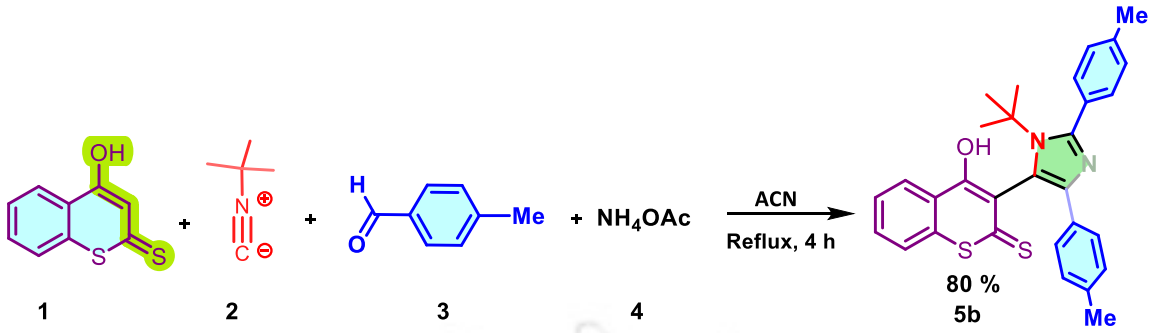

Entry	Solvent	Temperature	Time (h)	% Yield [b]
1.	ACN	RT	24	NR
2.	ACN	50 °C	12	30
3.	**ACN**	**Reflux**	**3**	**80**
4.	DMSO	RT-120°C	1-4	NR
5.	DMF	RT-120°C	1-4	Trace
6.	DCM	Reflux	4	NR
7.	Toluene	RT-110°C	1-4	Trace
8.	H_2O	100 °C	4	NR
9.	Ethanol	Reflux	1-4	NR

[a]All the reactions were performed using (0.2 mmol) 4-hydroxydithiocoumarin(1a), (0.2 mmol) *tert*-butyl isocyanide(2a), (0.2 mmol) ammonium acetate(4), and (0.2 mmol) aryl aldehyde(3a) in 1 mL acetonitrile. [b]Isolated yield. RT: Room Temperature, NR: No reaction. DMF = *N, N-dimethylformami*de.

Table 2. Substrate Scope [a,b]

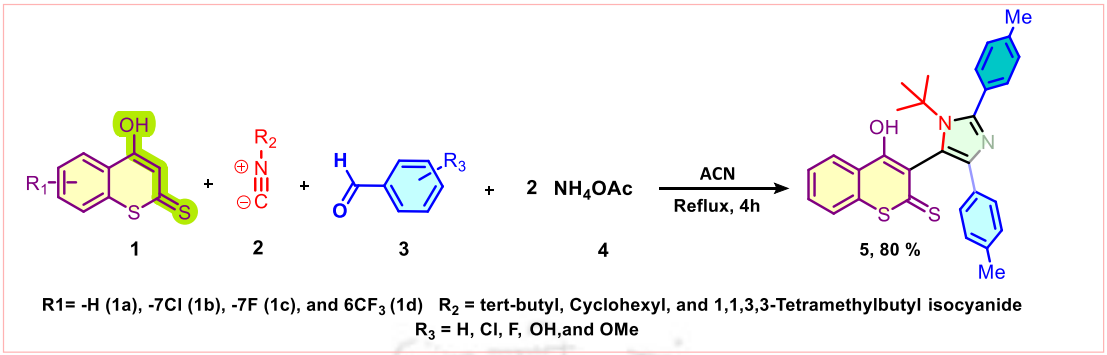

R1= -H (1a), -7Cl (1b), -7F (1c), and 6CF_3 (1d) R_2 = tert-butyl, Cyclohexyl, and 1,1,3,3-Tetramethylbutyl isocyanide
R_3 = H, Cl, F, OH,and OMe

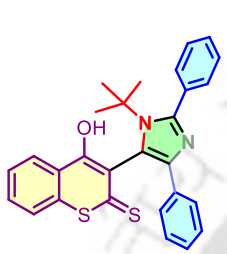

5a, 89%

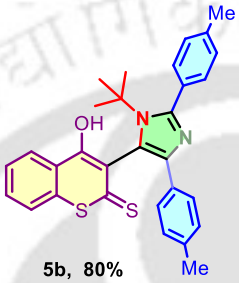

5b, 80%

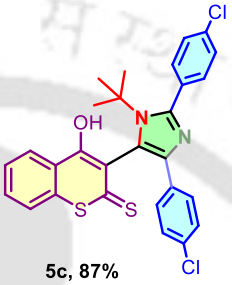

5c, 87%

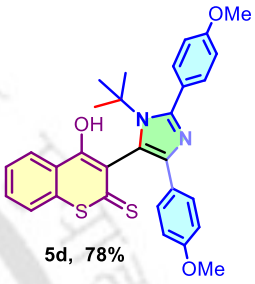

5d, 78%

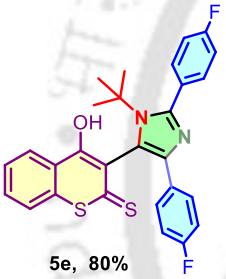

5e, 80%

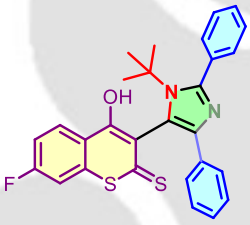

5f, 87%

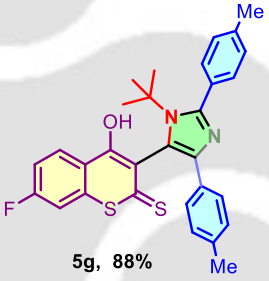

5g, 88%

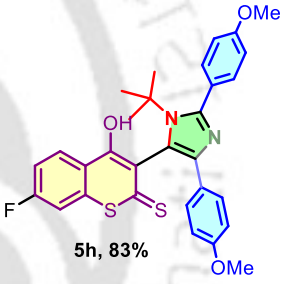

5h, 83%

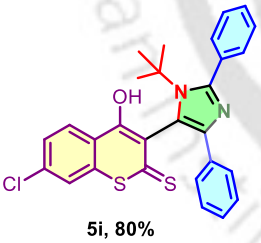

5i, 80%

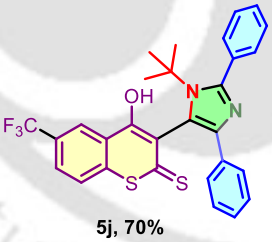

5j, 70%

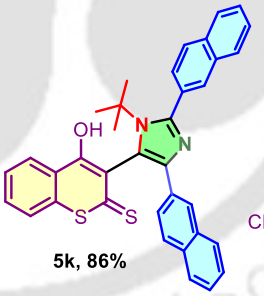

5k, 86%

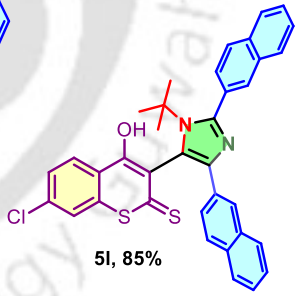

5l, 85%

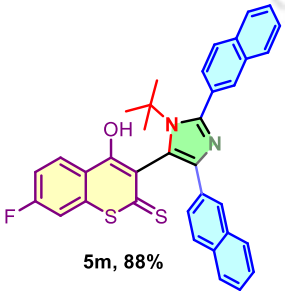

5m, 88%

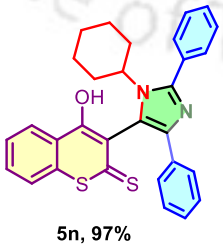

5n, 97%

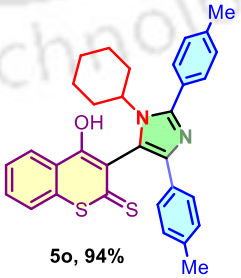

5o, 94%

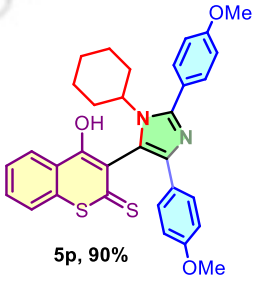

5p, 90%

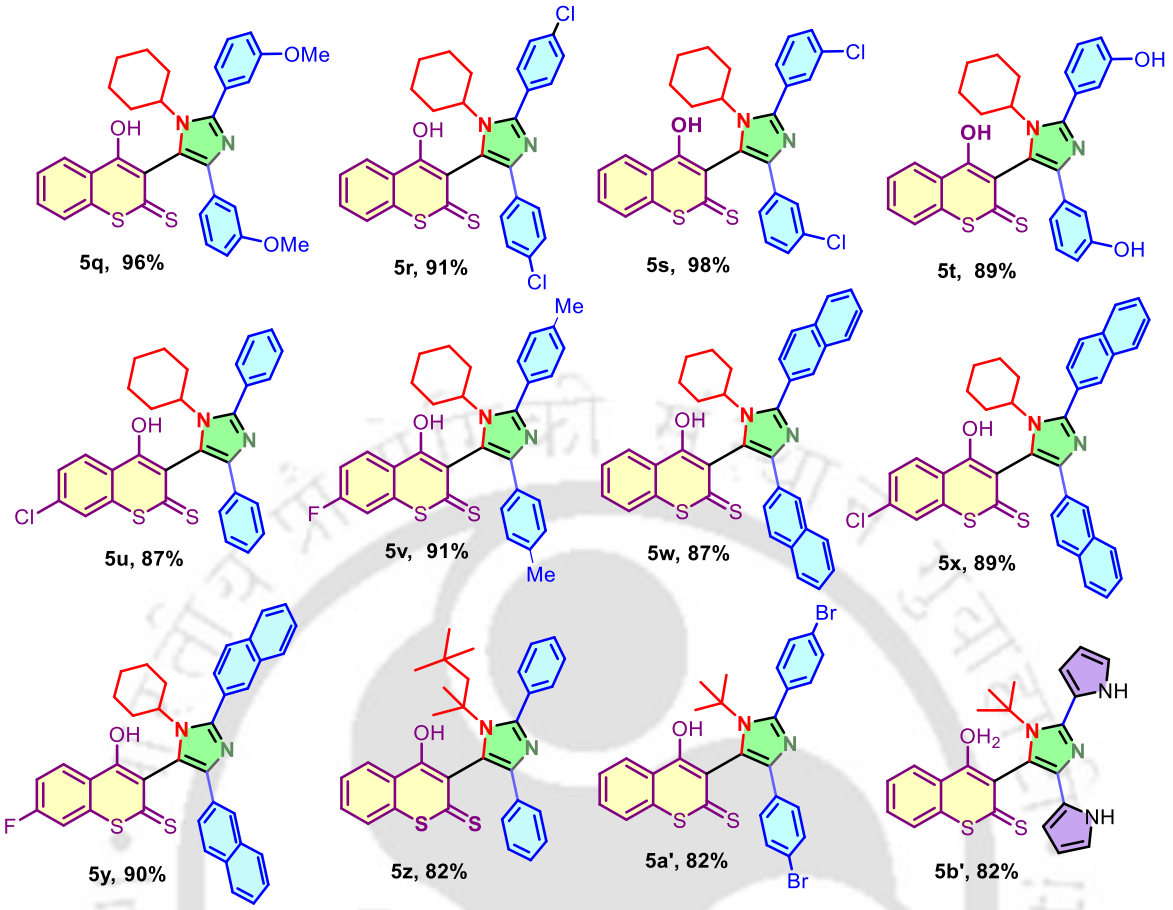

[a] All the reactions were performed using 4-hydroxydithiocoumarin derivatives(1) (0.2 mmol), isocyanide(2), ammonium acetate 4 (0.2 mmol), and aryl aldehyde (3) (0.4 mmol) in 1 mL acetonitrile at reflux temperature. Isolated yield.[b]

To explore the substrate scope, several reactions were performed under the optimised conditions (Table 2, entry 3). Initially, 4-hydroxydithiocoumarin was reacted with tert-butyl isocyanide and a series of aryl aldehydes bearing either electron-withdrawing or electron-donating substituents, affording the corresponding products **5a–e** in good yields (78–87%). Similarly, when 7-F (**1b**), 7-Cl (**1c**), and 6-CF_3 (**1d**), along with *tert*-butyl isocyanide, were reacted with different aryl aldehydes, they furnished the anticipated products 5f-j in good yields **(70-88%)**. In the case of bulky aryl aldehydes such as 9-anthracenecarboxyaldehyde, 1-naphthaldehyde, and 2-naphthaldehyde, only 2-naphthaldehyde yields the desired product 5j-m **(85-88%)**.

Notably, no desired product was obtained in the former two cases, which may be due to steric hindrance, and also in the case of nitro aryl aldehydes, no desired product was obtained.

Furthermore, cyclohexyl isocyanide was used instead of *tert*-butyl isocyanide to explore how different starting materials react. By changing both 4-hydroxydithiocoumarin and the arylaldehyde, we successfully synthesized compounds **5n-y** with yields ranging from **87-97%**. The reaction was also investigated with 1,1,3,3-tetramethyl isocyanide, and only **5z** could be synthesized in this case. Similarly, a heteroaldehyde (pyrrole-2-carbaldehyde) was used, and polyheterocycle molecule **5b′** was obtained with 82% yield.

Table 3. Possible mechanism

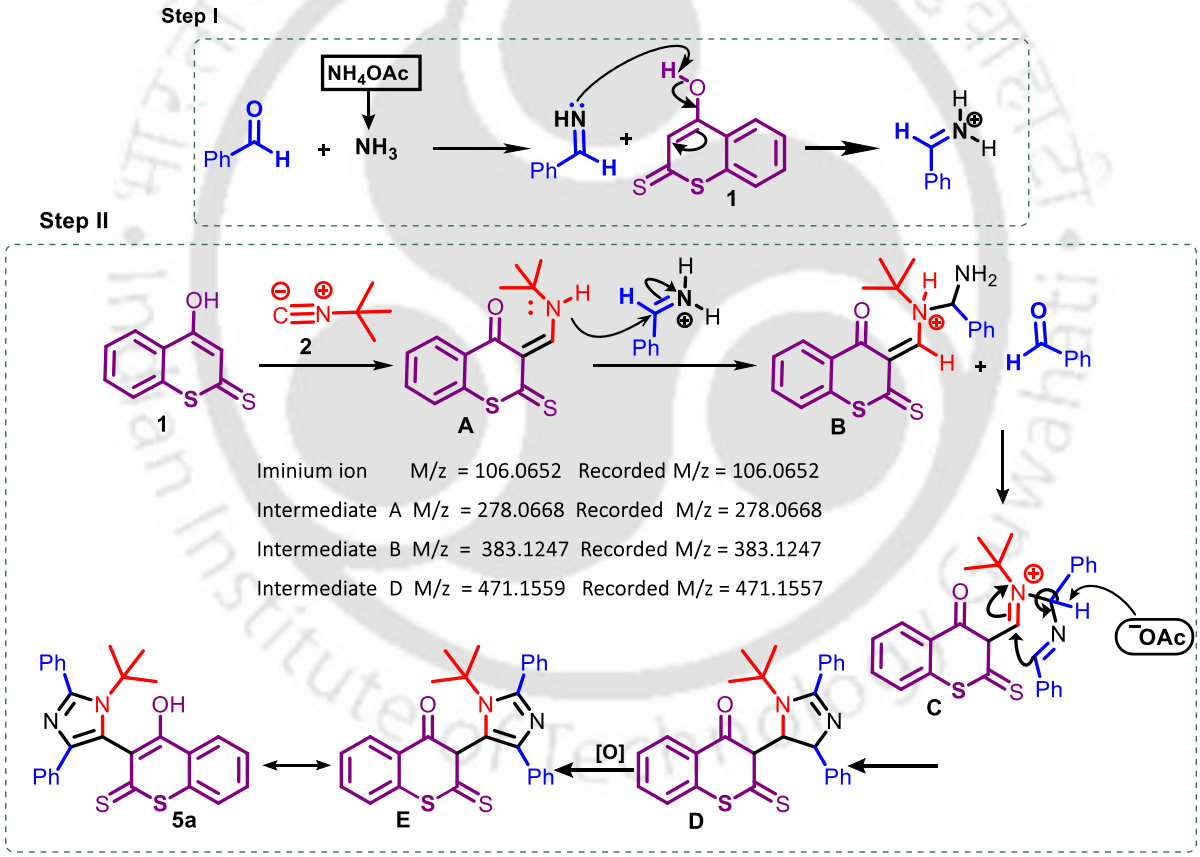

Schematic diagram of Reaction pathway

This mechanism is established based on previously reported literature, mass intermediates observed in HRMS, and the isolated product obtained during the experiment.

In the first step, upon heating, ammonium acetate generates NH_3, which reacts with an aryl aldehyde to form an imine intermediate, as shown in Table 3. The imine abstract proton from the 4-hydroxydithiocoumarin gives rise to the iminium ion. In the second step, 4-hydroxydithiocoumarin reacts with isocyanide **2** to form intermediate **A**, which then undergoes a nucleophilic addition to the iminium ion generated in the first step, forming intermediate **B.**

Intermediate **B** reacts with another molecule of aryl aldehyde through its amine group to form **intermediate C**, which subsequently transforms into **intermediate D**. Intermediate **D** then undergoes oxidation to yield **intermediate E**, which, upon tautomerization, affords the final product **5a**.

5.3. Biological application

The biological study was carried out with our collaborator, Professor S. S. Ghosh and his research scholar, Pijush Kanti Khanra, at the IIT Guwahati in the Department of Bioscience and Bioengineering.

Material and methods

5.3a. Target Prediction of the mother compound, 5a

The Swiss target prediction web server (https://www.swisstargetprediction.ch/) was employed to identify potential macromolecular targets of the synthesized mother compound **5a**. The SMILES identifier of **5a** was generated from its 3D SDF structure and subsequently used as input for target prediction analysis.

5.3b. Bioinformatic gene expression analysis

To assess the cancer-relevance of the predicted macromolecular targets, multiple bioinformatic platforms were used. EnrichR (https://maayanlab.cloud/Enrichr/), SDF (https://ualcan.path.uab.edu/) and DepMap (https://depmap.org/portal/) were used to assess gene–cancer correlations. Gene dependencies following CNR1 knockout were retrieved from the DepMap database, and the functional roles of affected genes were further explored using KEGG ontology enrichment and Reactome pathway analyses. In addition, UALCAN was utilized to perform patient survival analyses based on CNR1 expression levels in breast cancer,

as well as to evaluate the differential expression of the top 15 predicted target genes in TCGA TNBC samples.

5.3c. STRING correlation analysis

For correlation analysis between the two gene clusters associated with PI3K/Akt and MAPK signalling—derived from the set of genes affected by CNR1 knockout (DepMap dataset)—the STRING database (https://string-db.org/) was utilised. Correlation robustness was assessed using STRING confidence scores, where genes connected by a single string were considered to exhibit a medium confidence level (score ≥ 0.5), while genes connected by two or more strings were classified as having high confidence (score ≥ 0.7).

5.3d Preparation of CNR1 macromolecule and ligands, followed by molecular docking

The crystal structure of Cannabinoid Receptor 1 (CNR1; PDB ID: 7V3Z) was retrieved from the RCSB Protein Data Bank (RCSB PDB: Homepage) and pre-processed using BIO*VIA* Discovery Studio Visualizer to remove water molecules and non-essential ligands, as previously described by Khanra *et al*. 2025 [29]. Ligand preparation involved converting the synthesised compounds from the ".mol" format to the three-dimensional ".sdf" format. Molecular docking was performed using PyRx 0.9.2, following the established protocols of Khanra et al. (2025, 29), to evaluate the binding affinities of 28 synthesised ligands against CNR1. Post-docking analyses, including hydrogen bond mapping and amino acid interaction profiling, were conducted for the top five compounds using BIO*VIA* Discovery Studio Visualizer.

5.3e. Pharmacokinetic property prediction and drug-likeness property analysis

Drug-likeness and pharmacokinetic properties were systematically evaluated for the synthesized mother compound **5a** and the top five derivatives with the highest docking scores. Pharmacokinetic profiling was performed in silico using pkCSM (https://biosig.lab.uq.edu.au/pkcsm/prediction), which predicts parameters encompassing absorption, distribution, metabolism, excretion, and toxicity (ADMET).

Following ADMET characterization, the drug-likeness of the mother compound **5a** was further assessed using SwissADME (http://www.swissadme.ch/). By providing the canonical SMILES of **5a** as input, key descriptors—including Lipinski's rule of five, PAINS alerts, topological polar surface area (TPSA), and bioavailability score—were determined, thereby offering insights into its suitability as a potential therapeutic candidate.

5.3f. Cell culture conditions

The human breast cancer cell lines MDA-MB-231 (triple-negative breast cancer, TNBC) was procured from the National Centre for Cell Science (NCCS, Pune, India). Cells were cultured in Dulbecco's Modified Eagle's Medium (DMEM, high glucose; Sigma-Aldrich, USA) supplemented with additional ingredients including sodium bicarbonate, 10% fetal bovine serum (FBS; Gibco, USA) and 100 µg/mL penicillin and 100 µg/mL streptomycin (Thermo Fisher Scientific, USA). Cultures were maintained at 37 °C in a humidified incubator under an atmosphere of 5% CO_2.

5.3g. Cell *via*bility assay

To validate the in silico docking results, the anticancer activity of the lead compounds was assessed using an MTT [3-(4,5-dimethylthiazol-2-yl)-2,5-diphenyl-2H-tetrazolium bromide] cell *via*bility assay in MDA-MB-231 TNBC cells. Based on docking outcomes, compounds **5l** and **5m**, which exhibited the highest binding affinities to CNR1, were selected for evaluation. Cells were seeded at a density of 5 × 10^3 cells per well in 96-well plates (Thermo Scientific™) and allowed to adhere for ~30 h before treatment. Dose–response studies were performed using concentrations of 5, 10, 15, 20, 30, 40, and 50 µM for **5l**, and 9, 25, 40, 55, 70, 80, and 90 µM for **5m**. Untreated controls were included for normalization, with *via*bility set at 100%. 48 hours after treatment, the MTT assay was performed as previously described. *Via*ble cells reduced MTT to the insoluble formazan via NADPH oxidoreductase activity, and the crystals were solubilised in DMSO prior to absorbance measurements at 570 and 630 nm. Cell *via*bility (%) was calculated relative to untreated controls using the formula reported by Sen *et al.* 2023.[30] Cell *via*bility (%)=([〖(Abs 〗_570- 〖Abs〗_630) treated cells])/([(〖Abs 〗_570- 〖Abs〗_(630)) control cells]) X 100 IC_{50} optimization and data normalization were determined by nonlinear regression analysis (log[inhibitor] vs. normalised response, variable slope) in GraphPad Prism (version 6), following established protocols by Khanra *et al*. 2025.[29]

5.3h. Reactive oxygen species (ROS) generation assay

Following IC_{50} optimization for compounds **5l** and **5m**, MDA-MB-231 cells were seeded at a density of 2 × 10^5 cells per well in 6-well plates under four conditions: untreated–unstained, untreated–stained, **5l**-treated, and **5m**-treated. Upon reaching ~70% confluency, cells were treated with **5l** or **5m** at their respective IC_{50} concentrations, while controls remained untreated. After 24 h, cells were incubated with 10 µM DCFDA (2′,7′-dichlorofluorescein diacetate) for

30 min under cell culture conditions. The untreated–unstained group served as the negative staining control. In the presence of hydroxyl, peroxyl, and related ROS, DCFDA was oxidized to DCF (2′,7′-dichlorofluorescein), producing green fluorescence.[30] Fluorescent images were acquired using the ZOE™ Fluorescent Cell Imager (Bio-Rad) with a green filter, under fixed imaging parameters (gain: 16, exposure: 380 ms, intensity: 94, contrast: 17). Images were saved in ".tif" format, and fluorescence intensity was quantified using "ImageJ" software.

5.3i. Live-dead imaging

For live–dead analysis, MDA-MB-231 cells were seeded at 2×10^5 cells per well in 6-well plates under identical conditions to the ROS assay (untreated–unstained, untreated–stained, **5l**-treated, **5m**-treated). Following 48 h of treatment with **5l** or **5m** at their IC_{50} concentrations, adherent cells were stained with a dual-staining mixture of Calcein AM (4 μM) and propidium iodide (PI, 4 μM) for 30 min at cell culture conditions. The untreated–unstained condition served as a negative staining control. Calcein AM fluoresces green upon intracellular esterase activity in intact cytoplasm, marking *via*ble cells, whereas PI enters compromised membranes and intercalates with nuclear DNA, identifying dead cells[31]. After incubation, the stained cells were imaged using the ZOE Fluorescent Cell Imager (Bio-Rad), equipped with green and red fluorescence filters. Green fluorescence indicated live cells, while red fluorescence corresponded to dead populations. Images were captured in ".tif" format under fixed image setting parameters (gain: 19, exposure: 340 ms, intensity: 51, contrast: 23). Quantification of fold changes in live and dead populations across treatment conditions was performed using "ImageJ" software.

5.3j. Statistical significance analysis

Statistical analyses were performed to assess the significance of data from cell *via*bility, ROS generation, and live–dead assays. All computations were conducted using GraphPad Prism (v6.0.0; GraphPad Software, San Diego, CA, USA). Experiments included at least two independent biological replicates, with technical triplicates where applicable. Data are presented as mean ± standard error of the mean (SEM). For multiple comparisons within a dataset, one-way ANOVA was applied. A p-value ≤ 0.05 was considered statistically significant.

5.3k. Results

5.3l. Target prediction and macromolecular selection

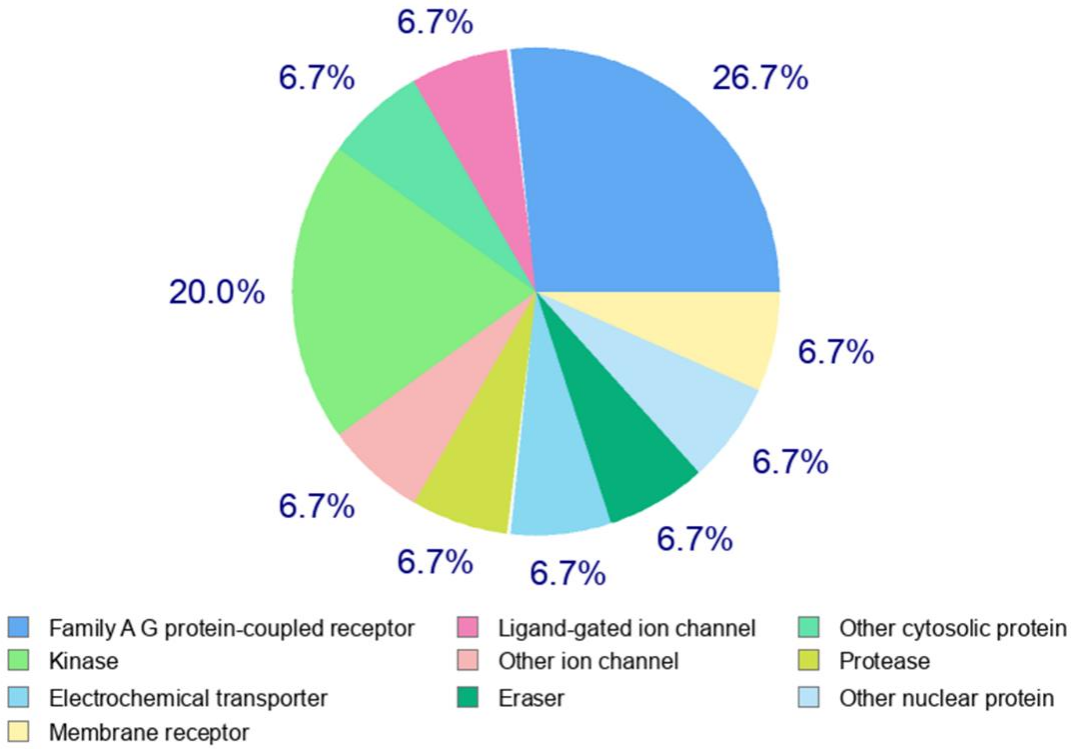

Figure 3. The Pi-diagram, illustrating the probability distribution of interactions between the ligand compound 5a and various families of target macromolecules. Each segment is color-coded to represent a specific macromolecular class, highlighting the relative likelihood of 5a binding across different targets.

Target prediction of compound **5a**, based on its canonical SMILES, revealed a predominant enrichment for G protein–coupled receptors (26.7%), followed by kinases (20%). Other predicted categories, including transporters, membrane receptors, ion channels, proteases, and nuclear proteins, each accounted for 6.7% **Figure 3.** Nineteen targets exhibited ≥10% binding probability, with cannabinoid receptor 1 (CNR1) emerging as the most prominent candidate, supported by 816 annotated three-dimensional activity records, alongside other GPCRs.

5.3m. Bioinformatics-driven gene expression analysis of CNR1 and other predicted targets in the context of cancer aggravation

To investigate the role of CNR1 in cancer signalling, genes affected by CNR1 knockout were retrieved from the DepMap dataset and analyzed using the EnrichR platform. KEGG pathway enrichment **Figure 4A** and Reactome pathway analysis **Figure 4C** revealed significant associations with cancer-related signalling and transduction pathways. Notably, many of the affected genes were enriched in the MAPK and PI3K–Akt signalling cascades, as well as in cancer metabolism, underscoring the regulatory contribution of CNR1 to tumour progression. Consistent with these findings, STRING correlation mapping **Figure 4D** demonstrated strong associations between CNR1 and genes in both the PI3K–Akt and MAPK pathways. The left cluster of **Figure 4D** corresponds to genes from the PI3K–Akt signalling pathway, while the right cluster represents genes from the MAPK signalling pathway, as identified through KEGG enrichment in **Figure 4A**. Consistent with these findings, STRING correlation mapping **Figure 4D** demonstrated strong associations between CNR1 and genes in both the PI3K–Akt and MAPK pathways.

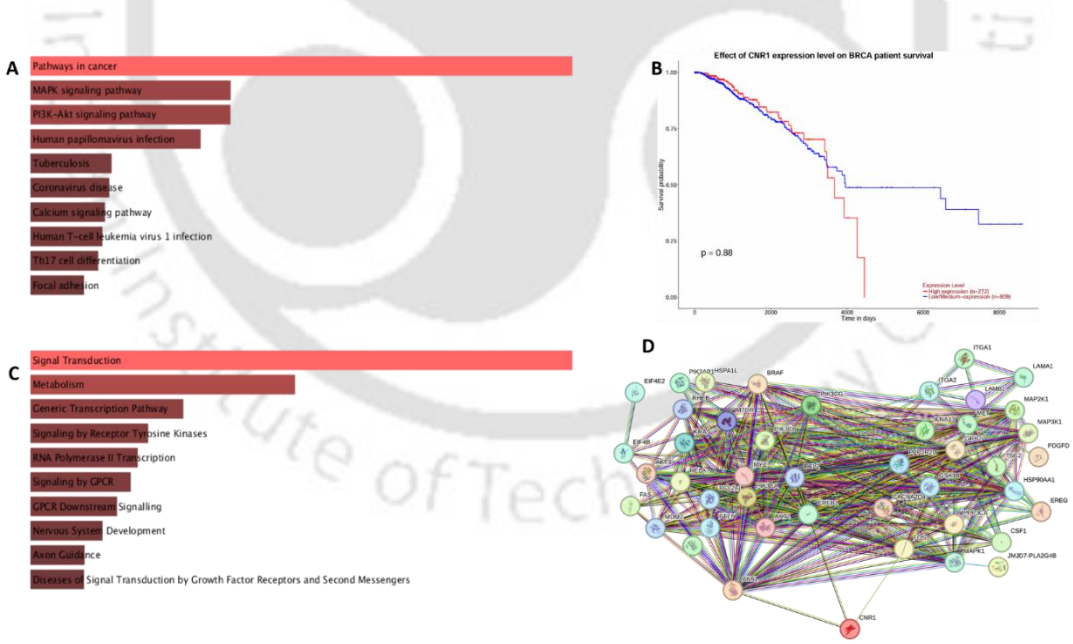

Figure 4. Regulatory impact of genes affected by CNR1 knockout (DepMap dataset) on cancer and cancer-associated signalling pathways, as identified by KEGG ontology enrichment (panel A) and Reactome pathway analysis (panel C). Panel B illustrates the survival patterns of breast cancer patients stratified by differential CNR1 expression, while panel D shows the transcript per million (TPM) expression levels of CNR1 across different stages of TCGA breast cancer samples compared with normal tissues.

The left cluster of **Figure 4D** corresponds to genes from the PI3K–Akt signalling pathway, while the right cluster represents genes from the MAPK signalling pathway, as identified through KEGG enrichment in **Figure 4A**. Importantly, CNR1 served as a connecting node, linking the "PI3K–Akt signalling pathway" cluster *via* AKT1 and CREB1, and bridging the "MAPK signalling pathway "cluster through FOS. This robust clustering pattern validates the KEGG enrichment results **Figure 4A** and highlights the integrative role of CNR1 in coordinating PI3K–Akt and MAPK signalling in cancer progression.

In addition to CNR1, analysis of 14 other genes (Supplementary Table S2) revealed marked upregulation, particularly in triple-negative breast cancer (TNBC) TCGA samples **Figure 5**. Genes including CNR2, GPR55, GPR18, GLRA1, ALOX**5a**P, RCE1, SLC6A9, SIRT2, and TSPO exhibited elevated expression relative to normal tissues. Key oncogenes, such as EGFR, KDR, MDM2, SIRT2, and ERBB2—encoding epidermal growth factor receptor (ErbB-1), vascular endothelial growth factor receptor 2, p53-binding protein Mdm2, NAD-dependent deacetylase sirtuin 2, and receptor protein-tyrosine kinase ErbB-2, respectively—have established roles in TNBC progression and its hallmark features.[33] Survival analysis further indicated that higher CNR1 expression correlates with poor prognosis: patients with elevated CNR1 levels survived up to ~4,000 days, whereas those with lower expression survived over ~8,000 days **Figure 4B**.

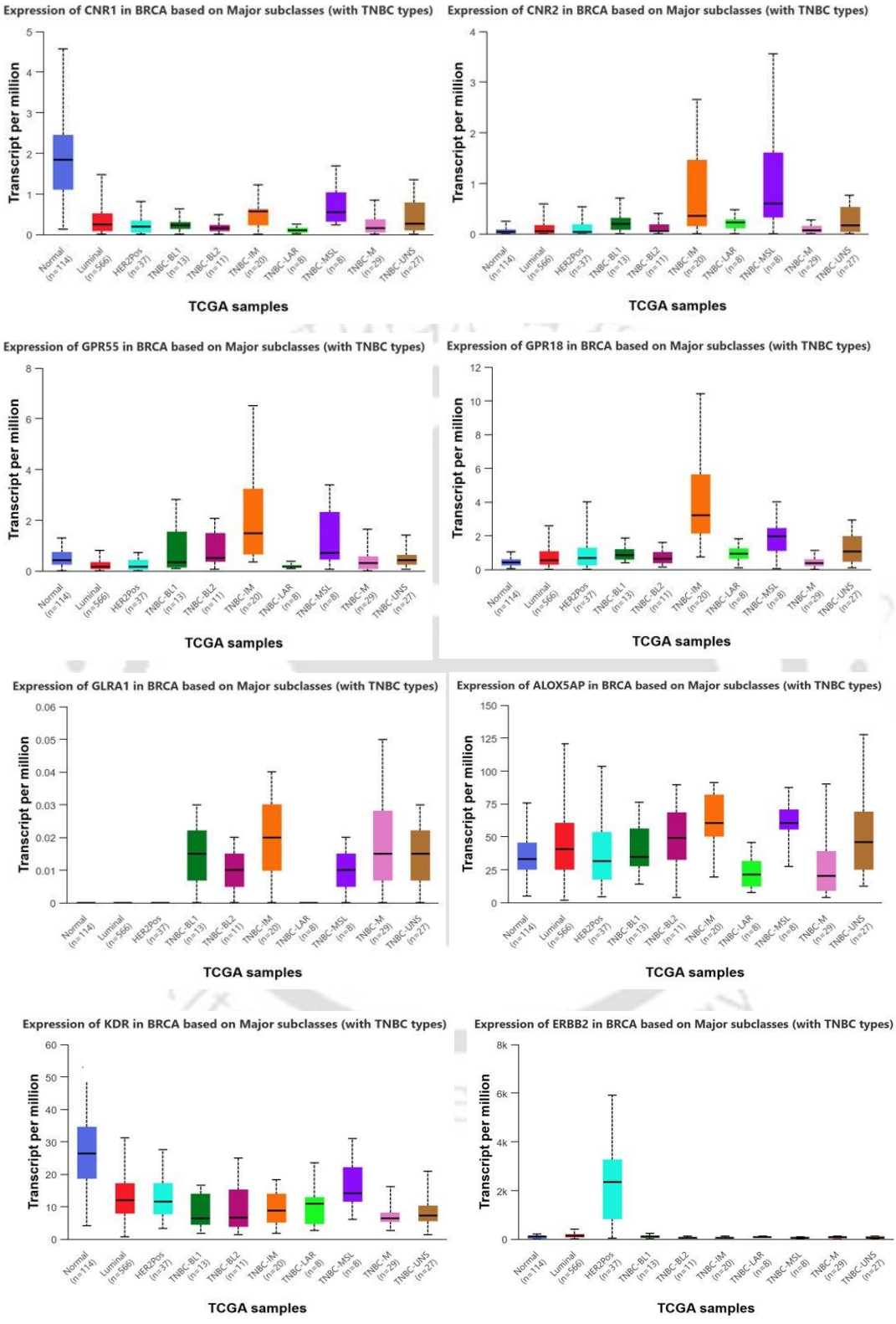
Expression of CNR1 in BRCA based on Major subclasses (with TNBC types)
Transcript per million
TCGA samples
Expression of CNR2 in BRCA based on Major subclasses (with TNBC types)
Transcript per million
TCGA samples
Expression of GPR55 in BRCA based on Major subclasses (with TNBC types)
Transcript per million
TCGA samples
Expression of GPR18 in BRCA based on Major subclasses (with TNBC types)
Transcript per million
TCGA samples
Expression of GLRA1 in BRCA based on Major subclasses (with TNBC types)
Transcript per million
TCGA samples
Expression of ALOX5AP in BRCA based on Major subclasses (with TNBC types)
Transcript per million
TCGA samples
Expression of KDR in BRCA based on Major subclasses (with TNBC types)
Transcript per million
TCGA samples
Expression of ERBB2 in BRCA based on Major subclasses (with TNBC types)
Transcript per million
TCGA samples

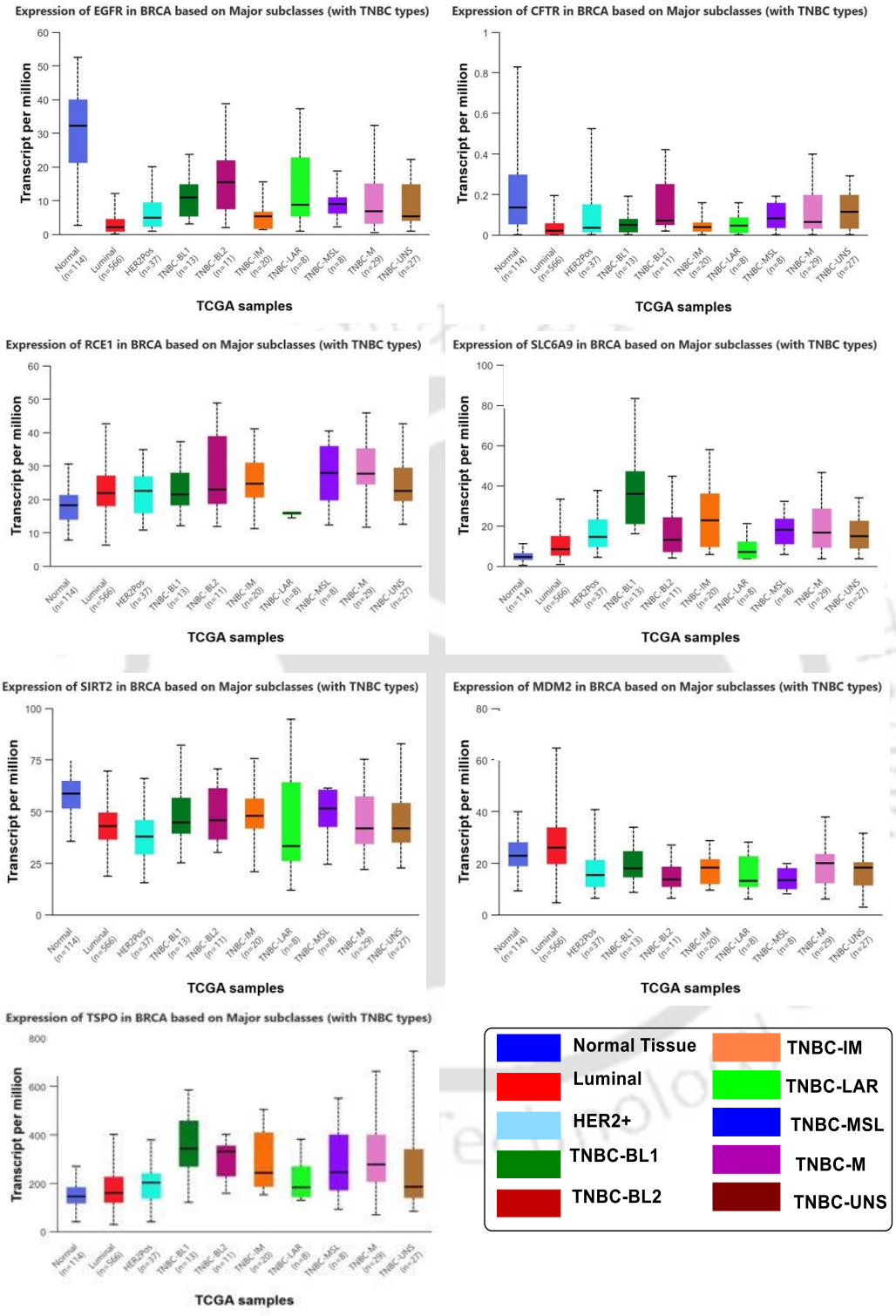

Figure 5. Differential expression of the top 15 predicted target genes across TNBC samples compared with normal tissues, luminal, and HER2⁺ TCGA cohorts. Expression patterns are displayed using distinct color codes to highlight subtype-specific variations.

Table 4. Key amino acid interactions of CNR1 with the five top-ranked compounds, highlighting critical binding residues involved in ligand recognition.

Name of the synthesized compounds	Number of hydrogen bonds (HBs)	Interacting residue(s) formed HB(s)	No. of additional interactions	Types of additional interactions and pertinent amino acid residues
5k	1	Tyr 296	14	Van der Waals (Gln 1045, Pro 1123, Gly 1144, Val 1143, Glu 1122, Ile 297, Ala 211, Tyr 292), Pi-Pi (Tyr 215, Phe 1121) Pi-alkyl (Ala 293, Ile 212), Pi-cation (His 219)
5l	2	Tyr 296, Tyr 215	12	Van der Waals (Gln 1045, Pro 1123, Gly 1144, Val 1143, Glu 1122, Ile 297, Ala 211, Tyr 292), Pi-Pi (Phe 1121) Pi-alkyl (Ala 293, Ile 212), Pi-cation (His 219)
5m	2	Tyr 296, Gln 1045	11	Van der Waals (Pro 1123, Gly 1144, Val 1143, Glu 1122, Ile 297,Ala 211, Tyr 292), Pi-Pi (Phe 1121) Pi-Alkyl (Ala 293, Ile 212), Pi-cation (His 219)
5w	0		18	Van der Waals (Phe 1124, Gly 1125, Glu 1122, Val 1127, Gly 1039, Tyr 1109, Ile 1038, Gly 1073, Ile 1072, Leu 1100, Met 1099), Pi-sigma (Leu 1126) Pi-alkyl (Lys 300, Pro 1123, Arg 1040), Pi-cation (Lys 1046, Asp 1042)
5x	0		14	Van der Waals (Gln 1045, Tyr 1120, Pro 1123, Gln 1045, Glu 1122, Arg 1147, Val 1143, Gly 1144, Tyr 292, Ile 297), Pi-Pi (Tyr 296) Pi-alkyl (Ala 293), Unfavorable donor-donor (Tyr 215), Pi-cation (His 219, Phe 1121)

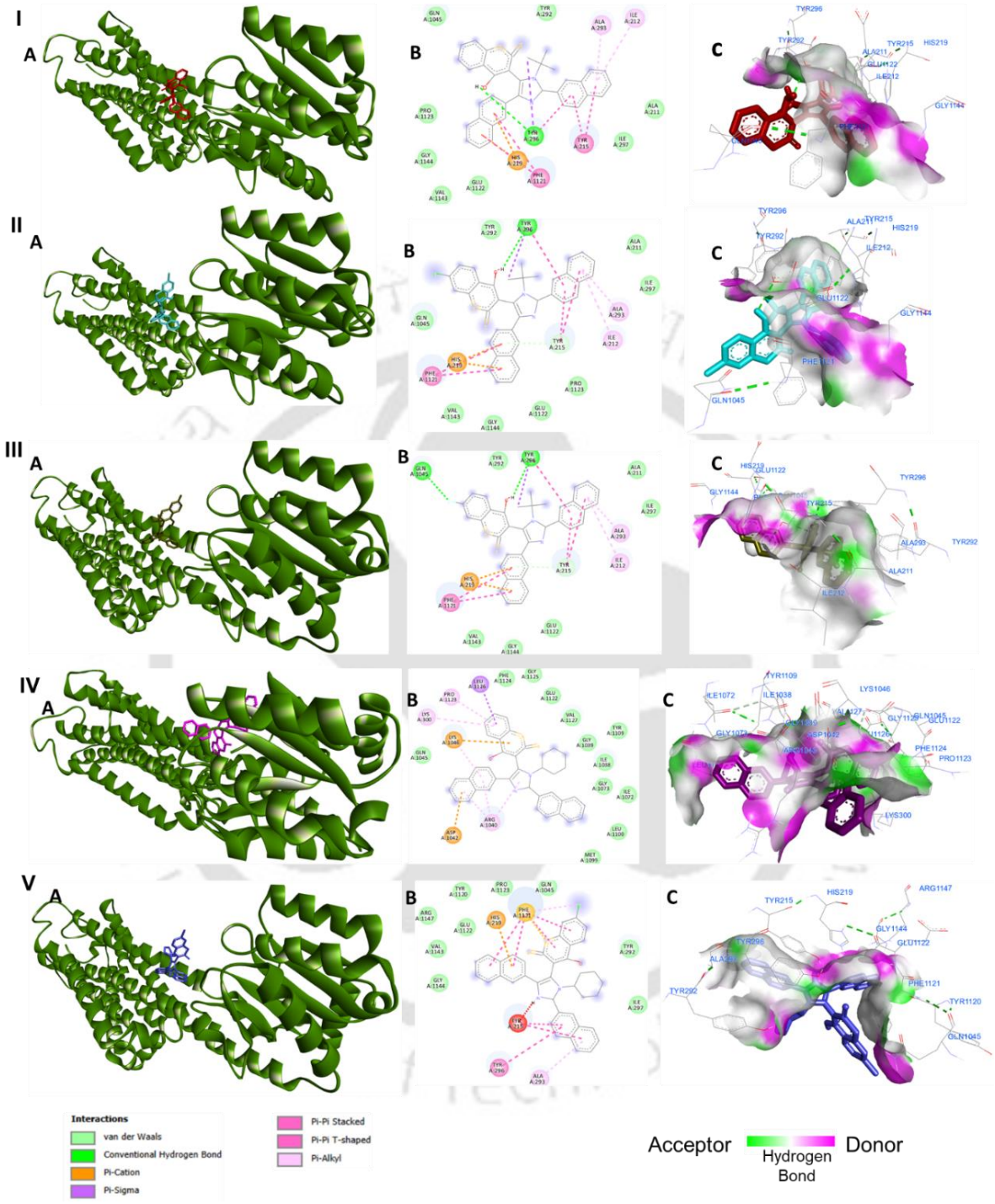

Figure 6. In silico 2D interaction profiles of docked ligands 5k (I), 5l (II), 5m (III), 5w (IV), and 5x (V) within the binding pocket of CNR1 (panel A). Panel B illustrates the corresponding amino acid interactions and bond types, depicted using distinct color codes. Panel C shows hydrogen bond cloud formations adjacent to the interaction zones for each of the five ligands.

5.3o. ADMET pharmacokinetic profiling analysis

ADMET(absorption, distribution, metabolism, excretion, and toxicity) profiling was performed to evaluate the pharmacokinetic characteristics of the synthesized compounds. The five top-performing candidates, identified by their superior docking scores, were subjected to ADMET analysis, the results of which are summarized in **Table 5.**

Property	Model Name	Compounds				
		5k	**5l**	**5m**	**5w**	**5x**
Absorption	Water solubility (log mol/L)	-2.894	-2.894	-2.893	-2.913	-2.912
	Caco2 permeability (log Papp in 10^{-6} cm/s)	0.786	0.78	0.837	0.098	0.091
	Human intestinal absorption (%)	87.273	86.483	87.419	85.396	84.433
	Skin Permeability (log Kp)	-2.735	-2.735	-2.735	-2.735	-2.735
	P-glycoprotein substrate	Yes	Yes	Yes	No	No
	P-glycoprotein inhibitor	Yes	Yes	Yes	Yes	Yes
Distribution	Plasma protein binding (fraction unbound in Fu)	0.367	0.365	0.37	0.352	0.349
	Volume distribution (L/ kg)	-0.212	-0.223	-0.205	-0.219	-0.227
	BBB penetration (log BB)	0.189	0.168	0.042	0.699	0.679
Metabolism	CYP2D6 substrate	No	No	No	No	No
	CYP3A4 substrate	Yes	Yes	Yes	Yes	Yes
	CYP1A2 inhibitor	Yes	Yes	Yes	Yes	Yes
	CYP2C19 inhibitor	No	No	No	No	No
	CYP2C9 inhibitor	No	No	No	Yes	Yes
	CYP2D6 inhibitor	Yes	Yes	Yes	Yes	Yes
	CYP3A4 inhibitor	No	No	No	No	No
Excretion	Total Clearance [Log (ml/ min/ kg]	0.365	0.256	0.266	0.449	0.34
	Renal OCT2 substrate	No	No	No	Yes	Yes
Toxicity	AMES toxicity	No	No	Yes	No	Yes
Excretion	Total Clearance [Log (ml/ min/ kg]	0.365	0.256	0.266	0.449	0.34
	Max. tolerated dose (human) [log (mg/kg/day)]	0.438	0.438	0.438	0.438	0.438
	hERG I inhibitor	No	No	No	No	No

	Rat oral acute toxicity (LD50) [mol/kg]	2.535	2.542	2.522	2.482	2.491
	Hepatotoxicity	Yes	No	Yes	No	No
	Skin Sensitization	No	No	No	No	No

5.3p. Absorption property

The absorption behavior of the selected compounds was evaluated using multiple parameters, including water solubility, human intestinal absorption (HIA), P-glycoprotein (P-gp) substrate and inhibitor properties, Caco-2 cell permeability, and skin permeability. Among these, Caco-2 permeability showed the most evident differences across compounds. Compounds with logarithmic Caco-2 permeability values

greater than −0.9 are generally considered highly permeable with favorable bioavailability. Based on this threshold, compounds **5k**, **5l**, and **5m** exhibited moderate permeability indices. Consistent with this trend, the compounds followed the order **5m** > **5k** > **5l** > **5w** > **5x** for HIA. Notably, compounds with HIA values exceeding 90% are regarded as having high intestinal absorption [34] whereas the tested candidates displayed moderate absorption potential. In terms of P-gp interactions, three compounds (**5k**, **5l**, and **5m**) were identified as substrates, yet all five acted as inhibitors of P-gp activity. This dual property is particularly relevant, as inhibition of P-gp can mitigate efflux-mediated multidrug resistance [35].Collectively, these findings suggest that the five shortlisted compounds hold strong potential as candidates against drug-resistant TNBC cells, reinforcing their capability for further *in vitro* evaluation to substantiate their anticancer efficacy.

5.3q. Distribution throughout the body

A VDss value above 0.45 indicates extensive tissue distribution, whereas values below −0.15 reflect limited distribution. The tested compounds exhibited moderate VDss values, suggesting balanced distribution across body fluids. Plasma protein binding analysis revealed unbounddrug fractions of ~0.35–0.37, which fall within the acceptable range of 0.02–1.0 for drug-like compounds [34].values, suggesting balanced distribution across body fluids. Plasma protein binding analysis revealed unbound drug fractions of ~0.35–0.37, which fall within the acceptable range of 0.02–1.0 for drug-like compounds [34]. These values imply that the compounds are less likely to remain bound to plasma proteins and more prone to hepatic and intestinal metabolism, thereby reducing systemic circulation persistence [29]. BBB permeability assessment demonstrated compound-specific variation. Compounds **5x** and **5w** exhibited

logBB values exceeding 0.3, indicative of high BBB penetration and potential central nervous system toxicity. By contrast, compound **5m** showed minimal BBB permeability (logBB = 0.0042), making it a more favorable therapeutic candidate owing to its poor brain distribution and reduced risk of neurotoxicity [36].

5.3r. Metabolism

Cytochrome P450 (CYP) enzymes play a central role in drug metabolism[34] acting both as substrates and inhibitors that influence pharmacokinetic behavior and therapeutic specificity. As summarized in Table 2, none of the five tested compounds were identified as CYP2D6 substrates, while all were predicted to be metabolized by CYP3A4, indicating that CYP3A4 is the primary enzyme mediating their biotransformation. Notably, all five compounds inhibited CYP1A2, a cytochrome isoform implicated in tumor-promoting activity [37], thereby suggesting a potential anticancer benefit beyond their primary mechanism of action. In contrast, no inhibitory activity was observed against CYP2C19, highlighting the compounds' selective and specific interactions with cytochrome isoforms.

5.3s. Excretion

Organic cation transporter 2 (OCT2) is a key renal uptake transporter that facilitates the clearance of excretory metabolites from the kidney. Drug-like candidates that undergo renal clearance typically display negligible substrate affinity for OCT2[34]. In contrast, predictive results indicated substrate affinity for compounds **5x** and **5w**, whereas **5k**, **5l**, and **5m** showed no such interaction, supporting the prioritization of **5l** and **5m** for *in vitro* validation studies. Assessment of total excretory clearance further revealed that all five compounds exhibited moderate clearance rates, with **5w** displaying the highest predicted clearance value.

5.3t. Toxicity profiling

Toxicity profiling revealed that compound **5l** exhibited the most favourable safety profile, showing no evidence of AMES mutagenicity, hepatotoxicity, or skin sensitisation. Importantly, none of the five compounds demonstrated inhibitory activity against the hERG (human ether-a-go-go) channel, a critical regulator of the cardiac action potential, thereby minimising the risk of cardiotoxicity. Assessment of dosage safety indicated that all five compounds remained below the threshold of concern for the maximum tolerated dose [log (MTD) > 0.477], with predicted values averaging ~0.438 log(mg/kg/day). Furthermore, all candidates displayed high LD50 values, consistent with low acute toxicity, in line with prior observations by Bhattacharya

et al. (2024.34 Collectively, these results underscore the favourable toxicity profiles of the five shortlisted compounds, with **5l** emerging as the safest candidate.

5.3u. Drug likeness property and bioactivity analysis of the synthesized mother compound:

Drug-likeness profiling was conducted to assess the pharmacokinetic suitability of the synthesized mother compound (**5a**). As summarized in supplementary table S4, **5a** satisfied Lipinski's rule of five with one violation and exhibited an optimal oral bioavailability score of 0.55, placing it within the desirable drug-like chemical space. Consistent with Lipinski, Veber, and Egan criteria, the topological polar surface area (TPSA) of **5a** was within the recommended threshold (≤140 Å²), supporting favourable oral absorption. [38,39] Further analysis revealed that **5a** possessed two hydrogen bond acceptors and one hydrogen bond donor, along with a LogP value of 3.86. This lipophilicity index (LogP ≤ 5) reflects an appropriate balance between solubility and membrane permeability, reinforcing its classification as a drug-like candidate. Collectively, these findings suggest that **5a** exhibits favourable drug-likeness properties and merits further development. [38]

1.4 *In vitro* anti-cancer activity evaluation of 5l and 5m *via* decreasing cell *via*bility gradients and heightening reactive oxygen species (ROS) generation

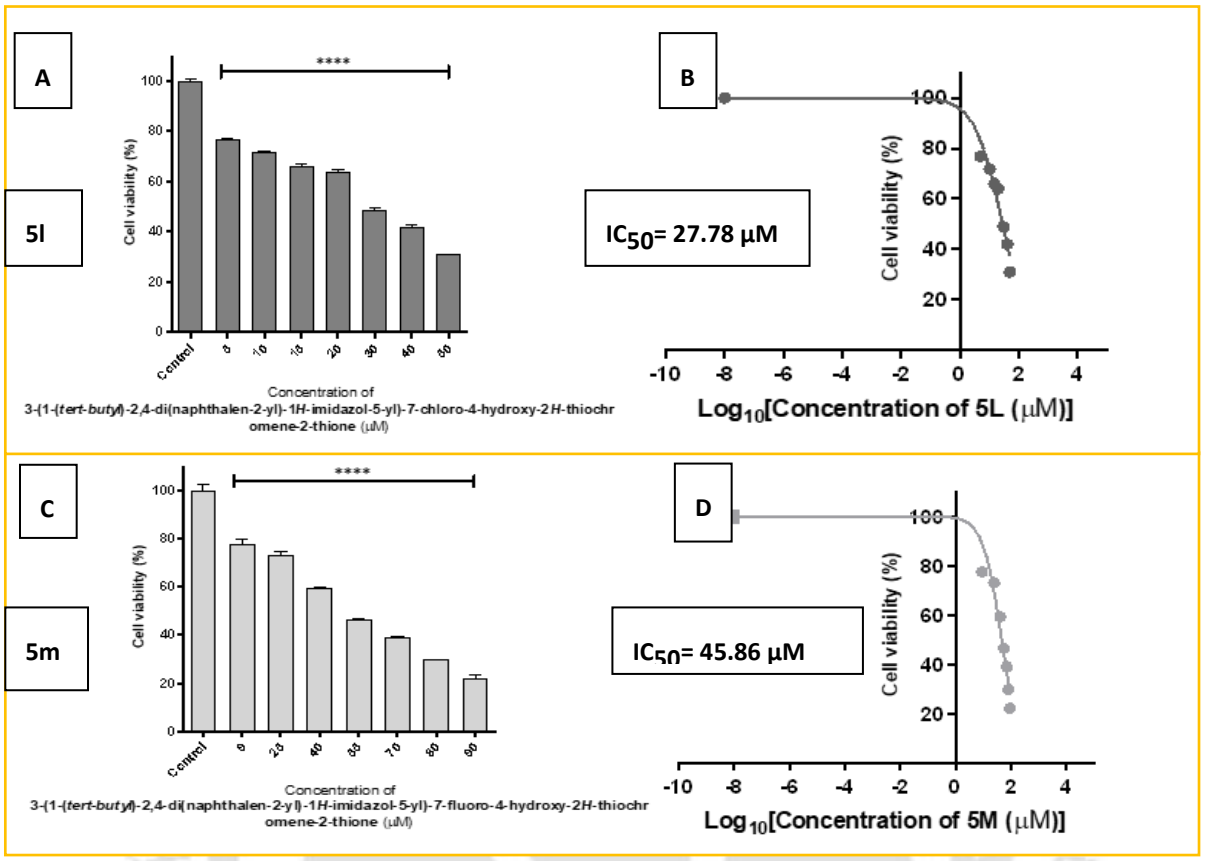

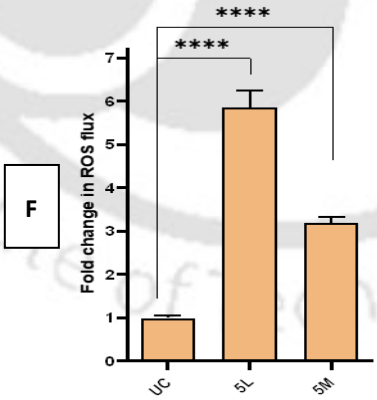

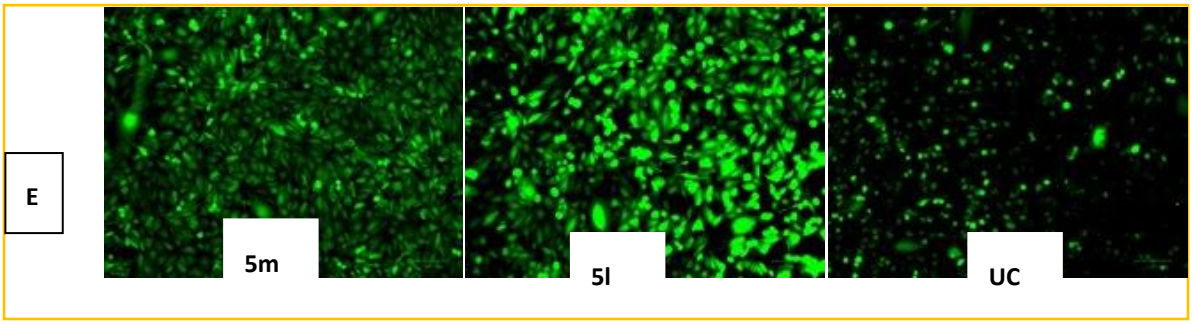

Figure 7 : Dose-dependent reduction in cell *via*bility (%) of MDA-MB-231 cells treated with **5l** (panels A, B) and **5m** (panels C, D). Panel E shows the increase in ROS generation under **5l**- and **5m**-treated conditions compared with the untreated control (UC). The induction of ROS is further validated by the fold-change in ROS flux (panel F). Data represent mean ± SEM from at least two independent experiments. Statistical significance: ns, not significant ($p > 0.05$); *$p \leq 0.05$; **$p \leq 0.01$; ***$p \leq 0.001$; ****$p \leq 0.0001$.

Following virtual screening, two lead compounds (**5l** and **5m**), identified by their highest binding affinities (lowest binding energy), were selected for *in vitro* validation. Cytotoxicity was assessed in MDA-MB-231 triple-negative breast cancer (TNBC) cells, a model known to overexpress CNR1.[40] Dose–response analysis revealed half-maximal inhibitory concentrations (IC_{50}) of 27.78 µM for **5l** **Figure**. **7A** and 45.86 µM for **5m Figure 7C**, with **5l** demonstrating greater potency. Consistent with these values, cell *via*bility decreased to ~30% upon **5l** treatment and ~20% with **5m** at the highest tested concentrations **Figure 7 B**, **D**. Mechanistic studies further indicated that **5l** induced higher levels of intracellular reactive oxygen species (ROS), with a 5.86-fold increase compared to untreated controls, whereas **5m** elicited a 3.2-fold increase after 24 h at their respective IC_{50} concentrations **Figure 7E, F**; Supplementary Table S5). These findings suggest that **5l** exerts stronger cytotoxic effects, potentially mediated through ROS-driven oxidative stress, which may lead to the activation of cell death pathways.[41]

5.3v. 2D live-dead imaging detected the declining cell density with increasing dead cell numbers upon IC50 dosage conditions of treatment groups

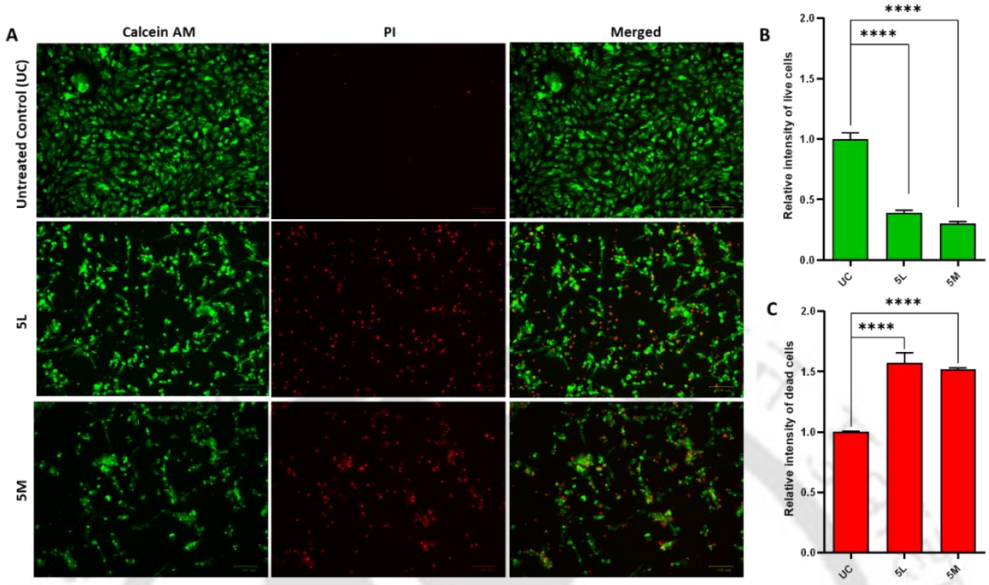

Figure 8: Increase in PI-stained dead cell populations and corresponding decrease in Calcein AM–stained live cells following **5l** and **5m** treatments compared with the "untreated control" (UC) (panel A). The merged image confirms the absence of overlap between live and dead cell populations. Panels B and C validate these findings by quantifying the fold-change in live and dead cell populations, respectively. Data represent mean ± SEM from at least two independent experiments. Statistical significance: ns, not significant ($p > 0.05$); *$p \leq 0.05$; **$p \leq 0.01$; ***$p \leq 0.001$; ****$p \leq 0.0001$.

Consistent with the reduction in cell *via*bility, both **5l**- and **5m**-treated groups exhibited a marked increase in propidium iodide (PI)-positive dead cells, with 1.58-fold and 1.52-fold increases, respectively, compared with untreated controls (Supplementary Table S6; **Figure 8**. **6C**). Conversely, Calcein AM staining revealed proportional decreases in live cell populations, corresponding to 2.56-fold (**5l**) and 3.3-fold (**5m**) reductions in *via*ble cells, in line with the cell *via*bility curves (**Figure 7**, D; **Figure 8** B). Together, these findings validate the IC_{50} concentrations of **5l** and **5m** and confirm their cytotoxic activity against MDA-MB-231 TNBC cells.

Discussions

This study elucidates the biological relevance of newly synthesized tasted compounds with pronounced anti-cancer properties. *In vitro* analyses demonstrated robust inhibition of cellular proliferation in aggressive triple-negative breast cancer (TNBC) cells. The MDA-MB-231 cell line, a widely used TNBC model, harbours multiple point mutations that confer resistance to standard chemotherapeutics such as mitoxantrone, [42] doxorubicin, paclitaxel, [43] cis-platin, [44] highlighting the therapeutic challenge posed by this cancer subtype. Among the synthesized compounds, two lead candidates, **5l** and **5m**, exhibited significant anti-proliferative activity with IC_{50} values of 27.78 μM and 45.86 μM, respectively. This was accompanied by a 5.86-fold and 3.2-fold increase in reactive oxygen species (ROS) production, implicating ROS-mediated mediated cytotoxicity, may activate cell death machinery and subsequent decrease in cell *via*bility .[41] The observed decline in *via*ble cell populations alongside a concomitant increase in dead cells further corroborates the cytotoxic potential of **5l** and 5m, supporting IC_{50} optimization derived from cell *via*bility assays.

Pharmacokinetic evaluation *via* ADMET profiling indicated a favourable toxicity profile for **5l**, while both **5l** and **5m** demonstrated suitable metabolic stability and moderate excretory clearance. Notably, both compounds exhibited low plasma protein binding and negligible blood-brain barrier permeability, suggesting minimal neurotoxicity and efficient systemic distribution. [34] These features collectively reinforce their translational potential for *in vivo* applications. Comprehensive bioinformatic analyses identified CNR1, a G-protein coupled receptor implicated in TNBC progression and the amplification of cancer hallmarks [40], as the putative target. Molecular docking studies revealed strong 2D binding interactions of **5l** and **5m** with CNR1, achieving the highest docking scores among the 28 tested compounds, thereby validating the observed *in vitro* efficacy. Additionally, the mother compound, **5a**, exhibited favorable drug-likeness properties, with only one violation of Lipinski's rule of five, no PAINS alerts, optimal topological polar surface area (TPSA), and bioavailability scores consistent with Lipinski, Veber, and Egan criteria.[38] Collectively, these findings highlight the therapeutic potential of **5l** and **5m,** along with their mother scaffold **5a**, as promising candidates for the treatment of TNBC, providing a strong rationale for further preclinical and translational investigations. Techniques such as ^{1}H NMR, ^{13}C NMR, IR, and mass spectrometry.

5.4. Experimental section

Procedure for the synthesis of 3-(1-(*tert*-butyl)-2,4-diphenyl-1*H*-imidazol-5-yl)-4-hydroxy-2*H*-thiochromene-2-thione derivatives

A mixture of 0.20 mmol (39 mg) 4-hydroxydithiocoumarin, 0.20 mmol (22 µL)tert-butyl isocyanide, 0.20 mmol (15 mg) ammonium acetate, and 0.40 mmol (26 µL) tolualdehyde in 1 mL acetonitrile was stirred in a 25 mL round-bottomed flask at reflux temperature. The reaction was monitored from time to time by using TLC. After three hours, the reaction was completed, and the crude residue was filtered using filter paper 150 mm and washed thoroughly with 10 mL ethyl acetate and hexane 6:4 ratio, respectively. The desired product was isolated with an 80% yield (79mg) and characterised by various spectroscopic techniques.

Conclusion:

In the current study, we proposed a convenient and easy synthetic strategy for the synthesis of highly substituted Bis-heterocycle (BHC) imidazole derivatives using 4-hydroxydithiocoumarin, isocyanide, ammonium acetate, and aldehydes. Moreover, we observed that the reactivity of 4-hydroxydithiocoumarin, which is an ambient nucleophile, with another nucleophile, isocyanide, to form an intermediate enamine regioselectively at the C3 position of 4-hydroxydithiocoumarin *via in situ* conversion of isocyanide to an electrophile. Among the newly synthesised compounds, 5l and 5n exhibit anticancerous activity in TNBC cell lines. An unusual pattern was also observed in a single-crystal XRD, resulting in a helical structure. The key features of this protocol include catalyst-free, high atom economy, low E-factor, ease of handling, good yield, no column chromatography required for separation, and shorter reaction time, making it a very efficient and attractive procedure for synthesising tetra-substituted Bis-Imidazole derivatives. Moreover, we also observed the dominance of the reactivity of isocyanide over aryl aldehyde with 4-hydroxydithiocoumarin under our reaction conditions.

Characterisation Table:

3-(1-(*tert*-butyl)-2,4-diphenyl-1*H*-imidazol-5-yl)-2-thioxothiochroman-4-one (5a) 1 A

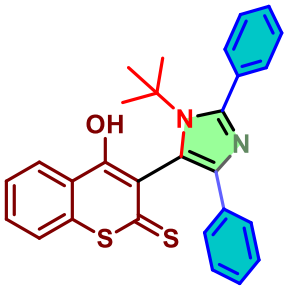

pale yellow crystalline solid (83 mg, 89%) mp 375-377 °C,^{1}H NMR (400 MHz, Chloroform-*d*) δ 8.09 (d, *J* = 6.8 Hz, 1H), 7.75 (d, *J* = 7.1 Hz, 2H), 7.67 (dd, *J* = 14.6, 7.3 Hz, 3H), 7.58 – 7.54 (m, 2H), 7.51 – 7.46 (m, 1H), 7.38 (d, *J* = 7.4 Hz, 1H), 7.35 – 7.21 (m, 4H), 1.51 (s, 9H). ^{13}C NMR (100 MHz, Chloroform-*d*) δ 184.1, 174.9, 143.8, 140.5, 131.4, 131.2, 131.0, 130.5, 130.3, 128.6, 128.3, 128.1, 127.2, 125.8, 122.9, 63.6, 30.6. IR(KBr)ν_{max}/cm^{-1} 2943 (C− H), 1135 (C=S), HRMS (ESI):m/z $[M+H]^+$ calcd. for $C_{27}H_{25}N_2OS_2$, 469.1403 found 469.1404.

3-(1-(*tert*-butyl)-2,4-di-*p*-tolyl-1*H*-imidazol-5-yl)-4-hydroxy-2*H*-thiochromene-2-thione

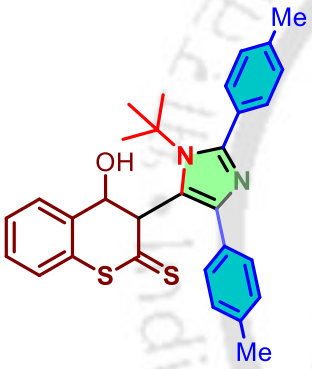

(5b) A light yellow solid (79 mg, 80%) mp 336-338 °C,^{1}H NMR (400 MHz, DMSO-d_6) δ 14.46 (s, 1H), 8.08 (dd, *J* = 8.0, 1.1 Hz, 1H), 7.62 (d, *J* = 7.9 Hz, 2H), 7.50 – 7.40 (m, 5H), 7.38 – 7.29 (m, 2H), 7.09 (d, *J* = 8.1 Hz, 2H), 2.44 (s, 3H), 2.21 (s, 3H), 1.50 (s, 9H). ^{13}C NMR (150 MHz, DMSO-d_6) δ 184.1, 174.8, 143.6, 141.1, 140.5, 137.7, 131.0, 130.8, 130.4, 130.3, 129.1, 128.8, 128.0, 127.1, 125.7, 122.8, 63.6, 30.5, 21.0, 20.7. IR(KBr)ν_{max}/cm^{-1} 2953 (C−H), 1137 (C=S), HRMS (ESI):m/z $[M+H]^+$ calcd. for $C_{30}H_{29}N_2O_3S_2$, 497.1716 found 497.1715.

3-(1-(*tert*-butyl)-2,4-bis(4-chlorophenyl)-1*H*-imidazol-5-yl)-4-hydroxy-2*H*-thiochromene

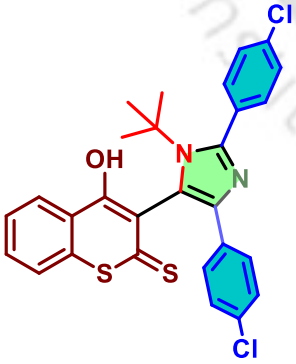

-2-thione (5c) A light yellow solid (93 mg, 87%) mp 310-312 °C, ^{1}H NMR (500 MHz, DMSO-d_6) δ 8.08 (d, *J* = 7.9 Hz, 1H), 7.66 (t, *J* = 11.0 Hz, 4H), 7.55 (d, *J* = 8.4 Hz, 2H), 7.48 (t, *J* = 7.4 Hz, 1H), 7.36 (d, *J* = 7.9 Hz, 1H), 7.35 – 7.26 (m, 3H), 1.46 (s, 9H). ^{13}C NMR (100 MHz, DMSO-d_6) δ 175.0, 152., 143.4, 140.7, 132.9, 130.5, 130.4, 128.7, 128.6, 128.2, 122.9, 78.3, 30.9. IR(KBr)ν_{max}/cm^{-1} 2933 (C−H), 1133 (C=S), HRMS (ESI):m/z $[M+H]^+$ calcd. for $C_{28}H_{23}Cl_2N_2OS_2$, 537.0623 found 537.0621.

3-(1-(*tert*-butyl)-2,4-bis(4-methoxyphenyl)-1*H*-imidazol-5-yl)-4-hydroxy-2*H*-thiochromene-2-thione (5d) 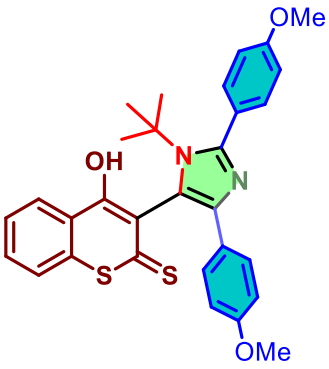

A light brown solid (82 mg, 78%) mp 388-390 °C,^{1}H NMR (400 MHz, Chloroform-*d*) δ 14.58 (s, 1H), 8.09 (d, *J* = 9.0 Hz, 1H), 7.56 (t, *J* = 7.8 Hz, 1H), 7.49 (t, *J* = 7.5 Hz, 1H), 7.38 (d, *J* = 7.6 Hz, 1H), 7.31 (dd, *J* = 17.1, 9.1 Hz, 5H), 7.17 (dd, *J* = 22.2, 7.8 Hz, 2H), 6.86 – 6.76 (m, 1H), 3.87 (s, 3H), 3.59 (s, 3H), 1.54 (s, 9H). ^{13}C NMR (150 MHz, Chloroform-*d*) δ 184.2, 174.8, 158.9, 140.5, 131.7, 130.5, 130.3, 129.9, 129.3, 128.0, 125.7, 123.2, 122.8, 119.3, 116.8, 112.0, 64.0, 55.6, 54.7, 30.5. IR(KBr)ν_{max}/cm^{-1} 2929 (C−H), 1135 (C=S), HRMS (ESI):m/z $[M+H]^+$ calcd. for $C_{30}H_{29}N_2O_3S_2$, 529.1614 found 529.1596.

3-(1-(*tert*-butyl)-2,4-bis(4-fluorophenyl)-1*H*-imidazol-5-yl)-4-hydroxy-2*H*-thiochromene-2-thione (5e) 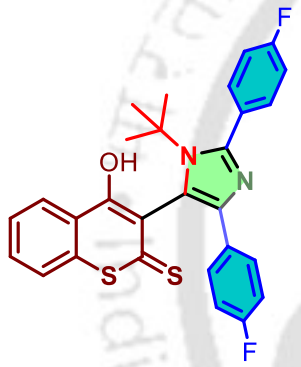

A light yellow solid (80 mg, 80%) mp 372-374 °C,^{1}H NMR (600 MHz, Chloroform-*d*) δ 8.10 (d, *J* = 8.0 Hz, 1H), 7.91 – 7.79 (m, 2H), 7.59 (dd, *J* = 8.8, 5.5 Hz, 2H), 7.55 – 7.46 (m, 3H), 7.38 (d, *J* = 7.8 Hz, 1H), 7.35 – 7.30 (m, 1H), 7.18 (t, *J* = 8.8 Hz, 2H), 1.51 (s, 9H). ^{13}C NMR (100 MHz, Chloroform-*d*) δ 184.28, 174.91, 164.07 (d, *J* = 160.2 Hz), 162.38, 160.83, 142.77, 140.50, 133.68 (d, *J* = 9.0 Hz), 131.64, 130.59, 130.28, 129.54 (d, *J* = 8.3 Hz), 128.78 (d, *J* = 2.3 Hz), 125.86, 122.89 (d, *J* = 10.7 Hz), 122.86, 115.92 (d, *J* = 22.1 Hz), 115.41 (d, *J* = 21.7 Hz), 30.62.IR(KBr)ν_{max}/cm^{-1} 2943 (C−H), 1139 (C=S), HRMS (ESI):m/z $[M+H]^+$ calcd. for $C_{28}H_{23}F_2N_2OS_2$, 505.1214 found 505.1214.

3-(1-(*tert*-butyl)-2,4-diphenyl-1*H*-imidazol-5-yl)-7-fluoro-4-hydroxy-2*H*-thiochromene-2-thione 6 (5f) 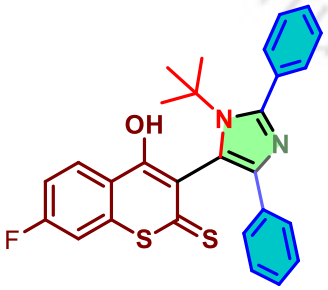

.A yellow solid (84 mg, 87%) mp 383-385 °C,^{1}H NMR (400 MHz, Chloroform-*d*) δ 14.66 (s, 1H), 8.13 (dd, *J* = 8.9, 6.1 Hz, 1H), 7.74 (d, *J* = 7.0 Hz, 2H), 7.67 – 7.61 (m, 2H), 7.55 (dd, *J* = 8.2, 1.3 Hz, 2H), 7.30 (ddd, *J* = 19.5, 10.6, 4.8 Hz, 5H), 7.18 – 7.13 (m, 1H), 1.50 (s, 9H). ^{13}C NMR (100 MHz, DMSO-d_6) δ 183.9, 174.1, 163.1 (d, *J* = 251.1 Hz), 143.8, 142.9, 142.8, 131.2, 131.1, 131.0, 128.6, 128.3, 127.2, 127.1, 122.9, 113.6 (d, *J* = 22.2 Hz), 109.0 (d, *J* = 24.0 Hz),

63.8, 30.6. IR(KBr)ν_{max}/cm^{-1} 2942 (C−H), 1136 (C=S), HRMS (ESI):m/z $[M+H]^+$ calcd. for $C_{28}H_2FN_2OS_2$, 487.1309 found 487.1296.

3-(1-cyclohexyl-2,4-di-*p*-tolyl-1*H*-imidazol-5-yl)-7-fluoro-4-hydroxy-2*H*-thiochromene-2-thione (5g) 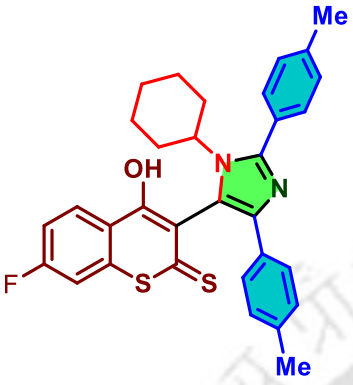

A yellow solid (95 mg, 88%) mp 363-365 °C,^{1}H NMR (600 MHz, Chloroform-*d*) δ 8.12 (dd, *J* = 8.9, 6.0 Hz, 1H), 7.65 (d, *J* = 8.2 Hz, 2H), 7.47 (d, *J* = 8.7 Hz, 2H), 7.33 – 7.31 (m, 1H), 7.19 – 7.14 (m, 3H), 6.86 (d, *J* = 8.6 Hz, 2H), 3.87 (s, 3H), 3.69 (s, 3H), 1.50 (s, 9H).^{13}C NMR (150 MHz, Chloroform-*d*) δ 183.7, 174.1, 163.8, 162.2, 160.2 (d, *J* = 295.1 Hz), 143.4, 142.9 (d, *J* = 9.3 Hz), 132.5, 131.0 (d, *J* = 9.4 Hz), 130.1, 128.6, 127.2, 123.0, 114.0, 113.7, 113.6, 113.5, 108.9 (d, *J* = 24.0 Hz), 55.5, 55.0, 50.9, 30.5. IR(KBr)ν_{max}/cm^{-1} 2925 (C−H), 1135 (C=S), HRMS (ESI):m/z $[M+H]^+$ calcd. for $C_{32}H_{30}FN_2OS_2$, 541.1778 found 529.1606.

3-(1-(*tert*-butyl)-2,4-*bis*(4-methoxyphenyl)-1*H*-imidazol-5-yl)-7-fluoro-2-thioxothioch-roman-4-one(5h) 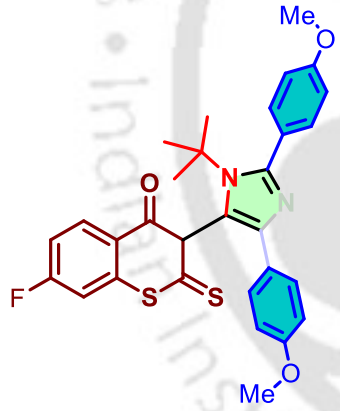

A brown solid (90 mg, 83%) mp 383-385 ^{1}H °C ,NMR (500 MHz, DMSO-d_6) δ 14.34 (s, 1H), 8.16 – 8.09 (m, 1H), 7.66 (d, *J* = 7.8 Hz, 2H), 7.46 (d, *J* = 8.3 Hz, 2H), 7.32 (d, *J* = 9.1 Hz, 1H), 7.16 (t, *J* = 9.8 Hz, 3H), 6.86 (d, *J* = 8.3 Hz, 2H), 3.87 (s, 3H), 3.69 (s, 3H), 1.49 (s, 9H). ^{13}C NMR (150 MHz, Chloroform-*d*) δ 183.7, 174.1, 163.8, 162.2, 160.2 (d, *J* = 294.8 Hz), 143.4, 142.9 (d, *J* = 9.3 Hz), 132.5, 131.0 (d, *J* = 9.6 Hz), 130.1, 128.6, 127.2, 123.0, 114.0, 113.7, 113.6, 113.5, 108.9 (d, *J* = 24.2 Hz), 55.5, 55.08, 50.9, 30.5. IR(KBr)ν_{max}/cm^{-1} 2931 (C−H), 1132 (C=S), HRMS (ESI):m/z $[M+H]^+$ calcd. for $C_{30}H_{28}FN_2O_3S_2$, 547.1520 found 547.1513.

3-(1-(*tert*-butyl)-2,4-diphenyl-1*H*-imidazol-5-yl)-6-chloro-4-hydroxy-2*H*-thiochromene-2-thione. (5i)

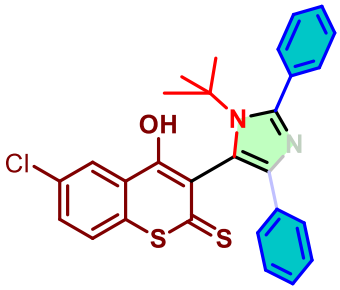

A light yellow solid (80 mg, 80%) mp 303-305 °C , ^{1}H NMR (400 MHz, Chloroform-*d*) δ 8.00 (d, *J* = 2.3 Hz, 1H), 7.61 (d, *J* = 7.1 Hz, 2H), 7.53 (dd, *J* = 9.5, 5.1 Hz, 5H), 7.51 – 7.48 (m, 1H), 7.42 (d, *J* = 8.5 Hz, 1H), 7.22 – 7.11 (m, 3H), 1.45 (s, 9H). ^{13}C NMR (100 MHz, DMSO-d_6) δ 173.8, 167.8, 133.3, 132.5, 131.3, 130.5, 129.7, 129.0, 128.6, 128.3, 127.6, 127.1, 125.3, 51.5, 31.3. IR(KBr)ν_{max}/cm^{-1} 2943 (C−H), 1139 (C=S), HRMS (ESI):m/z [M+H]$^{+}$ calcd. for $C_{26}H_{24}ClN_2OS_2$, 503.1013 found 503.1001.

3-(1-(*tert*-butyl)-2,4-diphenyl-1*H*-imidazol-5-yl)-4-hydroxy-6-(trifluoromethyl)-2*H*-thiochromene-2-thione (5j).

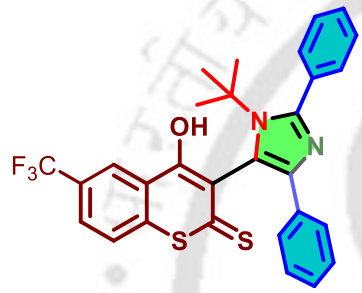

A brownish crystalline solid (75 mg, 70%) mp 393-395 °C,^{1}H NMR (400 MHz, DMSO-d_6) δ 8.64 (s, 1H), 8.24 (d, *J* = 8.6 Hz, 2H), 8.15 (dd, *J* = 8.5, 1.9 Hz, 2H), 7.89 – 7.85 (m, 1H), 7.41 – 7.30 (m, 2H), 7.26 – 7.17 (m, 4H), 6.92 (s, 1H), 1.20 (s, 9H).IR(KBr)ν_{max}/cm^{-1} 2943 (C−H), 1143 (C=S), HRMS (ESI):m/z [M+H]$^{+}$ calcd. for $C_{29}H_{24}F_3N_2OS_2$, 537.1277 found 537.1254.Because of very low solubility ^{13}C was not able to record.

3-(1-(*tert*-butyl)-2,4-di(naphthalen-2-yl)-1*H*-imidazol-5-yl)-4-hydroxy-2*H*-thiochromene-2-thione (5k).

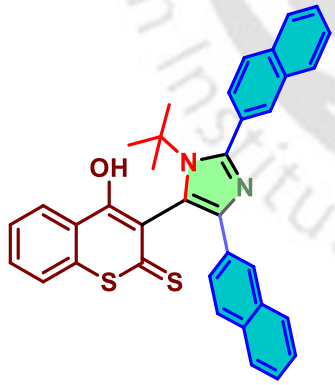

A yellow solid (97 mg, 86%) mp 378-380 °C,^{1}H NMR (600 MHz, Chloroform-*d*) δ 8.45 (s, 1H), 8.23 – 8.08 (m, 5H), 7.84 (dd, *J* = 22.1, 7.0 Hz, 3H), 7.77 – 7.67 (m, 4H), 7.52 – 7.44 (m, 3H), 7.40 (d, *J* = 7.8 Hz, 1H), 7.32 (t, *J* = 7.2 Hz, 1H), 1.58 (s, 9H). ^{13}C NMR (150 MHz, Chloroform-*d*) δ 184.3, 175.0, 172.4, 143.9, 140.5, 133.4, 132.5, 132.3, 131.8, 131.2, 130.5, 130.3, 128.5, 128.1, 128.0, 127.8, 127.6, 127.5, 127.3, 126.5, 125.7, 124.8, 122.8, 64.3, 30.8. IR(KBr)ν_{max}/cm^{-1} 2925 (C−H), 1133 (C=S), HRMS (ESI):m/z [M+H]$^{+}$ calcd. for $C_{36}H_{29}N_2OS_2$, 569.1716 found 569.1710.

3-(1-(*tert*-butyl)-2,4-di(naphthalen-2-yl)-1*H*-imidazol-5-yl)-7-chloro-4-hydroxy-2*H*-thiochromene-2-thione (5l). 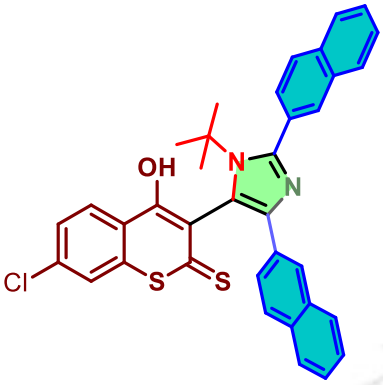

A yellow solid (102 mg, 85%) mp 380-382 °C,^{1}H NMR (500 MHz, Chloroform-*d*) δ 9.55 (s, 1H), 8.93 (s, 1H), 8.61 (s, 1H), 8.54 – 8.41 (m, 1H), 8.13 – 7.97 (m, 4H), 7.85 (dd, *J* = 29.8, 7.0 Hz, 3H), 7.63 – 7.52 (m, 4H), 7.34 (d, *J* = 7.4 Hz, 1H), 7.07 (d, *J* = 34.4 Hz, 1H), 1.58 (s, 9H). ^{13}C NMR (125 MHz, Chloroform-*d*) δ 189.3, 178.9, 174.5, 147.4, 142.8, 141.2, 139.3, 138.5, 137.7, 137.4, 136.7, 135.0, 133.8, 133.7, 133.0, 132.8, 132.4, 131.9, 131.7, 131.4, 129.7, 127.1, 71.0, 30.8 .IR(KBr)ν_{max}/cm^{-1} 2930 (C− H), 1129 (C=S), HRMS (ESI):m/z $[M+H]^+$ calcd. for $C_{36}H_{28}ClN_2OS_2$, 603.1326 found 603.1304.

3-(1-(tert-butyl)-2,4-di(naphthalen-2-yl)-1H-imidazol-5-yl)-7-fluoro-4-hydroxy-2H-thiochromene-2-thione (5m). 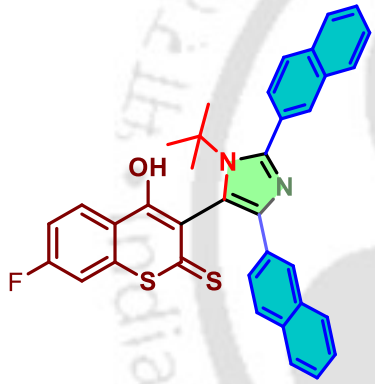

A yellow solid (94 mg, 88%) mp 369-371 °C, ^{1}H NMR (400 MHz, DMSO-d_6) δ 14.92 (s, 1H), 8.46 (s, 1H), 8.22 – 8.11 (m, 4H), 7.84 (d, *J* = 8.8 Hz, 2H), 7.76 – 7.66 (m, 4H), 7.48 (dd, *J* = 6.1, 3.3 Hz, 2H), 7.35 (dd, *J* = 9.1, 2.5 Hz, 2H), 7.16 (td, *J* = 8.7, 2.5 Hz, 2H), 1.58 (s, 9H). ^{13}C NMR (100 MHz, DMSO) δ 184.7, 174.7, 164.8, 162.3, 144.4, 143.3, 143.2, 133.9, 132.9, 132.9, 131.7, 131.5, 131.4, 129.0, 128.8, 128.7, 128.3, 128.2, 127.9, 127.6, 127.6, 127.2, 127.0, 125.2, 114.2, 114.0, 109.5, 109.3, 31.1. IR(KBr)ν_{max}/cm^{-1} 2939 (C−H), 1137 (C=S), HRMS (ESI):m/z $[M+H]^+$ calcd. for $C_{36}H_{28}FN_2OS_2$, 587.1622 found 158.1617.

3-(1-cyclohexyl-2,4-diphenyl-1*H*-imidazol-5-yl)-2-thioxothiochroman-4-one (5n) 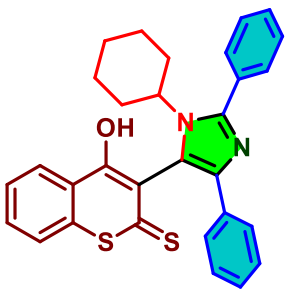

A yellow solid (95 mg, 97%) mp 306-308 °C**,** ^{1}H NMR (400 MHz, Chloroform-*d*) δ 8.09 (dd, *J* = 8.0, 1.1 Hz, 1H), 7.83 – 7.76 (m, 2H), 7.72 (dd, *J* = 14.9, 7.3 Hz, 3H), 7.65 – 7.60 (m, 2H), 7.54 – 7.48 (m, 1H), 7.42 (d, *J* = 7.3 Hz, 1H), 7.34 (qd, *J* = 6.2, 5.2, 3.3 Hz, 3H), 7.28 (t, *J* = 7.3 Hz, 1H), 4.03 – 3.89 (m, 1H), 1.99 (dd, *J* = 22.9, 11.7 Hz, 2H), 1.68 – 1.53 (m, 3H), 1.37 (q, *J* = 13.4, 12.4 Hz, 2H), 0.96 (dq, *J* = 23.6, 11.5, 10.0 Hz, 2H), 0.66 (q, *J* = 13.0 Hz, 1H). ^{13}C NMR (100 MHz,

Chloroform-*d*) δ 185.4, 174.4, 142.8, 140.4, 131.8, 131.1, 131.1, 130.6, 130.2, 129.0, 128.6, 128.3, 128.0, 126.5, 125.9, 123.0, 59.1, 32.6, 32.1, 25.8, 25.6, 24.6. IR(KBr)ν_{max}/cm^{-1} 2933 (C−H), 1133 (C=S), HRMS (ESI):m/z $[M+H]^+$ calcd. for $C_{30}H_{27}N_2OS_2$, 495.1559 found 497.1715.

3-(1-cyclohexyl-2,4-di-*p*-tolyl-1*H*-imidazol-5-yl)-4-hydroxy-2*H*-thiochromene-2-thione

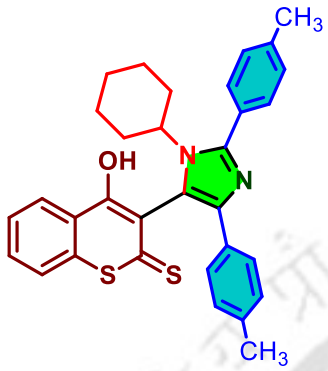

(5o), A brownish crystalline solid (98 mg, 94%) mp 393-395 °C,^{1}H NMR (400 MHz, Chloroform-*d*) δ 14.53 (s, 1H), 8.08 (dd, *J* = 8.0, 1.5 Hz, 1H), 7.65 (d, *J* = 7.9 Hz, 2H), 7.55 – 7.46 (m, 5H), 7.43 – 7.38 (m, 1H), 7.36 – 7.30 (m, 1H), 7.15 (d, *J* = 8.0 Hz, 2H), 3.96 (tt, *J* = 12.4, 3.4 Hz, 1H), 2.46 (s, 3H), 2.24 (s, 3H), 1.98 (dd, *J* = 18.8, 12.7 Hz, 2H), 1.71 – 1.53 (m, 3H), 1.40 (dq, *J* = 12.7, 8.8, 6.4 Hz, 2H), 0.97 (dddd, *J* = 26.3, 16.3, 12.7, 9.3 Hz, 2H), 0.77 – 0.61 (m, 1H). ^{13}C NMR (100 MHz, Chloroform-*d*) δ 185.4, 174.4, 142.6, 141.8, 140.4, 138.0, 130.7, 130.6, 130.5, 130.2, 129.6, 129.2, 128.7, 128.0, 126.5, 125.9, 125.5, 123.0, 122.3, 118.5, 59.1, 32.5, 32.0, 25.8, 25.6, 24.6, 21.1, 20.8. IR(KBr)ν_{max}/cm^{-1} 2943 (C−H), 1143 (C=S), HRMS (ESI):m/z $[M+H]^+$ calcd. for $C_{32}H_{31}N_2OS_2$, 523.1872 found 523.1872.

3-(1-cyclohexyl-2,4-*bis*(4-methoxyphenyl)-1*H*-imidazol-5-yl)-4-hydroxy-2*H*-thiochromene-2-thione (5p), A brownish crystalline solid (99 mg, 90%) mp 332-334 °C, ^{1}H NMR (400 MHz, DMSO-d_6) δ 8.08 (d, *J* = 8.0 Hz, 1H), 7.67 (d, *J* = 8.5 Hz, 2H), 7.52 (dd, *J* = 8.8, 6.8 Hz, 3H), 7.40 (d, *J* = 7.8 Hz, 1H), 7.33 (t, *J* = 7.5 Hz, 1H), 7.21 (d, *J* = 8.7 Hz, 2H), 6.90 (d, *J* = 8.8 Hz, 2H), 3.94 (m, 5.5 Hz, 1H), 3.88 (s, 3H), 3.70 (s, 3H), 2.05 – 1.90 (m, 2H), 1.71 – 1.53 (m, 3H), 1.41 (d, *J* = 11.4 Hz, 2H), 1.08 – 0.87 (m, 2H), 0.69 (dt, *J* = 13.4, 3.5 Hz, 1H). ^{13}C NMR (125 MHz, DMSO-d_6) δ 185.3, 174.5, 161.5, 159.2, 142.5, 140.5, 132.2, 130.6, 130.3, 129.8, 128.1, 127.9, 123.0, 118.9, 114.4, 114.0, 59.0, 55.6, 55.1, 32.1, 25.8, 25.7, 24.7. IR(KBr)ν_{max}/cm^{-1} 2932 (C− H), 1133 (C=S), HRMS (ESI):m/z $[M+H]^+$ calcd. for $C_{32}H_{31}N_2O_3S_2$, 555.1771 found 555.1770.

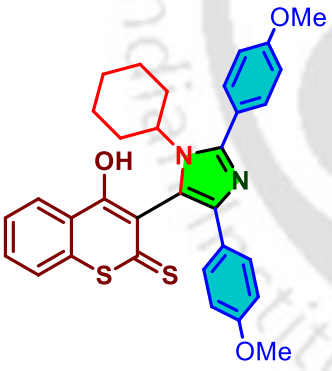

3-(1-cyclohexyl-2,4-bis(3-methoxyphenyl)-1*H*-imidazol-5-yl)-4-hydroxy-2*H*-thiochrom-ene -2-thione (5q), 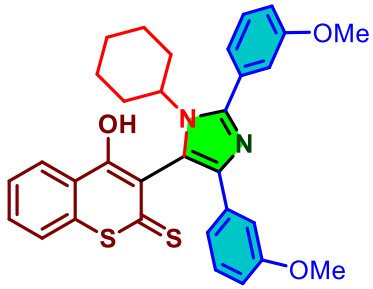

A light yellow crystalline solid (106 mg, 96%) mp 314-316 °C , ^{1}H NMR (400 MHz, Chloroform-*d*) δ 14.57 (s, 1H), 8.13 – 8.05 (m, 1H), 7.60 (t, *J* = 8.1 Hz, 1H), 7.54 – 7.48 (m, 1H), 7.42 (d, *J* = 7.3 Hz, 1H), 7.38 – 7.27 (m, 5H), 7.26 – 7.19 (m, 2H), 6.83 (d, *J* = 6.6 Hz, 1H), 3.99 (t, *J* = 12.3 Hz, 1H), 3.88 (s, 3H), 3.61 (s, 3H), 2.00 (dd, *J* = 21.7, 12.4 Hz, 2H), 1.64 (dd, *J* = 25.4, 14.9 Hz, 3H), 1.42 (d, *J* = 12.2 Hz, 2H), 0.98 (dq, *J* = 26.7, 16.0, 14.0 Hz, 2H), 0.70 (q, *J* = 16.1 Hz, 1H). ^{13}C NMR (100 MHz, DMSO-d_6) δ 185.47, 174.62, 159.31, 142.65, 140.48, 131.27, 130.78, 130.42, 130.29, 129.76, 128.11, 126.08, 123.16, 122.83, 118.76, 117.76, 115.91, 114.53, 111.67, 59.36, 55.76, 54.89, 32.61, 32.12, 25.88, 25.75, 24.78. IR(KBr)ν_{max}/cm^{-1} 2927 (C−H), 1139 (C=S), HRMS (ESI):m/z $[M+H]^+$ calcd. for $C_{32}H_{31}N_2O_3S_2$, 555.1771 found 555.1767.

3-(2,4-*bis*(4-chlorophenyl)-1-cyclohexyl-1*H*-imidazol-5-yl)-4-hydroxy-2*H*-thiochromene-2-thione (5r), 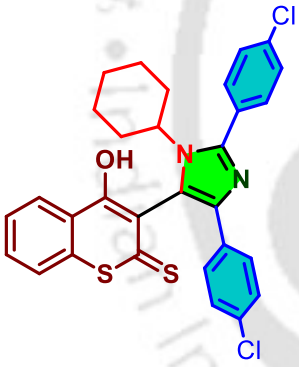

A yellow crystalline solid (91 mg, 102%) mp 323-326 °C, ^{1}H NMR (500 MHz, Chloroform-*d*) δ 8.09 (d, *J* = 7.9 Hz, 1H), 7.82 (d, *J* = 7.0 Hz, 2H), 7.75 (d, *J* = 8.1 Hz, 2H), 7.61 (d, *J* = 8.2 Hz, 2H), 7.51 (t, *J* = 7.5 Hz, 1H), 7.43 (t, *J* = 8.4 Hz, 3H), 7.34 (t, *J* = 7.5 Hz, 1H), 3.95 (t, *J* = 11.7 Hz, 1H), 1.97 (dd, *J* = 26.4, 11.0 Hz, 2H), 1.59 (d, *J* = 10.9 Hz, 3H), 1.38 (q, *J* = 12.7, 12.2 Hz, 2H), 0.98 (dq, *J* = 27.0, 12.8 Hz, 2H), 0.70 (q, *J* = 12.5 Hz, 1H). ^{13}C NMR (126 MHz, Chloroform-*d*) δ 185.5, 174.5, 142.1, 140.4, 136.6, 133.0, 132.5, 131.6, 130.7, 130.2, 129.2, 128.7, 128.2, 128.1, 126.0, 123.1, 118.5, 59.2, 39.5, 32.6, 25.8, 25.7, 24.7. IR(KBr)ν_{max}/cm^{-1} 2934 (C− H), 1140 (C=S), HRMS (ESI):m/z $[M+H]^+$ calcd. for $C_{30}H_{25}Cl_2N_2O_3S_2$, 563.0780 found 563.0780.

3-(2,4-*bis*(3-chlorophenyl)-1-cyclohexyl-1*H*-imidazol-5-yl)-4-hydroxy-2*H*-thiochromene-2-thione (5s)

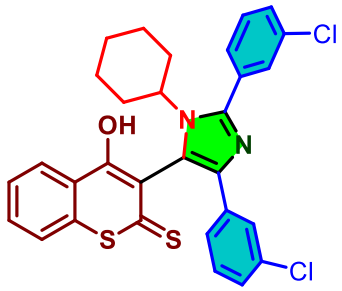

A yellow solid (110 mg, 98%) mp 369-371 °C, ^{1}H NMR (500 MHz, Chloroform-*d*) δ 8.09 (d, *J* = 7.7 Hz, 1H), 7.87 (s, 2H), 7.64 (s, 2H), 7.53 (q, *J* = 9.9, 9.3 Hz, 3H), 7.42 (d, *J* = 7.7 Hz, 1H), 7.34 (t, *J* = 7.2 Hz, 1H), 7.23 (t, *J* = 8.6 Hz, 2H), 3.94 (t, *J* = 11.6 Hz, 1H), 1.98 (dd, *J* = 32.8, 10.6 Hz, 2H), 1.59 (d, *J* = 11.5 Hz, 3H), 1.36 (dt, *J* = 24.4, 12.7 Hz, 2H), 1.10 – 0.87 (m, 2H), 0.69 (q, *J* = 12.2 Hz, 1H). ^{13}C NMR (125 MHz, Chloroform-*d*) δ 185.7, 174.6, 164.9, 163.1, 162.9, 161.1, 141.9, 140.4, 133.5, 133.4, 131.1, 130.8, 130.2, 128.9, 128.8, 128.3, 128.1, 126.0, 123.1, 121.8, 118.3, 116.4, 116.2, 115.8, 115.6, 59.3, 32.6, 32.2, 25.8, 25.7, 24.7. IR(KBr)ν_{max}/cm^{-1} 2937 (C− H), 1135 (C=S), HRMS (ESI):m/z $[M+H]^+$ calcd. for $C_{30}H_{25}Cl_2N_2O_3S_2$, 563.0780 found 563.0768.

3-(1-cyclohexyl-2,4-*bis*(3-hydroxyphenyl)-1*H*-imidazol-5-yl)-4-hydroxy-2*H*-thiochromene-2-thione (5t)

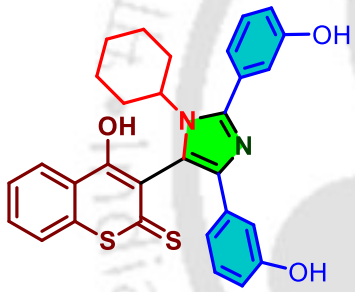

A yellow solid (93 mg, 89%) mp 336-338 °C, ^{1}H NMR (500 MHz, DMSO-d_6) δ 14.55 (s, 1H), 10.21 (s, 1H), 9.57 (s, 1H), 8.09 (d, *J* = 7.7 Hz, 1H), 7.56 – 7.27 (m, 4H), 7.24 – 6.94 (m, 6H), 6.69 (s, 1H), 4.00 – 3.90 (m, 1H), 2.00 – 1.89 (m, 2H), 1.65 (dd, *J* = 43.5, 11.6 Hz, 3H), 1.43 (d, *J* = 11.2 Hz, 2H), 1.29 – 1.18 (m, 1H), 1.02 – 0.92 (m, 1H), 0.71 (q, *J* = 11.9, 11.5 Hz, 1H). ^{13}C NMR (125 MHz, Chloroform-*d*) δ ^{13}C NMR (101 MHz, DMSO) δ 185.3, 174.4, 157.5, 157.3, 157.2, 152.7, 142.6, 140.5, 130.9, 130.6, 130.3, 129.5, 128.0, 125.9, 123.0, 121.1, 118.9, 117.3, 117.0, 113.6, 59.2, 32.5, 31.9, 30.8, 25.7, 24.6. IR(KBr)ν_{max}/cm^{-1} 2929 (C− H), 1133 (C=S), HRMS (ESI):m/z $[M+H]^+$ calcd. for $C_{30}H_{27}N_2O_3S_2$, 527.1458 found 527.1445.

7-chloro-3-(1-cyclohexyl-2,4-diphenyl-1*H*-imidazol-5-yl)-2-thioxothio chroman-4-one. (5u)

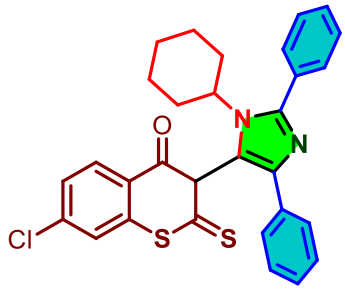

A pale yellow solid (91 mg, 87%) mp 336-338 °C, ^{1}H NMR (500 MHz, Chloroform-*d*) δ 8.08 (d, *J* = 8.0 Hz, 1H), 7.82 – 7.70 (m, 4H), 7.61 (d, *J* = 8.3 Hz, 2H), 7.51 (t, *J* = 7.6 Hz, 1H), 7.40 (t, *J* = 6.2 Hz, 3H), 7.33 (t, *J* = 8.1 Hz, 2H), 3.93 (t, *J* = 12.6 Hz, 1H), 1.96 (dd, *J* = 20.5, 12.4 Hz, 2H), 1.61 (q, *J* = 12.1, 10.0 Hz,

3H), 1.40 (t, *J* = 12.0 Hz, 2H), 0.98 (dd, *J* = 30.2, 14.0 Hz, 2H), 0.71 (q, *J* = 13.3 Hz, 1H). ^{13}C NMR (126 MHz, Chloroform-*d*) δ 185.1, 174.4, 142.1, 140.4, 132.4, 131.5, 131.0, 130.5, 130.2, 129.0, 128.5, 128.0, 127.8, 127.5, 127.1, 125.8, 123.0, 59.0, 32.5, 32.2, 25.8, 25.6, 24.6. IR(KBr)ν_{max}/cm^{-1} 2929 (C− H), 1137 (C=S), HRMS (ESI):m/z [M+H]$^+$ calcd. for $C_{30}H_{26}ClN_2OS_2$, 529.1170 found 529.1170.

3-(1-cyclohexyl-2,4-di-*p*-tolyl-1*H*-imidazol-5-yl)-7-fluoro-4-hydroxy-2*H*-thiochromene-2-thione (5v) A golden yellow solid (98 mg, 91%) mp 316-318 °C, ^{1}H NMR (400 MHz, Chloroform-*d*) δ 8.10 (dd, *J* = 8.9, 6.0 Hz, 1H), 7.58 (d, *J* = 7.6 Hz, 2H), 7.46 (dd, *J* = 17.7, 7.8 Hz, 4H), 7.33 (dd, *J* = 9.2, 2.6 Hz, 1H), 7.19 – 7.00 (m, 4H), 3.90 (s, 1H), 2.44 (s, 3H), 2.23 (s, 3H), 1.93 (s, 2H), 1.70 – 1.51 (m, 3H), 1.49 – 1.36 (m, 2H), 1.07 – 0.88 (m, 2H), 0.69 (q, *J* = 13.3 Hz, 1H). ^{13}C NMR (126 MHz, DMSO) δ 195.7, 185.4, 173.8, 163 (d, *J* = 251.2 Hz, 1C), 162.2, 142.8, 142.1, 138.3, 131.1, 130.6, 130.3, 129.7, 129.3, 128.8 (d, *J* = 3 Hz, 1C), 127.1, 126.6, 125.2, 118.3, 114.0 (d, *J* = 23.7 Hz, 1C), 109.2 (d, *J* = 23.7 Hz, 1C), 59.3, 32.6, 32.1, 25.8, 25.7, 24.7, 21.2, 20.8. IR(KBr)ν_{max}/cm^{-1} 2927 (C− H), 1135 (C=S), HRMS (ESI):m/z [M+H]$^+$ calcd. for $C_{32}H_{30}FN_2OS_2$, 541.1778 found 541.1710.

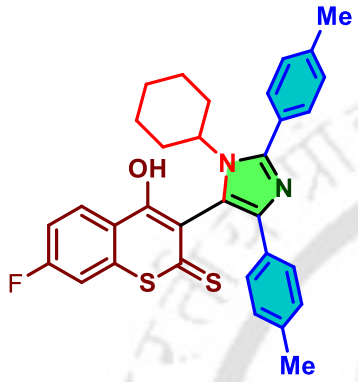

3-(1-cyclohexyl-2,4-di(naphthalen-2-yl)-1H-imidazol-5-yl)-4-hydroxy-2H-thiochromene-2-thione (5x). A orange solid (103 mg, 87%) mp 356-358 °C, ^{1}H NMR (400 MHz, DMSO-d_6) δ 14.98 (s, 1H), 8.53 (s, 1H), 8.24 (t, *J* = 12.6 Hz, 3H), 8.13 (dd, *J* = 10.5, 7.6 Hz, 2H), 7.94 – 7.82 (m, 3H), 7.81 – 7.70 (m, 4H), 7.51 (dd, *J* = 6.3, 3.2 Hz, 3H), 7.45 (d, *J* = 7.5 Hz, 1H), 7.35 (t, *J* = 7.9 Hz, 1H), 4.11 (t, *J* = 12.3 Hz, 1H), 2.10 (t, *J* = 11.3 Hz, 2H), 1.83 – 1.68 (m, 1H), 1.59 (t, *J* = 13.4 Hz, 2H), 1.48 (d, *J* = 12.3 Hz, 1H), 1.38 (d, *J* = 12.7 Hz, 1H), 1.00 (dd, *J* = 21.8, 12.8 Hz, 2H), 0.64 (q, *J* = 13.1 Hz, 1H). ^{13}C NMR (101 MHz, DMSO-d_6) δ 185.7, 142.9, 140.4, 133.7, 132.0, 131.9, 131.3, 130.6, 130.2, 128.7, 128.5, 128.2, 128.0, 127.9, 127.9, 127.6, 127.6, 126.4, 125.9, 124.1, 123.0, 118.4, 59.4, 25.7, 25.6, 24.6. . IR(KBr)ν_{max}/cm^{-1} 2926

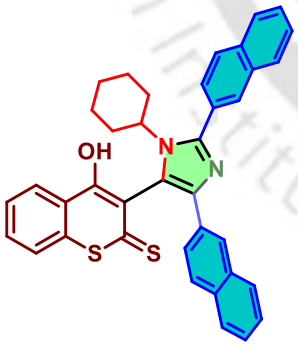

(C−H), 1143 (C=S), HRMS (ESI):m/z $[M+H]^+$ calcd. for $C_{38}H_{40}N_2OS_2$, 595.1873 found 595.1853.

7-chloro-3-(1-cyclohexyl-2,4-di(naphthalen-2-yl)-1H-imidazol-5-yl)-4-hydroxy-2H-thio chromene-2-thione (5x) A orange solid (111 mg, 98%) mp 366-368 °C, ^{1}H NMR (400 MHz, Chloroform-*d*) δ 8.50 (s, 1H), 8.22 (t, *J* = 12.3 Hz, 3H), 8.12 (t, *J* = 8.0 Hz, 2H), 7.93 – 7.81 (m, 3H), 7.79 – 7.68 (m, 4H), 7.54 – 7.42 (m, 4H), 7.36 – 7.31 (m, 1H), 4.09 (t, *J* = 11.6 Hz, 1H), 2.07 (d, *J* = 8.8 Hz, 2H), 1.75 (q, *J* = 11.1, 9.7 Hz, 1H), 1.65 – 1.33 (m, 4H), 0.98 (dq, *J* = 25.4, 12.8 Hz, 2H), 0.65 (t, *J* = 12.8 Hz, 1H). ^{13}C NMR (101 MHz, Chloroform-*d*) δ 174.62, 140.47, 133.72, 132.63, 132.11, 130.64, 130.60, 130.32, 128.72, 128.16, 128.07, 127.98, 127.92, 127.61, 126.71, 126.56, 125.93, 124.25, 123.08, 59.32 (d, *J* = 1.6 Hz), 32.66, 32.21, 25.79, 25.68, 24.67. IR(KBr)ν_{max}/cm^{-1} 2927 (C−H), 1133 (C=S), HRMS (ESI):m/z $[M+H]^+$ calcd. for $C_{38}H_{39}ClN_2OS_2$, 629.1483 found 629.1450.

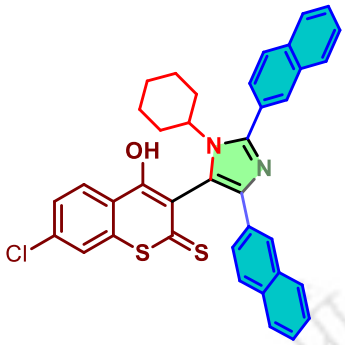

3-(1-cyclohexyl-2,4-di(naphthalen-2-yl)-1*H*-imidazol-5-yl)-7-fluoro-4-hydroxy-2*H*-thio chromene-2-thione (5y). A yellow solid (110 mg, 90%) mp 306-308 °C,^{1}H NMR (500 MHz, Chloroform-*d*) δ 15.06 (s, 1H), 8.48 (s, 1H), 8.21 (d, *J* = 14.2 Hz, 2H), 8.18 – 8.09 (m, 2H), 7.87 (q, *J* = 7.8, 7.3 Hz, 3H), 7.73 (dt, *J* = 22.8, 7.4 Hz, 4H), 7.54 – 7.46 (m, 2H), 7.38 (t, *J* = 10.2 Hz, 1H), 7.29 – 7.13 (m, 2H), 4.22 – 3.90 (m, 1H), 2.06 (d, *J* = 12.6 Hz, 2H), 1.74 (q, *J* = 12.9 Hz, 1H), 1.58 (t, *J* = 16.7 Hz, 2H), 1.46 (q, *J* = 12.5 Hz, 1H), 1.38 (d, *J* = 12.8 Hz, 1H), 0.99 (dq, *J* = 26.0, 13.3 Hz, 2H), 0.72 – 0.58 (m, 1H). ^{13}C NMR (101 MHz, Chloroform-*d*) δ 173.8, 163.1 (d, *J* = 251.0 Hz), 143.2, 142.8 (d, *J* = 9.2 Hz), 133.7, 132.6, 132.4, 132.1, 131.4, 131.2, 131.0, 130.9, 128.7, 128.4, 128.1, 127.9, 127.6, 127.1, 126.7, 126.5, 125.8, 124.2, 113.7 (d, *J* = 23.6 Hz), 109.2 (d, *J* = 23.5 Hz), 59.4, 32.6, 32.2, 25.7, 25.6, 24.6. IR(KBr)ν_{max}/cm^{-1} 2929 (C−H), 1137 (C=S), HRMS (ESI):m/z $[M+H]^+$ calcd. For $C_{38}H_{39}FN_2OS_2$, 613.1778 Found 613.1778.

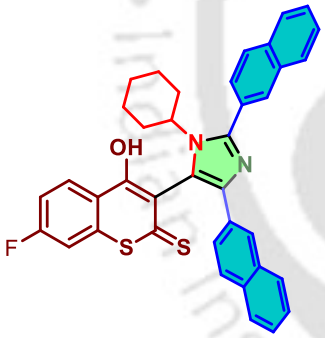

3-(2,4-diphenyl-1-(2,4,4-trimethylpentan-2-yl)-1H-imidazol-5-yl)-2-thioxothio chroman-4-one (5z) 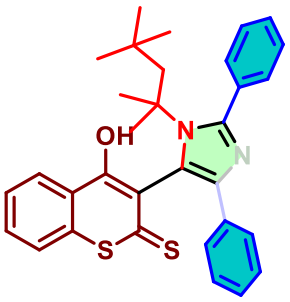

A orange solid (85 mg, 82%) mp 361-363 °C ^{1}H NMR (400 MHz, DMSO-d_6) δ 8.10 (d, J = 7.7 Hz, 1H), 7.76 – 7.71 (m, 2H), 7.69 – 7.64 (m, 2H), 7.61 – 7.53 (m, 3H), 7.50 – 7.46 (m, 1H), 7.38 (t, J = 8.1 Hz, 1H), 7.34 – 7.30 (m, 2H), 7.27 (d, J = 7.5 Hz, 2H), 2.21 (d, J = 14.9 Hz, 1H), 1.96 (d, J = 14.9 Hz, 1H), 1.59 (d, J = 13.0 Hz, 6H), 0.82 (s, 9H). ^{13}C NMR (126 MHz, DMSO-d_6) δ 184.54, 175.43, 174.43, 144.09, 141.00, 131.49, 130.92, 130.89, 129.74, 129.06, 128.80, 128.68, 128.56, 127.78, 126.85, 126.25, 123.33, 123.27, 54.16, 31.82, 31.30, 30.57, 30.02. IR(KBr)ν_{max}/cm^{-1} 2937 (C− H), 1142 (C=S), HRMS (ESI):m/z [M+H]$^{+}$ calcd. for $C_{32}H_{33}N_2OS_2$, 525.2029 found 525.2021.

3-(2,4-bis(4-bromophenyl)-1-(tert-butyl)-1H-imidazol-5-yl)-4-hydroxy-2H-thiochrom-ene-2-thione (5a′). 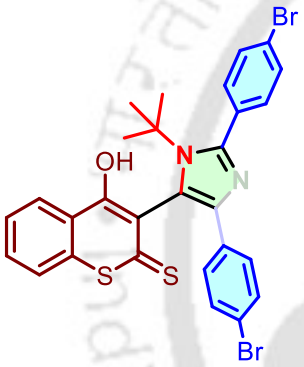

A yellow solid (91 mg, 82%) mp 351-353 °C,^{1}H NMR (400 MHz, Chloroform-d) δ 14.94 (s, 1H), 8.10 (d, J = 8.6 Hz, 1H), 7.86 (d, J = 8.4 Hz, 2H), 7.73 (d, J = 8.3 Hz, 2H), 7.51 (q, J = 8.8 Hz, 5H), 7.41 – 7.29 (m, 2H), 1.51 (s, 9H). ^{13}C NMR (126 MHz, DMSO) δ 184.3, 174.8, 142.8, 140.4, 133.0, 132.2, 131.7, 131.3, 130.5, 130.2, 129.3, 128.8, 128.1, 125.8, 125.1, 122.9, 122.5, 121.9, 64.0, 30.6. IR(KBr)ν_{max}/cm^{-1} 2924 (C− H), 1136 (C=S), HRMS (ESI):m/z [M+H]$^{+}$ calcd. for $C_{24}H_{23}N_4OS_2$, 624.9613 found 624.9590 and 626.9573.

7-chloro-3-(1-cyclohexyl-2,4-diphenyl-1*H*-imidazol-5-yl)-4-hydroxy-2*H*-thiochrome-ne-2-thione (5b′). 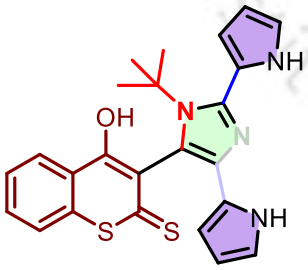

A yellow solid (91 mg, 82%) mp 321-323 °C, ^{1}H NMR (400 MHz, DMSO-d_6) δ 14.67 (s, 1H), 8.35 – 8.28 (m, 1H), 8.15 – 8.07 (m, 1H), 7.90 (dd, J = 4.9, 3.0 Hz, 1H), 7.72 – 7.66 (m, 1H), 7.58 – 7.54 (m, 1H), 7.50 (tt, J = 4.1, 2.0 Hz, 2H), 7.41 (d, J = 7.6 Hz, 1H), 7.38 – 7.31 (m, 1H), 7.30 – 7.25 (m, 1H), 1.54 (s, 9H).^{13}C NMR (101 MHz, DMSO) δ 183.8, 174.6, 140.4, 138.9, 131.8, 131.3, 130.6, 130.2, 129.8, 128.9, 128.5, 128.0, 127.7, 126.6, 125.9, 125.8, 125.5, 123.0, 122.9, 63.9, 30.1. IR(KBr)ν_{max}/cm^{-1} 2924 (C− H), 1136 (C=S), HRMS (ESI):m/z [M+H]$^{+}$ calcd. for $C_{24}H_{23}N_4OS_2$, 447.1308 found 447.1308.

Figure 8. Single Crystal XRD data of Compounds **5b**, **5g,** and **5o.**

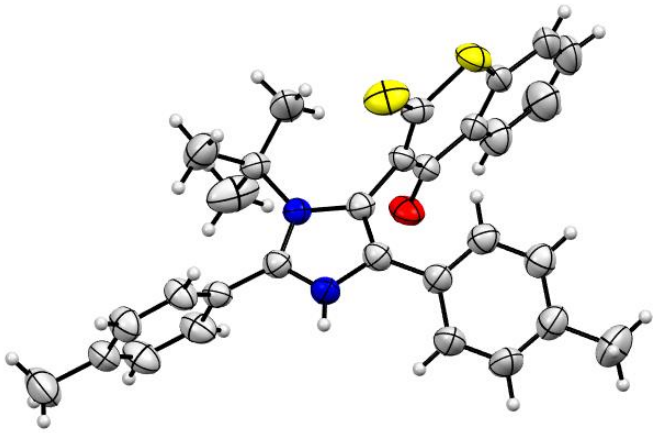

ORTEP Diagram of compound **5b** with CCDC number 2488799.

Entry	Identification Code	Compound 5b
01	Empirical formula	$C_{30}H28\,N_2OS_2$
02	Formula weight	496.66
03	Temperature	295 K
04	Wavelength	0.71073
05	Crystal system	Triclinic
06	Space group	p-1
07	Cell length	a 9.5477 (3) b 14.3505 (9) c 21.3607 (13)
08	Cell angle	α 103.134 (2) β 100.471 (2) γ 105.051 (2)
9	Cell volume	2660.7 (3)
10	Density	1.240 g/cm^3
11	Completeness to theta	0.997
12	Index ranges	h = 12 k = 18 l = 27
13	Theta (Max)	27.148
14	Cell formula units Z	4
15	CCDC no	2488799

Figure 9. Single Crystal XRD data of Compounds **5g**

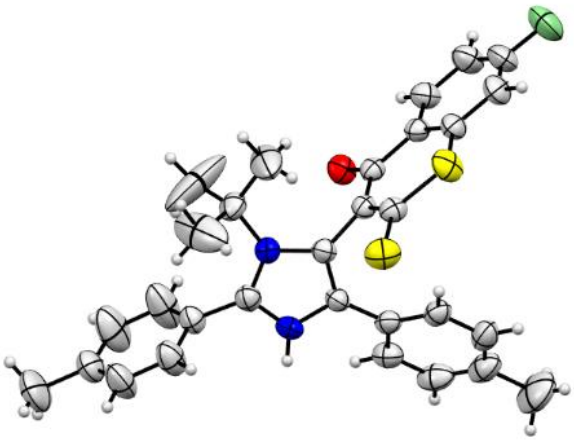

ORTEP Diagram of compound **5g** with CCDC number 2488801

Entry	Identification Code	Compound 5g
01	Empirical formula	$C_{32}H_{30}N_2OS_2$
02	Formula weight	522.70
03	Temperature	296 K
04	Wavelength	0.71073
05	Crystal system	Monoclinic
06	Space group	C 1 2/C1
07	Cell length	a 27.695 (11) b 9.440 (3) c 23.384 (9)
08	Cell angle	α 90 β 170.081 (18) γ 90
09	Cell volume	5443 (4)
10	Density	1.276
11	Completeness to theta	0.991
12	Index ranges	h = 32 k = 11 l = 27
13	Theta (Max)	24.999
14	Cell formula units Z	8
15	CCDC no	2488801

Figure 10. Single Crystal XRD data of Compounds **5o**

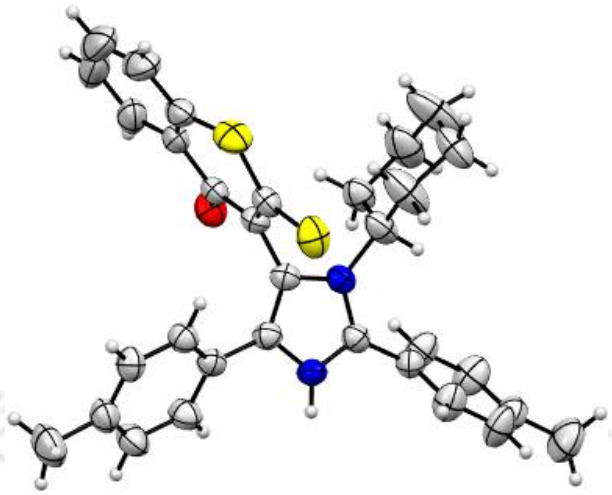

ORTEP Diagram of compound **5o** with CCDC number 2488804.

Entry	Identification Code	Compound 5o
01	Empirical formula	$C_{30}H27FN_2OS_2$
02	Formula weight	514.66
03	Temperature	298 K
04	Wavelength	0.71073
05	Crystal system	Triclinic
06	Space group	p-1
07	Cell length	a 9.5308 (4) b 14.4043 (6) c 21.8666 (12)
08	Cell angle	α 106.748(2) β 94.594 (2) γ 105.810 (1)
09	Cell volume	2724.6 (2)
10	Density	1.255 g/cm^3
11	Completeness to theta	0.998
12	Index ranges	h = 11 k = 17 l = 26
13	Theta (Max)	24.999
14	Cell formula units Z	4
15	CCDC no	2488804

Figure 11. ^{1}H NMR (500 MHz, DMSO-d_6) spectrum of compound **5n**

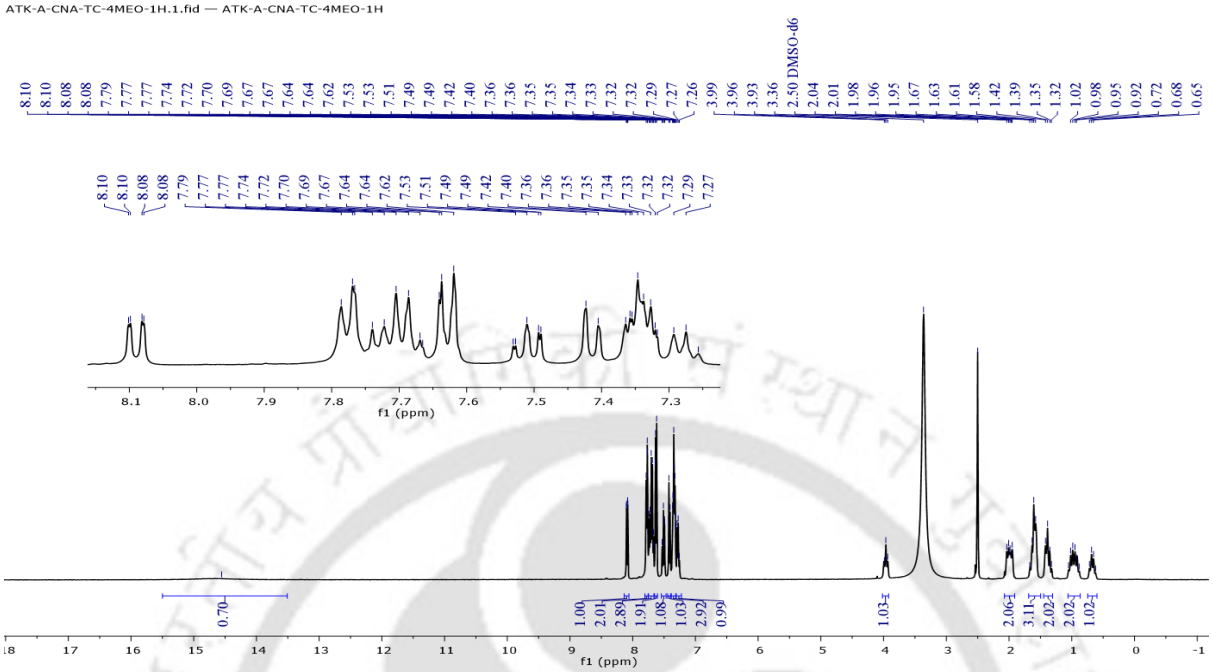

Figure 12. ^{13}C{^{1}H} NMR (125 MHz, DMSO-d_6) spectrum of compound **5n**

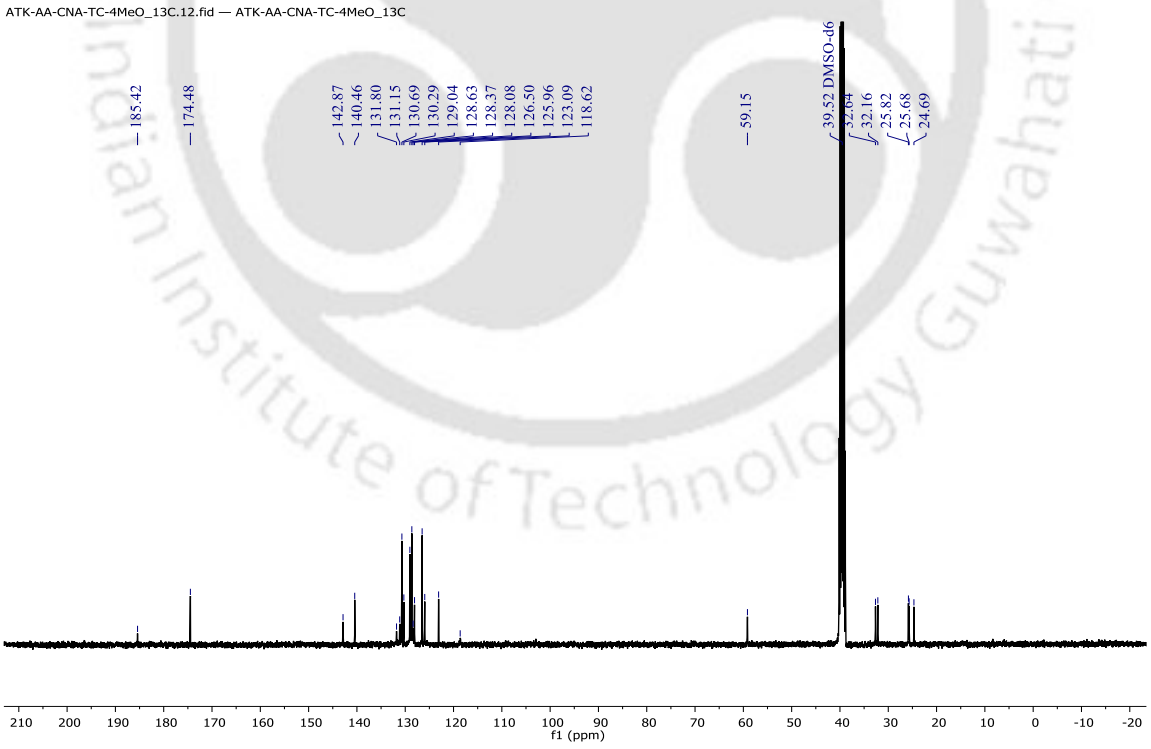

Figure 13. HRMS of compound 5n

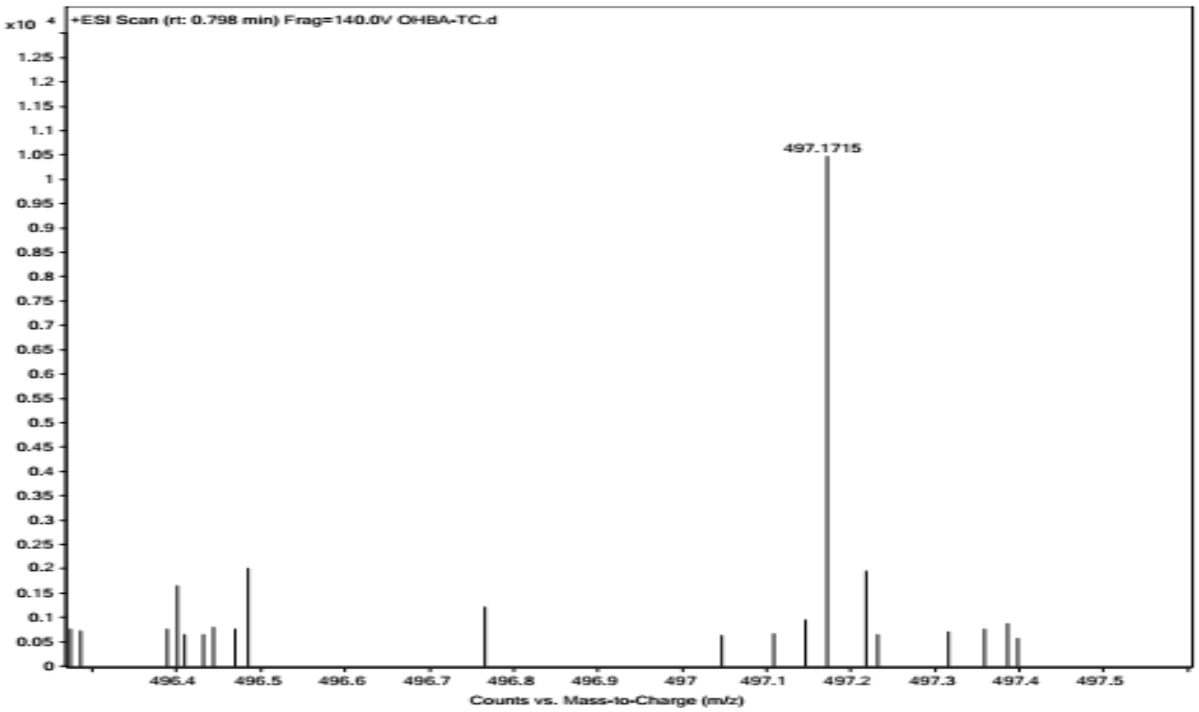

Figure 14. HRMS of Intermediate Iminium ion ,

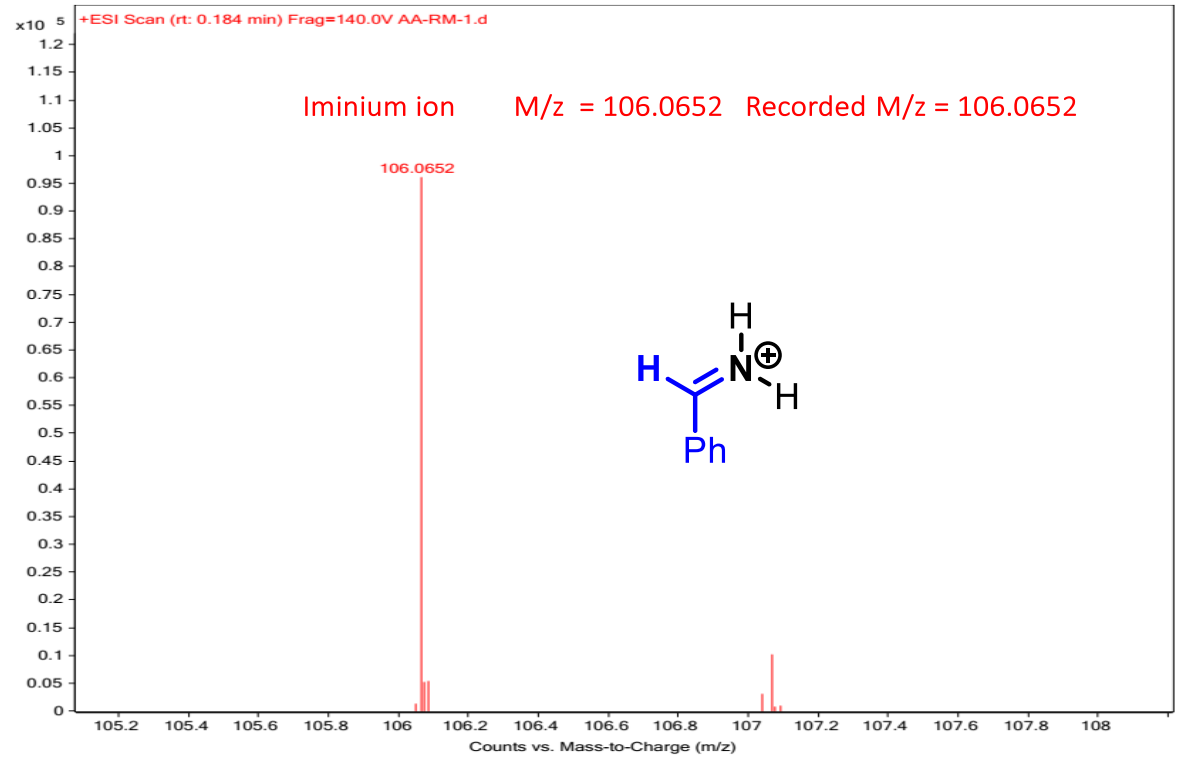

Figure 15. HRMS of Intermediate A

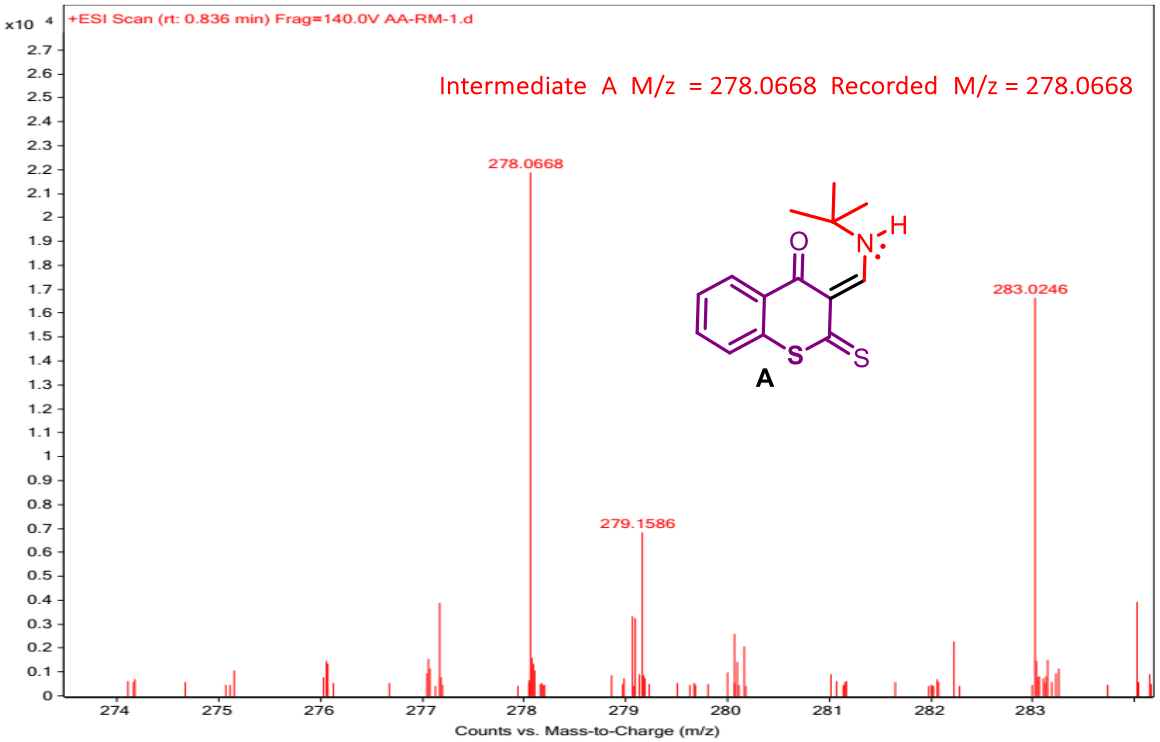

Figure 16. HRMS of Intermediate B

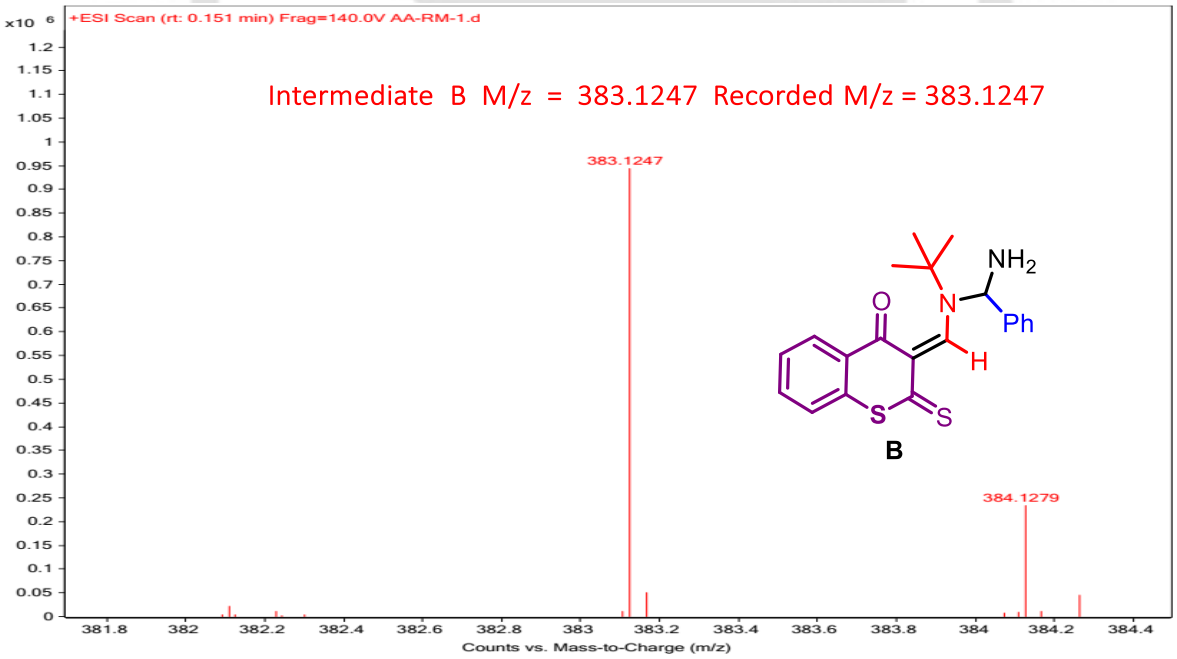

Figure 17. HRMS of Intermediate D

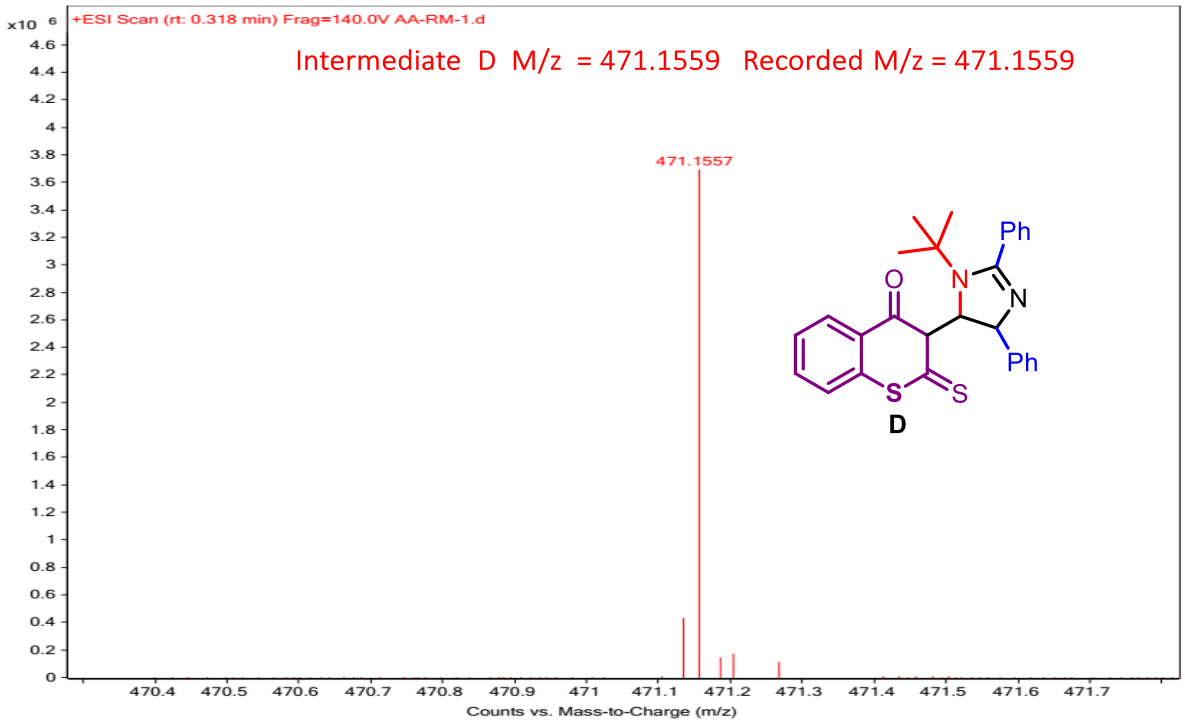

References:

1. S. Ishwar, Chemistry*Select.*, 2020, **5**, 8040-8061.
2. M. H. A. Al-Jumaili, A. A. Hamad, H. E. Hashem, A. D. Hussein, M. J. Muhaidi, Ahmed, A. H. A. Albanaa, F, Siddique, and E. A. Bakr, *J. Mol. Struct.*, 2023, **1271**, 133970.
3. J. Cao and X. Huang, *J. Com. Chem.*, 2010, **12**, 1-4.
4. A. Shaabani, and S. E. Motifs, *Mol. Divers.*, 2018, **22**, 207-224.
5. A. Thakur, G. Pereira, C. Patel, V. Chauhan, R. K. Dhaked, and A. Sharma. *J. Mol. Struct.*, 2020, **1206**, 127686.
6. A. M. S. Hebishy, M. S. Abdelfattah, A. Elmorsy, A. H. M. Elwahy, ZnO. *Synth. Commun.*, 2020, **50**, 980-996.
7. I. Khelifi, T. Naret, A. Hamze, J. Bignon, H. Levaique, M. C. Garcia Alvarez, J. Dubois, O. Provot, and M. Alami, *Eur. J. Med. Chem.*, 2019, **168**, 176-188.
8. A. Kamal, J. S. Reddy, M. J. Ramaiah, D. Dastagiri, E. V. Bharathi, M. V. Prem Sagar, S. N. C. V. L. Pushpavalli, P. Ray, and M. Pal-Bhadra, *MedChemComm.*, 2010, **1**, 355-358.
9. Y. Liu, X. Zhang, J. Li, X. Pei, S. Pang, and C. He, *JACS Au.*, 2025 **5**, 990-997.
10. S. Payamifar, M. Abdouss, and A. P. Marjani, *Arab. J. Chem.*, 2024, **17**, 105967.
11. I. A. Ibarra, A. Islas-Jácome, and E. González-Zamora. *Org. Biomol. Chem.*, 2018, **16**, 1402-1418.
12. A. Dömling, *Chem. Rev.*, 2006, **106**, 17-89.
13. A. R. Pawar, S. Yashmin, and A. T. Khan, *Org. Chem. Front.*, 2025, **12**, 1833-1841.
14. A. Mandal, and A. T. Khan, *Org. Biomol. Chem.*, 2024, **22**, 2339.
15. S. Bhattacharjee and A. T. Khan. *Tetrahedron Lett.*, **57**, 2016, 1831-1834.
16. Y. Gu, *Green Chem.*, 2012, **14**, 2091-2128.
17. A. Dömling, W. Wang, and K. Wang, *Chem. Rev.*, 2012, **112**, 3083-3135.
18. R. Ghomashi, S. Ghomashi, H. Aghaei, S. Massah and A. R. Massah, *Curr. Med. Chem.*, 2023, **30**, 4181-4255.

19. U. M. V. Basavanag, A. Islas-Jácome, A. Rentería-Gómez, A. S. Conejo, M. Kurva, J. O. C. Jiménez-Halla, J. Velusamy, G. Ramos-Ortíz and R. Gámez-Montaño, *New J. Chem.*, 2017, **41**, 3450-3459.
20. M. Masoudi, M. R. Shahbazi-Manshadi and M. Anary-Abbasinejad, *J. Heterocycl. Chem.*, 2019, **56**, 2772-2778.
21. R. B. Sparks and A. P. Combs, *Org. Lett.*, 2004, **6**, 2473-2475.
22. Y. Wang, Y. Li, T. Yu, W. Su, H. Ma, Y. Zhao, X. Li and H. Zhang, *Dyes Pigments*, 2020, **173**, 107958.
23. A. S. Nipate, C. K. Jadhav, A. V. Chate, K. S. Taur and C. H. Gill, *J. Heterocycl. Chem.*, 2020, **57**, 820-829.
24. M. Hossain, *Sci. J. Chem.*, 2018, **6**, 83-94.
25. A. Hamdi, W. Daoudi, M. Aaddouz, M. Azzouzi, H. Amhamdi, A. Elyoussfi, A. E. Aatiaoui, D. K. Verma, M. Abboud and M. Ahari, *Heliyon*, 2024, **10**, e31253.
26. M. Belal, S. Mondal, S. Yashmin, and A. T. Khan, *Org. Biomol. Chem.*, 2022, **20**, 715-726.
27. E. M. M. Abdelraheem, S. Khaksar, K. Kurpiewska, J. Kalinowska-Tłuścik, S. Shaabani, A. Dömling, *J. Org. Chem.*, 2018, **83**, 1441-1447.
28. L. Banfi, A. Basso, C. Lambruschini, L. Moni, and R. Riva, *Chem. Sci.*, 2021, **12**, 15445-15472.
29. P. K. Khanra, T. Kandasamy. and S. S. Ghosh, *Comput. Biol. Chem.*, 2025, **119**, 108575.
30. P. Sen, T. Kandasamy, and S. S. Ghosh, *Cell Signal*, 2023, **102**, 110529.
31. A. Mandal, S. Singh, S. Daimary, A. Arora, S. S. Nambiar, S. S. Ghosh, A.T. Khan, 2025, **57**, 2472-2485.

32. C. Gao, G. A. Xiao, Piersigilli, J. Gou, O. Ogunwobi, J. Bargonetti, *Breast Cancer Research*, 2019, **21**, 5-20.
33. Z. S. Lima, M. Ghadamzadeh, F. T. Arashloo, G. Amjad, M. R. Ebadi, and L. Younesi, *J. Hematol Oncol*, 2019, **12**, 38.
34. S. Bhattacharya, P. K. Khanra, A. Dutta, N. Gupta, Z. Aliakbar Tehrani, L. Severová, K. Šrédl, M. Dvořák, and E. Fernández-Cusimamani, *Int. J. Mol. Sci.*, 2024, **25**, 9650.
35. R. Callaghan, F. Luk, and M. Bebawy, *Drug Metabolism and Disposition*, 2014, **42**, 623-631.
36. B. Shaker, J. Lee, Y. Lee, M. S. Yu, H. M. Lee, E. Lee H. C. Kang, K. S. Oh, H. W. Kim, and D. A. Na, *Bioinformatics*, 2023, **39**, btad577.
37. C. C. Hong, B. K. V. Tang, Agarwal, L. Martin, D. Tritchler, M. Yaffe, and N. F. Boyd, *Breast Cancer Res.*, 2004, **6**, R338.
38. A. Daina, O. Michielin, and V. Zoete, *Sci Rep.*, 2017, **7**, 42717.
39. S. R. Veber, H. Y. Johnson D. F. Cheng, B. R. Smith, K. W. Ward, K. D. Kopple, *J. Med Chem.*, 2002, **45**, 2615-2623.
40. P. Li, Q. Lin, S. Sun, N. Yang, Y. Xia, S. Cao, W. Zhang, H. Q. Li, Guo, M. Zhu, Y. Wang, Z. Zheng, and S. Li, *Cell Death Dis.*, 2022, **13**, 808.
41. A. Patra, A. Arora, S. S. Ghosh, and G. Kaur Saini, *ACS Pharmacol Transl Sci.*, 2024, **7,** 2878-2893.
42. D. Carlisi, A. De Blasio, R. Drago-Ferrante, R. Di Fiore, G. Buttitta, M. Morreale, C. Scerri, R. Vento, and G. Tesoriere, *Cell Death Discov.*, 2017, **3**, 17078,
43. Y. KWON, S.Y. CHUN, K. S. NAM, and S. KIM, *Oncol. Rep.*, ,2015, **34,** 884-890.

Chapter VI

Summary

During my Doctoral Studies, I explored the reactivity of 4-hydroxydithiocoumarin with different types of reactants, and various interesting results were obtained, summarised in **Figure 1** below**.**

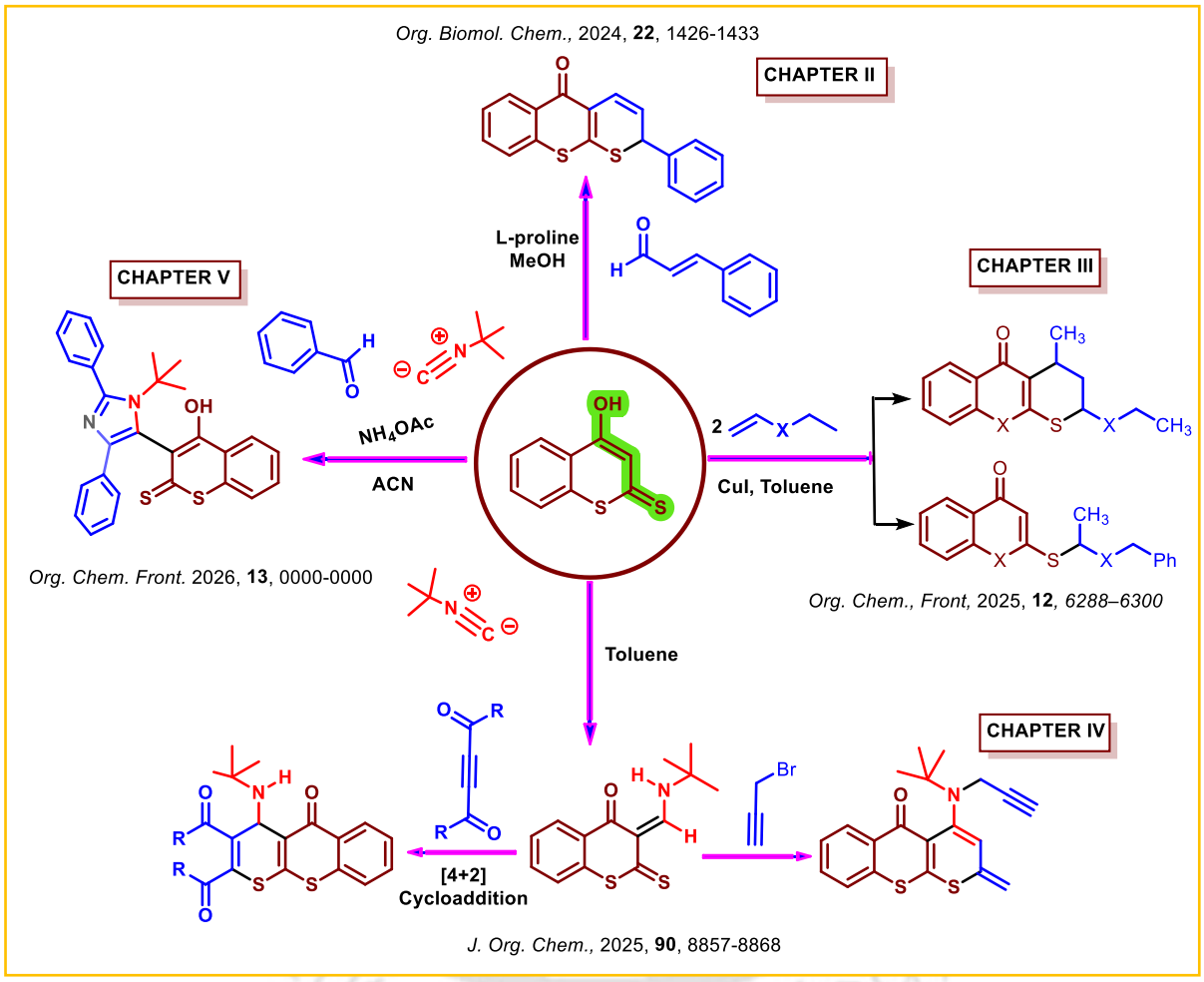

Future Scope

In the third chapter, we have successfully synthesised thiopyrano derivatives using vinyl ethers. These successful results can be extended towards the synthesis of fused thiophene derivatives by tuning the reaction conditions, as depicted in **Scheme 1**.

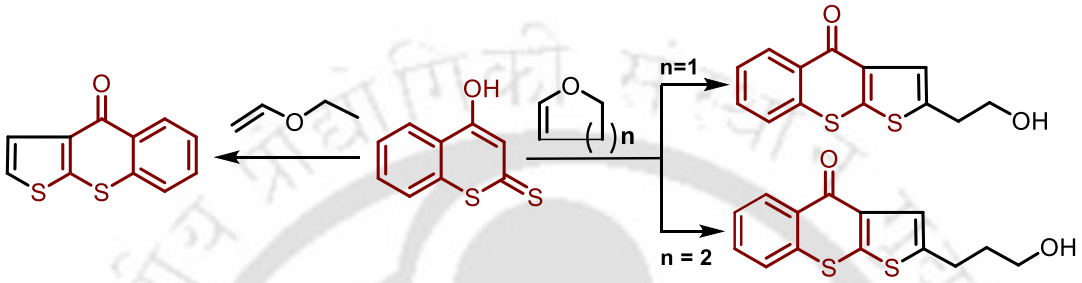

Scheme 1. Synthesis of Fused Thiophene and 2-Substituted Thiophene Derivatives

In addition, the present study can be further explored towards the synthesis of thiozole derivatives. The thiozoles are important heterocyclic compounds, as they constitute the core structure of several naturally occurring organosulfur compounds, such as penicillin and vitamin B1 (thiamine), as illustrated in **Figure 1** in **Chapter I**. 4-Hydroxydithiocoumarin can serve as a potential precursor for the synthesis of a new class of thiozole derivatives, as shown in **Scheme 2**.

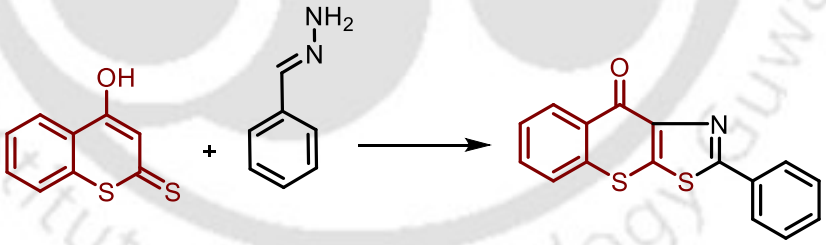

Scheme 2. Synthesis of Thiozole Derivatives

The following research papers were published from the PhD thesis work

1. **Ahmad Ali,** S. Faraz, and A. T. Khan, "L-Proline-catalysed synthesis of 2-aryl-2*H*,5*H* thiopyrano[2,3-*b*]thiochromen-5-ones from 4-hydroxydithiocoumarins and cinnamaldehyde derivatives." *Org. Biomol. Chem.,* **2024**, *22,* 1426-1433. DOI: 10.1039/d3ob02051g

2. **Ahmad Ali**, S. Begam, K. Mehta, P. V. Bharatam, A. T. Khan, "Regioselective Synthesis of (*E*)-3-((Alkylamino)methylene)-2-thioxothiochroman-4-one Derivatives and Their Regioselective Cycloaddition with Alkyne." *J. Org. Chem.,* **2025**, *90,* 8857-8868. DOI: 10.1021/acs.joc.5c00156

3. **Ahmad Ali**, S. Mondal, M. Sood, P. V. Bharatam, and A. T. Khan "Copper-catalysed regioselective *S*-alkylation and C-3(*H*)activation of 4-hydroxydi-thiocoumarin and 4-hydroxy-2*H*-chromene-2-thione: Easy access to 4-methyl-3,4-dihydrothiopyran derivatives." *Org. Chem. Front.* **2025**, *12*, 6388-6300. DOI: 10.1039/d5qo00949a

4. **Ahmad Ali,** N. Amin, S. Begam, P. K. Khanra, S. S. Ghosh and A. T. Khan "Green synthesis of a 4-hydroxydithiocoumarinimidazole bis-heterocycle scaffold, and its antiproliferative study and unusual single-crystal XRD pattern" *Org. Chem. Front.* **2026**, *13*, 2841-2857. DOI: 10.1039/d6qo00082g

Publications from other research work, which are NOT included in the PhD thesis

1. K. Mahato, S. Mondal, **A. Ali**, P. R. Bagdi, A. T. Khan, N. Arora, and S. S. Ghosh, "Unconventional sulfur transfer behaviour of 4-hydroxydithiocoumarin: An easy access to biologically potent 1,2-dithiolane scaffolds." *New J. Chem.,* **2023,** *47*, 1954-1965. DOI: 10.1039/d2nj04791h

2. S. Faraz, **A. Ali** and A. T. Khan, "$FeCl_3$-catalysed regioselective ring-opening of aryl oxirane with 4-hydroxycoumarin for the synthesis of furo[3,2-*c*]coumarins." *Org. Biomol. Chem.,* **2024,** *22*, 95-105. DOI: 10.1039/d3ob01721d

3. D. Kumar, **A. Ali,** M. Sood, P. V. Bharatam, A. T. Khan. "Reactivity study of 4-hydroxydithiocoumarin/4-hydroxythiocoumarin with vinyl ether/cyclic vinyl ether: synthesis of fused novel thiophene derivatives using CuO nanoparticles" *New J. Chem.,* **2026,** *50,* 0000-0000. DOI: 10.1039/D6NJ00650G

4. Afzal, E. Ali SK, **A. Ali,** M. Sood, P. V. Bharatam, and A. T. Khan "Substrate-based stereoselective Synthesis of (*E*) and (*Z*)-3-((alkylamino)methylene)-2-thioxochroman-4-one derivatives using 4-hydroxy-2*H*-chromene-2-thione and isocyanides submitted to *New J. Chem.* for publication

Oral/Posters presented at the Conferences

1. Research and Industrial Conclaves (RIC 2023) 14-16th May at IIT Guwahati
2. Frontiers in Chemical Science (FICS 2024) 2-4th December at IIT Guwahati
3. XIX J-NOST Conference 7th-9th October at IIT Gandhinagar
4. Research and Industrial Conclaves SNERGY 2025, 10-12th October SCIENTIFIQUE Thesis presentation (Oral) at IIT Guwahati

Organic & Biomolecular Chemistry

ROYAL SOCIETY OF CHEMISTRY

PAPER

View Article Online
View Journal | View Issue

Cite this: *Org. Biomol. Chem.*, 2024, **22**, 1426

L-Proline-catalysed synthesis of 2-aryl-2*H*,5*H*-thiopyrano[2,3-*b*] thiochromen-5-ones from 4-hydroxydithiocoumarins and cinnamaldehyde derivatives†

Ahmad Ali, Simra Faraz and Abu Taleb Khan *

Received 15th December 2023,
Accepted 11th January 2024

DOI: 10.1039/d3ob02051g

rsc.li/obc

The hitherto unreported synthesis of 2-aryl-2*H*,5*H*-thiopyrano[2,3-*b*]thiochromen-5-one derivatives was achieved from 4-hydroxydithiocoumarin and cinnamaldehyde using 20 mol% L-proline, an environmentally benign organocatalyst in methanol under reflux conditions. The current approach involves imine formation, followed by a Mannich reaction, instead of a 1,4-addition or thia-Michael reaction, and finally, cyclization. The salient features of this method are mild reaction conditions, broad substrate scope, good yield, atom economy, and shorter reaction time.

Introduction

Sulfur-containing heterocyclic compounds are gaining more attention from researchers because of their profound and immense biological importance, and their potential as useful precursors for drug design.[1a–c] Among organosulfur compounds, thiochromene and thiopyran exhibit many biological activities;[2a–c] the former is used to synthesize drugs in medicinal chemistry.[3] Our research group demonstrated the usefulness of 4-hydroxydithiocoumarin as the key starting material for the synthesis of new molecules by exploring its reactivity with various reactants, as well as their biological importance, which has been reviewed recently.[4] Earlier, we noted that the reaction of 4-hydroxydithiocoumarin and aromatic aldehyde using 10 mol% L-proline as a catalyst generated a pentacyclic molecule through the Knoevenagel reaction *via* a pseudo-three-component reaction depicted in Scheme 1a.[5] We have also observed that 4-hydroxydithiocoumarin reacts with β-nitrostyrene, which acts as a Michael acceptor, to provide an unusual oxime product as summarised in Scheme 1b.[6] The present study intends is to investigate whether cinnamaldehyde will behave similar to aromatic aldehyde or the reaction behavior will be like that of β-nitrostyrene products. Interestingly, it was observed that the reactivity of cinnamaldehyde was found to be different from aromatic aldehyde, as well as β-nitrostyrene, where a different product **3** was obtained, which is described in the manuscript. Therefore, we tried to explore the reactivity pattern of 4-hydroxydithiocoumarin by reacting it with α-β-unsaturated aldehyde using L-proline as an organocatalyst. Because of its versatile catalytic properties, it has recently been used in various organic syntheses, particularly in MCRs,[7a,b] as an asymmetric catalyst in an aldol reaction,[8] and Mannich reaction[9] with excellent enantioselectivity,[10a–c] regioselectivity,[11] and chemoselectivity.[12] Cravotto *et al.* reported[13] the synthesis of thiopyrano derivatives from 4-hydroxythiocoumarin and substituted α,β-unsaturated aldehydes.

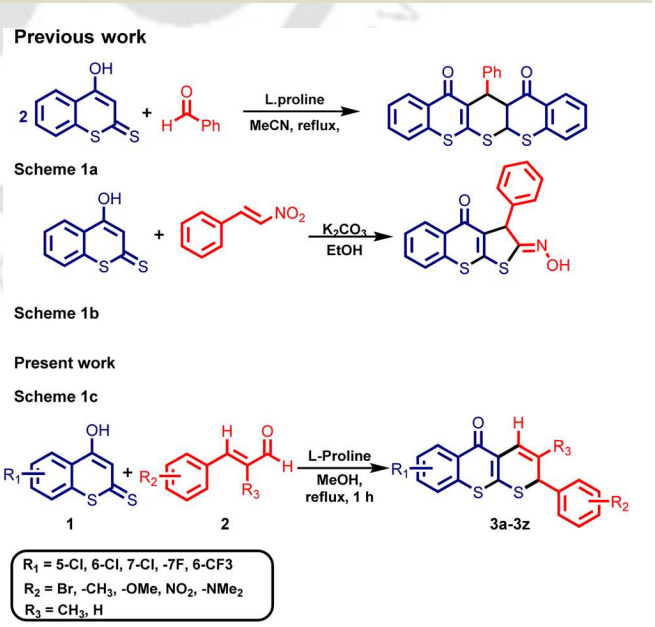

Scheme 1 Comparison of previous work with present work.

Department of Chemistry, Indian Institute of Technology Guwahati, Guwahati-781039, Assam, India. E-mail: atk@iitg.ac.in

†Electronic supplementary information (ESI) available. CCDC 2311036. For ESI and crystallographic data in CIF or other electronic format see DOI: https://doi.org/10.1039/d3ob02051g

ORGANIC CHEMISTRY FRONTIERS

RESEARCH ARTICLE

View Article Online
View Journal | View Issue

Cite this: *Org. Chem. Front.*, 2025, **12**, 6288

Copper-catalysed regioselective *S*-alkylation and C–3(H) activation of 4-hydroxydithiocoumarins and 4-hydroxy-2*H*-chromene-2-thione: easy access to 4-methyl-3,4-dihydrothiopyran derivatives†

Ahmad Ali,[a] Santa Mondal,[a] Mehak Sood,[b] Prasad V. Bharatam[b] and Abu Taleb Khan *[a]

Received 26th June 2025,
Accepted 1st August 2025

DOI: 10.1039/d5qo00949a

rsc.li/frontiers-organic

A useful and expedient synthetic route for the synthesis of 4-methyl-3,4-dihydrothiopyran derivatives (**3a–p** & **6a–o**) was accomplished by employing 4-hydroxydithiocoumarins/4-hydroxy-2*H*-chromene-2-thione and substituted vinyl ethers in the presence of 10 mol% Cu(I) iodide catalyst in toluene under reflux conditions. Notably, the reaction between 4-hydroxydithiocoumarin and ethyl vinyl sulfide (**4**) provided the cyclized products **5a–e**, whereas the reaction between 4-hydroxy-2*H*-chromene-2-thione and ethyl vinyl sulfide **4** gave only the hydrothiolation products **7a–c** under identical reaction conditions. Similarly, the reaction of 4-hydroxydithiocoumarin with phenyl vinyl ether also provided the hydrothiolation products **3q–s** instead of the expected cyclized products under similar reaction conditions. The present methodology involves the formation of two new C–C bonds and one C–S bond *via* regioselective *S*-alkylation and C-3 activation of 4-hydroxydithiocoumarin/4-hydroxy-2*H*-chromene-2-thione in a single step at the expense of one C–O/C–S bond. The current procedure possesses several positive features, such as a broad substrate scope, high regioselectivity, moderate to good yields, high atom economy, mild reaction conditions, and a shorter reaction time.

Introduction

Due to the prevalence of C–S bonds in numerous biological and pharmacological substances, there has been continuous interest in developing mild and effective processes for the formation of carbon–sulfur bonds.[1] Recently, both C–S coupling reactions and direct C–H functionalizations have been established for C–S bond formation.[2] Classical approaches for the construction of C–S bonds include either the direct coupling of organic halides with thiols or the addition of thiols to unsaturated C–C bonds. However, the synthesis of C–S bonds through hydrothiolation reactions and C(sp^2)–H activation has been less explored with electron-rich olefins, particularly vinyl ethers (VEs). VEs have numerous synthetic applications as monomers in polymer synthesis,[3] MCRs,[4] Diels–Alder reactions,[5] and Claisen rearrangements.[6] They have also been exploited in the synthesis of natural products, new physiologically active molecules, and heterocycles.[7] Montevecchi *et al.* demonstrated the synthesis of a thioether from a pseudo-heterocyclic thiol and vinyl ether in the presence of AIBN.[8] In addition, Yamashita *et al.* reported the synthesis of a pyrazole by using vinyl ether in the presence of a chiral Zr catalyst *via* C–H activation.[9] Still, the chemistry of vinyl ethers and their sulfur equivalents is under investigation and can be explored further to generate new transformations.[10] On the other hand, organosulfur compounds are abundant in nature and significantly impact medicinal chemistry.[9,11] Among various organosulfur compounds, thiopyran derivatives exhibit a wide variety of biological activities, such as antimicrobial,[12] antitumor,[13] anticancer,[14] and antiviral activities.[14] Over the past decade, our group has been actively involved in synthesizing various sulfur-containing biologically active hybrid molecules, using 4-hydroxydithiocoumarin as a key precursor, and its chemistry has also been reviewed by our research group.[11] Developing a more efficient route towards α-aryl thioethers from 4-hydroxydithiocoumarin/4-hydroxy-2*H*-chromene-2-thione under environmentally benign reaction conditions would be highly advantageous. In 2020, our research group demonstrated the synthesis

[a]*Department of Chemistry, Indian Institute of Technology Guwahati, Guwahati-781039, Assam, India. E-mail: atk@iitg.ac.in, prof.atkhan@gmail.com, ahmadzaki7782@gmail.com, santa.mondal47@gmail.com*
[b]*Department of Medicinal Chemistry, National Institute of Pharmaceutical Education and Research, S.A.S. Nagar, Mohali, 160062 Punjab, India. E-mail: mehaksood88@gmail.com, pvbharatam@niper.ac.in*

†This work is dedicated to my postdoctoral mentor, Professor Goverdhan Mehta, University Distinguished & Dr Kallam Anji Reddy Chair Professor, University of Hyderabad, on the occasion of his 82nd birthday.

JOC The Journal of Organic Chemistry

pubs.acs.org/joc Article

Regioselective Synthesis of (*E*)-3-((Alkylamino)methylene)-2-thioxothiochroman-4-one Derivatives and Their Regioselective Cycloaddition with Alkynes

Ahmad Ali, Sikhamoni Begam, Kriti Mehta, Prasad V. Bharatam, and Abu Taleb Khan*

Cite This: *J. Org. Chem.* 2025, 90, 8857−8868 Read Online

ACCESS | Metrics & More | Article Recommendations | Supporting Information

ABSTRACT: The catalyst-free reaction between 4-hydroxydithiocoumarin and isocyanide was investigated, yielding substituted (*E*)-3-aminomethylene-2-thioxothiochroman-4-one derivatives (**3**) regioselectively at the C-3 position of 4-hydroxydithiocoumarin. Cycloaddition of product **3** with acetylene-1,4-dicarboxylate ester afforded adduct **6** regioselectively in good yields. Substrates **3a** and **3e** reacted with propargyl bromide (**7**) in the presence of potassium carbonate in acetone, giving the unusual products **8a** and **8e**. DFT calculations explored the mechanism of **3e** formation and its reaction energy profile with alkynes. This protocol offers a broad substrate scope, good yields, ease of handling, catalyst-free conditions, high atom economy, regioselectivity, and a shorter reaction time.

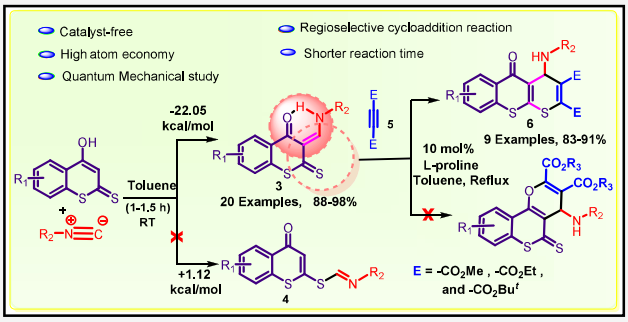

INTRODUCTION

Organo-sulfur compounds are being investigated in different research areas because of their remarkable biological and pharmaceutical importance, as well as their utility in diverse organic transformations.[1−4] Compounds derived from 4-hydroxycoumarin, such as the naturally occurring dicoumarol[5,6] and the non-natural warfarin,[7,8] exhibit anticoagulant activities. The analogs of 4-hydroxycoumarin (I), such as 4-hydroxythiocoumarin (II) and 4-hydroxydithiocoumarin (III), bear a structural resemblance (Figure 1).

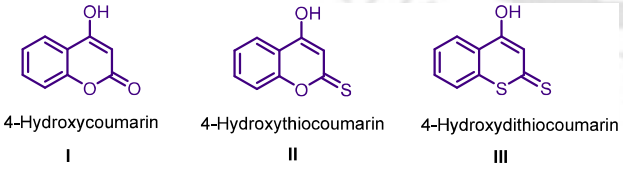

Figure 1. Analogues of 4-hydroxycoumarin.

Since 2014, our research group has extensively investigated the reactivity of 4-hydroxydithiocoumarin and demonstrated the synthesis of numerous new chemical entities by exploiting C-3 and C═S positions.[9−14] Recently, these successful results are also summarized in a review article.[15] 4-Hydroxydithiocoumarin can exist in three possible tautomeric forms[16] (Figure 2), generating three nucleophilic sites when treated with a base.

Since 1838, isocyanide has captured the interest of synthetic chemists because its terminal carbon atom can behave both as a nucleophile and an electrophile (α-addition).[17,18] This unique characteristic makes isocyanide a highly attractive starting material for creating new molecules. Isocyanides can also exist in two resonating forms (Figure 3).

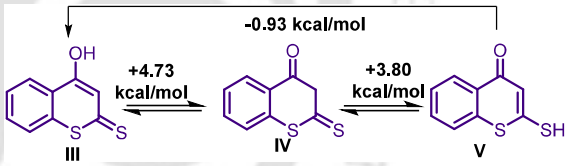

Figure 2. Three tautomeric forms of 4-hydroxycoumarin. **III** is the most stable form. The calculations were carried out using the B3LYP/6−31+G(d,p) level of DFT. All the energy values are estimated using the free energy (G) values. The relative energies of the reaction path are provided in kcal/mol.

Numerous new molecules have been synthesized in the pharmaceutical industry by utilizing isocyanides in various multicomponent reactions (MCRs).[19] Moreover, isocyanide-based MCRs, such as the Passerini[20] and Ugi reactions, are well documented for diversity-oriented synthesis.[21]

Received: January 22, 2025
Revised: June 1, 2025
Accepted: June 10, 2025
Published: June 19, 2025

https://doi.org/10.1021/acs.joc.5c00156
J. Org. Chem. 2025, 90, 8857−8868

ORGANIC CHEMISTRY FRONTIERS

RESEARCH ARTICLE

Cite this: *Org. Chem. Front.*, 2026, **13**, 2841

Green synthesis of a 4-hydroxydithiocoumarin-imidazole bis-heterocycle scaffold, and its antiproliferative study and unusual single-crystal XRD pattern

Ahmad Ali,[a] Nur Amin,[a] Sikhamoni Begam,[a] Pijush Kanti Khanra,[b] Siddhartha Sankar Ghosh[b,c] and Abu Taleb Khan*[a]

Received 21st January 2026,
Accepted 4th March 2026

DOI: 10.1039/d6qo00082g

rsc.li/frontiers-organic

This study introduces a catalyst-free, highly efficient synthetic strategy for constructing hitherto unreported tetra-substituted imidazole-bound bis-heterocyclic (BHC) derivatives *via* a pseudo-five-component reaction. The method provides selective reactivity at the C3 position of 4-hydroxydithiocoumarin, rather than the expected C=S, in which one equivalent each of 4-hydroxydithiocoumarin, isocyanide, and ammonium acetate and two equivalents of aryl aldehyde participate to form two C–C and two C–N bonds in a single operation. This protocol is distinguished by its remarkable atom economy (83.4%), an exceptionally low environmental factor (*E*-factor = 0.19), and environmentally benign reaction conditions. Moreover, this one-pot process affords good yields without the need for column chromatographic separation, thereby reducing the use of additional auxiliaries. Notably, the resulting BHC derivatives, **5l** and **5m**, exhibit promising antiproliferative activities, highlighting the potential impact of this sustainable synthetic approach. In addition, the newly developed product exhibits an unusual structural pattern, as observed by single-crystal XRD.

1. Introduction

Bis-heterocycles (BHCs) are organic compounds that contain two heterocyclic moieties within a single molecule.[1] These rings can be identical or different and are often connected *via* a covalent bond, a linker, or ring fusion.[2] The involvement of two heterocycles, rather than a discrete unit, in a single unit enhances the overall activity and orthogonal reactivity of functional groups.[3,4] Consequently, BHCs show vast applications in medicinal chemistry, pharmaceutical sciences, and in the development of new anticancer drugs.[5–8] Owing to these applications, scientists have constructed various BHCs *via* multicomponent reaction (MCR) approaches.[9–11] MCRs are considered a powerful synthetic toolbox for the construction of complex organic frameworks in a single step.[12–15] In a typical MCR, more than two reactants are combined in a single pot to produce the desired product, thereby enabling the generation of a wide variety of chemical entities simply by changing the starting materials. Some critical advantages of MCR are high-atom-efficiency, one-pot operation, ease of handling, creation of orthogonal reactive functional groups, and contributions to sustainability.[16,17] Wang, Y. *et al.* reported bis-heterocycles through an MCR using phenanthrene-9,10-dione, an aryl amine, and formyl-coumarin (Scheme 2a). Meanwhile, Ghomeshi *et al.* demonstrated bis-heterocycles (coumarin-imidazole) through a three-component reaction from 4-formyl-coumarin, benzil and ammonium acetate, as shown in Scheme 2b. 4-Hydroxydithiocoumarin is a known thio-analogue of 4-hydroxycoumarin, bearing three prominent nucleophilic reactive sites.[18] These multifunctional sites make 4-hydroxydithiocoumarin a fascinating and versatile building block in various organic transformations to access sulfur-containing heterocyclic compounds.[19–24] Building on this, in 2021, our research group reviewed the reactivity switch of 4-hydroxydithiocoumarin, summarising nearly all prior reactions.[25] Moreover, our previous study explored the reactivity of 4-hydroxydithiocoumarin, which is an ambient nucleophile, with another nucleophile, isocyanide, to form alkylamino methylene regioselectively at the C3 position of 4-hydroxydithiocoumarin *via* two-component reactions, as shown in Scheme 2c. In the literature, it is also reported that 4-hydroxydithiocoumarin reacts with aryl aldehydes *via* a Knoevenagel

[a]*Department of Chemistry, Indian Institute of Technology Guwahati, Guwahati-781039, Assam, India. E-mail: atk@iitg.ac.in, prof.atkhan@gmail.com, ahmadzaki7782@gmail.com, nuramin9495@gmail.com, begamsikhamoni@gmail.com*

[b]*Department of Biosciences and Bioengineering, Indian Institute of Technology Guwahati, Guwahati, 781039 Assam, India. E-mail: k.pijush@iitg.ac.in*

[c]*Centre for Nanotechnology, Indian Institute of Technology Guwahati, Guwahati-781039, Assam, India. E-mail: sghosh@iitg.ac.in; https://www.iitg.ac.in/SiddharthaGhosh*